Towards an in-depth view of the reproductive biology of *Schistosoma mansoni*: from gonad isolation to sub-transcriptomics and cell culture

Inaugural-Dissertation
zur Erlangung des Doktorgrades der Naturwissenschaften
(Dr. rer. nat.)
im Fachbereich Biologie und Chemie der
Justus-Liebig-Universität Gießen

vorgelegt von

Zhigang Lu

aus Hebei, V. R. China

Juni 2015

The present work was carried out at the Institute of Parasitology (Faculty 10), Justus Liebig University Giessen between October 2011 and February 2015 under the supervision of Prof. Dr. Albrecht Bindereif and Prof. Dr. Christoph G. Grevelding.

First supervisor: **Prof. Dr. Albrecht Bindereif**
Institute of Biochemistry, Justus Liebig University Giessen, Heinrich-Buff-Ring 58, 35392 Giessen, Germany

Second supervisor: **Prof. Dr. Christoph G. Grevelding**
Institute of Parasitology, BFS, Justus Liebig University Giessen, Schubertstr 81, 35392 Giessen, Germany

To my family

Abbreviations

1. Samples

bM	Male worms from couples obtained from mixed-sex (bisexual) infections
sM	Male worms obtained from single-sex infections
bT	Testes isolated from bM
sT	Testes isolated from sM
bF	Female worms from couples obtained from mixed-sex infections
sF	Females obtained from single-sex infections
bO	Ovaries isolated from bF
sO	Ovaries isolated from sF

2. Gene / protein

AQP	Aquaporin
Ago	Argonaut
BSA	Bovine serum albumin
CD36	CD36 Class B scavenger receptor
Cam4	Calmodulin 4
ESP	Eggshell precursor protein
EdU	5-ethynyl-2′-deoxyuridine
FGFR	Fibroblast growth factor receptor
FKBP12	FK506 binding protein 12
GPAT	Glycerol-3-phosphate acyltransferase
HIP	Hippocalcin
HSP	Heat shock protein
LDL	Low density lipoprotein
MCM	Mini-chromosome maintenance protein
NCS	Newborn cattle serum
npp	Neuropeptide precursor
NPP-5	Nucleotide pyrophosphatase/phosphodiesterase type 5
ORO	Oil Red O
PlK	Polo-like kinase
SPRM1hc	Schistosome permease 1 heavy chain
Tyr1	Tyrosinase 1

Vlg	Vasa-like-gene

3. Technical terms

BLAST	Basic local alignment search tool
bp	Base pairs
BP	Biological process
CC	Cellular component
CLSM	Confocal laser scanning microscopy
CPM	Counts per million
DEGs	Differentially expressed genes
DGE	Differential gene expression
ESTs	Expressed sequence tags
GO	Gene ontology
KEGG	Kyoto Encyclopedia of Genes and Genomes
MF	Molecular function
o/n	Overnight
p.i.	Post infection
RNA-Seq	RNA sequencing
RPKM	Reads per kilobase per million
RT	Room temperature
SAGE	Serial analysis of gene expression
WHO	World Health Organization
WISH	Whole mount in situ hybridization

4. Conserved protein domains

AAA	ATPases associated with a variety of cellular activities
ANK	Ankyrin repeats
ANX	Annexin repeats
ARF	ARF-like small GTPases
B41	Band 4.1 homologues
BROMO	Bromo domain
C1	Protein kinase C conserved region 1 (C1) domains (Cysteine-rich domains)
C2	Protein kinase C conserved region 2 (CalB)
CA	Cadherin repeats
CH	Calponin homology domain

cNMP	Cyclic nucleotide-monophosphate binding domain
DEXDc	DEAD-like helicases superfamily
EFh	EF-hand, calcium binding motif
EGF_CA	Calcium-binding EGF-like domain
EGF_Lam	Laminin-type epidermal growth factor-like domain
FN3	Fibronectin type 3 domain
HELICc	Helicase superfamily c-terminal domain
HOX	Homeodomain
IG_like	Immunoglobulin like
IGc2	Immunoglobulin C-2 Type
KH	K homology RNA-binding domain
KIND	Kinase non-catalytic C-lobe domain
LIM	Zinc-binding domain present in Lin-11, Isl-1, Mec-3
PDZ	Domain present in PSD-95, Dlg, and ZO-1/2
PH	Pleckstrin homology domain
PTPc	Protein tyrosine phosphatase, catalytic domain
RAB	Rab subfamily of small GTPases
RAN	Ran (Ras-related nuclear proteins) /TC4 subfamily of small GTPases
RhoGAP	GTPase-activator protein for Rho-like GTPases
RRM	RNA binding motif
SAM	Sterile alpha motif
SH3	Src homology 3 domains
SPEC	Spectrin repeats
STK	Serine/threonine kinase
STYKc	Protein kinase; unclassified specificity.
S_TKc	Serine/threonine protein kinases, catalytic domain
Spc7	Spc7 kinetochore protein
TBC	Domain in Tre-2, BUB2p, and Cdc16p
TPR	Tetratricopeptide repeats
TSP1	Thrombospondin type 1 repeats
UBCc	Ubiquitin-conjugating enzyme E2, catalytic domain homologues
UBQ	Ubiquitin homologues
vWA	von Willebrand factor A
WW	Domain with 2 conserved Trp (W) residues

Contents

1 Introduction

1.1 Schistosomiasis

Schistosomiasis, or bilharzia, is a parasitic disease caused by trematodes of the genus *Schistosoma*. The species *Schistosoma mansoni*, *S. japonicum*, *S. mekongi*, *S. guineensis* and *S. intercalatum* cause intestinal schistosomiasis, whereas *S. haematobium* triggers urogenital schistosomiasis (World Health Organization (WHO), 2014. Schistosomiasis. Fact sheet N°115. (www.who.int/mediacentre/factsheets/fs115/en/); Global Health Estimates. (www.who.int/healthinfo/global_burden_disease/en/); (Grimes et al., 2014)). As one of the most devastating tropical diseases worldwide, schistosomiasis affects more than 240 million humans being infected, about 780 million people are at risk of infection, and more than 200,000 die every year. With respect to its meaning as parasite-induced infectious disease, schistosomiasis is regarded as a neglected tropical disease and as number two worldwide second only to malaria. Schistosome infections mostly occur in tropical and subtropical areas, especially in Africa.

However, schistosomiasis is not only an agony for people living in endemic areas. Also travellers and immigrants are affected, a human health issue in industrialized countries (Hatz, 2005; Grobusch et al., 2003). Recent reports in Europe indicate the sudden emergence of urinary schistosomiasis, because travelers have been infected in southern Corsica (France). Climate changes are discussed to support environmental conditions for the settlement of *Bulinus* snails, which are the intermediate hosts of *S. haematobium* that was diagnosed in infected tourists from this Mediterranean area (de Laval et al., 2014).

Schistosomes can also infect animal vertebrate hosts and thus have an additional socio-economic impact. Prevalence studies indicate that about 530 million cattle are present in endemic regions of Africa and Asia, where infections rates vary from 31% to 81% (De Bont and Vercruysse, 1998). Especially in Asia water buffaloes play an important role because they can be infected by *S. japonicum*, one of several schistosome

species with high zoonotic potential (Huang and Manderson, 2005; Gray et al., 2009; Wang et al., 2009; Olveda et al., 2014).

1.1.1 Pathology

Not the parasitic worms as such but their eggs are responsible for the pathogenic consequences of schistosomiasis. Half of the eggs reach the environment by leaving the body with urine or faeces for completing the life cycle. The other half remain in the blood circulation and most of these eggs get trapped in the liver and spleen (for *S. mansoni* and *S. japonicum*) or in the bladder and ureter (for *S. haematobium*), where they cause severe inflammatory processes (Ross et al., 2002).

With respect to the clinical progression, schistosome infections can be divided into acute and chronic schistosomiasis. The acute infection is also called "Katayama fever" and is caused by eggs trapped in the liver and intestinal wall. The symptoms include fever, nausea, headache, an irritating cough and, in extreme cases diarrhoea accompanied with blood, mucus and necrotic material. These symptoms can last from a few weeks to several months (Conlon, 2005). The chronic intestinal and hepatosplenic schistosomiasis emerges years after infection. The pathogenic reaction is a cellular, granulomatous inflammation around trapped eggs, which leads to fibrosis, especially in the liver (Ross et al., 2002).

For infection with *S. haematobium*, the disease progression is chronical. The most frequently affected organ is the urinary bladder, and infections with this species are characterised by the occurrence of blood in the urine (haematuria). In addition, *S. haematobium* can cause urinary bladder cancer, and other schistosome species have been associated with liver, colorectal, and prostate cancers (Benamrouz et al., 2012; Honeycutt et al., 2014; Correia da Costa et al., 2014).

1.1.2 Schistosome life cycle

Schistosomes have a complex life cycle that involves an intermediate snail host and a final mammalian host (Figure 1.1). When released together with feces or urine into the water, miracidia hatch from the eggs under optimal conditions (warm temperature and sun light). The miracidia swim and following contact they penetrate a species-specific water snail, in which asexual reproduction takes place via mother and daughter sporocyst stages. The latter enter cercariogenesis to produce cercariae that are released from the snail as the life stage infectious for final hosts. Upon direct contact inside the water, cercariae penetrate the skin of the mammalian host and shed their forked tails.

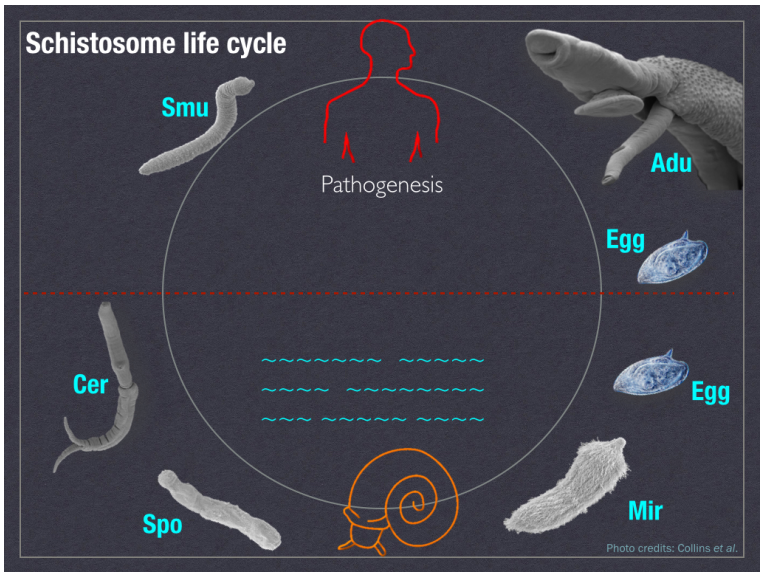

Figure 1.1: Schistosome life cycle. The developmental stages are presented in clockwise order. Adu: adult worms; Mir: miracidia; Spo: sporocysts; Cer: cercariae; Smu: schistosomula. Modified from (Collins and Newmark, 2013).

After a skin migration phase of a few hours, cercariae transform into schistosomula that enter the blood circulation and migrate to portal veins in the liver, where they mature into adult worms and start pairing. As constantly paired couples they migrate to the mesenteric venules of the gut (among other species *S. mansoni* and *S. japonicum*) or the bladder (*S. haematobium*). Mated females (size 7 to 20 mm) deposit eggs in the small venules of the portal and perivesical systems. The eggs actively migrate towards the lumen of the intestine (*S. mansoni* and *S. japonicum*) and of the bladder and ureters (*S. haematobium*). About half of the eggs will be lodged in tissues and half are eliminated with feces or urine (Bogitsh et al., 2013).

1.1.3 Control and treatment of schistosomiasis

Since schistosome infection is induced in the water when the cercariae penetrate the skin, it can be prevented by avoiding contact (e.g. swimming, wading and drinking) with water containing infected snails in endemic areas. Efforts to fight schistosomes include among others eliminating the snail intermediate-hosts that are required to maintain the parasite's life cycle (Centers for Disease Control and Prevention (CDC), 2012. Schistosomasis. Prevention & Control. (www.cdc.gov/parasites/schistosomiasis/prevent.html)). For the disease itself, the goal of treatment is to reduce egg production via the reduction of worm load, which might lead to a

reversal of hydronephrosis and the regression of periportal fibrosis and portal hypertension (Gryseels et al., 2006). Due to its high efficiency and its low cost Praziquantel (PZQ) has become the drug of choice for treatment, also because it is effective against all schistosome species. PZQ induces ultrastructural changes in the teguments of adult worms, resulting in increased permeability to calcium ions. They accumulate in the parasite cytosol, leading to muscular contractions and ultimate paralysis of adult worms. By damaging the tegument membrane, PZQ also exposes parasite antigens to host immune responses (Doenhoff et al., 2008; Reimers et al., 2015). However, this drug is not effective against the juvenile and larval stages of schistosomes and cannot prevent re-infection (El Ridi and Tallima, 2013). Treatment is most effective from four to six weeks after exposure onwards, when the infection has been established and the worms have fully matured. However, administration of PZQ is on a large-scale in many countries (Fenwick et al., 2003; Doenhoff et al., 2009). Low drug efficacy has been reported (Raso et al., 2004; Barakat and El Morshedy, 2011) and the fear of schistosome resistance to PZQ is discussed (Kusel and Hagan, 1999; Gryseels et al., 2001; Doenhoff et al., 2008; Wang et al., 2012). Because no vaccine is available yet, and because the number of drugs to fight schistosomes is alarmingly limited, the WHO has classified schistosomiasis as one of the most important diseases next to malaria and tuberculosis for which novel treatment concepts are urgently needed (WHO, 2014. Global Health Estimates. (www.who.int/healthinfo/global_burden_disease/en/)).

1.2 The unique reproductive biology of schistosomes

1.2.1 Schistosome reproductive organs

During evolution schistosomes have evolved two genders, while all other trematodes are hermaphrodites. The male reproductive organ is the testis, which consists of testicular lobes in which spermatogenesis occurs leading to sperm production. Sperms are transported via the vas deferens to the sperm vesicle of the male before it is delivered via the cirrus to the female, while the female resides in the ventral groove, the gynaecophoric canal, of its male partner (Mehlhorn, 2008; Fried and Graczyk, 1997). Form there sperm is taken up by the uterus of the female and migrates to the receptaculum seminis, which is part of the oviduct near the exit of the ovary extending into the oviduct (Figure 1.2). When primary oocytes leave the ovary, they get fertilized by sperms within the oviduct, complete meiosis, and migrate to the

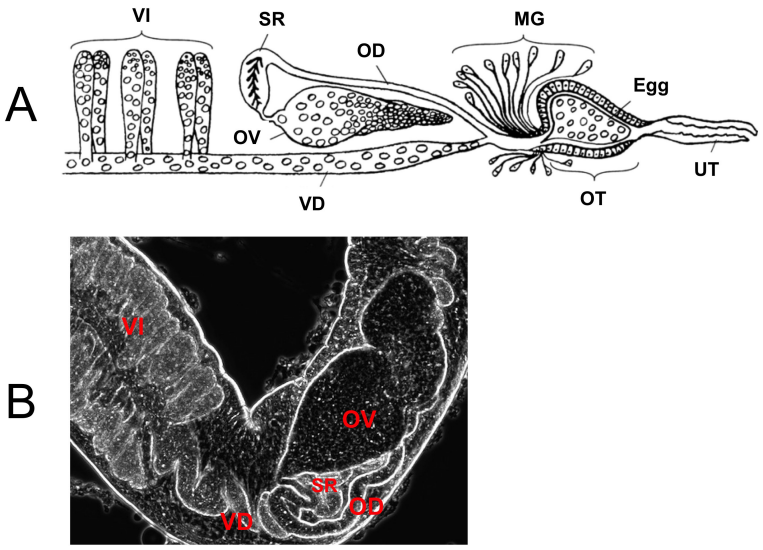

Figure 1.2: Schistosome female reproductive organs. A: a schematic view of the female reproductive organs (DeWalick et al., 2012; Gonnert, 1955b,a); B: phase-contrast microscopy showing among others the female's reproductive organs, vitellarium and ovary. VI: vitellarium; VD: vitelline duct; OV: ovary; OD: oviduct; SR: sperm reservoir/receptaculum seminis; MG: Mehlis' gland; OT: ootype; UT: uterus.

ootype, which is the egg-forming organ. For the females, ovary, vitellarium and ootype are the main reproductive organs, which are accompanied by several accessory tissues (vitelline duct, oviduct, and Mehlis' gland) (Figure 1.2).

1.2.2 Pairing and male-female interaction

Only when paired, the female schistosome starts to continuously produce eggs. Females from single-sex infections have a virgin character and are stunted in size, with underdeveloped ovary and a completely undeveloped vitellarium. Once paired with a male partner, mitogenic processes are induced and the development of female reproductive organs (ovary and vitellarium) is initiated (Shaw et al., 1977; Clough, 1981; Popiel and Basch, 1984; Kunz et al., 1995). As one consequence of this sexual maturation, the size of the female increases dramatically as the vitellarium develops that represents the biggest reproductive organ of a female. In addition primary oocytes differentiate and the ovary enlarges.

At the molecular level, increased mitotic activity was observed and egg-shell precursor genes (p14, p48 etc.) start to be expressed when a pairing contact has been established. Furthermore, the male is not only necessary to induce the reproductive development of the female but also to maintain its mature state (LoVerde et al., 2009;

Grevelding et al., 1997; Knobloch et al., 2002a). Because of this intimate contact between the partners, it has been hypothesized that the male releases some stimuli to the female. However, the biochemical nature of these stimuli is still unknown (Armstrong, 1965; Michaels, 1969; Basch and Basch, 1984; Basch and Nicolas, 1989). On the other hand, the female also exert a stimulatory effect on the male. Changes in levels of glutathione and lipids in the male as well as the expression of new antigens in the gynecophoric canal were observed when the male paired with a female partner (LoVerde et al., 2004b; Osman et al., 2006). Beyond that, gene transcription in males is widely influenced upon pairing as shown by microarray and SAGE-analyses comparing the transcriptomes of paired versus unpaired *S. mansoni* males (Fitzpatrick and Hoffmann, 2006; Williams et al., 2007; Leutner et al., 2013).

Interestingly, the pairing effect is reversible. Females separated from males will stop egg production and gradually degenerate until they are similar to females that were never paired before. If separated females are re-paired with males, mitogenic and differentiation processes are resumed and egg production will start again (Popiel and Basch, 1984; LoVerde and Chen, 1991; Kunz et al., 1995; Grevelding, 2004). The influence of the male even extends to the control of transcriptional processes of female-specifically transcribed genes with functions for reproduction (Grevelding et al., 1997).

1.3 Egg biosynthesis and schistosome reproduction

1.3.1 Development of vitelline cells

In paired females, vitelline cells undergo four developmental stages: S1 to S4. S1 cells are stem-cell like precursor cells, owning the ability of self-renewal and differentiation. Depending on the environmental signals, S1 cells can either produce two euqally-sized daughter cells through equal cell division; or by unequal division they produce two differently-sized daughter cells, one that maintains the stem cell-like character and the other one starting differentiation to S2, S3 and S4 cells (Kunz, 2001) (Figure 1.3 A).

By transmission electron microscopy (TEM), the cellular components were shown to be subject to changes during S1 to S4 cell differentiation. S1 cells have a large nucleus and a very low amount of cytoplasm. In S2 cells, the cytoplasmic volume increases and the nucleus/cytoplasm ratio becomes smaller compared to S1 cells. As cells enter the third stage (S3), vitelline globules are formed and the initial formation of vitelline droplets is observed. Finally, S4 cells represent mature vitelline cells, which contain

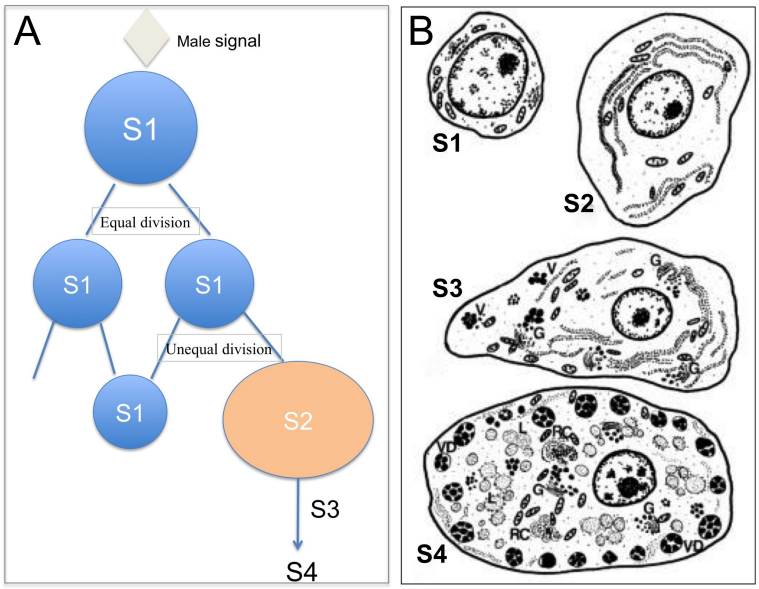

Figure 1.3: A schematic view of vitelline cells development through S1 to S4 (A, adapted from Kunz (2001)) with different cellular components (B, (Erasmus, 1975; Lu et al., 2015)). V, vitelline globules; G, Golgi complexes; VD, vitelline droplets; L, lipids; RC, ribosomal complex.

abundant vitelline droplets arranged at the periphery of these cells. The cytoplasms of S4 cells also contain lipid droplets, with glycogen particles at their periphery. Besides the cellular components, there is a considerable increase in the size of S1 to S4 cells, accompanied by the lowest nucleus/cytoplasm ratio (Erasmus, 1975) (Figure 1.3 B).

1.3.2 Egg biosynthesis

Depending on the species paired schistosomes produce 300-3,000 eggs per female per day (Moore and Sandground, 1956; Cheever et al., 1994). As all other trematodes, schistosomes produce composite eggs consisting of one fertilized oocyte, which is provided by the ovary and transported via the oviduct to the ootype as well as 30-40 mature vitelline cells that originate from the vitellarium being transported via the vitelloduct to the ootype (Shaw, 1987). Supported by serial contractions, vitelline cells start to release their granules containing egg-shell precursor proteins (eg. p14, p48). The egg-shell is finally formed by biochemical cross-linking processes of these precursors proteins (DeWalick et al., 2012). It was suggested that vitelline cells also provide nutrients, such as lipids and yolk, for the developing miracidium. The massive number of eggs produced each day requires that the vitellarium is a highly proliferative tissue and the largest organ of a paired female.

1.3.3 Signal transductions in the gonads

Because the successful continuation of the schistosome life cycle depends on egg formation, and since the pathology of schistosomiasis is mainly caused by the eggs, it is crucial to understand the reproductive development of this parasite. One research focus has been the reproductive biology of the female, which is mainly responsible for egg production and whose sexual maturation completely dependends on continuous pairing with the male. In the past decades many signaling molecules and pathways have been identified in the reproductive organs of *S. mansoni*. Among others these molecules comprise the transorming growth facotr (TGF) receptors, TGF-β I and II and members of the TGF-β signaling pathway such as FKBP12 and Smad molecules (LoVerde et al., 2007, 2009). Furthermore, several cellular tyrosinase kinases (CTKs) such as SmTK3, SmTK4, SmTK5 and SmTK6 have been identified as gonad-associated signaling molecules (Knobloch et al., 2007; Beckmann et al., 2010b). In addition, platyhelminth-specific integrin families have been identified and shown to interact with schistosome CTKs, especially with SmTK4 (Beckmann et al., 2012). The latter is part of a CTK complex interacting with the venus kinases receptor tyrosinase kinases VKR1 and VKR2 (Beckmann et al., 2010b). Both SmVKRs have been demonstrated to be transcribed in the gonads and to be involved in processes regulating oogenesis and spermatogenesis (Vanderstraete et al., 2014; Dissous et al., 2014). Other types of receptor tyrosine kinases (RTKs), such as FGFR A and B, were also shown to be transcribed in gonads and in addition regulated by pairing (Hahnel et al., 2014). They were also demonstrated to be important for somatic stem cells and germinal cells (Collins et al., 2013).

1.4 Schistosome cell culture

To facilitate research on schistosomes, which are not easy to maintain in laboratory setting, cell lines would be of great advantage and are internationally recognized as primary research needs (Quack et al., 2010; Ye et al., 2013; Hoffmann et al., 2014).

To overcome research limitations, different *in vitro* culture systems for parasites of all stages were developed. Among other systems the successful transformation of cercariae to schistosomulae was achieved *in vitro*, as well as the transformation from miracidia to sporocysts and finally to cercariae *in vitro* (reviewed by Quack et al. (2010) and Ye et al. (2013)). Although this is already remarkable progress, since the transformation of sporocysts to cercariae needs a few months (Ivanchenko et al., 1999),

it is not practical for experimental designs and it has not been able yet to complete the whole life cycle *in vitro*. One further obstacle is that adult worms cannot produce fertilized and completely developed eggs *in vitro* as efficiently and continuously as they would do it in the animal host (Ye et al., 2013). Without knowing the exact nutrients and further growth factors they require, cultured adult worms seem to be unable to reproduce efficiently in culture. Against this background the establishment of cell lines in the post-genomic era is of high interest (Quack et al., 2010; Hoffmann et al., 2014). In the past some research activities have been initiated towards this end.

The very initial isolation and maintaining of schistosome cells was reported in the 1970s. At this time a study reported the limited migration of cells from the cut ends of trypsinized worms (Capron and Dupas, 1972). Subsequent attempts included the optimizing of culture media with classical cell culture media (RPMI, DMEM or M199), or self-made media formulations (Basch, 1981), the supplementation of additives (salts supplement, lipid mixtures and growth factors) and the establishment of co-cultivation systems (schistosomula cells with host liver cells, or sporocyst cells with snail cells), which were mainly used for cells obtained from *S. mansoni* and *S. japonicum*. Under the given conditions, it was reported that schistosome cells can survive *in vitro* up to 246 days (Ming et al., 2006). Although some successes was noticed for primary cell cultivation, the division of cells was rarely observed and for a limited time period by applying extracellular matrix (ECM) protein and/or feeder cells. However, no continuously dividing cells were obtained up to now, which would be a prerequisite for passaging cells indefinitely (reviewed by Quack et al. (2010) and Ye et al. (2013)). In most cases, cultivated cells represented mixtures of different cell types. In comparison with cell lines from other invertebrates, a number of differences in the experimental approaches can be noticed. Thus it has been discussed to focus on the starting material which should be more homogeneous with respect to cell types, and appropriated cells should have a high proliferation potential. The latter can be found in juvenile stages or sporocysts but also in the gonads of adults, which harbor a lot of stem cell-like precursor cells, including germinal cells and/or somatic stem cells (Pan, 1980; Collins et al., 2013; Wang et al., 2013)).

1.5 Schistosome genome and *-omics* studies

The *Schistosoma* genome project was launched in 1994 driven by the WHO (LoVerde et al., 2004a). Since that time, various *-omics* studies have been performed including genomics, transcriptomics, proteomics, glycomics and metabolomics ((Hokke et al.,

2007; Chuan et al., 2010; Gobert, 2010; Nahum et al., 2012; Wilson, 2012; Wang and Hu, 2014)).

1.5.1 Genomics

Known *Schistosoma* species possess seven pairs of autosomes and one pair of sex chromosomes (female = ZW, male =ZZ), which range in sizes from 18 to 73 megabases (Mb) and can be distinguished by size, shape and C-banding (Grossman et al., 1981). The first drafts of genomes of *Schistosoma mansoni* (Puerto Rican isolate) and *S. japonicum* (Anhui isolate) were published in 2009, and in 2012 the *S. haematobium* (Egyptian isolate) genome was sequenced. The sizes of the nuclear genomes of these three species were determined to be 363 Mb (*S. mansoni*), 397 Mb (*S. japonicum*), and 385 Mb (*S. haematobium*) containing approximately 10,809, 13,469, and 13,073 protein-coding genes, respectively (Berriman et al., 2009; The *Schistosoma japonicum* Genome Sequencing and Functional Analysis Consortium, 2009; Young et al., 2012). Recently, the annotation of *S. mansoni* genome has been improved, by which the total number of genes was determined to be 10,852 (Protasio et al., 2012). The genome data of the other species are still in the draft stage.

1.5.2 Transcriptomics

With respect to *S. mansoni* gene transcription in different life stages, several studies have been carried out using different strategies, including expressed sequence tags (ESTs) (Franco et al., 1997; Verjovski-Almeida et al., 2003), serial analysis of gene expression (SAGE) (Williams et al., 2007; Taft et al., 2009), and RNA-Seq (Protasio et al., 2012; Almeida et al., 2012). The largest accumulation of EST data was proviced by Verjovski-Almeida *et al.*, who generated 163,000 ESTs from normalized cDNA libraries from six selected developmental stages of the parasite, resulting in 31,000 assembled sequences and 92% sampling of an estimated 14,000 gene complement of *S. mansoni*. The EST data were used as one of the components for the modeler to provide gene predictions in *S. mansoni* (Berriman et al., 2009). However, despite the relatively high transcript sampling achieved, coverage of transcripts was still fragmentary (Almeida et al., 2012).

Besides the transcriptome profiling of gene expression in different life stages, studies were also performed to investigate the pairing effect. Fitzpatrick and Hoffmann (2006) applied DNA microarray analyses to uncover pairing-regulated transcriptional profiles. They found that many of the regulated transcripts have roles

in red blood-cell consumption (e.g., ferritin-1 heavy chain, extracellular superoxide dismutase and aspartate aminotransferase), reproduction (e.g., polo-like kinase 1), egg-laying (e.g., p14, p48, fs800 and tyrosinase 1) and the stabilization of long-term physical contacts (e.g., SEC22 vesicle trafficking protein-like 1 and vesicular integral-membrane protein VIP36). Furthermore, they also detected many male biology-associated transcripts (e.g., Titin and paramyosin), which surprisingly had higher transcript levels in immature females than in mature ones.

Parker-Manuel et al. (2011) applied a microarray approach to explore the gene expression patterns in germ balls (embryonic cercaria), cercariae and day 3 schistosomula. For germ balls they found prominent protein-encoding genes, which were involved in cell division, but also proteases and potential immunomodulators. In addition, transcription of 1,731 genes was differentially regulated above 2-fold difference between germ balls and cercaria, and 1,066 were differentially transcribed between cercariae and day-3 schistosomula.

Cogswell et al. (2012) employed the SAGE technique to identify genes with different transcript abundance in mature (paired) and immature (unpaired) females, and further localized appropriate transcripts by whole mount *in situ* hybridizations (WISH). Some of the identified genes such as *cpeb* and *IF2* localised also in the reproductive rogans. Leutner et al. (2013) compared the whole transcriptome of males from single-sex (sM; unpaired) and mixed-sex (bM; paired) infections by a combined Microarray and SuperSAGE analyses. 526 and 253 genes were found to be differentially transcribed between sM and bM by these two techniques. Among these differentially expressed genes (DEGs) was follistatin, a TGF-beta pathway controlling molecule, which was down-regulated in bM. By yeast-two-hybrid analysis it was found to interact with inhibin/activin and bone morphogenic protein (BMP). The study also highlighted the potential role of neurotransmitters in male development.

Recently, Nawaratna et al. (2011, 2014) applied laser microdissection microscopy combined with microarray analysis to identify tissue-specific transcription profiles in *S. mansoni* including the gut, ovary, testis, vitellarium and oesophageal gland tissues. The authors found that, compared to the whole worm, 384 to 4,450 genes were up-regulated with at least 2-fold in the gut or the reproductive tissues. Although the microdissection approach is elegant, the resulting tissue might not be homogeneous. The same approach was performed before to identify tissue-specifically transcribed genes in *Schistosoma japonicum* females (Gobert et al., 2009), which resulted in 147 genes up-regulated in the gut, 4,149 genes in the ovary and 2,553 genes in the vitellaria.

1.5.3 Proteomics

Curwen et al. (2004) compared the *S. mansoni* soluble proteomes across four life-cycle stages (cercariae, lung-stage schistosomula, adult worms and eggs). They found that the protein patterns obtained by 2D separations of soluble proteins from different life-cycle stages were similar, and that the most abundantly expressed proteins are shared between different stages. A similar study was done for *Schistosoma japonicum* (Liu et al., 2006), which identified 1,181, 1,154, 1,375, 1,441, and 918 proteins from cercariae, hepatic schistosomula, adults, eggs, and miracidia, respectively. Another study tried to identify differentially expressed proteins between male and female *S. japonicum* after pairing (Cheng et al., 2005), which were involved in signal transduction, metabolism and transcriptional regulation etc. At the tissue level, no proteomic analysis has been done so far.

1.6 Aims of this study

The aims of this study were:

1). to identify genes that are transcribed in *S. mansoni* gonads (transcriptome) using RNA-Seq.

2). to investigate the effect of pairing on gene expression at the transcript level in the gonads, i.e. to identify differentially expressed genes between gonads from worms of single-sex infections versus mixed-sex infections.

3). to isolate and characterize vitelline cells from adult female worms based on a novel isolation approach for gonad tissue from *S. mansoni* (Hahnel et al., 2013).

2 Material and Methods

2.1 Ethics Statement

All animal experiments have been performed in accordance with the European Convention for the Protection of Vertebrate Animals used for experimental and other scientific purposes (ETS No 123; revised Appendix A) and have been approved by the Regional Council (Regierungspraesidium) Giessen (V54-19 c 20/15 c GI 18/10).

2.2 *Schistosoma mansoni* laboratory cycle

To maintain the parasite life cycle under laboratory conditions, *Biomphalaria glabrata* snails were used as intermediate hosts, and Syrian hamsters (*Mesocricetus auratus*) as final hosts. The laboratory-strain of *S. mansoni* originated from a Liberian isolate obtained from Bayer AG, Monheim (Grevelding, 1995). Adult worms were obtained by hepatoportal perfusion 46 (mixed-sex) or 67 (single-sex) days post infection.

2.2.1 Maintenance and infection of snails

Snails were kept in aerated snail-water at 26°C and a day-night light rhythm of 16/8 h. They were fed every second day with cucumber slices and once a week with frozen spinach. Snail infection was performed over night (o/n) in 12-well microtiter-plates with 2 ml snail-water in each well. Snails were placed separately into single wells and exposed to 10-15 miracidia each for polymiracidial infections, or only one miracidium for monomiracidial infection (Grevelding, 1999). On the following day, snails were placed back into aquaria, which were shaded after three weeks to prevent early egression of cercariae. Normally, cercariae egress four to five weeks post polymiracidial infection or up to ten weeks post monomiracidial infection (p.i.).

2.2.2 Infection of hamsters

For final-host infection by the paddling method (Dettman et al., 1989) eight to ten weeks old hamsters (Mesocricetus auratus) were used, which were obtained either from the institute's own breeding facility or from Janvier (France). Firstly, hamsters were bathed in warm (30°C) snail-water (1.5 cm high in a plastic container) for 45 to 60 min to soften the skin. After snail-water replacement, 1,500-2,000 cercariae were added and the hamsters kept within the container for additional 45 min to to become infected. Worm recovery (perfusion) occurred 46 days p.i. in case of mixed-sex infections or 67 days p.i. when unisexual infections had been performed.

2.2.3 Worm perfusion and *in vitro* culture

Perfusion was done according to a standard method with modifications (Smithers and Terry, 1965; Duvall and DeWitt, 1967). After anethesy sectioning occurred to open the ventral part of the hamster body to get access to the inner organs. The portal vein was scratched by a needle connected to a flexible tube and a bottle with pre-warmed (37°C) perfusion medium. The needle was subsequently introduced into the left heart chamber. Subsequently, the perfusion medium was pumped through the blood circulation, thus flushing the worms out of the portal vein system. Worms were collected by a brush pen and transferred to a petri dish containing worm-culture medium. If worms had already migrated to the mesenteric vein system, they were extracted by opening the veins separately. Following perfusion, worms were sorted to culture-medium according to their pairing status and then either kept at 37°C and 5% CO_2 in an incubator or washed with PBS and forwarded to following experiments (RNA extraction, gonad isolation, etc.)

2.3 Isolation and vitality check of gonads and cells

The isolation of organs or cells was done by a novel method established in our lab (Hahnel et al., 2013). The following diagram summarizes the steps performed (Figure 2.1):

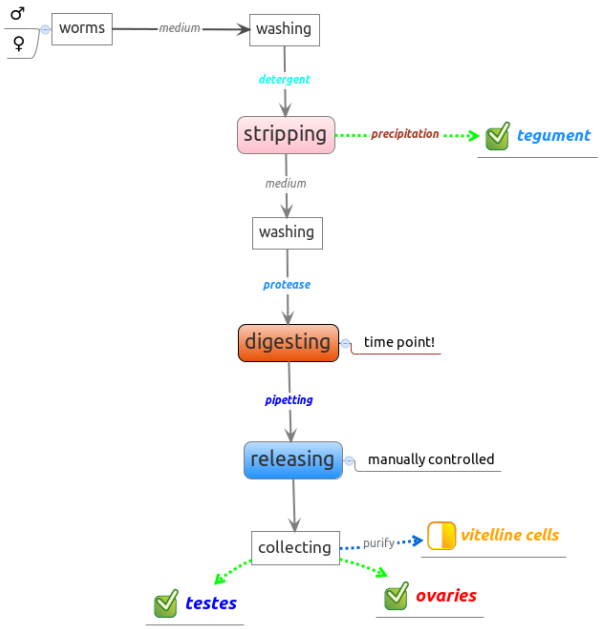

Figure 2.1: A schematic view of the gonad/cell isolation approach.

2.3.1 Ovaries & testes isolation

To get access to the gonads about 50 worms were transferred into 2 ml Eppendorf vessels. The medium was removed and the worms washed once with 2 ml M199 (non-supplemented). After removal of the medium "tegument stripping" was done for 2 x 5 min (females) or 3 x 5 min (males) in 400 µl stripping buffer (0.1% of each: Brij 35 (Roth, Germany), Nonidet P40 (NP-40; Fluka, Germany), Tween 80 (Sigma, Germany), and Triton X-405 (Sigma) in DEPC-PBS, pH 7.2-7.4; 0.2 µm filtered before use) at 1,200 rpm and 37°C. Afterwards, the worms were washed three times with 2 ml M199 (non-supplemented), and the medium was removed completely.

The following enzymatic digestion was performed by incubating the worms with 300-500 µl of elastase (Sigma E0258) solution (5 U/ml in non-supplemented M199) for 25-35 min at 650 rpm and 37°C. The shaking was stopped when the medium became clouded with small fragments, and the worms became soft and viscous. The tube was incubated in the heating block for 1 min. Afterwards, 1 ml M199 medium was added to the tube and 2-4 times gentle pipetting was performed to gradually break up and dissolve the worm cacarsses. The liquid was transferred into a 25 mm dish filled with 2 ml M199, which was placed under an inverted microscope (Leica) to check and collect gonads. Intact and clean gonads were collected by pipetting with 10 µl tips and transferred into a dish with fresh medium. The gonads were then transferred

to another dish with M199 (with or w/o supplement, depending on the purpose) for purification. If necessary, pipetting was performed again for several times to manually release or clean the organs.

Following collecting, most organs were transferred into an RNAase- and DNA-free vessels on ice, spinned down at 6,000*g* for 2 min and frozen at -80°C. In parallel, 5-10 organs were stained with 0.4% Trypan Blue for vitality check.

2.3.2 Isolation of vitellaria and vitelline cells

Vitelline cells were isolated based the protocol for ovaries and testes with slight modifications. Elastase digestion was stopped earlier (20-25 min) when the musculature was disrupted but ovaries/testes were not yet released. Then worms were transferred into a 25 mm dish containing 200 µl fresh medium and incubated for 0.5-1 min. At this point vitelline cells started to be released. These cells were collected by transferring the worms several times to fresh medium and continuous sampling by pipetting using 10 µl pipette tips. Alternatively, cells were collected by centrifugation of the medium after the worms had been removed. The purity of vitelline cells was checked by bright-field microscopy. Remaining tissue fragments were removed by pipetting if necessary and cell suspension was filtered through a 30 µm sieve (Merck Millipore, Germany).

Complete and partial vitellaria were occasionally obtained during the enzymatic digestion step and carefully separated from worms using feather-weight forceps. It appeared more difficult to isolate pure vitellarium tissue compared to vitelline cells.

2.3.3 Vitality of isolated gonads/cells

Trypan-blue staining Besides the morphological check by bright-field microscopy, collected gonads/cells were also stained immediately with 10 µl of 0.4% Trypan Blue solution (Sigma). After about 1 min, the dead cells were stained blue.

Fluorescent staining Cell viability was monitored by double staining using fluorescent dyes Hoechst 33342 (Sigma), which labels nuclei and, as an indirect viability indicator, SYTOX Orange (Life Technologies, Germany), which is a nucleic acid stain penetrating plasma membranes of dead or dying cells only. Stock solutions were prepared in dH_2O at concentrations of 2 mM for Hoechst 33342 or 5 µM for SYTOX Orange, and kept in dark at -20°C until use. Staining solution was prepared

freshly in M199, with a final concentration of 4 µM (Hoechst 33342) or 0.5 µM (SYTOX Orange).

For testis and ovary staining, 30 µl M199 medium containing 5-10 organs was mixed with 30 µl Hoechst 33342 solution and 30 µl SYTOX Orange solution. The mixture was incubated at 37°C for 15 min and then transferred onto a slide. To stain vitellarium tissue, tissue fragments were transferred into 1.5 ml vessels. After the fragments subsided the medium supernatant was carefully removed by pipetting. Vitelline cells were enriched by centrifugation at 2,000*g* for 2 min ahead of staining. To this end, 25 µl staining solution was added to tissue fragments/cells, followed by an incubation at 37°C for 15 min. Subsequently, the staining solution was removed, and 50 µl M199 was added for washing. Finally, the stained tissue/cells were mounted on glass slides with Roti-Mount FluorCare mounting solution (Roth) and kept in the dark until detection.

Fluorescence signals were captured on an Olympus IX 81 microscope with the following settings: UV filter (Ex filter 360-370 nm, Em filter 420-460 nm) to detect Hoechst 33342; Blue filter (Ex filter 470-495 nm, Em filter 510-550 nm) to detect autofluorescence (for vitellaria and vitelline cells); and Green filter (Ex filter 540-550 nm, Em 575-625 nm filter) to detect SYTOX Orange.

2.4 Protein extraction and analysis

2.4.1 Buffers and solutions

Buffers for SDS-PAGE

2 x SDS extraction buffer: 20% glycerol, 10% 2-Mercaptoethanol, 6% SDS, 10mM pyrogallol in buffer (0.5 M Tris pH 6.8 and 0.4% SDS), supplemented with Proteinase Inhibitor Cocktail (Sigma). 1 x buffer was diluted with dH_2O.
2 x SDS sample buffer (Laemmli buffer): 2 x extraction buffer plus 0.004% bromophenol blue.
1 x SDS-PAGE running buffer: 25 mM Tris base, 190 mM glycine, 0.1% SDS, pH 8.3.

Buffers for Western Blot

Tank blot buffer: 25 mM Tris, 192 mM glycine, 20% methanol and 0.06% SDS in dH_2O, pH 8.3.
10 x Ponceau S Red staining solution: 2% Ponceau S in 30% trichloroacetic acid and 30% sulfosalicylic acid. Incubate on an agitator for 5 min.

Coomassie Blue staining solution: 40% dH_2O, 10% acetic acid, 50% methanol and 0.25% Coomassie Brilliant Blue R-250.
Destaining solution for Coomassie-Blue: 67.5% distilled water, 7.5% acetic acid, and 25% methanol.
Blocking buffer: 10 x ROTI-BLOCK (Roth) was diluted to 1 x with dH_2O.
PBST: 1x PBS plus 0.1% Tween-20.

Buffers and solutions for Silver Staining

Fixative: 50 ml ethanol, 10 ml acetic acid, 40 ml H_2O and 0.5 ml 37% formaldehyde.
Washing solution: 50 ml ethanol and 50 ml dH_2O.
Sensitizing solution: 63.7 mg $Na_2S_2O_3$ or 0.1g $Na_2S_2O_3$-$5H_2O$ in 50 ml dH_2O, freshly prepared.
Staining solution: 0.1 g $AgNO_3$ in 50 ml dH_2O then add 37.5 µl 37% formaldehyde; freshly prepared.
Developer: 3 g Na_2CO_3, 0.127 mg $Na_2S_2O_3$/0.2 mg $Na_2S_2O_3$-$5H_2O$ in 50ml dH_2O then add 25 µl 37% formaldehyde; freshly prepared.
Stopping solution: 60 ml acetic acid, 220 ml ethanol and 220 ml dH_2O.

2.4.2 Protein extraction and quantification

Whole worm proteins were extracted by either using 283 females and 100 males from unisexual infections, or 100 females and 50 males from mixed-sex infections. Collected into separate 2 ml Eppendorf tubes, the worms were first washed once with M199 and then once with PBS to remove host proteins. After that, 500 µl 2 x SDS sample buffer was added into each tube. Proteins were extracted by several times of sonication until no worm fragments were visible anymore. In between all tubes were kept in ice to prevent heating of the samples. Subsequently, the samples were denatured at 100°C for 10 min and centrifuged at 13,000*g* for 10 min. The supernatant was transferred to new tubes and stored at -20°C.

For testis and ovary protein preparation, 300 ovaries or testes were obtained by the organ isolation protocol and transferred in 100 µl 1x SDS sample buffer. Samples were denatured at 100°C for 10 min and centrifuged at 13,000*g* for 10 min. The supernatant was transferred to a new tube and stored at -20°C until use.

For recovery of tegument protein from mixed-sex worms, 100 males or 150 females were washed once with M199 followed by another wash with stripping buffer to remove the medium and host proteins; tegument protein was obtained by 6 x stripping

with 10 x stripping buffer (1% of each detergent: Brij 35, Nonidet P40 (NP-40), Tween 80, and Triton X-405 in DEPC-PBS, pH 7.2-7.4; 0.2 µm filtered before use) at 37°C, 12,000 rpm. All fractions were collected and the protein was precipitated by chloroform-methanol. Finally, 500 µl 2x SDS buffer was added to dissolve the protein, which was centrifuged 13,000*g* for 10 min. The supernatant was transferred into another tube and stored at -80°C until use.

The average protein amount in each worm/organ was determined with The Pierce BCA Protein Assay Kit and further by densitometric analysis using BSA as standard. ImageJ was used for densitometric analyses (Schneider et al., 2012).

2.4.3 Silver staining

About 1.5-2.0 µg protein of each sample was taken for silver staining. For organs, it was equivalent to 6 sT, 5.4 bT, 60 sO and 4.2 bO. The loading volume was controlled to be at most 10 µl in order to produce sharp and clear bands.

For the staining, the gel was firstly fixed in Fixative solution o/n or at least 1 h at RT in a plastic bowl, followed by 2 x 25 min washing in Washing-solution. After a brief sensitising for 1 min with Sensitising-solution, the gel was washed 3 x 20 s with dH_2O. Staining was performed in Staining-solution for 20 min at RT. Subsequently, the gel was washed for another 3 x 20 s with dH_2O. The gel was then transferred into another plastic bowl and development was done by adding the Developer followed by gentle shaking until bands were clearly visible. Immediately after that, the gel was washed for 20 s in dH_2O and the reaction was stopped by incubating in Stop-solution for 10 min. Finally the gel was washed for 3 x 10 min in dH_2O and stored in 1% acetic acid at 4°C. ,

2.4.4 Western blot

For SDS-PAGE, 15% separating gels were used to separate proteins that are smaller than 20 kDa, and 12% or 10% separating gels were applied for proteins around 70 kDa. Running condition was defined as 80 V for the stacking gel and 120 V for the separating gel. After that, the gel and membrane were soaked in pre- cold tank blot buffer for at least 30 and 15 min, respectively. Tank blotting was performed at 4°C, with 40 V – 80 mA o/n or 100 V – 320 mA for 1 h. After blotting, the membrane was briefly stained with 1 x Ponceau S Red (Sigma) staining solution to check blotting efficiency, which was also used to cut the membrane into pieces according to proteins of different molecular weight (MW) sizes. To remove the Ponceau S stain, the membrane was

gently rinsed several times with dH_2O.

For blocking the membrane was incubated with Roti-Block solution at RT for 30 min on a shaker. Subsequently, the membrane was incubated with the primary antibody that was diluted with the same Roti-Block solution (dilutions were show in Table 2.1) at 4°C o/n and washed 3 x 15 min with PBST at RT followed by incubation with the HRP-conjugated secondary antibody (Goat anti Rabbit) at RT for 1 h. Afterwards, a second washing step was applied as described above.

Table 2.1: Antibody dilutions for western blot

Smp_Nr	Abbreviation	Dilution	Reference
Smp_106930	SmHSP70	1:20,000	Moser et al. (1990)
Smp_037540.2	SmSPRM1hc	1:600	Krautz-Peterson et al. (2007)
Smp_005740	SmAQP	1:400	Faghiri and Skelly (2009)
Smp_079230	SmFKBP12	1:5,000	Rossi et al. (2002)

Finally the Enhanced Chemiluminescent (ECL) kit (Pierce) was used to detect the signals, which were exposed to Kodak X-ray film.

2.5 Proteomic analyses in ovaries

To perform an initial proteome analysis in a kind of pilot experiment, 120 paired worms were separated directly after perfusion for protein isolation. Performing the organ isolation method resulted in the recovery of 100 ovaries, which were kept in 2 Eppendorf tubes with 50 organs in each that were stored at -20°C until use. Proteome analysis was done by nano-LC-ESI-MS/MS analysis in cooperation with TopLab (Munich, Germany). To this end ovaries were first treated with 25 µl 8 M urea/0.4 M NH_4HCO_3 for 10 min in an ultrasonic bath. The lysed cells were centrifuged through a QIAshredder (QIAGEN). The proteins in the flow were reduced with dithiothreitol, alkylated with iodoacetamide, and digested with trypsin o/n.

An aliquot of the tryptic digest was analyzed by nano-LC-ESI-MS/MS. The HPLC separation was performed on an Ettan MDLC (GE Healthcare). The peptides were dissolved in 0.1% formic acid, loaded with a flow rate of 6 µl/min on a C18 trapping column (C18 PepMap 100, 5 micron particle size, 300 microns ID, 5 mm length, LC Packings) and finally separated on an analytical column (PepMap 100 C18, 3 micron particle size, 75 microns id, 15 cm length). Eluant A was 0.1% formic acid, an eluant B

84% acetonitrile and 0.1% formic acid. The gradient used was 0-30% B for 80 minutes, 30-60% B for 30 minutes, 100% B for 10 minutes.

Mass spectrometry was done with a linear ion trap mass spectrometer (Thermo LTQ Orbitrap, Thermo Electron), which was connected online to the nano-LC system. The LTQ Orbitrap was operated in parallel mode, with the scanning in the Orbitrap Precursormassen (mass range 300-2,000 m / z 60,000 FWHM resolution at m / z 400) and the same three data-dependent MS /MS in the LTQ ion trap.

With the software Proteome Discoverer (Thermo Scientific) an exclusion list was created from the first run of peptide masses. In a second run peptides with a reject mass width of + / - 10 ppm were not re-fragmented and thus additional peptides could be analyzed with low signal intensity.

The MS/MS data from both runs were merged and compared with databases containing all sequences from *Schistosoma mansoni* (UniProt: SwissProt and TREMBL) using the Mascot software (Matrix Science, UK). A Peptide Mass Tolerance of +/- 50 ppm and a Fragment Mass Tolerance of +/- 0.35 Da were used. For the fragmented peptides ion score cut-off was set to 25. Usually, only one or two peptides were fragmented for the other identified proteins with lower score. These may be proteins that were present only in very small amounts in the sample. The rate of false-positively identified proteins increases with a lower score.

2.6 RNA extraction and RT-PCR

2.6.1 RNA extraction

Total RNA was extracted with Trizol / Chloroform as previously described in detail (Hahnel et al., 2013; Beckmann et al., 2010b).

Whole worm total RNA Between 20-50 male or female worms were collected into separate 1.5 ml tubes. 300 µl Trizol were added into each tube and the worms were mechanically hormogenized with plastic pitsons. After filling Trizol to 500 µl, the tubes were kept at RT for 5 min. Afterwards, 100 µl chloroform was added into each tube and the tubes were vigorously shaked for 15 sec, and left on the bench for settling down (3-10 min).

Following centrifugation at 12,000*g* and 4°C for 10 min, the aqueous phase was transferred into new tubes, and 250 µl of isopropanol were added. After brief vortexing, the tubes were kept at -20°C o/n. Afterwards, the tubes were centrifuged

at 12,000*g* and 4°C for 10 min. Most liquid was removed and 1 ml ice-cold 75% ethanol was added to the pellet for washing. Centrifugation was repeated, the pellets were washed again and subsequently dried at RT for 5 min. The total RNA was resuspended in 20 µl DEPC-H_2O.

Gonad and cell total RNA Gonads or cells were collected as soon as possible after elastase digestion into RNase-free tubes. The samples were concentrated by centrifugation at 6,500*g* for 2 min at RT, and the supernatant was discarded. Total RNA was extracted using PeqGOLD TriFast reagent (Peqlab) according to the manufacturers' instructions. Briefly, 50 µl TriFast-solution was added to the tube immediately after the removal of medium. To completely disrupt the cells, three freeze-thaw cycles were performed using liquid nitrogen. After that, TriFast-solution was supplemented to a final volume of 500 µl and the extract kept for 5 min at RT. After adding 100 µl chloroform, the extract was vortexed vigorously for 15 s and then centrifuged at 4°C and 12,000*g* for 10 min. The upper aqueous phase was carefully transferred to a new tube, and total RNA was precipitated by adding 250 µl isopropanol and glycogen (1 µl; RNase-free PeqGOLD glycogen, Peqlab). After incubation at -20°C o/n, the RNA was concentrated by centrifugation at 4°C and 12,000*g* for 10 min. The supernatant was removed and the RNA pellet washed with 75% ice-cold ethanol, dried at RT, and finally resuspended in 20 µl DEPC-H_2O.

2.6.2 RNA analyses using the Angilent bioanalyser

Quality and quantity of total RNA from schistosome whole worms and gonads were checked by Agilent 2100 Bioanalyser using the Agilent RNA 6000 Pico Kit according to manufacturer's instruction. For each sample, 1 µl of DEPC-H_2O diluted RNA (50 pg-5 ng) was loaded onto the chip.

2.6.3 Reverse Transcription / cDNA synthesis

Following a non-enzymatic gDNA wipeout step, cDNA synthesis was done with 200 ng total RNA as template using the QuantiTect Reverse Transcription Kit (Qiagen) and a mixture of random oligo hexamers and oligo-dT primers. The reaction was performed at 42°C for 30 min, with a final step at 95°C for 5 min to inactivate the reverse transcriptase.

2.6.4 PCRs

RT-PCRs were performed in a total volume of 25 µl containing 1 µl of the synthesized cDNA, and 1x reaction buffer B (80 mM Tris-HCl, 20 mM $(NH_4)_2SO_4$, 0.02% w/v Tween20, 2.5 mM $MgCl_2$), 200 µM dNTPs, 400 nM of each primer, and 2.5 units Fire-Pol Taq polymerase (Solis BioDyne). With respect to the base compositions of the primers used (Table 2.2), PCR conditions were as follows: 95°C for 5 min, 35 cycles of 95°C for 30 s, 54-60°C for 45 s, 72°C for 45 s, and a final extension at 72°C for 5 min.

Table 2.2: Primers for RT-PCR

Gene Abbr.	Smp_Nr	Primers (5'->3')	$A_{(T)}$°C
SmHsp70	Smp_106930	TGGTACTCCTCAGATTGAGGT	59
		ACCTTCTCCAACTCCTCCC	
Sm_p14	Smp_131110	CCTATGGCGGTGATTATGG	60
		GGCTGGGTTTGTAAGTGC	
SmTyr1	Smp_050270	GCCTAGATTAGAACATGCTTCTG	58
		CCTCTTTCTAGATTTCTGACAACC	
SmCD36	Smp_011680	TGTCTGCTTGTCTAAGTTATGG	56.4
		TAGAATCGTGCTTTACATCAGG	
SmVlg3	Smp_068440	GATCTGGTTGAATTGCTTCGTG	58
		GTTGTGGATGTTGAAGTCTAGG	
SmFGFR A	Smp_175590	CCAACATCGTCATCATCGTC	54.8
		CTGCCCAGAAATTGATTCCAG	
SmFGFR B	Smp_157300	GAGTATCTGCGTCGTCATCG	59
		CACTAGTTTCAGTACGACCATC	
SmAgo2-1	Smp_179320	TGTAGATGTAAGTGCCAGGG	54.8
		GCTGACGAATTACAACTCCG	
SmNanos2	Smp_051920.2	CGCAATTCACCAATCAAACC	56.4
		CCATTGTTCCGGCAAAATGC	
SmESP	Smp_000430	GTTCCAATTACCAACCAACGTC	58
		GTTTCCGTTACCACCATAATTACC	
SmCam4	Smp_032990	ATGAATGTTCCAATAACTCGTGAAG	56
		AAGTGCTCTTGTTAATTCTGGTAAAC	
SmORAI	Smp_076650.x	ACGTTGTTACTTCTTCAGTACTCC	58
		ACTTTGTAGGTAGTAAGCGCAC	

SmHIP	Smp_085650	GCTATTTATGCGATGGTTGGC	58
		GACTCTGAGGTATCAGGAATGAC	
SmKK7	Smp_194830	TGAAGCTCTACTTCATTTTCTTTCTG	59
		TTAGTCATGCAATTTATGTTCATCA	
SmAQP	Smp_005740	GACCAATCCGTCAGCATCTC	59
		GATGAATAGGCCACCAACTTC	
SmNPP5	Smp_153390.2	TGCTCCTAAGAAGTCAGCAGA	59
		ATCTGTTGATATTGGCAAAGCTTC	

2.7 Transcriptome analyses of testes, ovaries and whole worms by RNA-Seq

2.7.1 RNA extraction

RNA extraction was done as described before and 100 ng of total RNA from each sample was used for RNA-Seq. In total 8 samples were analysed and all samples except sO (ovaries of single-sex females, generated by mono-miracidial infection) have 3 biological replicates (n = 3; Table 2.3). BT (testes from males obtained from mixed-sex infection) and bO (ovaries from females obtained from mixed-sex infection) were isolated immediately after worm couples were separated following perfusion (= bM and bF; males and females, respectively, obtained from mixed-sex infection). All worms were used to isolate RNA or gonads within 8 h after perfusion.

Table 2.3: Number of worms/organs used for RNA-Seq

Sample	# Replicates	# Organs for each replicate
bM	3	10
sM	3	10
bT	3	39-89
sT	3	57-136
bF	3	10
sF	3	50
bO	3	50-57
sO	2	323-816

2.7.2 Library preparation and sequencing

Sample libraries (23 in total) were made with TruSeq RNA Library Preparation Kit (Illumina). All 23 libraries were multiplexed in one pool (23-plex tags) and sequenced on Illumina HiSeq 2500 with 100 bp paired end reads. About 40 Gb data was generated in total, which resulted in 1.67 Gb data per sample. This was approximately 100 x coverage of 16 Mb' *S. mansoni* transcriptome. Each sample was sequenced in parallel in two lanes (= two technical replicates) and then the mapping sequence files ('.bam') were merged. Samples were named consecutively with replicate number i.e. bM1, bM2 andbM3, which stood for each replicate of bM samples.

2.7.3 RNA-Seq data processing

The working pipeline for data processing was as follows: tophat2 (mapping) -> HTSeq_count (read counts) -> edgeR (Differential gene expression analysis) -> Blast / Gene Ontology analysis. Firstly, mapping sequence files ('.bam') were merged by *samtool merge* (Li et al., 2009). Afterwards, counts were calculated by "htseq-count" from the merged '.bam' files (23 in total, one per sample). For proteins with different splice variants, only the longest was recorded. The count table was delivered to R for differential gene expression analysis.

2.7.4 Differential gene expression analyses at the transcript level

For differential gene expression, edgeR (Robinson et al., 2010) was used with raw count values as input. The file with read counts and gene lengths (Supplementary file No. 01-1) was imported into R and raw RPKM (Reads Per Kilobase per Million mapped reads) values were calculated (Supplementary file No. 01-2). For filtering lowly expressed tags, we estimated RPKM < 2 as background signal. Therefore, only genes whose RPKM is large than 2 in all replicates of at least one sample were defined as "expressed/transcribed" and were kept for downstream analysis. Read counts of the rest genes were then normalised for differential expression analysis. Besides, mean RPKM values (Supplementary file No. 02) were calculated based on normalised reads for generating barplots and heatmaps.

To investigate the effect of pairing-status, gender or tissue-origin on gene transcription, a GLM (generalized linear model) approach with defined contrasts (McCarthy et al., 2012) was applied to calculate $\log_2$(Fold Change) and FDR (False Discovery Rate, equivalent to adjusted p values; (Benjamini and Hochberg, 1995))

values between the samples. The comparisons were set as follows: i) pairing effect: bM/sM, bT/sT, bF/sF, and bO/sO; ii) gender effect: bM/bF, sM/sF, bT/bO, and sT/sO; iii) tissue effect: bT/bM, sT/sM, bO/bF and sO/sF. The cut-offs for significant differential gene expression was: fold-difference > 1.5 for all comparisons; FDR < 0.05 for bM/sM and bT/sT, FDR < 0.005 for all the rest comparisons.

2.7.5 Gonad-enriched versus worm-enriched transcripts

To highlight genes, which in contrast to whole worms were transcribed preferentially or exclusively in both or individual gonads, average gene expression in gonads were compared to those in worms. Genes with at least 4-fold difference were considered as differentially transcribed between worms and organs. The lists of genes were then manually revised according to the transcription patterns to keep the comparison more accurate, especially for those sample-specifically transcribed genes that might have been wrongly categorized due to a compensation to the rest of samples.

2.7.6 Males-sF-enriched transcripts

To detect gene transcripts enriched in males and sF, the average transcript amount of (males + sF) was compared to the average of the rest samples using the edgeR package in R. FDR and logFC values were calculated and the former was set to 0.005. To assure specific transcripts, genes were filtered by comparing their RPKM values as follows: "sF>2x bF & sF > 2x sO & bM > 2x bT". In addition a manual inspection was done.

2.7.7 House-keeping genes

House-keeping candidate genes were discovered by using a GLM approach in edgeR, which worked as an ANOVA-like test to find genes whose transcription did not show significant difference between any two of the eight samples. Further cut-off was set as 5% FDR and 1.4-fold difference (see scripts in Supplementary file No. 03-1 for the above mentioned analyses).

2.7.8 Functional analysis of gene products *in silico*

Gene Ontology (GO) enrichment analysis was performed with the TopGO (Alexa and Rahnenfuhrer, 2010) package for R, where $p < 0.01$ and nodesize = 10 were set for

identifying significantly enriched categories (scripts are included in Supplementary file No. 03-2). Gene annotations were obtained from the GeneDB database v4.0 (www.genedb.org; Supplementary file No. 04).

Besides, protein sequences were also blasted against the KEGG KO group using BSH-method (KAAS (http://www.genome.jp/tools/kaas/); performed on 16 February 2015 with default parameters) to find orthologs (indicated by "[K]"; Supplementary file No. 05).

Additionally, conserved domains were identified by NCBI Batch CD-Search using the default CDD database (cdd v3.13, E-value cut-off 0.01; performed on 20 February 2015), which includes NCBI-curated domains and data imported from Pfam, SMART, COG, PRK, and TIGRFAM (Supplementary file No. 06). Protein sequences of specific genes were also blasted against the *C. elegans* / *Drosophila* / Zebrafish and planarian databases to find potential homologs, which was done by using the program Blast+ (Camacho et al., 2009). Multiple sequences alignment was done using Clustal Omega with default settings (http://www.ebi.ac.uk/Tools/msa/clustalo/).

2.8 Adhesion of vitelline cells

To enhance cell attachment, Poly-L-Lysine (PLL; Biochrom AG, Germany), laminin (Sigma), Cell-Tak (BD Biosciences, Germany) and serum (newborn cattle serum, Sigma) were either used alone or in combination for the coating of slides. Working solutions: PLL (1 mg/ml) was 1:1 diluted with dH_2O; laminin was diluted with medium at a final concentration of 16 µg/ml. Cell-Tak (1.85 mg/ml in 5% acetic acid) was applied in the hand-spreading way suggested by the manufacturer.

Vitelline cell adhesion was first tested in the following way: PLL + laminin, laminin only, Cell-Tak and serum. This was done by covering the whole slide or only a specific area of its center (about 1 cm in diameter).

For the combination of PLL and laminin, diluted PLL (30-40 µl) was dropped on the center of slide, which was then placed on a heating block. After PLL was completely evaporated, laminin was added on top and incubated at RT for 30-40 min. Rest laminin was removed and the slide air-dried. The slides were stored at 4°C for later use.

Cell-Tak-based adhesion was performed as follows: 3-5 µl Cell-Tak was dropped on the slide and spread to form a thin film. After at least 20 min at RT, Cell-Tak evaporated and the slides were rinsed twice with distilled water. After air-drying, the slides were stored at 2-8°C for up to two weeks. Serum-free medium turned out to be advantageous to attach cells. For adhesion, a drop of cell suspension was placed on

the coated area, followed by 10-20 min to allow the cells to sink down and to attach. Afterwards, the medium was replaced with pre-warmed serum-containing medium.

2.9 Neutral lipid staining

2.9.1 Oil Red O staining of neutral lipids

Solutions

Oil Red O Stock solution: 300 mg ORO powder (Sigma #O-0625) dissolved in 100ml isopropanol. The mixture was stirred o/n and kept dark at RT.
Oil Red O Working solution: 3 parts of ORO Stock was mixed with 2 parts of PBS. The mixture was kept at RT for 15 min followed by 0.2 µm filtration. For blank control, 60% isopropanol was prepared by diluting with dH_2O or PBS.

Staining

For ORO staining, 10 worms were washed 1x with PBS. Fixation was done by incubating worms with 4% formaldehyde (in PBS) at RT for at least 1h. Subsequently, dehydration was achieved by replacing formaldehyde with 60% isopropanol and incubation for 15 min. The worms were then stained with ORO working solution at a final concentration of 0.18% at RT for 3-5 h, in the dark on a shaker. The material was rinsed afterwards with BPST (1 x PBS plus 0.3% triton x-100) and mounted with Aquatex (Merck). For the quantification of ORO, stained worms were incubated in 100% isopropanol on a shaker until no ORO color remained within the worms (about 30 min). OD_{490} values were measured using 100% isopropanol as blank.

For staining of adhered cells, cells werre attached onto slides that had been pre-coated with PLL and laminin and then fixed for 15 min and dehydrated for 5 min, and dried completely at RT. The staining process was shortened to 15 min.

2.9.2 Fluorescence staining of neutral lipids

Isolated vitelline cells were collected in a 1.5 ml vial and concentrated by centrifugation at 2,000*g* for 2 min. Most of the medium was removed from the supernatant of the cell pellet and 50 µl of each dye (Hoechst 33342: 4 µM in M199; HCS LipidTOX Deep Red Neutral Lipid Stain: 1:1,000 in M199; Life Technologies) was added to the vial and the cells resuspended by careful pipetting. Staining was done at 37°C for 50 min in the dark. Thereafter, the stained cells were washed once

with M199 and mounted onto glass slides with Roti-Mount FluorCare mounting solution (Roth). Microscopic analyses were done by confocal laser-scanning microscopy (CLSM; Leica TCS SP2 microscope) with the following settings for detection: Hoechst 33342: Ex 405 nm, Em 420-470 nm; autofluorescence: Ex 405 nm, Em 500-550 nm; LipidTOX Deep Red: Ex 633 nm, Em 650-670 nm.

2.10 Electron microscopy

2.10.1 Scanning electron microscopy (SEM)

Following vitellarium isolation vitelline cells were collected as described above. For scanning electron microscopy (SEM; Zeiss DSM 982 microscope) vitelline cells were seeded onto a 12 mm glass slide, which had been sterilized by 100% ethanol and precoated with poly-L-lysine (PLL) and laminin. Briefly, 50 µl PLL (0.05 mg/ml in dH_2O; Biochrom AG) was dropped on the center of one round glass slide and kept on a heating plate (37°C) until the liquid evaporated. Then, 50 µl laminin (16 µg/ml in M199; Sigma) was added on top of the PLL layer and the slide kept at RT for 40 min. Superfluous liquid was removed afterwards and the slide kept at 4°C until use. For adhering, cell suspension was transferred on top of PLL-laminin double layer and kept at room temperature (RT) for 20 min. Afterwards, cells were fixed in 2% glutaraldehyde in 0.1 M PBS (pH 7.4) at RT for 2 h on a shaker, followed by rinsing for 10 min in 0.1 M PBS, osmium fixation in 2% OsO_4 at RT for 30 min, and another rinsing steps in ddH_2O for 2 x 5 min. The preparation was then dehydrated shortly in 30% and 50% ethanol on ice on a shaker and finally kept in 70% ethanol at 4°C o/n. On the following day, dehydration was continued in 80%, 90%, 96%, and 100% ethanol for 10 min each, on ice on a shaker. Finally, the cells were critical-point dried (cpd030, Bal-tec), mounted on SEM-holders and gold sputtered (scd004, Balzers).

Cells were observed in a FEG scanning electron microscope (DSM982, Zeiss) at 3kV. Images were recorded using a secondary electron (SE)-detector with the voltage of the collector grid biased to + 300 V in order to improve the signal-to-noise ratio and to reveal optimal topographical contrast.

2.10.2 Transmission electron microscopy (TEM)

For transmission electron microscopy (TEM) the vitelline cells were fixed in 2% glutaraldehyde in 0.1 M PBS (pH 7.4) at RT for 3 h, embedded in gelatine (Fluka), post fixed in 1% osmium tetroxide, washed, and incubated in 1% aqueous uranyl acetate

(Polysciences, Germany) o/n at 4°C. Specimens were dehydrated in an ethanol series and embedded in LR White (Agar Scientific, UK). From the blocks cured by heat, ultrathin sections were cut and finally contrasted in uranyl acetate and lead citrate. Ultrathin sections were inspected by TEM (EM912a/b – ZEISS, Germany) at 120 kV under zero-loss conditions. Images were recorded at slight under focus using a 2k x 2k slow-scan ccd camera (TRS).

2.11 Ca^{2+}-imaging on vitelline cells

Vitelline cells were collected as described above and suspended in M199 medium. To achieve adherence of vitelline cells for subsequent Ca^{2+}-imaging experiments, glass slides were precoated with a combination of PLL and laminin as mentioned above. Cell suspensions were kept on slides for 20 min to achieve cell adhesion.

To measure Ca^{2+}, Fura-2 (Life Technologies) was used, an aminopolycarboxylic acid, which as a ratiometric fluorescent dye binds free intracellular Ca^{2+}. Fura-2 is excited at wavelengths of 340 nm and 380 nm, and the ratio of the emissions directly correlates to the amount of intracellular Ca^{2+}. For superfusion of attached vitelline cells, Tyrode solution was used (135 mM NaCl, 5.4 mM KCl, 10 mM HEPES, 12.2 mM glucose, 1.25 mM $CaCl_2$ and 1 mM $MgCl_2$ in dH_2O, pH 7.4). For the Fura-2 loading of vitelline cells, 6 µl Fura-2 (1 mg/ml in DMSO; Life Technologies) and 6 µl Pluronic F-127 (Life Technologies) were dissolved in 2 ml Tyrode solution to incubate the cells at 37°C for 1 h ahead of imaging. Cyclopiazonic acid (CPA) (10 µM; Sigma) was applied as a blocker of Ca^{2+}-ATPases to inhibit intra cellular Ca^{2+} transport. Furthermore, Gadolinium (Gd^{3+}, 5 µM; Sigma) was applied as a capacitative Ca^{2+}- entry blocker.

2.12 Fluorescence-activated cell sorting (FACS)

The purpose of FACS was to separate S1-S4 stage cells according to differences in their auto-fluorescence intensities and size or granularity. After isolation, cells were centrifuged at 2,000*g* for 2 min and resuspended in 500 µl PBS with 1 mM EDTA and 25 mM HEPES. The density was approximately 1 x 10^6 – 1 x 10^7 cells/ml. Cells were stained with Hoechst 33342 at a final concentration of 4 µM. Unstained cells were used as control. Hoechst-stained cells were then stained with SYTOX Red (Life Technologies) to exclude dead cells. Analysis was done on BD Biosciences FACS Aria III flow cytometer, with violet (Ex 405nm for Hoechst 33342), blue (488 nm for autofluorescence) and red (633 nm for SYTOX Red) lasers.

3 Results

Because schistosome reproduction plays substantial roles not only for maintaining the parasite´s life cycle but also for the pathologic consequences of schistosomiasis in infected humans or animals, this work mainly focused on characterizations of the defined reproductive organs (the testis, ovary, and vitellarium) with respect to morphological and molecular aspects. The results are presented in three main parts: 1) characterization of testes and ovaries at the levels of morphology, and protein expression; 2) sub-transcriptome analyses of testes and ovaries, including investigations of pairing effects, and comparisons of gonad versus whole worm transcriptomes; 3) isolation and characterization of vitellaria and vitelline cells.

3.1 Organ isolation efficiency

Based on the organ isolation approach developed in our laboratory (Hahnel et al., 2013) testes, ovaries and vitellaria (see below) were extracted from adult worms. The efficiency of organ isolation varied from organ to organ and between the genders. The yield for testes isolation from adult male *S. mansoni* was 60-80%, independent of the pairing-status. The yield of ovaries was 70-85% from paired females (bO) and 80-90% from females that had never been paired before (sO). In general, the testicular lobes turned out to be more fragile when extracted than the ovaries.

3.2 Morphological and molecular analyses of isolated testes and ovaries

3.2.1 Light microscopy

With respect to male gonads, testes from paired (bT) versus unpaired (sT) males showed similar morphological characteristics as shown before in another study (Neves et al., 2005). They exhibited comparable sizes and consisted of 8-10 individual lobes.

Inside each lobe spermatocytes at different stages of developmental were observed (see Fig 3.1 as a representative example). In contrast, ovaries from unpaired (sO) females, which contain only undifferentiated oogonia, are much smaller than those from paired (bO) ones. Ovaries from paired females consisted of two parts: the smaller anterior area containing oogonia, and the larger posterior part that contains mature, primary oocytes (see Figure 3.2).

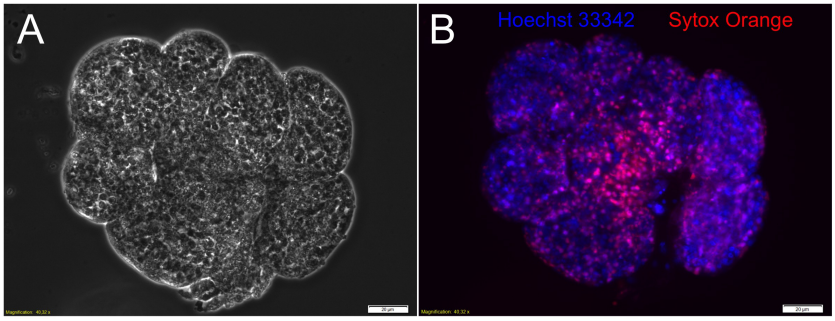

Figure 3.1: Microscopical pictures of testes obtained from a paired male, stained with Hochest 33342 (blue) and SYTOX Orange (red). A: phase-contrast; B: fluorescent microscopy. Scale bars: 20 μm.

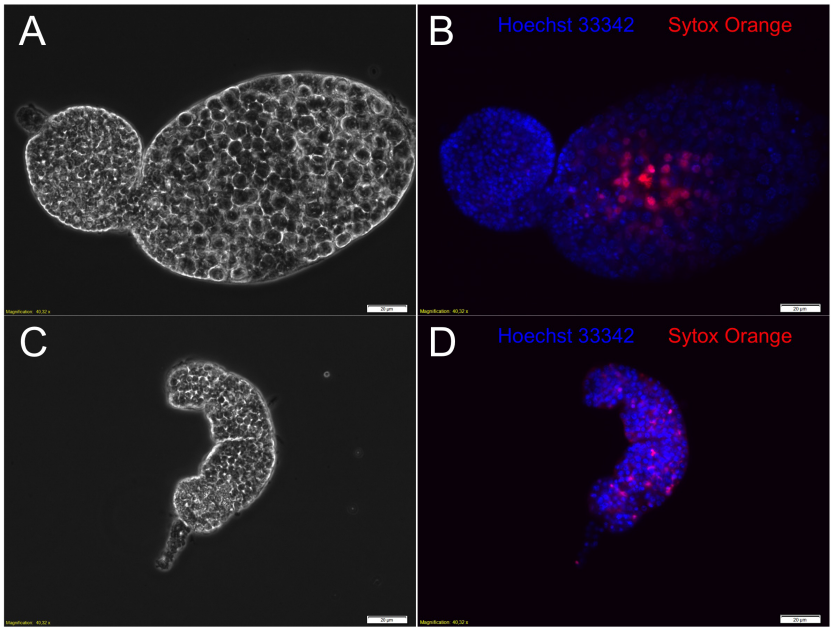

Figure 3.2: Ovaries isolated from paired females (A and B) or unpaired females (C and D), stained with Hochest 33342 (blue) and SYTOX Orange (red). A and C: phase contrast; B and D: fluorescent microscopy. Scale bars: 20 μm.

Cell vitality inside the gonads was determined by SYTOX Orange staining. The dye is cell-impermeant and, therefore, only dead cells will allow the dye to pass through the membrane and to stain the nucleic acids. Hoechst 33342 nucleic acid stain is a cell-permeant nuclear counterstain that emits blue fluorescence when bound to dsDNA. Cells stained by both dyes showed blue and purple signals during fluorescence microscopy. The latter is due to an overlay of blue and red. This result indicated that some gonad cells were less vital than others. Furthermore, comparing the amount of purple-stained cells between the organs showed that cells inside the ovary had a higher vitality than those from isolated testicular lobes.

Cell size measurement by light microscopy

The sizes of cells inside gonads were measured on an Olympus IX81 microscope, with the software Cell Dimension (Olympus). Diameters of the longest orientation were recorded. From the measurements performed it was determined that mature oocytes had diameters of about 11-13 μm and spermatocytes, immature oocytes as well as oogonia revealed sizes between 2.5-5 μm (Table 3.1).

Table 3.1: Size measurement of gonad cells (μm in diameter)

Cell type	Size range	Mostly
Immature oogonia	3-5	3-4
Immature oocytes	2.5-5	2.5-4
Mature oocytes	6-11	9-11
Spermatocytes	2.5-5.5	3-4

3.2.2 Electron microscopy of ovaries

Whole ovaries were processed for electron microscopic (SEM and TEM) analyses. Figure 3.3 shows the SEM image of one oocyte and one oogonia cell (A), and the intracellular components of an oocyte as visualized by TEM (B).

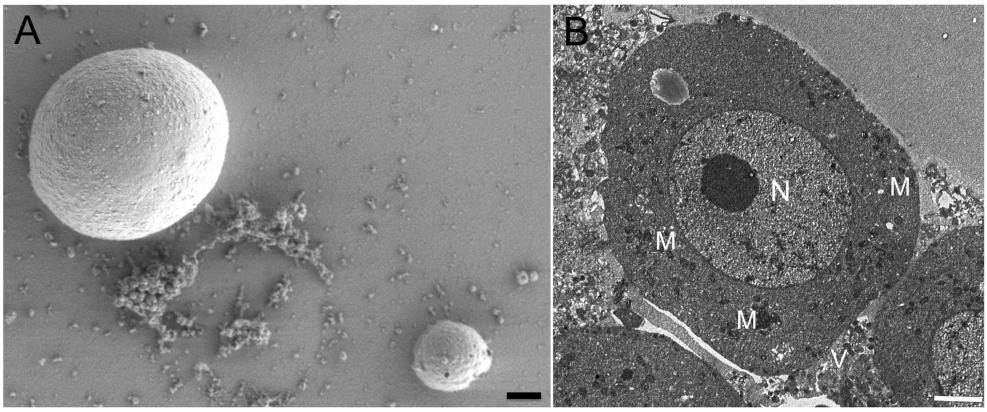

Figure 3.3: Electron microscopy analyses of ovaries. A: scanning electron microscopy; B: transmission electron microscopy. N: nucleus; M: mitochondria; V: vesicles. Scale bars: 2 μm.

3.2.3 Quantification and quality of worm and gonad proteins

The average amount of protein per worm or gonad was determined by BCA and densitometric analysis. The results showed that the amount of total protein in sO is less than 1/10 of that in bO, while the protein amounts of sT and bT were similar (Table 3.2. Values for sT and sO were estimated by silver staining intensities).

Table 3.2: Average protein amount in each individual worm and organ

Sample	Average protein amount (μg)
bM	89.2
sM	85.7
bT	0.3
sT	0.3
bF	33.8
sF	10.1
bO	0.4
sO	0.03

For quality control, 1.5 μg of each worm and gonad protein was analysed by SDS-PAGE and subsequent silver staining (Figure 3.4). All isolated protein samples showed a wide molecular weight distribution, ranging from 10 kDa to nearly 250 kDa. For proteins around 55 kDa, some differences were observed between the bisexual and unisexual gonads.

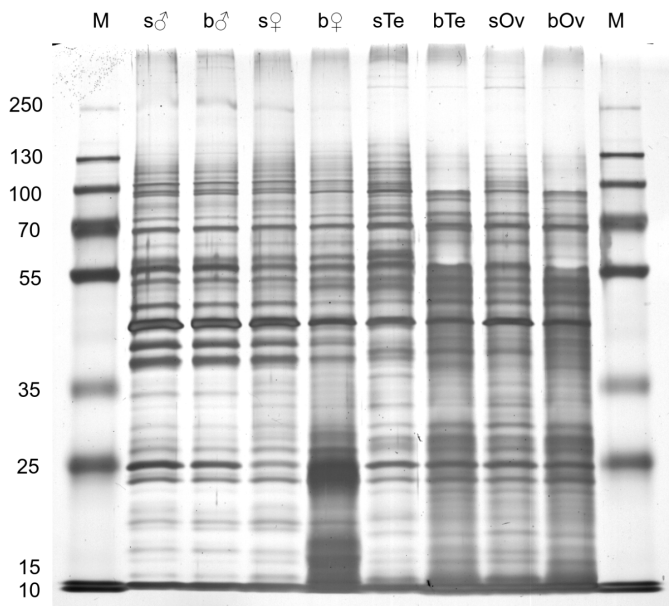

Figure 3.4: Silver-stained proteins extracted from *S. mansoni* adult worms (Mars and Venus symbols) and gonads (testes [Te] and ovaries [Ov]) of unpaired (s) and paired (b) individuals. M: protein-size marker.

3.2.4 Protein expression levels in the gonads

Western blot analysis was performed to investigate the gonad-dependent expression patterns of the following proteins: SPRM1hc, HSP70, Aquaporin and FKBP12 (Figure 3.5). These schistosome proteins had been characterized before by others, and appropriate antibodies were kindly provided by Dr. Patrick Skelly (SPRM1hc, Aquaporin; (Faghiri and Skelly, 2009; Krautz-Peterson et al., 2007)) and Dr. Mo Klinkert (HSP70, FKBP12; (Moser et al., 1990; Rossi et al., 2002)). Tegument protein of adults of both genders were extracted and used for control purpose.

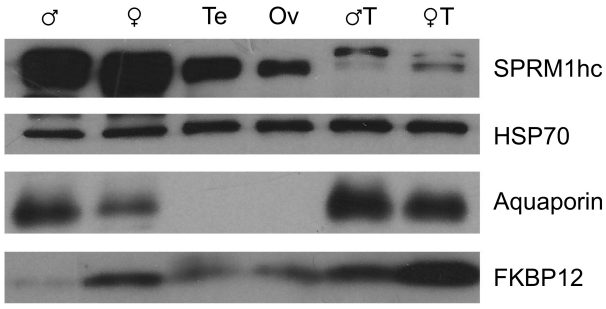

Figure 3.5: Detection of protein expression by Western blot analysis. Mars and Venus symbols indicate the gender of adult worms or the tegument fractions obtained from males or females; T = tegument protein, Te = testes, Ov = ovaries.

The Western blot result showed that SPRM1hc and aquaporin were detected to be expressed in whole worm and the tegument of both genders, which was expected. The former was also detected in both testes and ovaries, while aquaporin not detected in either gonad. HSP70 and FKBP12 were expressed in all samples.

3.2.5 Proteome of ovaries

To get a first insight into the protein composition of ovaries, a first proteome analysis was performed in collaboration with TopLab (Germany). To this end ovaries were isolated from paired females and used for protein extraction. By nano-LC-ESI-MS/MS method a total of 814 proteins were detected, among which 395 proteins have a minimal score of 100. Among those 395 proteins, there were 60 ribosomal proteins, 7 translation initiation factors, 7 heat shock proteins, 5 RNA helicases, and 11 histones (Table 3.3). The complete list of identified proteins can be found in Supplementary files No. 07-1 and 07-2.

Table 3.3: A selection of proteins identified in bO

Smp_	Product
036220, 108390, 162370, 194870	histone
001830, 003410, 004940, 007900	ribosomal protein
000480, 001170, 034190, 039400	eukaryotic translation initiation factor
003970, 030690, 073500, 083410	translation elongation factor
003660, 013790, 133120, 211330	RNA helicase
069130, 072330, 097380, 106930	heat shock protein
002550, 009310, 070200, 079290	RNA binding protein
002880, 038100, 039000	ATP synthase
040680, 200180	dynein light chain
001360	thymidylate kinase
002510	pyruvate dehydrogenase (lipoamide)
003990	triosephosphate isomerase 1a
004780	immunophilin
006550	glutaredoxin
008660	gelsolin
008070	thioredoxin
079230	FKBP12
033710	vasa-like 1
179320	argonaute

212930	cyclin h

3.3 Transcriptome analyses of adult worms and gonads

To get deeper insights into gene transcription within the gonads, RNA-Seq analyses were performed with RNA from testes (T), ovaries (O), as well as whole males (M) and females (F) of mixed-sex infections (b-) and single-sex (s-) infection. At least two biological replicates, and two technical replicates were prepared for analyses. Sequences were mapped to the *S. mansoni* genome (assembly version 5) and reads were counted. The section below describes the RNA-Seq result.

3.3.1 Basic data exploration

RNA-Seq reads and library sizes

The total QC-passed reads ranged from 43 million to 110 million, and the average was 63 million. Among the total reads, 84.5% mapped to the *S. mansoni* genome (see Appendix 7.1 for details). Further analyses concentrated on protein-coding genes with the longest splice variants (10,818 Smp numbers), thus no attention was given to reads from microRNAs, rRNAs as well as the splice variants of protein-coding genes. Depending on the samples, reads originated from those genes consisted of 37-79% of total mapped reads. Figure 3.6 shows the library sizes (total reads for coding genes) of all samples.

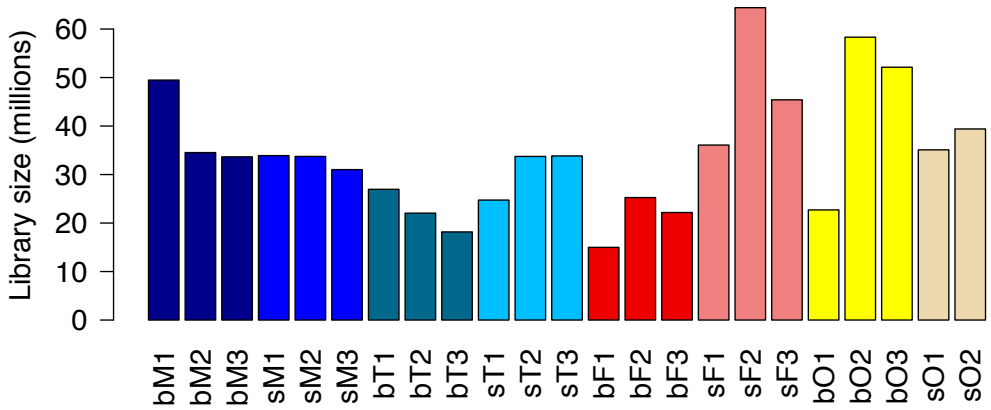

Figure 3.6: Library sizes of all samples. M = male, T = testis, F = female, O = ovary; b: samples from mixed-sex infections (paired), s: samples from single-sex infections (unpaired).

Pearson's correlation between replicates

To investigate the reproducibility among the biological replicates used, Pearson's correlation (showed in r values) was calculated between the replicates (indicated as R1, R2 and R3) of all samples based on their log2-transformed RPKM values, which were calculated using the edgeR package (Robinson et al., 2010). All samples showed good correlations between the replicates ($r > 0.98$; Table 3.4), which proved that the biological samples used were of consistent quality.

Because all replicates showed good correlations, the mean RPKM value of all replicates for each sample was calculated and used for further analysis.

Table 3.4: Pearson's correlations between sample replicates

Samples	R1 - R2	R2 - R3	R1 - R3
bsMales	0.9859	0.9946	0.9841
ssMales	0.9982	0.9950	0.9943
bsTestes	0.9835	0.9838	0.9873
ssTestes	0.9927	0.9845	0.9815
bsFemales	0.9818	0.9951	0.9803
ssFemales	0.9950	0.9927	0.9934
bsOvaries	0.9949	0.9975	0.9963
ssOvaries	0.9911	–	–

RPKM thresholds and number of transcribed genes

To get an overview of RPKM distribution and the effect of RPKM threshold, an examination was done on the number of genes in each group by changing different RPKM thresholds from 0 to 10. The corresponding numbers of transcribed genes can be seen in Table 3.5.

Table 3.5: RPKM threshold and number of transcribed genes

Category/Threshold	0	0.1	0.5	1	2	5	10
Across 8 samples	10,127	10,015	9,673	9,488	9,224	8,724	8,149
bM	9,672	9,507	9,047	8,725	8,280	7,405	6,446
sM	9,681	9,515	9,027	8,708	8,273	7,372	6,359
bT	8,806	8,649	8,314	8,064	7,757	7,254	6,603
sT	9,325	9,039	8,485	8,174	7,838	7,330	6,680
bF	9,275	9,123	8,529	8,103	7,573	6,753	5,855

sF	9,707	9,501	9,053	8,779	8,425	7,603	6,564
bO	8,913	8,419	7,782	7,433	7,016	6,350	5,745
sO	9,376	9,143	8,574	8,195	7,800	7,182	6,533

With a cut-off of RPKM = 2 a total of 1,049-1,897 genes whose RPKM between 0 and 2 were excluded for analysis. The total RPKM values of these genes comprised less than 0.5% of the library sizes (data not shown), which had little effect on further DGE analysis. When the threshold was increased to 5 or 10, the number of genes decreased dramatically.

RPKM distributions

Density plots were generated from the $\log_2$(RPKM+0.001) values as a method to check RPKM distributions. All samples exhibited bimodal distributions, with the first peak representing the percentage of genes without any reads and the second peak showing the highest RPKM density (Figure 3.7).

After removing genes whose RPKM was < 2 in at least one replicate of one sample, 9,224 (out of 10,818) genes were kept for further analysis. The number of transcribed genes detected in each sample, as well as the average RPKM based on all genes were determined and shown in Table 3.6.

Table 3.6: Number of transcripts and average expression

Sample	#genes	Average RPKM
bM	8,280	110.2
sM	8,273	119.9
bT	7,757	89.4
sT	7,838	87.0
bF	7,573	144.9
sF	8,425	120.4
bO	7,016	120.9
sO	7,800	79.8

Interestingly, the numbers of transcribed genes in "single-sex" samples (s, before pairing) were almost all higher than those in "mixed-sex" samples (b, after pairing), especially for females and ovaries, although their average gene expression levels were lower than the paired counterparts.

Furthermore, venn diagrams were created to show the distribution of genes in all worm and gonad samples (Figure 3.8). Although numbers of transcribed genes in

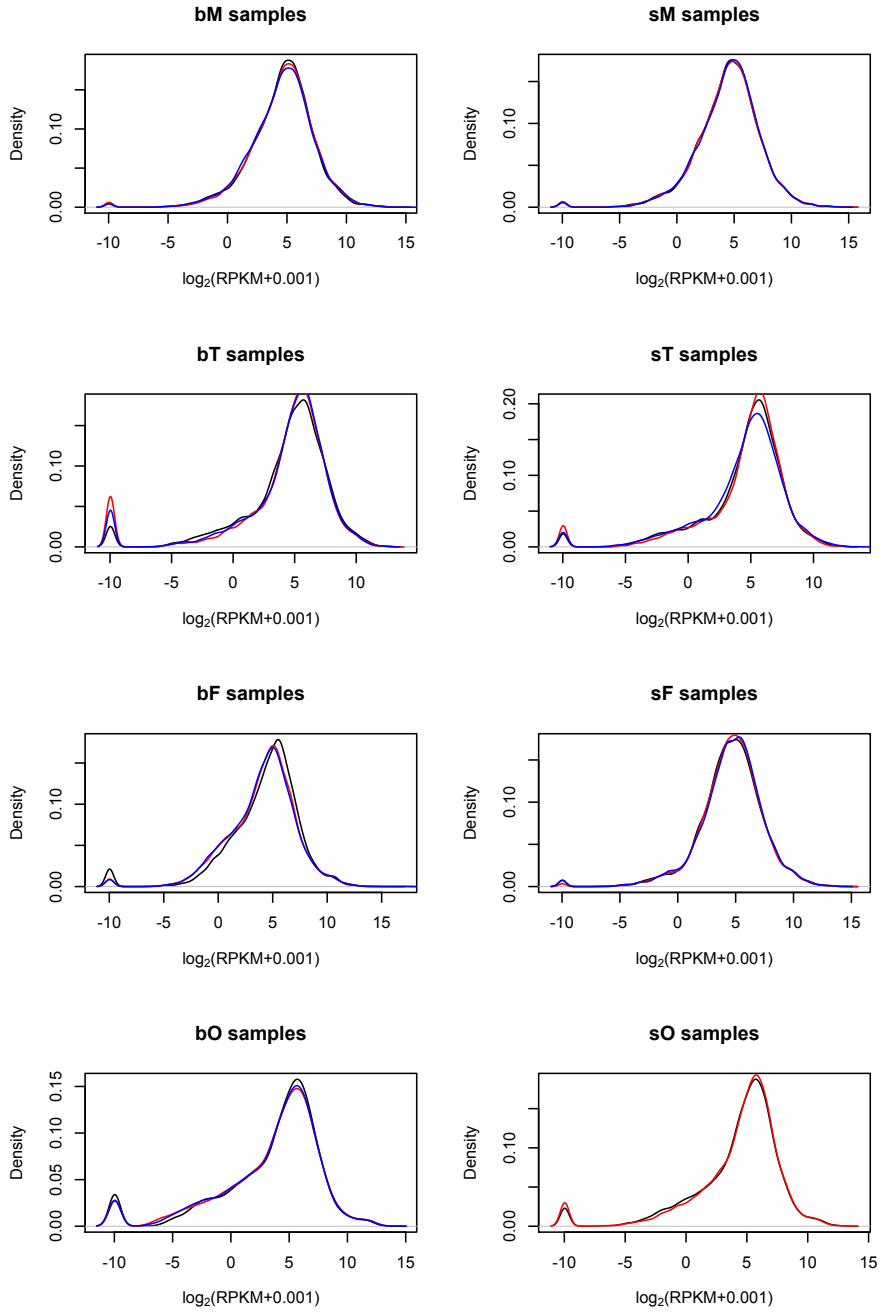

Figure 3.7: RPKM distribution across the samples. Different colors indicate replicates. Black curve: replicate 1; red curve: replicate 2; blue curve: replicate 3. All samples showed bimodal distributions. The first peaks indicate the percentage of genes without any reads (RPKM = 0), and the second peaks show the highest RPKM densities.

one or more samples were calculated, the information should be combined with the following DGE analysis to reduce the RPKM threshold bias.

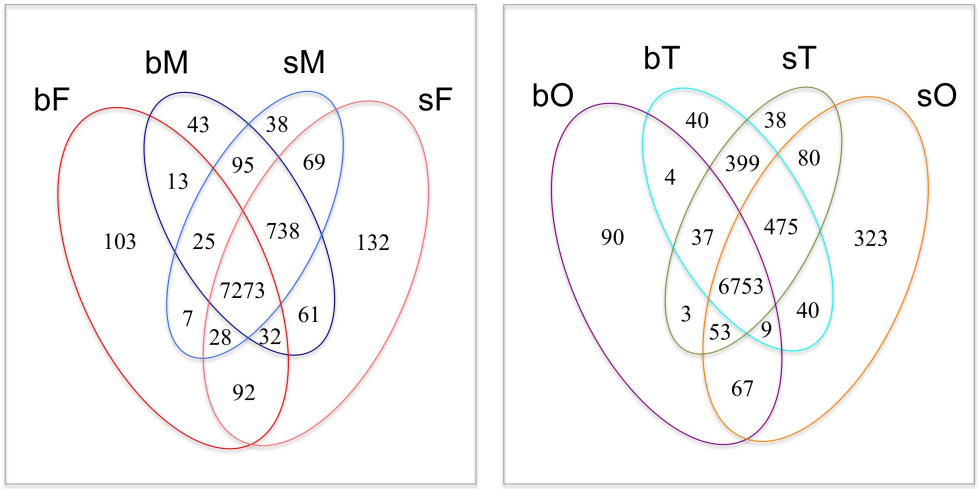

Figure 3.8: Venn diagram of transcribed genes in worm and gonad samples. Note that although they showed sample specificity, the numbers might not represent real information because of the RPKM threshold bias.

Hierarchical clustering of top 100 highly expressed genes

According to their average RPKMs in all 23 samples, the top 100 highly expressed genes were selected to make a hierarchical clustering (Figure 3.9). Among the genes investigated, *p14* (Smp_131110) was calculated to be expressed at the highest level (average RPKM = 17,275.6). This is in perfect agreement with further, independent studies showing that this egg-shell precursor protein gene is one of the most abundantly expressed genes in schistosomes (Chen et al., 1992; DeWalick et al., 2011).

Several ubiquitously and abundantly expressed genes were also listed, including *GAPDH* (Smp_056970), heat shock protein 70 gene *HSP70* (Smp_106930) and *α-tubulin* (Smp_090120). Besides these, there were transcripts coding for ribosomal proteins. Different patterns can be seen from the clusters obtained. For instance, in testes (bT and sT) highest transcript amounts were found for genes such as *histone H3* (Smp_082240), *α-tubulin* (Smp_090120) and *histone H1* (Smp_003770). Highly transcribed in bO were mainly genes coding for ribosomal protein genes and translation elongation factors.

Interestingly, some genes were also clustered into a bM/sM/sF group. Details about genes in this cluster will be discussed later. The complete list of these top 100 genes is given in the Supplementary file No. 08.

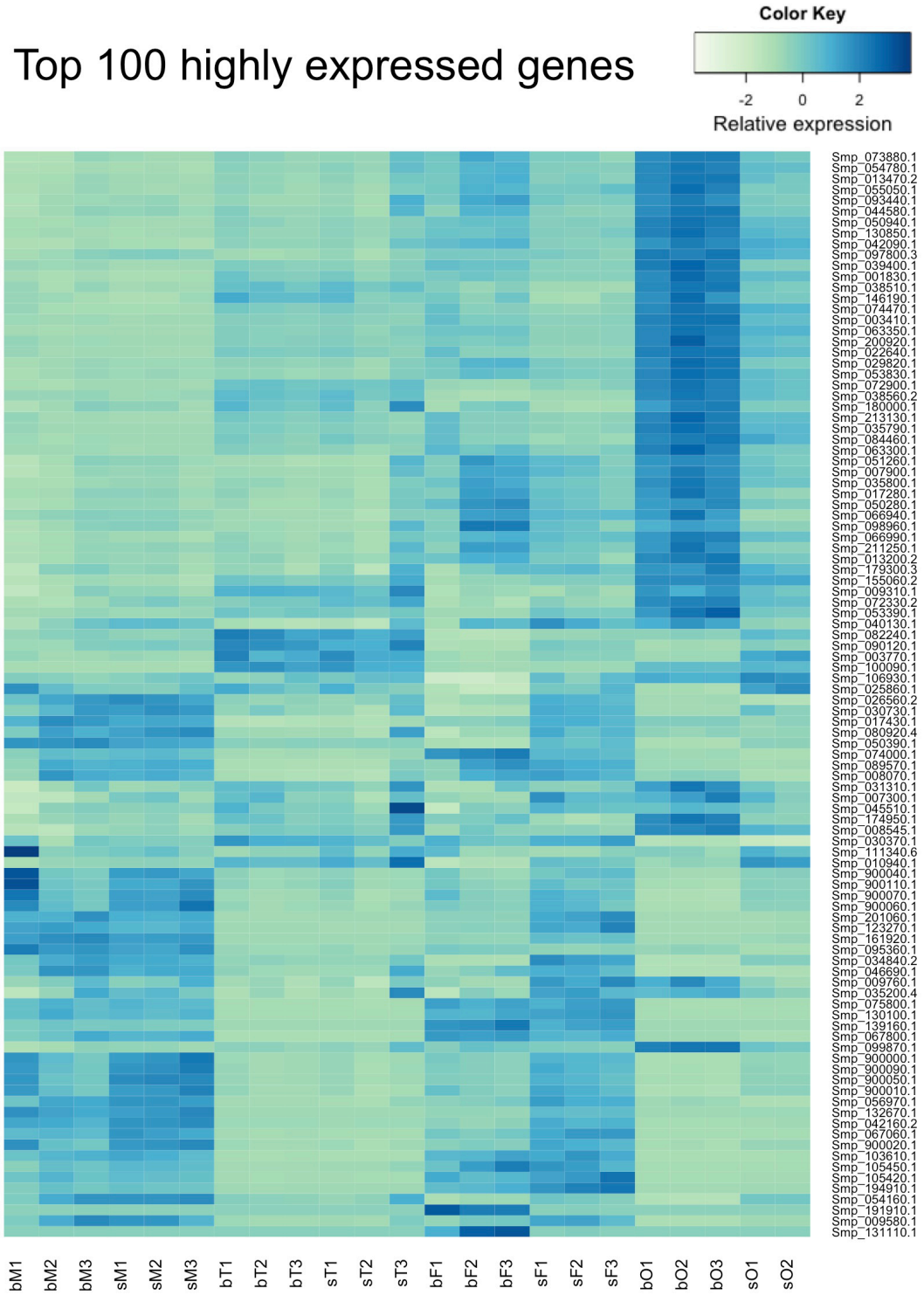

Figure 3.9: Hierarchical clustering of top 100 highly expressed genes in all samples. White color indicates lowest expression level among 23 samples and dark-blue color indicates highest expression level.

3.3.2 Differential gene expression at the transcript level: affecting factors

Among all 8 whole worm and gonad samples, the following three factors influencing gene expression at the transcript level were investigated:

1). Pairing effect: i.e. comparisons between paired ("b" samples) and unpaired ("s" samples);

2). Gender effect: comparison between male samples (M) and female samples (F);

3). Tissue effect: i.e. whole worms versus gonad samples (T; O).

Given the fact that pairing plays a critical role in the development of reproductive organs especially for ovaries and vitellaria, pairing-induced differential gene expression was the main focus of this study. In addition, the effects of gender and tissue on gene expression were also be covered in my analysis and appropriate results will be shown.

Multidimensional scaling

To get an overview about the effect of these three factors on gene expression, the multidimensional scaling was calculated to estimate the distances between samples. This was achieved by either using "leading Log2 Fold Change (lLFC)" or by calculating "Biological Coefficient of Variation (BCV)". Both calculations were based on values from top 500 genes (Figure 3.10).

From the multidimensional scaling calculations of both methods, sO and bO samples well separated into two separate clusters. The same was found for the sF/bF samples, indicating that the transcript profiles of genes in ovaries and female worms were largely affected by pairing. In contrast, sT and bT samples occurred in one cluster, and the same applied for the sM/bM samples, indicating that pairing had only little effects on gene expression in this gender. This tendency was also observed in the hierarchical clustering of all genes (Appendix 7.2).

All gonad samples were found to cluster distantly from their worm counterparts. This was expected with regard to tissue-specific gene expression, which should remarkably differ from that of whole worms.

Coinciding with the former findings, all testis samples clustered separately from the ovary samples. It is noteworthy, however, that the distances between sF and males were shorter than that between bF and males. This phenomenon is discussed later.

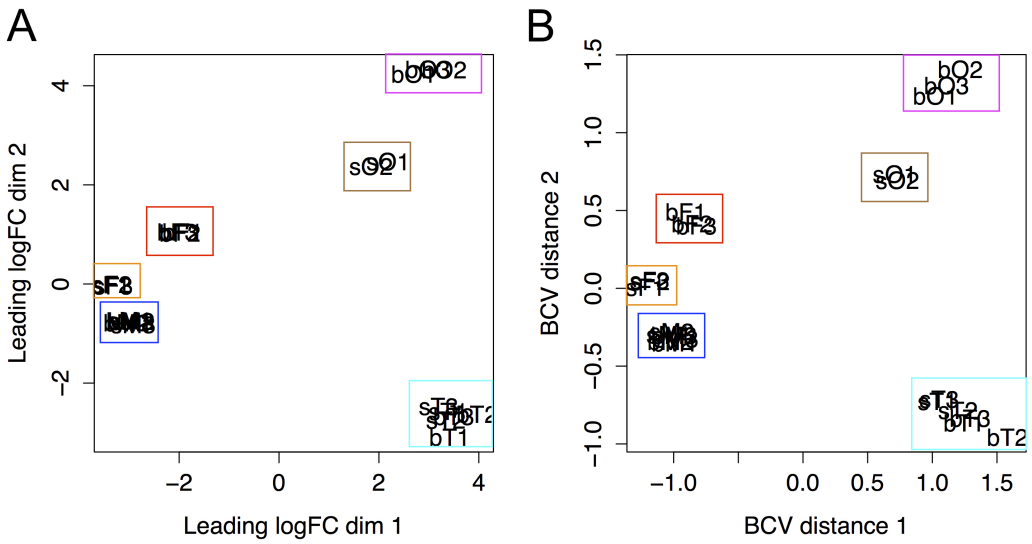

Figure 3.10: Multidimensional scaling (MDS) of all samples including the biological replicates (bM 1-3 [blue], sM 1-3 [blue], bT 1-3 [cyan], sT 1-3 [cyan], bF 1-3 [red], sF 1-3 [orange], bO 1-3 [magenta], sO 1-2 [brown]). A, MDS calculated by leading logFC (lFC); B, MDS calculated by Biological Coefficient of Variation (BCV). Both methods correspondingly revealed that bF and sF form separate clusters as well as bO and sO. In contrast, bM and sM cluster very closely, as well as bT and sT. It is noteworthy that the sF cluster located closer to the bM/sM cluster than to the bF cluster.

Numbers of differentially expressed genes

Effect of pairing-status To evaluate the effect of pairing, gender or tissue on gene expression in these samples, the numbers of differentially expressed genes (DEGs) were calculated based on the discussed factors. Fold difference cut-off was set at 1.5 (or 2.0). Cut-off for the false discovery rates (FDR, = adjusted p) were set at < 0.005 for most comparisons, and at < 0.05 for the comparisons between bM versus sM, as well as bT versus sT.

With respect to the pairing effect, transcripts detected in bM were compared to those from sM, bF compared to sF, bT to sT, and bO to sO. Table 3.7 shows the corresponding number of DEGs originated from each comparison, of which the fold change cut-off was set to 1.5 (2.0).

For genes transcribed in males and testes, only 3-5% were found to be significantly regulated by pairing with > 1.5-fold difference (FDR < 0.05), and less than 2% of them had a > 2-fold difference in transcript amounts. In contrast, pairing-affected transcripts occurred more frequently in females and ovaries, > 43% of the genes exhibited at least a 1.5-fold difference in the transcript levels, and about 30% have a > 2-fold change

in transcript amounts (FDR < 0.005). Furthermore, the comparisons between paired and unpaired worms and their reproductive organs showed that the number of DEGs between males and between testes were lower than the appropriate numbers of DEGs in females and ovaries. This confirmed the estimation of multidimensional scaling which showed nearly one cluster for males and one for testes, but two distinct separate clusters for bF and sF, as well as for bO and sO. In all comparisons at least 1/3 of the pairing-affected DEGs revealed fold-difference between 1.5 and 2.0. (Supplementary files No. 09-12). Detailed analyses will be shown in sections 3.3.6 and 3.3.7.

Table 3.7: Effect of pairing on the number of differentially expressed genes

Comparison	bM/sM	bF/sF	bT/sT	bO/sO
# up in paired	313 (118)	1,591 (737)	96 (48)	1,752 (950)
# up in unpaired	113 (23)	2,157 (1,752)	147 (65)	1,848 (1,461)
# total DEGs	426 (141)	3,748 (2,489)	243 (113)	3,600 (2,411)
# total genes	8,422	8,573	7,931	7,934
% DEGs	5.1 (1.7)	43.7 (29.0)	3.1 (1.4)	45.4 (30.4)

FDR < 0.05 (bM/sM and bT/sT) or 0.005 (bF/sF and bO/sO); fold-change cut-off: 1.5 (2.0)

Effect of gender To investigate the gender effect, transcripts of male worms and testes were compared to their female counterpart (bM-bF, bT-bO, sM-sF and sT-sO). Table 3.8 shows the corresponding number of DEGs based on each comparison, and the fold change cut-offs were set to 1.5 (2.0).

Table 3.8: Effect of gender on the number of differentially expressed genes

Comparison	bM/bF	bT/bO	sM/sF	sT/sO
# up in male	2,444 (1,920)	2,458 (1,991)	680 (268)	1,800 (1,333)
# up in female	1,939 (1,002)	2,171 (1,301)	765 (400)	1,037 (497)
# total DEGs	4,383 (2,922)	4,629 (3,292)	1,445 (668)	2,837 (1,830)
# total genes	8,510	7,970	8,590	8,277
% DEGs	51.5 (34.3)	58.1 (41.3)	16.8 (7.8)	34.3 (22.1)

FDR < 0.005; fold-change cut-off: 1.5 (2.0)

The comparison of transcripts in samples of male origin with those of female origin showed that 51-58% of the transcripts in samples from mixed-sex infections had

at least a 1.5-fold difference, and 34-41% the transcripts differed > 2-fold difference (FDR<0.005). The gender effect of samples from single-sex infection was smaller, especially comparing sM and sF. Here only 16.8% of the transcribed genes exhibited a > 1.5-fold change and 7.8% a > 2-fold change (Supplementary files No. 13-16).

Effect of tissue-origin To investigate the tissue effect, comparisons were made between bT and bM, sT and sM, bO and bF, as well as sO and sF. Table 3.9 includes the corresponding number of DEGs from each comparison. The cut-off of fold change for each comparison was set to 1.5 (2.0).

Table 3.9: Effect of tissue on the number of differentially expressed genes

Comparison	bT/bM	bO/bF	sT/sM	sO/sF
# up in gonad	2,741 (2,008)	2,209 (1,309)	2,792 (2,098)	2,134 (1,451)
# up in worm	2,737 (2,248)	2,325 (1,852)	2,617 (1,976)	2,946 (2,427)
# total DEGs	5,478 (4,256)	4,534 (3,161)	5,409 (4,074)	5,080 (3,878)
# total genes	8,783	8,810	7,931	8,840
% DEGs	62.4 (48.5)	51.5 (35.9)	68.2 (51.4)	57.5 (43.9)

FDR < 0.005; fold-change cut-off: 1.5 (2.0)

The effect of tissue seemed to be similar among the comparisons. In all situations, more than 50% of the detected genes were significantly differentially transcribed between the whole worm and the gonad (FDR < 0.005, fold-difference > 1.5) (see Supplementary files No. 17-20). Detailed analysis will be provided in sections 3.3.9, 3.3.10 and 3.3.11.

3.3.3 Transcriptomes of testes and ovaries

Genes with conserved domains

The Conserved Domain Database (CDD) includes NCBI-curated domains, as well as domain models imported from a number of external source databases (Pfam, SMART, COG, PRK, TIGRFAM). By applying a NCBI Batch CD-search, 6,200 genes (79.9% of the genes detected) in bT were found to contain putative conserved domains in the CDD database (E-value < 0.01). Pfam entries were found for 5,828 (75.1%) of these genes. For bO genes, 5,687 genes (81.1%) showed conserved domains (E-value < 0.01), and 5,353 had pfam hits. The SMART resource focuses on modular

signaling domain, which can provide information on a protein's cellular role, binding partners and subcellular localization. The top 50 pfam / SMART entries were listed as follows (Table 3.10):

Table 3.10: Top 50 pfam/SMART entries of bT and bO genes

Pfam ID	Annotation	#bT	#bO	SMART ID	Annotation	#bT	#bO
pfam00069	Pkinase	183	155	smart00220	S_TKc	180	152
pfam12796	Ank_2	141	121	smart00360	RRM	143	141
pfam00400	WD40	138	127	smart00320	WD40	136	125
pfam00076	RRM_1	135	130	smart00060	FN3	95	48
pfam14259	RRM_6	124	124	smart00487	DEXDc	86	86
pfam07679	I-set	120	75	smart00490	HELICc	80	79
pfam00023	Ank	108	92	smart00382	AAA	74	77
pfam00041	fn3	92	45	smart00410	IG_like	73	45
pfam13414	TPR_11	81	74	smart00248	ANK	72	60
pfam00271	Helicase_C	80	79	smart00228	PDZ	70	62
pfam13855	LRR_8	70	56	smart00326	SH3	52	51
pfam00153	Mito_carr	68	68	smart00249	PHD	50	49
pfam12799	LRR_4	66	49	smart00239	C2	45	39
pfam00270	DEAD	65	65	smart00612	Kelch	43	35
pfam13499	EF-hand_7	63	57	smart00150	SPEC	43	42
pfam00595	PDZ	61	54	smart00233	PH	42	39
pfam13465	zf-H2C2_2	59	44	smart00322	KH	40	36
pfam00071	Ras	55	51	smart00184	RING	38	34
pfam13637	Ank_4	51	43	smart00132	LIM	38	26
pfam08477	Miro	45	41	smart00176	RAN	37	34
pfam00628	PHD	45	44	smart00028	TPR	35	33
pfam00435	Spectrin	43	43	smart00252	SH2	33	26
pfam00168	C2	41	35	smart00180	EGF_Lam	33	28
pfam13895	Ig_2	39	31	smart00112	CA	33	26
pfam01344	Kelch_1	37	29	smart00408	IGc2	31	21
pfam00412	LIM	37	24	smart00335	ANX	30	15
pfam00053	Laminin_EGF	37	30	smart00271	DnaJ	30	29
pfam00013	KH_1	37	33	smart00054	EFh	30	27
pfam01391	Collagen	35	32	smart00175	RAB	29	27
pfam00169	PH	34	33	smart00033	CH	29	29

pfam00004	AAA	34	33	smart00456	WW	27	25
pfam07690	MFS_1	32	31	smart00212	UBCc	26	26
pfam00307	CH	32	31	smart00194	PTPc	26	22
pfam00018	SH3_1	32	31	smart00750	KIND	25	21
pfam00017	SH2	32	26	smart00409	IG	25	18
pfam13893	RRM_5	31	31	smart00295	B41	25	20
pfam00520	Ion_trans	31	20	smart00787	Spc7	24	22
pfam00226	DnaJ	31	30	smart00100	cNMP	24	19
pfam00191	Annexin	31	15	smart00404	PTPc_motif	23	20
pfam00005	ABC_tran	31	30	smart00389	HOX	22	11
pfam13833	EF-hand_8	30	26	smart00324	RhoGAP	22	21
pfam00028	Cadherin	30	24	smart00297	BROMO	22	22
pfam00335	Tetraspannin	29	21	smart00213	UBQ	22	22
pfam00102	Y_phosphatase	29	25	smart00109	C1	22	17
pfam07714	Pkinase_Tyr	28	24	smart00221	STYKc	21	19
pfam13424	TPR_12	27	22	smart00179	EGF_CA	21	15
pfam00397	WW	27	25	smart00164	TBC	21	19
pfam00515	TPR_1	26	25	smart00454	SAM	20	20
pfam00179	UQ_con	26	26	smart00209	TSP1	19	15
pfam05483	SCP-1	25	16	smart00177	ARF	19	18

3.3.4 Gene Ontology (GO) enrichment analysis

GO enrichment analyses were performed for bT and bO genes according to the Biological Processes assignments (Ashburner et al., 2000). Significantly enriched categories were selected ($p < 0.01$). Numbers of genes involved in different biological processes were shown below for bT (Figure 3.11) and bO (Figure 3.12).

The enrichment for genes in testes and ovaries did not reveal much difference concerning the biological processes. General cellular process such as translation, cell cycle, ribosome biogenesis and transport were significantly enriched. In the enrichment for bT genes one category named "striated muscle contraction" was not easy to interpret. It turned out that the genes associated with this category encode proteins that have motor functions, such as dynein and myosin, or have ciliary structures, such as rootletin and coiled coil domain-containing proteins. These genes are probably involved in sperm motility (Inaba, 2003; Nagy et al., 2008; Werner and Simmons, 2008; Grigoryan and Keating, 2008).

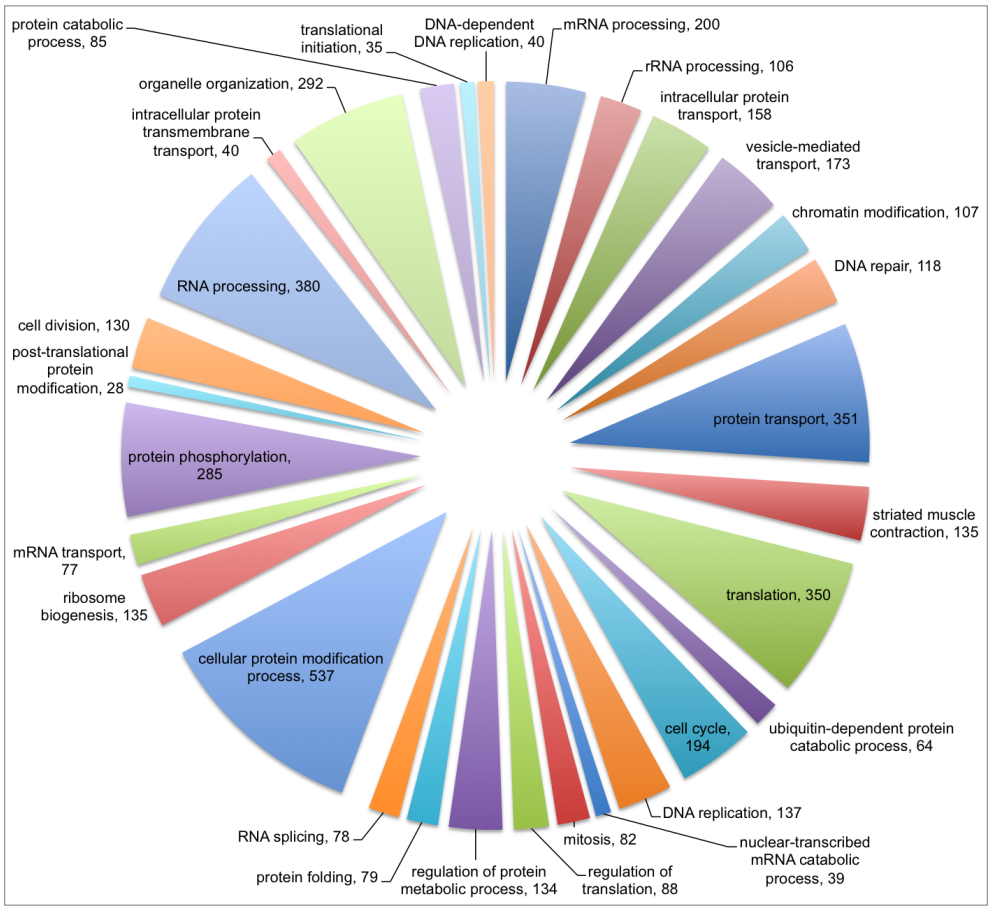

Figure 3.11: GO enrichment of bT genes by biological process. The numbers of genes involved in each process were included. Top significantly enriched processes include cellular protein modification process, RNA processing, translation, protein transport, organelle organization, protein phosphorylation, etc.

3.3.5 Marker genes

Because marker genes are important tools for different kinds of molecular analyses, an effort was undertaken to search such genes was done in the given data sets. To this end, border limits were defined to avoid the arbitrary cut-off of RPKM = 2, especially for unexpressed genes. We defined RPKM > 2 in one sample as transcribed and RPKM < 0.1 in the other as almost non-transcribed.

For testes 182 genes were found to be transcribed in bT but not in Ov. Genes whose annotations contain "[K] " at the beginning indicated that they have orthologs in the KEGG database. Table 3.11 shows a selection of non-hypothetical genes whose RPKM was > 10 in most cases. These genes include several transcription factors, tektin,

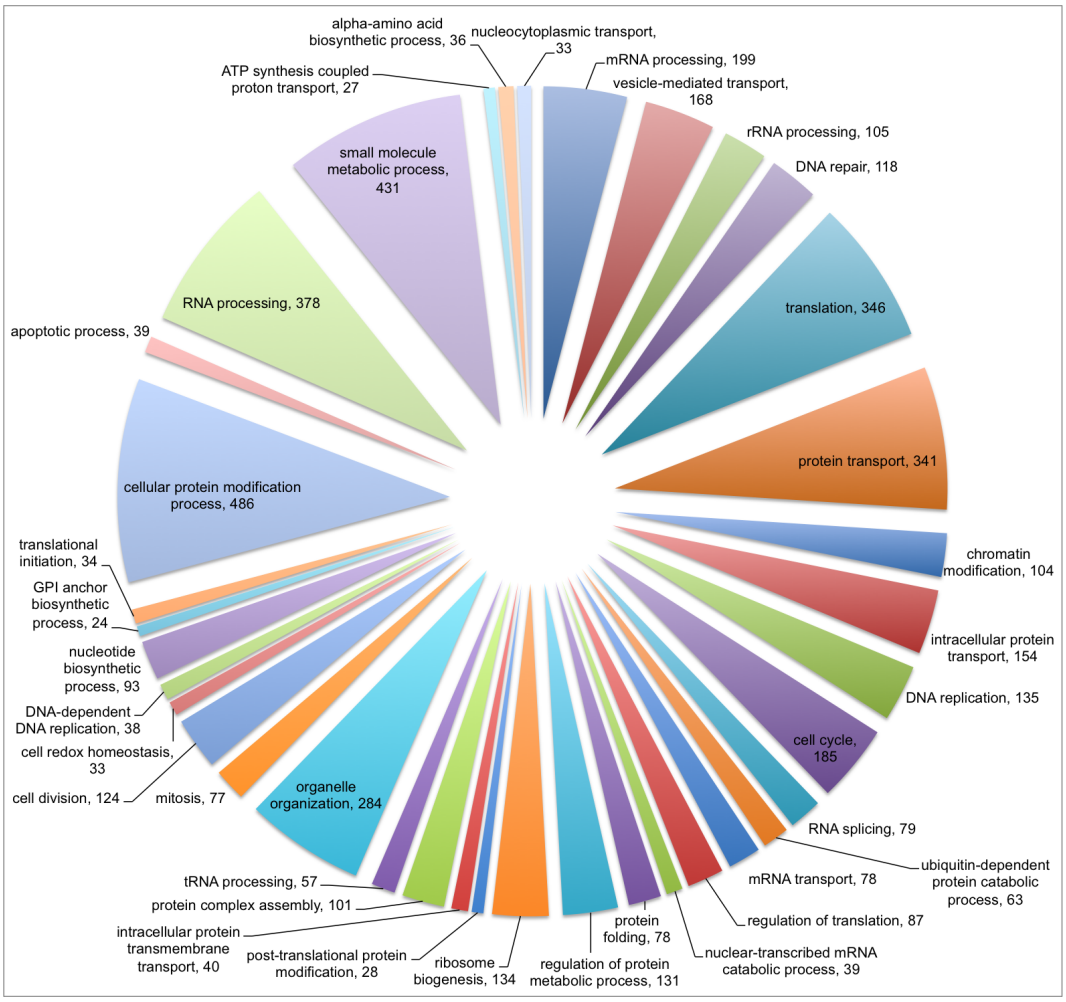

Figure 3.12: GO Enrichment of bO genes by biological process. The numbers of genes involved in each process were included. Top significantly enriched processes include cellular protein modification process, small molecule metabolic process, RNA processing, translation, protein transport, etc.

kelch protein genes, dynein genes, and others. The complete list can be found in the Appendix 7.3.

Table 3.11: Genes expressed in bT but not in bO

GeneID	RPKM_bT	Product
Smp_009630.1	20.67	homeobox protein SIX6
Smp_018120.1	14.23	[K] kinesin protein KIF9
Smp_028130.1	67.38	protein FAM78B
Smp_059600.1	9.89	[K] tektin 3
Smp_062490.1	56.55	[K] heart and neural crest derivatives expressed
Smp_079600.1	67.04	two pore calcium channel protein 1
Smp_080650.1	224.50	cAMP-dependent protein kinase regulatory chain CAP-ED
Smp_080820.1	69.08	G-protein coupled receptor fragment
Smp_085690.1	33.66	cAMP-dependent protein kinase catalytic subunit PKA/STK
Smp_094930.1	41.50	early growth response protein 1 (EGR)
Smp_104210.1	51.41	[K] opsin receptor
Smp_114970.1	51.58	WD repeat-containing protein 52
Smp_122170.1	155.27	phd finger protein 10
Smp_126250.1	48.08	tetratricopeptide repeat protein 21b
Smp_131240.1	61.75	transcription factor
Smp_136100.1	163.87	kelch protein 10
Smp_141230.1	183.38	[K] dual specificity tyrosine (Y) phosphorylation DYRK
Smp_142220.1	123.22	apobec1 complementation factor
Smp_143970.1	110.32	kelch protein 10
Smp_144540.1	109.22	zinc finger and putative transcriptional repressor
Smp_146420.1	20.24	spindle assembly checkpoint component MAD1
Smp_148040.1	53.14	DC STAMP domain-containing protein 1
Smp_148160.1	62.55	spermatogenesis-associated protein 6
Smp_150920.1	28.20	[K] synaptotagmin
Smp_151740.1	21.15	run and tbc1 domain-containing protein
Smp_152200.1	129.97	M-phase inducer phosphatase 3 cdc25
Smp_154790.1	34.78	DC STAMP domain-containing protein 2
Smp_158370.1	22.73	[K] tubulin monoglycylase TTLL3

Smp_159520.1	26.19	acidic fibroblast growth factor intracellular
Smp_160310.1	41.31	lysosomal alpha mannosidase
Smp_164150.1	46.85	tau tubulin kinase 1 STK-CK1
Smp_171010.1	147.42	EF hand domain (C terminal)-containing 2
Smp_176170.1	14.78	venom allergen (val) protein
Smp_179050.1	41.02	[K] homomeric kinesin Kif17
Smp_198810.1	19.37	mitogen activated protein kinase 15
Smp_212280.1	99.07	dynein heavy chain

A number of 33 genes were abundantly transcribed in bO but not in bT. Table 3.12 shows the non-hypothetical ones. This list includes two cytoplasmic polyadenylation element binding (CPEB) protein genes, two thyroid hormone receptor genes, the calmodulin, the ephrin receptor and others. The complete list can be found in the Appendix 7.4.

Table 3.12: Genes expressed in bO but not in bT

GeneID	RPKM_bO	Product
Smp_032970.1	6.78	calmodulin protein
Smp_070360.1	223.60	[K] cytoplasmic polyadenylation element binding (CPEB)
Smp_077850.1	2.02	actin
Smp_081620.1	4.73	[K] SmHox4
Smp_087320.1	227.30	TPA-induced protein 11B mouse
Smp_093790.1	2.50	prokaryotic membrane lipoprotein lipid
Smp_098340.1	8.27	[K] gamma glutamylcyclotransferase
Smp_118960.1	17.42	jun protein
Smp_134490.1	8.27	thyroid hormone receptor alpha
Smp_137460.1	119.35	cytoplasmic polyadenylation element binding (CPEB)
Smp_139480.1	2.21	[K] ephrin receptor
Smp_142700.1	8.43	neuronal acetylcholine receptor subunit alpha 4
Smp_145020.1	4.92	[K] glutamate semialdehyde dehydrogenase
Smp_146940.1	3.10	innexin
Smp_156140.1	6.63	tripartite motif protein trim9
Smp_163750.1	4.07	otoferlin
Smp_164140.1	131.53	opsin receptor

Smp_168410.1	4.52	tripartite motif protein trim9
Smp_169160.1	3.19	ATP-dependent DNA ligase, IPR000859
Smp_174260.1	26.24	thyroid hormone receptor alpha
Smp_176510.1	5.33	RIMS-binding protein 2
Smp_191690.1	14.32	tumor susceptibility gene 101 protein

3.3.6 Pairing effect 1: differential gene expression in testes and ovaries

DEG analysis was done with the GLM approach and by defining the contrast (bT-sT or bO-sO). Fold change values (log_2FC) and FDR (false discovery rate) values were calculated for each gene and the cut-off was defined as: fold change > 1.5 for both comparisons; FDR < 0.005 for ovaries and < 0.05 for testes.

Against the background of a pairing-influence, transcripts of 243 genes were significantly differentially expressed between bT and sT indicating that their transcription occurred pairing-dependently. Among those, 96 were up-regulated in bT and 147 were up-regulated in sT (Figure 3.13 A; Supplementary file No. 09).

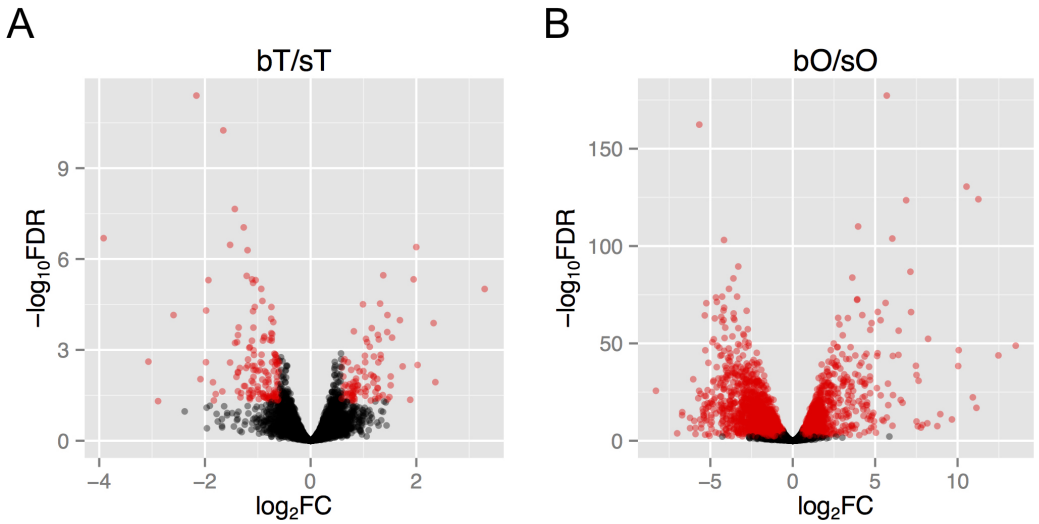

Figure 3.13: Differentially expressed genes in testes (A, bT/sT) and ovaries (B, bO/sO) revealed by Volcano plots. Red points indicate differentially expressed genes (>1.5-fold difference; FDR < 0.05 (testes) or 0.005 (ovaries)).

In contrast to the testes a remarkable high number of genes in the ovary was affected by pairing. Transcripts of 3,600 genes were significantly differentially expressed between bO and sO, of which 1,752 were up-regulated in bO and 1,848 up-regulated in sO (Figure 3.13: B; Supplementary file No. 10).

These results confirm a previous hypothesis from our working group that was based on a first qPCR analysis of a small number of selected genes whose transcript profiles were comparatively analysed in testes and ovaries from paired and unpaired male and female *S. mansoni*. From the obtained data it was concluded that a set of genes in the gonads is under the direct control of pairing (Hahnel et al., 2014).

By combining the DGE analysis for testes and ovaries, all genes transcribed in either gonad (in total 7,970) were divided into the following 8 categories (1.1 - 3.4; Figure 3.14). Genes that have orthologs in the KEGG database are indicated with '[K] ' at the beginning of their annotations. Genes with IDs in bold will be selected for discussion later. The selection was based on their transcript abundance, transcription patterns and potential functions for gonad development. In most cases, hypothetical genes (1,873 in total) were not listed in this selection. Genes showing significant similarities (FDR < 0.01) to those in other organisms will be partially discussed. The complete gene list and expression profiles can be found in the Supplementary files No. 21-28.

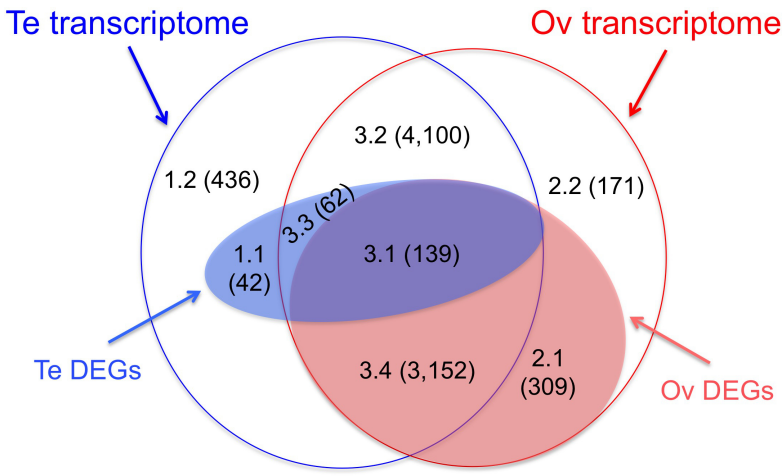

Figure 3.14: Venn diagram of transcribed genes in testes and ovaries. According to their transcription profiles, genes transcribed in the gonads were divided into eight categories: 1.1 (testes-specific and pairing-affected genes), 1.2 (testes-specific and pairing-unaffected genes), 2.1 (ovaries-specific and pairing-affected genes), 2.2 (ovaries-specific and pairing-unaffected genes), 3.1 (pairing-affected genes in both gonads), 3.2 (pairing-unaffected genes in both gonads), 3.3 (transcription of genes affected by pairing in testes but not in ovaries), and 3.4 (transcription of genes affected by pairing in ovaries but not in testes).

1.1 Testes-specific and pairing-affected genes A total of 42 genes were found to be transcribed specifically in testes and to be affected by paring. Among these, 39 genes were up-regulated after pairing. Table 3.13 shows a representative selection; genes without functional annotations were left out. This category includes a synaptotagmin gene (Smp_150920) whose transcription was increased by about 2-fold after pairing. Another gene encodes the M-phase inducer phosphatase 3 (Cdc25) and its transcription was elevated by 1.75-fold (Figure 3.15). The putative cell cycle-associated gene SmCdc25 exhibited similarities (blastp, E-values $< 10^{-5}$) to orthologs from *C. elegans* (Cdc25.1-Cdc25.4; (Ashcroft et al., 1998)) and one of the two Cdc25s (String and Twine; (Courtot et al., 1992)) from *Drosophila* (Twine, data not shown). To get information on products and expression patterns of all the genes in this category, see Supplementary file No. 21.

Table 3.13: A selection of genes whose transcription occurred testes-specifically and affected by pairing

GeneID	RPKM_bT	$\log_2$(bT/sT)	Product
Smp_080820.1	69.08	0.83	G protein-coupled receptor fragment
Smp_130250.1	82.39	0.99	dual specificity Serine/Threonine kinase
Smp_135480.1	80.79	0.62	intraflagellar transport protein 88
Smp_140170.1	13.68	1.37	irregular chiasm C roughest protein
Smp_150920.1	28.20	1.06	synaptotagmin
Smp_152200.1	129.9	0.81	M-phase inducer phosphatase 3
Smp_167100.1	15.48	1.30	peptidase M8 domain-containing protein
Smp_198240.1	11.09	1.28	anosmin 1

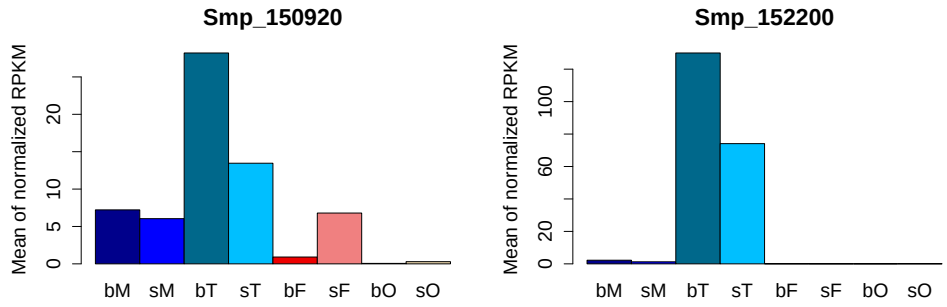

Figure 3.15: Expression profiles of selected genes from Category 1.1. Smp_150920 is a putative synaptotagmin gene and Smp_152200 is a gene putatively coding for an M-phase inducer phosphatase Cdc25 ortholog.

1.2 Testes-specific and pairing-unaffected genes A total of 436 genes showed no significance in their transcript fold changes (FDR > 0.05) after pairing. This category includes genes encoding transcription factors, protein kinases, dynein proteins, tektin proteins, as well as one *SPATIAL* (Stromal Protein Associated With Thymii And Lymph Node Homolog) and one *elav* (Emryonic Lethal, Abnormal Vision) gene (Table 3.14; Figure 3.16). By a multiple-blast approach, the ELAV protein of *S. mansoni* showed high similaritiy to ELAVs from close relatives such as the flatworm *Macrostomum lignano* and the planarian *Schmidtea mediterranea* (Figure 3.17). The complete list of genes of this category and their expression profiles are available in Supplementary file No. 22.

Table 3.14: A selection of genes whose transcription occurred testes-specifically and unaffected by pairing

GeneID	RPKM_bT	Product
Smp_009630.1	20.67	homeobox protein SIX6
Smp_009800.1	19.75	serine:threonine protein kinase Nek10
Smp_018940.1	117.95	calmodulin
Smp_082830.1	34.74	[K] Dynein intermediate chain
Smp_094930.1	41.50	early growth response protein (egr)
Smp_099770.1	18.21	tetraspanin
Smp_104210.1	51.41	opsin receptor
Smp_128330.1	63.55	ets-related
Smp_136100.1	163.87	kelch protein 10
Smp_141230.1	183.3	[K] dual specificity tyrosine (Y) phosphorylation DYRK
Smp_144540.1	109.22	zinc finger and putative transcriptional repressor
Smp_151040.1	155.97	cyclin-dependent kinase 5 activator 1
Smp_170210.1	61.51	[K] tektin 2 (testicular)
Smp_194750.1	54.03	protein SPATIAL
Smp_194950.1	146.80	[K] ELAV protein 2

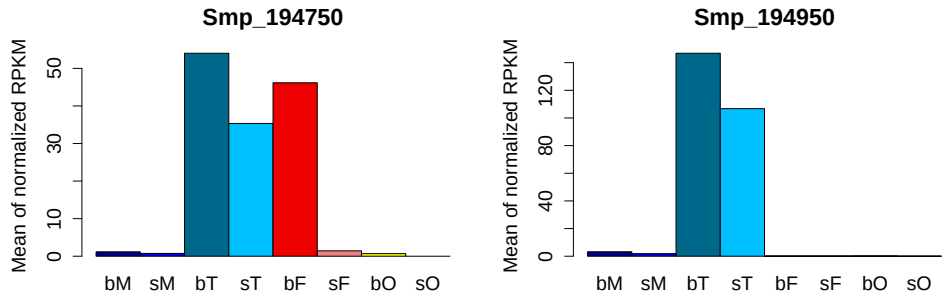

Figure 3.16: Expression profiles of selected genes from Category 1.2. Smp_194750 encodes the SPATIAL protein and Smp_194950 is a ELAV potein gene.

2.1 Ovary-specific and pairing-affected genes A total of 309 genes were found to be ovary-specifically transcribed and affected by pairing, including genes encoding a tyrosinase, two CPEB proteins, transcription factors, transporters, and others. A selection of genes with high amounts of transcripts (RPKM > 10) is shown in Table 3.15. Among other genes, the *tyrosinase* has little transcript amounts in sO but its transcript number increased dramatically after pairing (198-fold). Similar transcript patterns were found for the *cpeb* gene (Smp_070360) and *synaptotagmin* gene (Smp_150350) (Figure 3.18). The complete list with expression profiles can be found in Supplementary file No. 23.

Table 3.15: A selection of genes whose transcription occurred ovary-specifically and affected by pairing

GeneID	RPKM_bO	$\log_2$(bO/sO)	Product
Smp_013540.1	53.48	7.63	[K] tyrosinase
Smp_056700.1	185.32	3.91	membrane-associated RING finger protein
Smp_070360.1	223.60	10.5	[K] cytoplasmic polyadenylation element binding (CPEB)
Smp_080360.1	475.19	6.41	PLAC8
Smp_087320.1	227.30	3.38	TPA-induced protein 11B mouse / zinc finger
Smp_104970.1	23.13	3.34	leucine rich repeat-containing protein 70
Smp_129920.1	27.22	7.58	sodium-dependent neurotransmitter transporter
Smp_130970.1	53.83	4.68	G2 mitotic specific cyclin B3

Smp_137460.1	119.35	4.23	cytoplasmic polyadenylation element binding
Smp_141570.1	14.08	12.4	TWiK family of potassium channels protein (4TM
Smp_150350.1	348.45	6.04	synaptotagmin XIV
Smp_156320.1	10.25	6.66	[K] norepinephrine:norepinephrine transporter
Smp_166560.1	22.36	4.05	[K] zinc-finger homeobox protein 1
Smp_174260.1	26.24	5.10	thyroid hormone receptor alpha
Smp_176940.1	43.03	6.87	cationic amino acid transporter

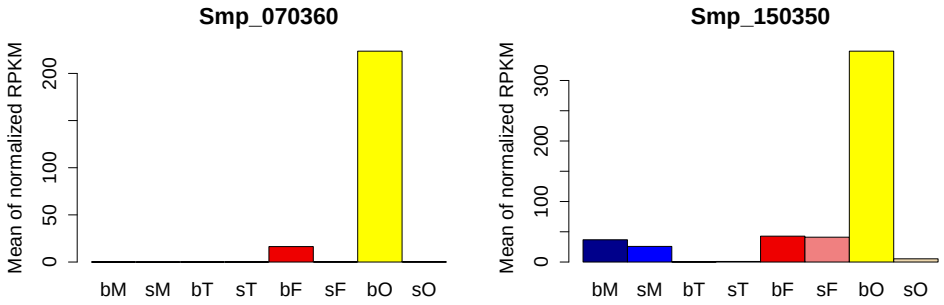

Figure 3.18: Expression profiles of selected genes from Category 2.1. Smp_070360 encodes a cytoplasmic polyadenylation element binding (CPEB) protein and Smp_150350 is a synaptotagmin gene.

2.2 Ovary-specific and pairing-unaffected genes The occurrence of transcripts of 171 genes appeared ovary-specific and not affected by pairing. Table 3.16 shows a selection of these genes, which includes the SOX transcription factor (Smp_076600) and a regulator of G-protein signaling gene (Smp_210800) with their transcript profiles in Figure 3.19. The complete list of all 171 genes is attached as Supplementary file No. 24.

Table 3.16: A selection of genes whose transcription occurred ovary-specifically and unaffected by pairing

GeneID	RPKM_bO	Product
Smp_021190.1	13.00	histidine kinase
Smp_076600.1	10.30	transcription factor SOX
Smp_118960.1	17.42	jun protein

Smp_130370.1	10.87	elongation of very long chain fatty acids
Smp_191690.1	14.32	tumor susceptibility gene 101 protein
Smp_210800.1	9.29	regulator of G protein signaling

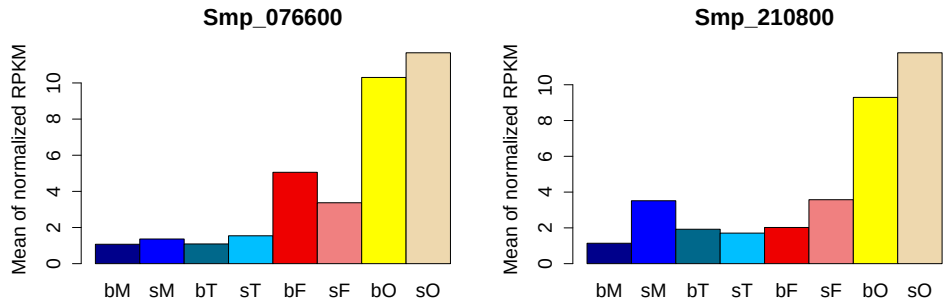

Figure 3.19: Expression profiles of selected genes from Category 2.2. Smp_076600 encodes the SOX transcription factor and Smp_210800 encodes the regulator of G protein signaling (RGS domain).

3.1 Pairing-affected genes in both gonads A total of 139 genes showed differential expression in both testes and ovaries. The table (3.17) provides an overview about the identified genes and shows also the regulation pattern of non-hypothetical proteins (number of non-hypothetical genes / number of total genes). Transcript profiles of Smp_146810 (diaphanous) and Smp_147550 (twik family of potassium channels) were shown in Figure 3.20. The transcript profiles of all genes of this category are listed in Supplementary file No. 25.

Table 3.17: Genes whose transcriptions were affected by pairing in both testes and ovaries

GeneID	$\log_2$(bT/sT)	$\log_2$(bO/sO)	Product
A: up-regulated in both testes and ovaries (5/9)			
Smp_000050.1	0.93	2.12	transient receptor potential cation channel
Smp_025370.1	0.82	3.29	lipopolysaccharide induced transcription factor regulating TNF alpha
Smp_146810.1	1.20	4.35	diaphanous
Smp_147550.1	0.80	5.12	twik family of potassium channels
Smp_149820.1	0.72	3.08	[K] glycoprotein N acetylgalactosamine 3-beta galactosyltransferase

B: down-regulated in both testes and ovaries (59/79)

Smp_000200.1	-0.93	-1.71	NEDD4 binding protein 2 2
Smp_006860.1	-0.79	-2.86	PDZ and LIM domain protein Zasp
Smp_012440.1	-0.84	-0.86	glucose transport protein
Smp_015050.1	-0.63	-0.70	[K] choline kinase
Smp_018170.1	-1.52	-1.86	zinc finger protein
Smp_019310.1	-1.08	-4.57	dynein light chain
Smp_027430.1	-0.71	-1.42	EF hand domain-containing family member A2
Smp_034120.1	-0.62	-0.91	[K] synaptosomal associated protein 23 kDa
Smp_042770.1	-0.73	-0.86	TBC1 domain family 0
Smp_045550.1	-1.06	-4.05	[K] annexin
Smp_046360.1	-1.10	-1.85	zinc finger protein 143
Smp_047640.1	-0.83	-3.46	ferritin, heavy polypeptide 1
Smp_047650.1	-0.73	-3.58	[K] ferritin, heavy polypeptide 1
Smp_047660.1	-1.18	-4.06	[K] ferritin, heavy polypeptide 1
Smp_047680.1	-1.18	-4.08	ferritin, heavy polypeptide 1
Smp_049240.1	-1.40	-2.49	major egg antigen
Smp_049250.1	-1.04	-2.33	major egg antigen
Smp_049270.1	-0.67	-3.00	major egg antigen (p40)
Smp_053420.1	-0.67	-1.35	fermitin family 1
Smp_059980.1	-1.08	-4.37	[K] arginase
Smp_071390.1	-1.08	-4.61	[K] adenylate kinase
Smp_072210.1	-0.68	-1.21	zinc finger protein 395
Smp_077720.1	-0.78	-3.31	annexin
Smp_077980.1	-1.08	-2.69	[K] neuroendocrine convertase 2
Smp_093930.2	-0.64	-3.37	[K] receptor tyrosine kinase EGFR A
Smp_096390.1	-1.43	-2.37	16 kda calcium binding protein
Smp_096410.2	-1.14	-3.82	16 kda calcium binding protein
Smp_105360.1	-0.89	-1.06	neurogenic locus notch protein
Smp_114620.1	-0.98	-1.75	adenosinetriphosphatase
Smp_123000.2	-0.81	-2.38	ski oncogene
Smp_125350.1	-1.37	-1.01	BC026374 protein (S09 family)
Smp_125890.1	-0.94	-0.76	[K] dna photolyase

Smp_127000.1	-1.33	-3.07	large neutral amino acids transporter small
Smp_127990.1	-1.16	-2.77	MEG 13
Smp_128230.1	-0.66	-1.70	neurogenic locus notch protein
Smp_131580.1	-0.67	-2.03	[K] lysosomal alpha mannosidase
Smp_133250.1	-0.70	-1.31	discoidin domain-containing receptor 2
Smp_133690.1	-0.66	-3.21	discoidin domain-containing receptor 2
Smp_134870.1	-1.84	-2.20	early growth response protein
Smp_138880.1	-1.07	-1.97	[K] RNA binding protein fox 1 1
Smp_140000.1	-1.11	-2.46	tetraspanin CD63 receptor
Smp_144700.1	-0.60	-0.85	5′ AMP-activated protein kinase subunit gamma
Smp_145890.1	-0.70	-2.53	adamTS protein 3
Smp_147680.1	-1.97	-3.06	EF hand-containing, Ca^{2+} binding
Smp_150730.1	-1.09	-0.71	discoidin domain-containing receptor 2
Smp_154490.1	-1.26	-1.96	ras associating and dilute domain-containing protein
Smp_158510.1	-1.26	-1.67	[K] diacylglycerol O-acyltransferase 1
Smp_160830.1	-0.72	-1.33	[K] phospholipase d3
Smp_166530.2	-1.65	-3.07	[K] phospholipase A
Smp_168000.1	-1.00	-2.57	monocarboxylate transporter
Smp_168980.1	-0.66	-2.80	adenylate cyclase
Smp_173210.1	-0.88	-0.79	zinc finger protein XlCOF6
Smp_175720.1	-0.89	-3.83	[K] E3 ubiquitin protein ligase TRIM9
Smp_176610.1	-0.59	-2.72	[K] BTB:POZ domain-containing protein
Smp_185680.1	-1.52	-1.75	major egg antigen
Smp_186020.1	-1.37	-1.85	major egg antigen
Smp_196250.1	-0.62	-2.78	[K] supervillin
Smp_213910.1	-1.07	-3.15	type IV collagen alpha 1 chain

C: differentially regulated in testes and ovaries (38/51)

Smp_008450.1	0.59	-2.08	leucine rich repeat and death domain-containing protein
Smp_014570.1	1.33	-1.54	saposin,IPR008139
Smp_015190.1	0.81	-2.05	serine rich repeat protein
Smp_040680.1	1.19	-3.08	[K] dynein light chain

Smp_059170.2	1.03	-4.00	troponin i
Smp_070630.1	1.27	-2.34	protein unc 112
Smp_074150.1	0.71	-2.03	annexin
Smp_083770.1	0.85	-4.79	anoctamin 7
Smp_092020.1	1.31	-3.69	cement protein 3B variant 2
Smp_123020.1	0.66	-2.60	protein serine:threonine kinase
Smp_123270.1	1.00	-1.28	Sj Ts1
Smp_126500.1	0.82	-1.90	[K] tensin C1 domain-containing phosphatase
Smp_139160.1	1.29	-1.75	SmCL2 peptidase (C01 family)
Smp_141920.1	0.79	-1.65	SH3 and multiple ankyrin repeat domains protein
Smp_148430.1	0.94	-1.46	hook protein
Smp_164380.1	0.77	-3.02	[K] protein KINase family member (kin 1)
Smp_173030.1	2.00	-3.74	aminopeptidase A (M01 family)
Smp_179170.1	1.52	-2.35	hemoglobinase (C13 family)
Smp_179370.1	3.23	-2.53	low density lipoprotein (LDL) receptor
Smp_199490.1	0.81	-1.31	diacylglycerol kinase zeta iota
Smp_002930.1	-1.67	3.55	[K] histone H2A
Smp_003110.1	-1.17	2.04	nadrin protein
Smp_046430.1	-0.74	0.80	[K] ubiquitin carboxyl terminal hydrolase
Smp_049890.1	-0.69	0.79	[K] WD repeat domain-containing protein 83
Smp_053900.1	-0.66	3.07	[K] beta hexosaminidase subunit beta
Smp_086960.1	-0.86	1.36	[K] lipoyltransferase 1, mitochondrial
Smp_095090.1	-0.69	0.72	solute carrier family 37
Smp_105080.1	-1.11	1.55	[K] endonuclease G
Smp_135260.1	-0.59	2.19	[K] ethanolaminephosphotransferase 1
Smp_148050.1	-0.62	0.84	[K] glutaminyl tRNA synthetase
Smp_148660.1	-0.60	1.01	[K] DNA ligase 4
Smp_152610.1	-0.85	1.07	protein hook 3
Smp_153730.1	-0.59	2.08	[K] protein LAS1
Smp_159140.1	-0.68	3.03	[K] solute carrier organic anion transporter family
Smp_159920.1	-1.00	6.07	protocadherin 11

Smp_161250.1	-0.63	0.81	microphthalmia associated transcription factor
Smp_174740.1	-0.71	1.11	small subunit processome component 20
Smp_211160.1	-0.77	0.63	ATP-dependent RNA helicase DHX33

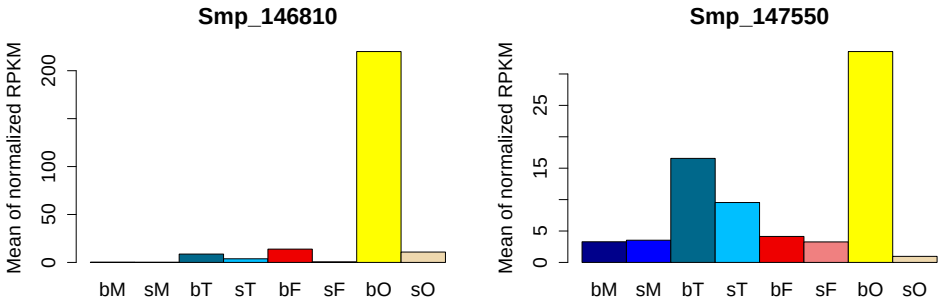

Figure 3.20: Expression profiles of selected genes from Category 3.1. Smp_146810 is a diaphanous protein gene and Smp_147550 encodes a protein belonging to the twik family of potassium channels.

3.2 Pairing-unaffected genes in both gonads Transcripts of 4100 genes showed no significant changes by pairing in both gonads, including among other genes the DNA replication licensing factors MCM (mini-chromosome maintenance proteins) 2-8, vasa-like genes 1-3, argonaut, origin recognition complex (ORC) subunits, and the protein tyrosine protein kinases (PTKs) SmTK3, SmTK5 and VKR2 (Table 3.18). These schistosome PTKs have been shown before to be transcribed in the gonads of *S. mansoni* and to be involved in reproduction-associated differentiation processes (Kapp et al., 2001, 2004; Knobloch et al., 2002b; Beckmann et al., 2010a; Buro et al., 2013; Vanderstraete et al., 2014). The transcript profiles of Smp_124570 (leucin ziper protein) and Smp_136600 (protein lin 9) are presented in Figure 3.21 and these two genes will be discussed later. The complete list of genes of this category and their expression profiles are available in Supplementary file No. 26.

Table 3.18: A selection of genes that are transcribed pairing-independently in both testes and ovaries

GeneID	RPKM_bT	RPKM_bO	Product
Smp_000260.1	261.46	126.27	[K] proactivator polypeptide saposin
Smp_006550.1	329.13	601.14	glutaredoxin 3
Smp_008070.1	868.91	1,831.17	[K] thioredoxin

Smp_008545.1	1,248.86	2,943.65	[K] heat shock protein 60 HSP60
Smp_026030.1	22.56	38.11	DNA repair and recombination protein RAD54B
Smp_032500.1	164.68	258.20	[K] DNA replication licensing factor mcm7
Smp_036500.1	57.02	46.08	nhr 48 / constitutive androstane receptor (CAR)
Smp_042210.1	43.58	46.76	[K] origin recognition complex subunit 4 ORC
Smp_042980.1	56.57	75.67	[K] mevalonate kinase
Smp_046500.2	354.94	764.60	[K] proliferating cell nuclear antigen PCNA
Smp_048430.1	186.39	244.65	[K] thioredoxin glutathione reductase
Smp_052910.1	1,191.54	409.17	[K] S-phase kinase associated protein skp1
Smp_055310.1	77.08	70.47	[K] histone lysine n methyltransferase setd8
Smp_055890.1	286.79	445.65	[K] ribonucleoside diphosphate reductase subunit M2
Smp_056360.8	1,101.95	1,168.20	Sm-npp-17
Smp_056760.1	451.74	425.00	[K] protein disulfide isomerase
Smp_058690.1	370.13	361.30	[K] glutathione peroxidase
Smp_059800.1	136.62	141.39	[K] trans-prenyltransferase, putative
Smp_068440.1	66.78	67.83	vasa-like gene 3
Smp_080730.1	592.15	489.46	STK / cyclin dependent kinase 1 (CDC2
Smp_082810.2	222.25	269.54	[K] cell polarity protein; Cdc42
Smp_082850.2	89.00	129.14	[K] cullin
Smp_085910.1	26.55	37.63	smad family member smad2
Smp_093310.1	139.23	161.38	[K] transcription factor E2F5
Smp_103160.2	68.78	59.47	[K] FAA4 Long-chain-fatty-acid–CoA ligase 4
Smp_124570.1	752.42	32.05	leucin zipper protein
Smp_128310.1	28.94	26.14	[K] xylosyltransferase I
Smp_130430.1	152.91	121.62	[K] isopentenyl-diphosphate delta-isomerase
Smp_133660.1	87.67	41.95	protein lin 9
Smp_147400.1	32.59	41.99	[K] sestrin 1
Smp_149260.1	103.14	116.71	[K] kinesin family 1

Smp_150270.1	78.49	54.04	[K] cullin 1
Smp_153310.1	72.25	125.53	cell polarity protein; lethal giant larvae Llgl
Smp_153500.1	15.72	23.49	tyrosine protein kinase VKR2
Smp_158050.1	143.90	79.19	[K] global transcription activator snf2l2 CHD
Smp_162340.1	20.85	26.94	[K] serine:threonine protein kinase ATR
Smp_168520.1	81.83	35.75	[K] acetyl-CoA synthetase
Smp_170110.1	30.46	77.23	high density lipoprotein binding protein
Smp_179070.1	93.81	55.78	ribosomal protein S6 kinase beta 2
Smp_179320.1	333.37	661.09	argonaute ago2-1

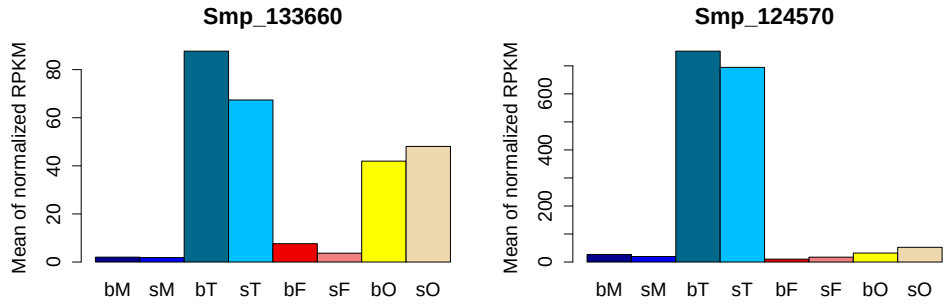

Figure 3.21: Expression profiles of selected genes from Category 3.2. Smp_133660 encodes the protein lin 9 and Smp_124570 encodes a leucin zipper protein.

3.3 Transcription of genes affected by pairing in testes but not in ovaries The transcription of 62 genes was affected by pairing in testes but not in ovaries, of which a selection is shown in Table 3.19. This includes the genes encoding a von-Willebrand factor A (vWA) domain-containing protein (Smp_127480) and a DNA double strand break repair rad50 ATPase (Smp_181450), whose transcript profiles are shown in Figure 3.22. The transcript profiles of all genes of this category are listed in Supplementary file No. 27.

Table 3.19: A selection of genes whose transcription was pairing-affected in testes but not in ovaries

GeneID	logFC_Te	Product
Smp_008660.1	-1.08	[K] gelsolin
Smp_011150.1	-0.79	[K] threonine aspartase 1
Smp_034410.1	-0.66	[K] cathepsin F (C01 family)

Smp_053300.1	-1.98	[K] histone H4
Smp_065240.1	-1.43	[K] GDP fucose protein O fucosyltransferase 1
Smp_090890.1	-0.87	proto oncogene STK
Smp_127480.1	0.64	von-Willebrand factor A domain-containing 3B
Smp_130210.1	-0.78	[K] ATP-dependent RNA helicase DDX11
Smp_130920.1	0.62	multiple C2 and transmembrane domain-containing protein
Smp_131780.1	-0.90	[K] CUG BP and ETR3 factor
Smp_135160.1	0.85	dual specificity protein phosphatase 10
Smp_137730.1	1.03	alpha(13)fucosyltransferase
Smp_139830.1	0.79	integrin alpha FG GAP repeat containing protein
Smp_152230.1	-0.73	WD repeat-containing protein 24
Smp_165440.1	-1.05	[K] netrin receptor unc 5
Smp_181450.1	0.70	DNA double strand break repair rad50 ATPase
Smp_189960.1	-0.63	nuclear pore complex protein Nup153
Smp_190070.1	-1.83	WD repeat and FYVE domain-containing protein 3

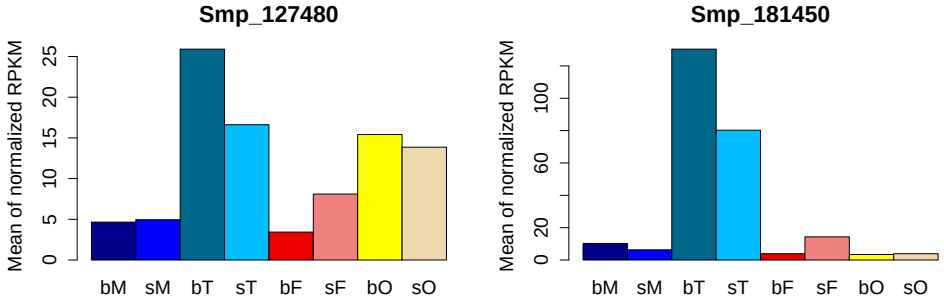

Figure 3.22: Expression profiles of selected genes from Category 3.3. Smp_127480 encodes a protein containing the vWA domain and Smp_181450 is a gene coding for the DNA double-strand break repair rad50 ATPase.

3.4 Transcription of genes affected by pairing in ovaries but not in testes In this last category, the transcription of 3152 genes was found to be pairing-affected in ovaries but not in testes. This category includes among other genes the receptor PTK VKR1, and the cellular PTKs SmTK4 and SmTK6. Furthermore, FGFR a and b, polo-like kinases (PlKs) 1 and 4, nanos2, and ADP ribosylation factors. Again, many of these genes have been shown before to be transcribed in the gonads (Beckmann et al., 2010a, 2011; Long et al., 2010; Hahnel et al., 2014). Smp_166150 (MELK) and Smp_198690

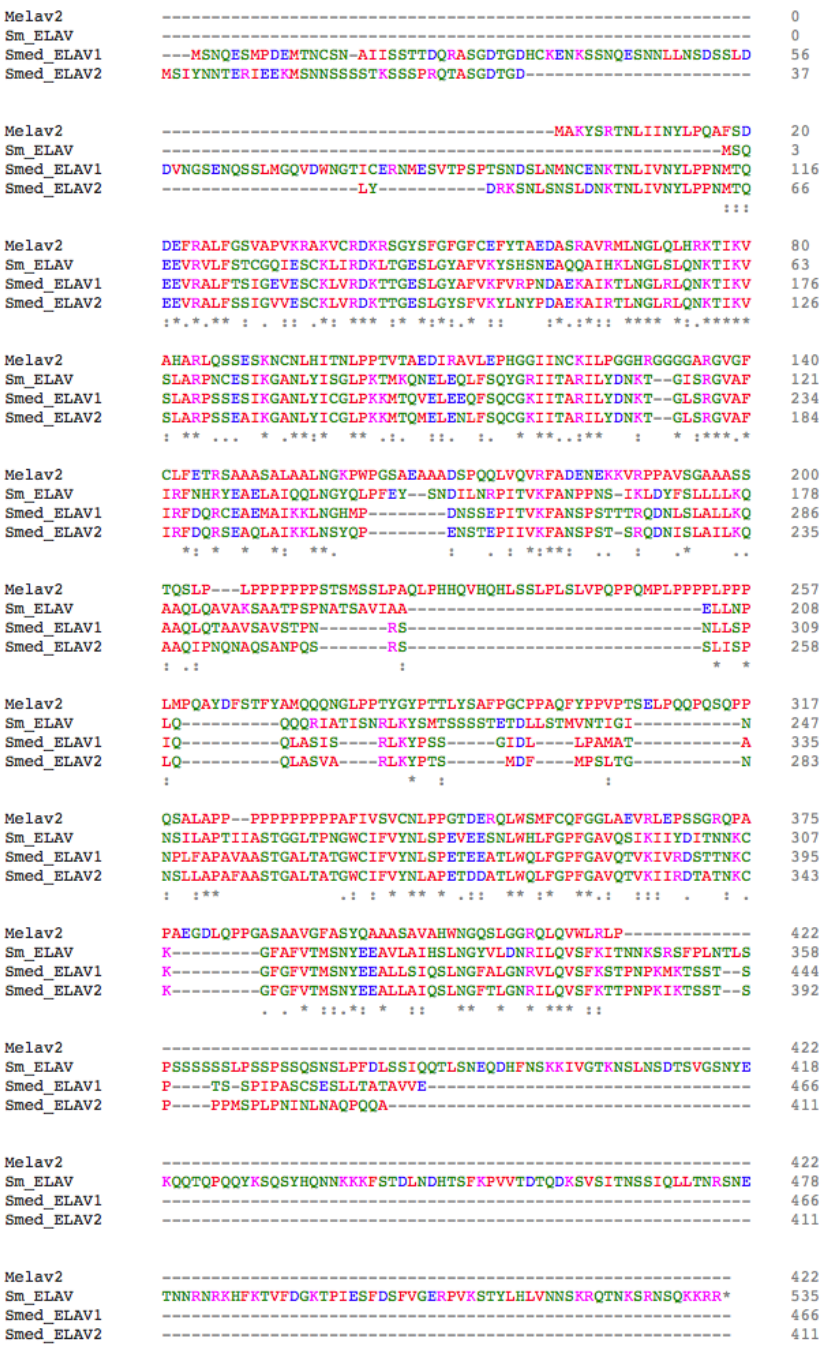

Figure 3.17: Multiple alignment of ELAVs from *Macrostomum lignano* (Melav), *S. mansoni* (Sm_ELAV) and *Schmidtea mediterranea* (Smed_ELAV1 and Smed_ELAV2). Sm_ELAV shares 35% identity with Melav, 63% with Smed_ELAV1, and 61% with Smed_ELAV2.

(HMG-CoA synthase) will be discussed later and their transcript profiles are shown in Figure 3.23. The complete list of genes of this category and their expression profiles are available in Supplementary file No. 28.

Table 3.20: A selection of genes whose transcription was pairing-affected in ovaries but not in testes

GeneID	logFC_Ov	Product
Smp_000130.1	-1.3	[K] hormone sensitive lipase
Smp_001170.1	1.26	[K] eukaryotic translation initiation factor 3
Smp_001360.1	0.72	[K] thymidylate kinase
Smp_006920.1	0.77	SmTK6
Smp_009600.1	0.77	[K] PlK1
Smp_011000.1	-1.65	[K] lysosomal acid lipase-related
Smp_011680.1	-1.59	CD36 class B scavenger receptor
Smp_013060.1	-0.99	[K] smad family member smad1
Smp_019790.1	0.74	VKR1
Smp_026400.1	3.35	thyrotroph embryonic factor
Smp_026510.1	-0.83	[K] dual specificity mitogen activated protein MEK1
Smp_030870.1	-1.87	interleukin 1 receptor associated kinase SIMPL
Smp_033950.2	1.12	Smad4
Smp_038970.1	-1.46	long chain fatty acid coenzyme A ligase
Smp_045650.1	-2.56	growth arrest specific 8 GAS8
Smp_046410.1	2.51	[K] tektin 2 (testicular)
Smp_048690.1	-1.91	enkurin
Smp_049760.1	0.93	[K] TGF-beta receptor 1
Smp_051920.2	-2.86	nanos2
Smp_052390.1	1.69	[K] origin recognition complex subunit 5 ORC
Smp_054470.1	-1.38	[K] thioredoxin
Smp_056350.1	0.90	[K] mitotic spindle assembly checkpoint protein
Smp_058360.1	1.72	[K] chloride channel protein
Smp_059480.1	-4.40	tryparedoxin peroxidase
Smp_060070.1	0.82	[K] septin 7
Smp_060160.1	-2.74	sperm flagellar protein 1
Smp_073500.2	0.93	[K] elongation factor (ef-tu)
Smp_079230.1	1.57	[K] FKBP12
Smp_079410.1	-1.19	[K] PlK4

Smp_105480.1	-2.39	[K] ADP ribosylation factor protein 6 like
Smp_123190.1	-2.59	[K] ADP ribosylation factor protein 2 binding
Smp_149460.1	-2.41	[K] SmTK4
Smp_157300.1	-2.12	FGFR B
Smp_159930.1	-1.12	[K] ADP ribosylation factor 3
Smp_166150.1	0.91	maternal embryonic leucine zipper kinase MELK
Smp_175590.1	-2.95	FGFR a
Smp_198690.1	1.20	HMG-CoA synthase

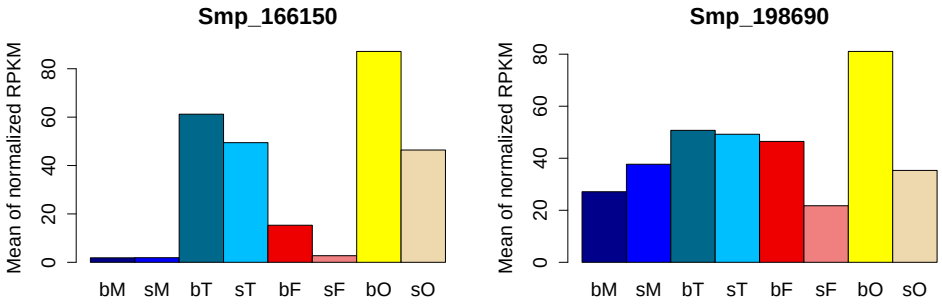

Figure 3.23: Expression profiles of selected genes from Category 3.4. Smp_166150 is a gene coding for the maternal embryonic leucine zipper kinase (MELK) and Smp_198690 encodes the 3-hydroxy-3-methylglutaryl-coenzyme A (HMG-CoA) synthase.

3.3.7 Pairing effect 2: differential gene expression in males and females

An overview of pairing effect on gene expression in male or female worms is shown in the volcano plots in Figure 3.24.

When the transcriptomes of adult males were compared (bM versus sM), transcripts of 313 genes were up-regulated in bM and that of 113 were up-regulated in sM (> 1.5 fold difference; FDR < 0.05). The latter included *follistatin*, a gene identified as differentially transcribed between bM and sM in a former study (Leutner et al., 2013). Table 3.21 shows several examples of appropriate non-hypothetical genes. The complete list of DEGs was attached as Supplementary file No. 11.

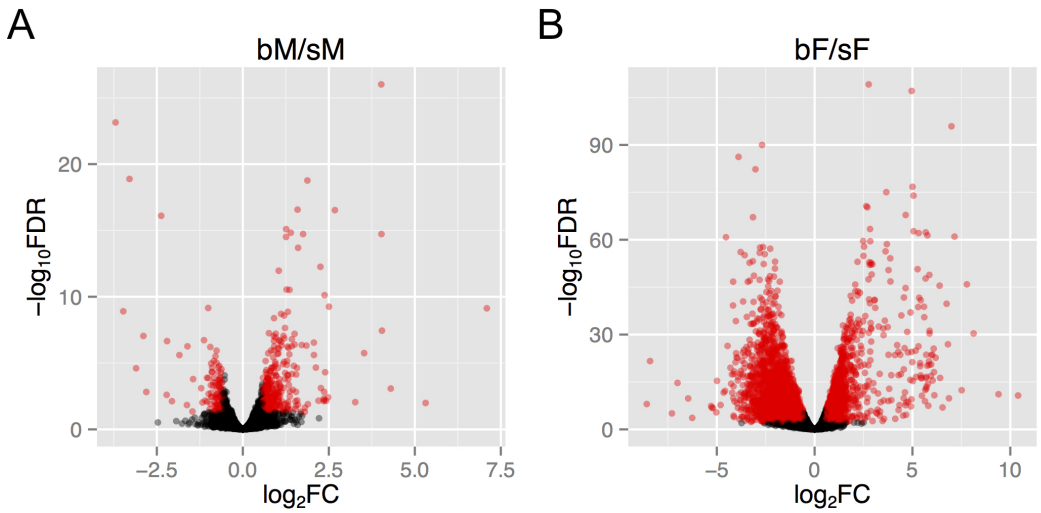

Figure 3.24: Differentially expressed genes revealed by Volcano plots. Red points indicate differentially expressed genes (> 1.5-fold difference; FDR < 0.05 (A, male comparison) or 0.005 (B, female comparison)).

Table 3.21: Examples of transcripts up-regulated in bM or sM

GeneID	$\log_2$(bM/sM)	Product
Up-regulated in bM		
Smp_174520.1	4.30	dynein light chain
Smp_158480.1	4.03	AMP-dependent ligase
Smp_168940.1	4.02	NAD-dependent epimerase:dehydratase
Smp_158150.1	3.25	reticulocalbin 2
Smp_136110.1	2.68	leucine rich repeat-containing protein 68
Smp_160040.1	2.51	abnormal long morphology protein 1
Smp_170340.1	2.50	[K] collagen alpha 1(IV) chain
Smp_135230.1	2.39	tyrosine decarboxylase family member (tdc 1)
Smp_195090.1	2.38	tegument-allergen-like protein
Smp_052230.1	2.35	papilin
Smp_158750.1	2.24	[K] forkhead box protein C2 B
Smp_154010.1	2.20	halobacterial transducer protein VI
Smp_171580.1	2.12	[K] aromatic amino acid decarboxylase
Up-regulated in sM		
Smp_036470.1	-3.7	oxalate:formate antiporter
Smp_141800.1	-3.29	oxalate:formate antiporter

Smp_187840.1	-3.10	long chain fatty acid coenzyme ligase
Smp_038970.1	-2.89	long chain fatty acid coenzyme A ligase
Smp_163170.1	-2.20	sodium:potassium dependent atpase beta subunit
Smp_079960.1	-2.06	[K] tubulin beta 2C chain
Smp_212760.1	-1.84	kinesin, putative
Smp_210800.1	-1.62	regulator of G protein signaling 7
Smp_123300.1	-1.44	follistatin
Smp_072330.2	-1.09	[K] heat shock protein
Smp_121920.1	-1.04	[K] vesicular amine transporter
Smp_022430.1	-1.04	brain protein 44 protein 2 like
Smp_034550.1	-1.01	[K] alpha actinin
Smp_083720.1	-1.00	[K] phosphate carrier protein mitochondrial

For females (bF versus sF), transcripts of 1,591 genes were up-regulated in bF and 2,157 genes were up-regulated in sF (> 1.5 fold difference; FDR < 0.005). Genes related to the egg-shell biosynthesis were all up-regulated in bF as expected, which included the tyrosinases, egg-shell proteins (p14, p48, egg-shell precursor, etc.). Besides that, several ribosomal proteins, RNA helicases, DNA replication licensing factors and translation initiation factors were also up-regulated in bF. In contrast, genes up-regulated in sF included several calcium-binding proteins (e.g. calmodulin), aquaporins, dyneins, innexins, protocadherins and others (Table 3.22). For information about all female DEGs see Supplementary file No. 12.

Table 3.22: Examples transcripts up-regulated in bF or sF

GeneID	$\log_2$(bF/sF)	Product
Up-regulated in bF		
Smp_197780.1	10.40	lin 7 protein
Smp_029620.1	9.40	homeobox protein SMOX 4
Smp_145490.1	7.78	poly(rC) binding protein 2:3:4
Smp_130780.1	7.51	monocarboxylate transporter
Smp_134490.1	7.05	thyroid hormone receptor alpha
Smp_070360.1	6.99	[K] cytoplasmic polyadenylation element binding
Smp_041880.1	6.81	peptide (allatostatin:somatostatin)
Smp_013540.1	6.74	[K] tyrosinase
Smp_050270.1	6.41	[K] tyrosinase 1
Smp_000430.1	6.19	egg-shell protein

Smp_000270.1	6.03	fs800
Smp_155310.1	6.02	tetraspanin CD63 receptor
Smp_077890.1	5.96	trematode Eggshell Synthesis domain-containing protein
Smp_141450.2	5.94	female reproductive tract protease GLEANR 897
Smp_112450.1	5.88	trematode Eggshell Synthesis domain-containing protein
Smp_137460.1	5.86	cytoplasmic polyadenylation element binding
Smp_095980.1	5.85	extracellular superoxide dismutase (Cu Zn) SOD
Up-regulated in sF		
Smp_032980.1	-8.58	calmodulin protein
Smp_032970.1	-8.41	calmodulin protein
Smp_099670.1	-7.89	lipoprotein receptor
Smp_032990.1	-7.01	calmodulin 4
Smp_003600.1	-6.87	DM9 domain-containing protein
Smp_079260.1	-6.76	LIM:homeobox protein Lhx2
Smp_140350.1	-5.74	homeobox protein ARX
Smp_034160.1	-5.56	jagged protein
Smp_193600.1	-5.29	glutamate (NMDA) receptor subunit epsilon 2
Smp_180350.1	-5.20	opsin receptor
Smp_194330.1	-5.02	synaptotagmin
Smp_206190.1	-4.65	complement C1q tumor necrosis factor
Smp_161600.1	-4.58	sox transcription factor
Smp_158160.1	-4.45	RNA binding protein lin 28
Smp_036470.1	-4.45	oxalate:formate antiporter
Smp_114565.1	-4.27	SmHox8 (fragment)
Smp_156220.1	-4.23	receptor type tyrosine protein phosphatase delta
Smp_142390.1	-4.21	innexin unc 9

3.3.8 Gender effect: differential gene expression between male (M+T) and female (F+O) samples

To investigate the gender effect in general, the average transcript amounts of male samples (bM, sM, bT, sT) was compared to that of female samples (bF, sF, bO, sO). FDR was set to 0.005, and fold difference to 2. Furthermore, to make the comparison more

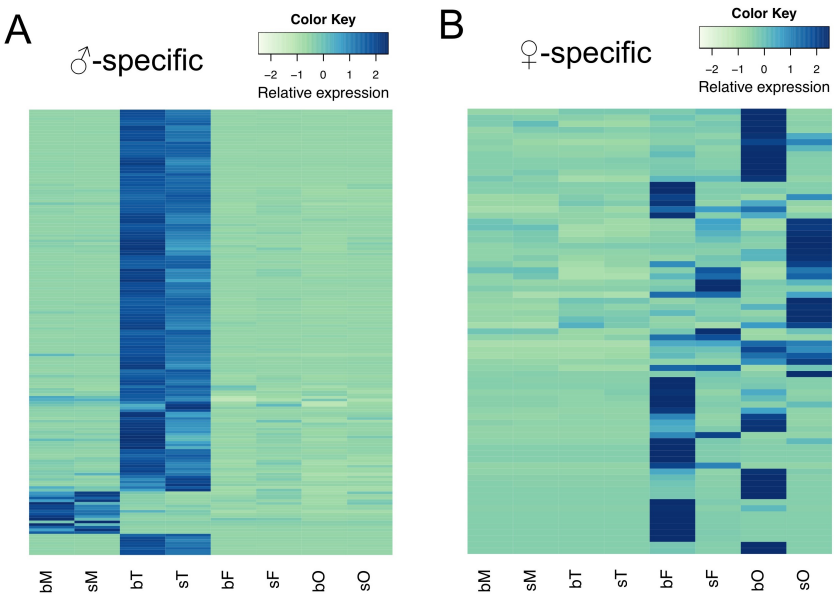

Figure 3.25: Hierarchical clustering of male- and female-specific transcripts. Mars symbol: male samples (bM/sM/bT/sT), Venus symbol: female samples (bF/sF/bO/sO).

specific, the RPKM values in all samples of one group were set to < 2 as unexpressed. This resulted in a total of 168 and 73 genes that were male- and female-specifically transcribed, respectively (Figure 3.25). Transcripts in the former group were mainly enriched in testes samples, which contained among other genes the M-phase indcer phosphatase 3 (cdc 25, Smp_152200), a kelch protein gene (Smp_143970), the ELAV gene (Smp_194950), several dyneins and HOX genes. Transcripts enriched in female samples included the CPEBs (Smp_070360 and Smp_137460), a G2:mitotic specific cyclin (Smp_130970), a tyrosinase (Smp_050270) and others. The complete gene list and expression profiles can be see in Supplementary files No. 29 and 30.

3.3.9 Tissue effect 1: DEGs from bT/bM and bO/bF comparisons

When comparing the whole gene transcript profiles between bT and bM, transcript numbers of 5,996 genes were detected to be significantly different (FDR < 0.005) (Figure 3.26 A). Among these, 5,478 genes showed at least a 1.5-fold difference in transcription, of which 2,741 were up-regulated in bT and 2,737 were up-regulated in the whole males.

The genes whose transcription was up-regulated in bT included those encoding ribosomal proteins, RNA helicases, DNA replication licensing factors, dynein chains, the ELAV protein (see also section 3.3.6), CDKs, translation initiation and elongation factors, intraflagellar transport proteins, kinesins, STKs and others. Genes with up-regulated transcription levels in bM encode ADP-ribosylation factor proteins, E3

ubiquitin protein ligases, NADH dehydrogenase subunits, cadherins, dyneins, innexins, neuropeptides, myosins, protocadherins, synaptotagmins, channel proteins, zinc finger proteins and others.

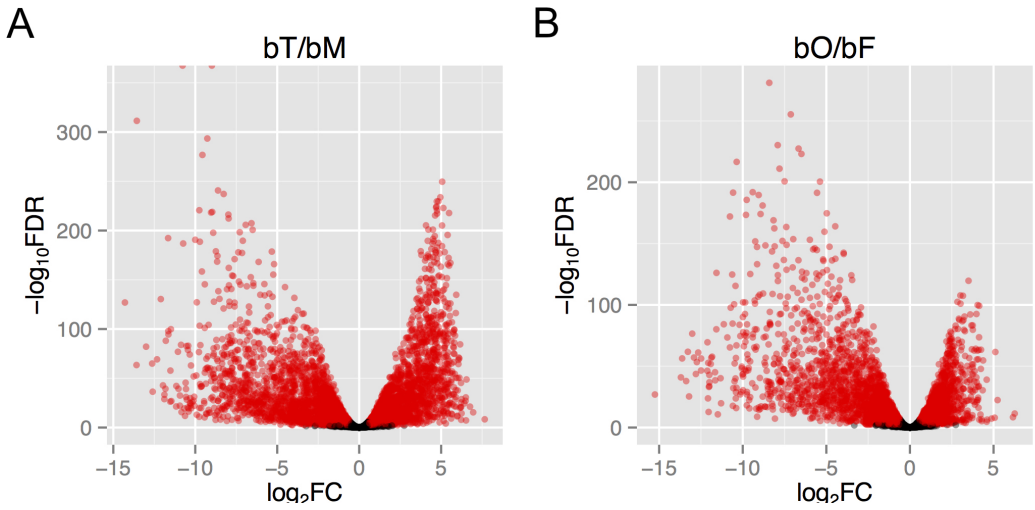

Figure 3.26: Differential gene expression between bT and bM, bO and bF revealed by Volcano plots. Red points indicate differentially expressed genes (>1.5-fold difference; FDR < 0.005 (A, bT compared to bM; B, bO compared to bF)).

For the comparison between bO and bF, transcript profiles of 5,021 differentially expressed genes were significant (FDR < 0.005) (Figure 3.26 B). Among them, 4,534 showed at least a 1.5-fold difference, of which 2,209 were up-regulated in bO and 2,325 were up-regulated in bF.

Genes up-regulated in bO included ribosomal proteins, RNA helicases and polymerases, DNA replication licensing factors, cyclins and CDKs, tRNA synthetases, translation initiation and elongation factors, kinesins, STKs, zinc finger proteins and others. Genes up-regulated in bF included ADP ribosylation factor proteins, aquaporins, E3 ubiquitin protein ligases, NADH dehydrogenase subunits, egg-shell proteins, annexins, cadherins, dyneins, channel proteins, transporters, fatty acid amide hydrolases, ferritins, innexins, neuropeptides, phospholipases, protocadherins, STKs, tegument-allergen-like proteins, tyrosine kinases, zinc-finger proteins, and others.

3.3.10 Tissue effect 2: DEGs from sT/sM and sO/sF comparisons

The transcript profiles between sT and sM, as well as sO and sF were also compared. For the former, the transcription of 2,792 genes were significantly up-regulated (> 1.5-fold difference) in sT and 2,617 up-regulated in sM (FDR < 0.005). For the latter, the

transcription of 2,134 genes was significantly up-regulated (>1.5-fold difference) in sO and 2,946 up-regulated in sF (FDR < 0.005).

Genes up-regulated in sT or sM were similar to the comparison of bT to bM. Genes up-regulated in sO contained RNA helicases, DNA and RNA polymerases, DNA replication licensing factors, and others similar to those up-regulated in bO. Genes up-regulated in sF represented ADP ribosylation factors, ATP synthases, E3 ubiquitin protein ligases, GTP binding proteins, NADH dehydrogenases, cadherins, dyneins, CDKs, innexins, channel proteins, and others.

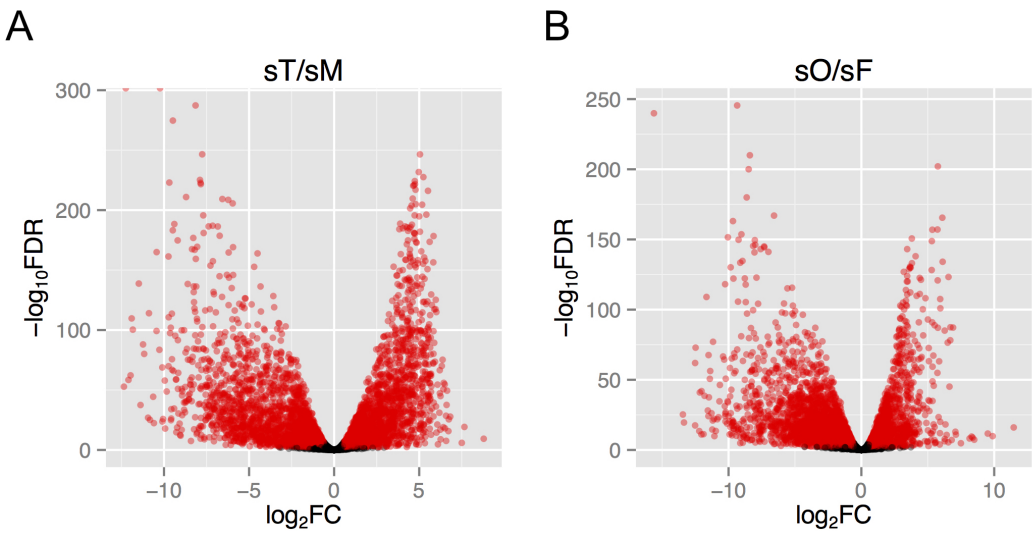

Figure 3.27: Differential gene expression between sT and sM, sO and sF revealed by Volcano plots. Red points indicate differentially expressed genes (>1.5-fold difference; FDR < 0.005 (A, sT compared to sM; B, sO compared to sF)).

By combining all genes whose transcription was up-regulated in gonads (section 3.3.9 and 3.3.10), 1,012 genes were found in all four groups. This indicated a gonad-bias of occurrence of transcripts of these genes, which are transcribed at least with a > 1.5-fold difference compared to the whole worm samples. The complete list of all 1,012 genes can be found in Supplementary file No. 31.

To get an overview of the identities and putative functional characteristics of these genes, GO enrichment analysis was perform based on the categories of biological process (Figure 3.28 A) and molecular function (Figure 3.28 B). The main processes these genes are involved in included RNA biosynthetic process, cell cycle, DNA replication, DNA repair, chromosome organization, nuclear division, ribosome biogenesis and mitosis. Protein products of about half of these genes (557 out of 1,012) have binding activities, which include nuclear acid binding and ATP binding.

Besides, 63 gene products have ATPase activity, 49 possess helicase activity, 48 show motor activity and 39 with actin binding and 32 have calmodulin-binding activity.

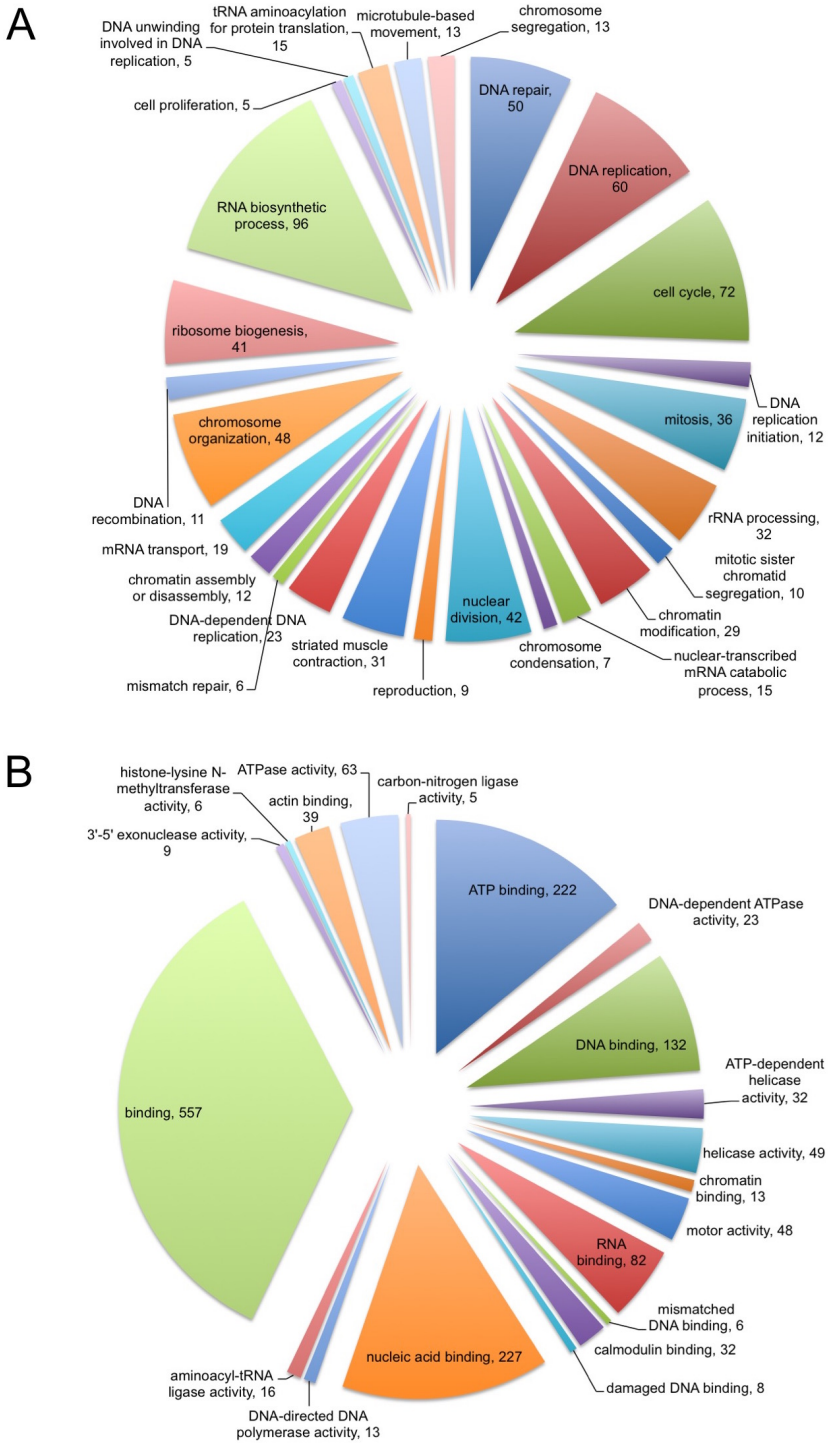

Figure 3.28: GO enrichment of genes up-regulated in all gonads by biological process (A) and by molecular function (B). The numbers of genes involved in each process were included.

3.3.11 Tissue effect 3: gonad-enriched versus worm-enriched transcripts

Another approach to find gonad-enriched transcripts in general is to compare the average gonad reads with average worm reads. By this 905 genes were found to be transcribed at least 4-fold higher in gonads than in whole worms (see Figure 3.29 A), of which 852 genes overlapped with the above combined 1,012 genes. This approach indicated that these genes have specialized functions in the gonads. In contrast, 1,326 genes were more abundantly transcribed in the whole worms (Figure 3.29 B), indicating that they play may more important roles in tissues other than gonads. The complete lists of gonad- and worm-enriched genes were attached as Supplementary files No. 32 and 33.

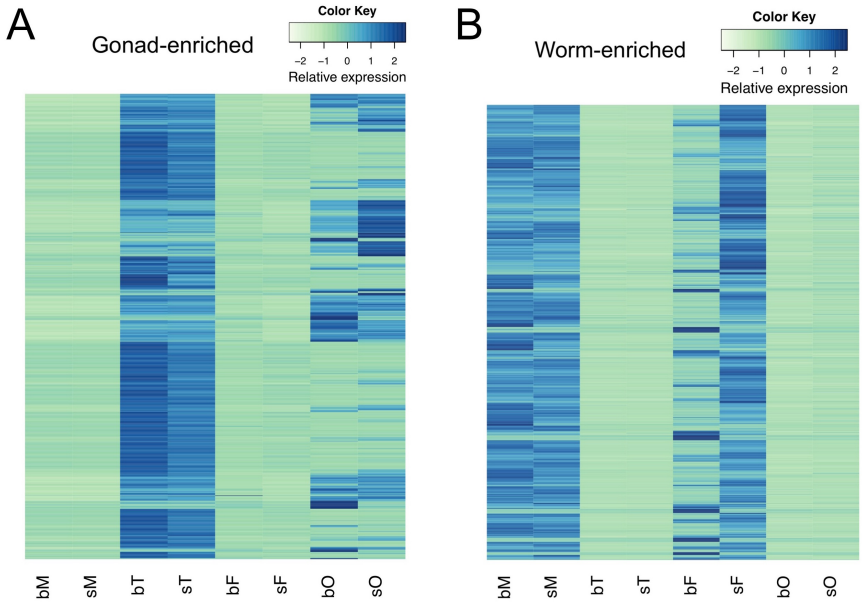

Figure 3.29: Hierarchical clustering of gonad- (A) and worm-enriched (B) transcripts. Most of gonad-enriched genes are transcribed in testes, and most of worm-enriched genes are transcribed simultaneously in males and sing-sex females.

3.3.12 Combined factors influencing gene transcription

Besides the above mentioned effect of single factors, the transcription of most genes has been found to be influenced by combined factors. For instance, the transcripts enriched in males and sF were found to be influenced by both pairing and tissue. The transcripts enriched in testes and bF were affected by all three factors.

Males-sF cluster

From the analysis of worm-enriched transcripts by hierarchical clustering (Figure 3.29 B), it became obvious that many genes were simultaneously expressed at high levels in males as well as in single-sex females. By comparing the average RPKM of (Males + sF) to the average of the rest, and through manual examination, a total of 841 genes (7.8% of total *S. mansoni* genes) were found to be transcribed more abundant in Males-sF than in all other samples (> 7.8-fold difference; FDR < 0.005). Table 3.23 shows a selection of these genes. The complete list can be found in the Supplementary file No. 34.

Table 3.23: A selection of transcripts enriched in males and sF

Gene_ID(s)	Product
Smp_124000, Smp_163630, Smp_172180, Smp_163710, Smp_085840	MEG family members
Smp_124050, Smp_199890, Smp_070240	venom allergen-like proteins
Smp_194960, Smp_154190, Smp_194970	25 kDa integral membrane proteins
Smp_000900, Smp_007070, Smp_018690, Smp_088360, Smp_118040	neuropeptide receptors
Smp_068510, Smp_158980, Smp_158990, Smp_151600	neuronal calcium sensors
Smp_037510, Smp_140850, Smp_140860, Smp_142390	innexin unc 9
Smp_086530, Smp_169200	tegument-allergen-like protein
Smp_128590	laminin gamma 3 chain
Smp_137940	guanylate kinase
Smp_059530.2	tetraspanin
Smp_211020	cell adhesion molecule
Smp_160880	phosphatidylcholine sterol acyltransferase
Smp_194830	KK7
Smp_153390.2	NPP-5
Smp_003440	stomatin
Smp_062560	[K] secreted frizzled protein

Smp_154600	[K] acetylcholinesterase
Smp_121660	IDL peptide
Smp_139970	calmodulin 4

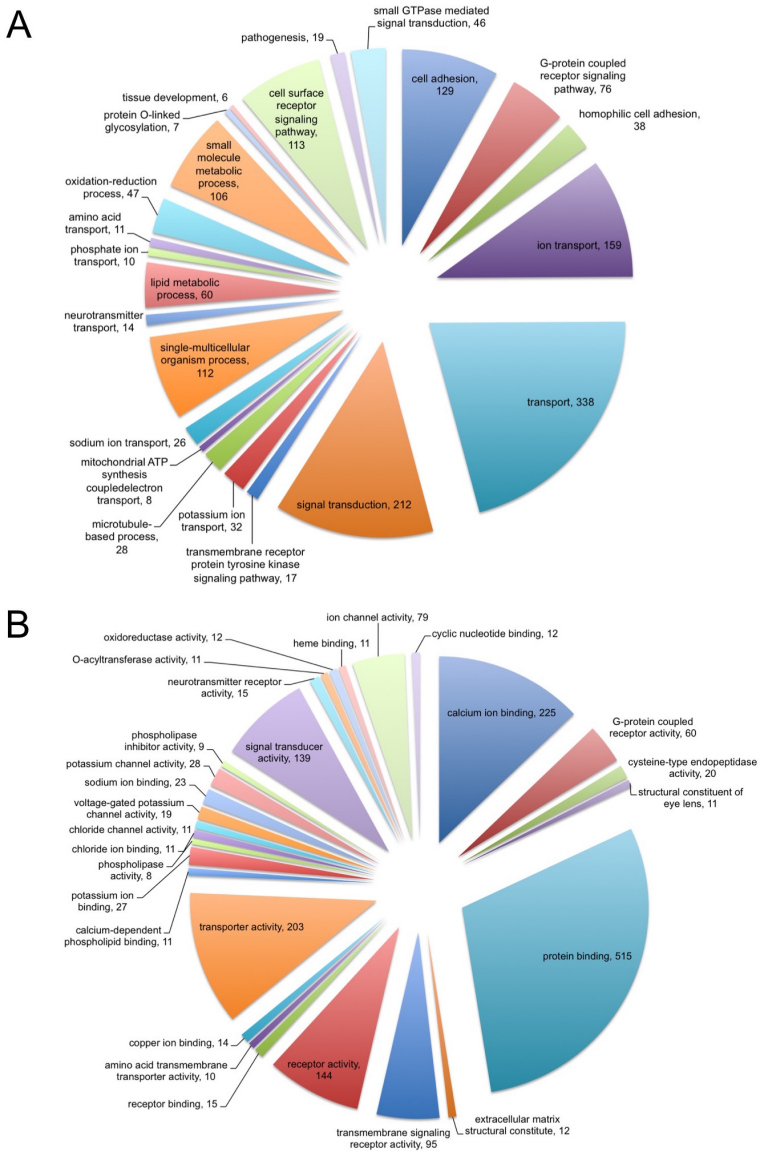

Figure 3.30: Gene ontology enrichment anlysis of transcripts enriched in the males-sF cluster. A, enrichment based on biological process; B, enrichment based on molecular function.

According to gene ontology enrichment analyses (Figure 3.30), these genes are mainly involved in transport, cell adhesion, signal transduction and development, including a number of micro-exon genes (MEGs), cell adhesion molecules, neuropeptide receptors, and GPCR. Form the point of molecular function, these genes mainly have binding and receptor functions.

Testes-bF cluser

Several gene transcripts were found to be enriched in both testes and bF, but not in bO. This suggests that some genes might have the same function in the testes and vitellarium, but not in the ovary. Figure 3.31 shows their expression profiles.

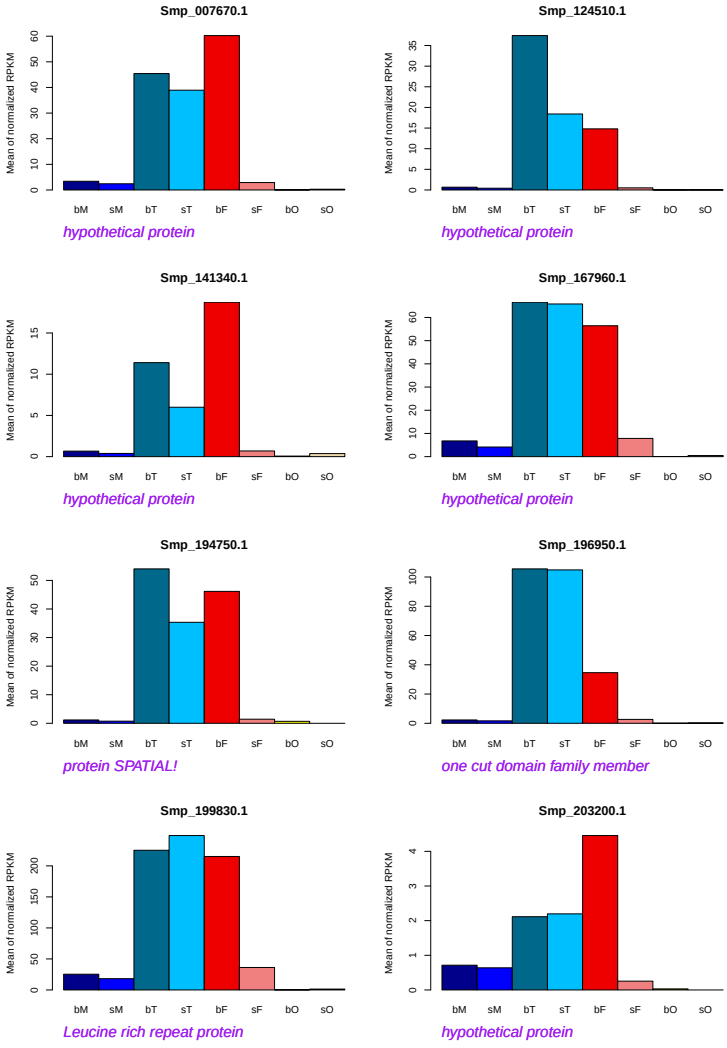

Figure 3.31: Expression profiles of transcripts enriched in testes and bF. Because these genes are barely transcribed in the ovary, they possibly function in both testes and the vitellarium.

3.3.13 Potential house-keeping genes

Surprisingly, in these data sets, a number of commonly used house-keeping genes including *actin*, *tubulin* and *GAPDH*, were found to be differentially transcribed among the eight samples (see Supplementary file No. 35-1). For instance, GAPDH (Smp_056970) was significantly differentially transcribed between whole worms and

gonads, as well as between bM and sM. The same applied to two actins (Smp_161920 and Smp_161930), which in addition were also differentially transcribed between bF and sF. Therefore, they are not suitable for quantification analyses such as qPCRs. A search for potential house keeping genes with non-significant differences in transcription was performed for i) all samples, and ii) for worm samples only.

House-keeping genes for all samples

A total of 15 candidate genes were found to be expressed with < 1.23-fold difference between any two samples (FDR > 0.05). Thus, they might be suitable as housekeepers for all samples (Table 3.24; Supplementary file No. 35-2).

Table 3.24: Potential house-keeping genes for all sample comparisons

Gene_ID	Product
Smp_005050.1	oxidoreductase HTATIP2
Smp_008900.1	[K] eukaryotic translation
Smp_018760.1	[K] neutral alpha glucosidase AB
Smp_048940.1	[K] vacuolar protein sorting-associated protein
Smp_064020.4	[K] PAB-dependent poly(A)-specific ribonuclease
Smp_065110.1	[K] LETM1 and EF hand domain-containing protein 1
Smp_073940.1	actin-interacting protein 1
Smp_104960.1	[K] syntaxin 6
Smp_106260.1	transcription factor iib
Smp_129570.1	hypothetical protein
Smp_138760.1	[K] ADP ribose pyrophosphatase, mitochondrial
Smp_152080.1	hypothetical protein
Smp_152510.1	CWF19 protein 1
Smp_153490.1	[K] GDP mannose 4,6 dehydratase
Smp_166290.1	[K] serine:threonine protein phosphatase 2A

House-keeping genes for worm samples

A total of 57 candidate genes did not show significant differences in the transcription level among the worm samples. Besides the 15 genes mentioned above, 42 other candidate genes were potentially suitable as house-keeping genes for worm samples. Table 3.25 shows some examples, the complete list of genes can be found in the appendix 7.5.

Table 3.25: A selection of house-keeping genes for adult worms

Gene_ID	Product
Smp_007260.2	sarco:endoplasmic reticulum calcium ATPase
Smp_012560.1	o-methyltransferase
Smp_012970.1	myotubulari
Smp_096320.1	[K] kelch protein 20 like
Smp_102920.1	[K] tRNA dimethylallyltransferase
Smp_154420.1	[K] clathrin heavy chain
Smp_163640.1	[K] phosphatidylinositol
Smp_186830.1	oligomeric Golgi complex component
Smp_193410.1	mitochondrial uncoupling protein

3.3.14 Expression patterns of genes involved in different biological processes

Genes related to stem cells and neoblasts

From sporocyst-enriched genes analysed in a different study, 581 genes were identified that shared similarities with planarian neoblast-enriched genes (Wang et al., 2013) , indicating their roles in stem-cell proliferation and differentiation. In my data set these genes were expressed at a higher level compared to the average expression level of all genes. This applies in particular for their transcript amounts in the gonads, in which 1.72 to 2.38-fold differences were determined (Table 3.26).

Table 3.26: Average RPKM of neoblast- and sporocyst-enriched (NSe) genes compared to the average of all genes

Sample	Average_all genes	Average_NSe genes	Fold difference
bM	110.2	131.1	1.19
sM	119.9	148.0	1.23
bT	89.4	154.0	1.72
sT	87.0	156.2	1.80
bF	144.9	196.5	1.36
sF	120.4	161.0	1.34
bO	120.9	288.3	2.38
sO	79.8	161.8	2.03

The hierarchical clustering is shown in Figure 3.32. Among these genes, many have been shown in independent studies before to be important for gonad development like polo-like kinase 1 (Long et al., 2012), vasa-like genes 1-3 (Skinner et al., 2012), FGFR a and b (Collins et al., 2013; Hahnel et al., 2014), argonaute (Wang et al., 2013) and PCNA (Wang et al., 2013). Their expression profiles are shown below (Figure 3.33).

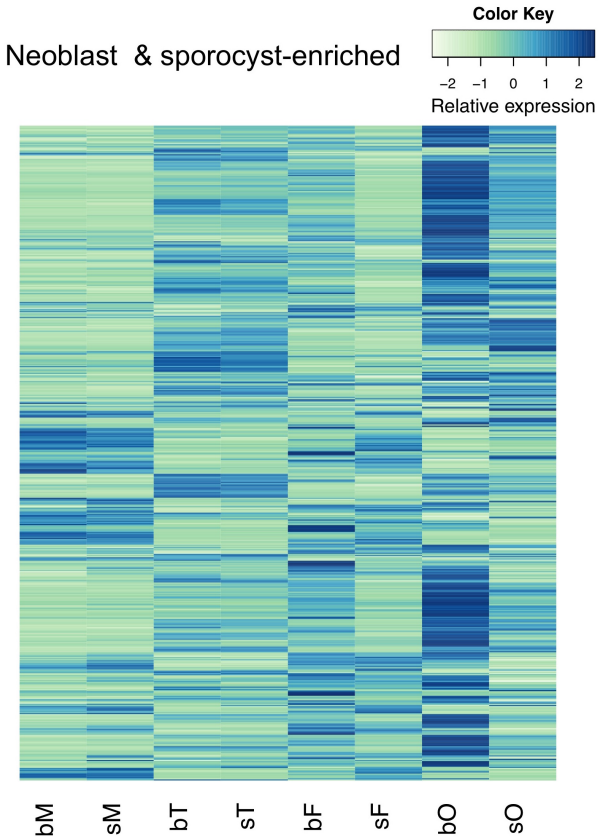

Figure 3.32: Hierarchical clustering of neoblast- and sporocyst- enriched genes. Many of those stem cell-related genes have highest expression in bO indicating higher mitotic activity.

Genes involved in neural development

With regard to a former study from our lab where evidence was obtained for roles of neuronal processes during male-female interaction (Leutner et al., 2013), I also checked genes that are involved in such processes. Of 61 genes predicted in a previous study to be involved in neural processes (Berriman et al., 2009), 39 were found in my study to be transcribed in the adult stage (Figure 3.34).

Among these, Smp_051410 (a junction protein with a claudin domain), and Smp_141250 (protein jagged) showed preferential expression in testes. Smp_166150 (maternal embryonic leucine zipper kinase, MELK) was expressed preferentially in

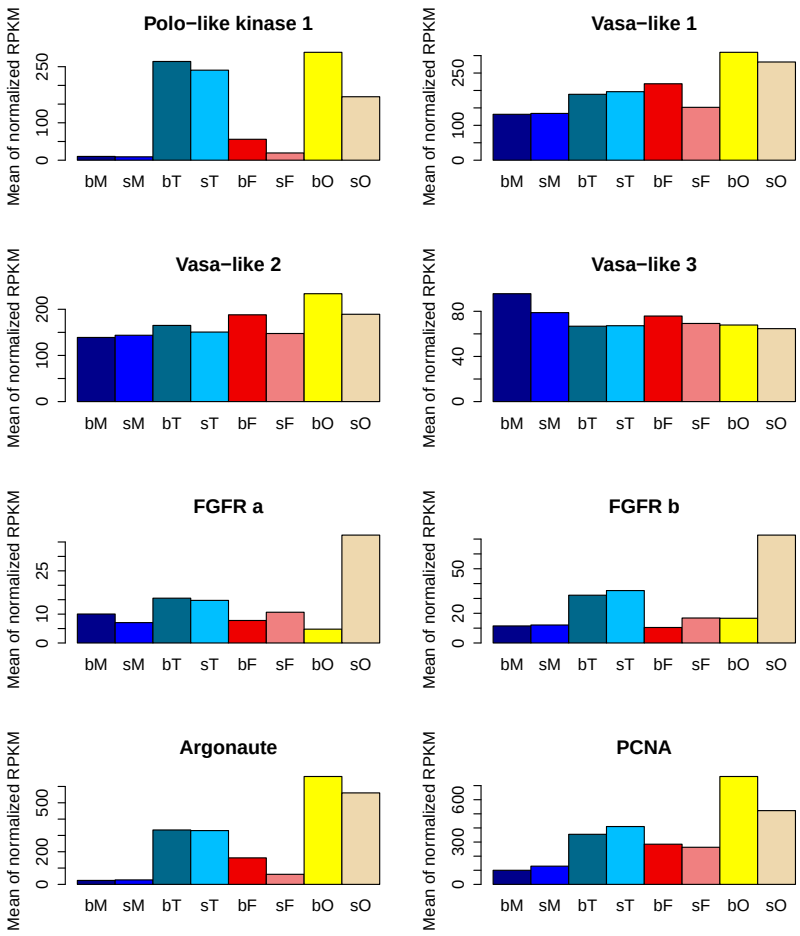

Figure 3.33: Expression profiles of selected genes. These genes have been shown in other studies to be related to stem cell functions. Here they are demonstrated to be transcribed in both gonads.

testes and ovaries. Smp_186930 (homeobox protein nk2) and Smp_135370 (neurogenic locus protein delta like) were preferentially expressed in bO and sO, respectively.

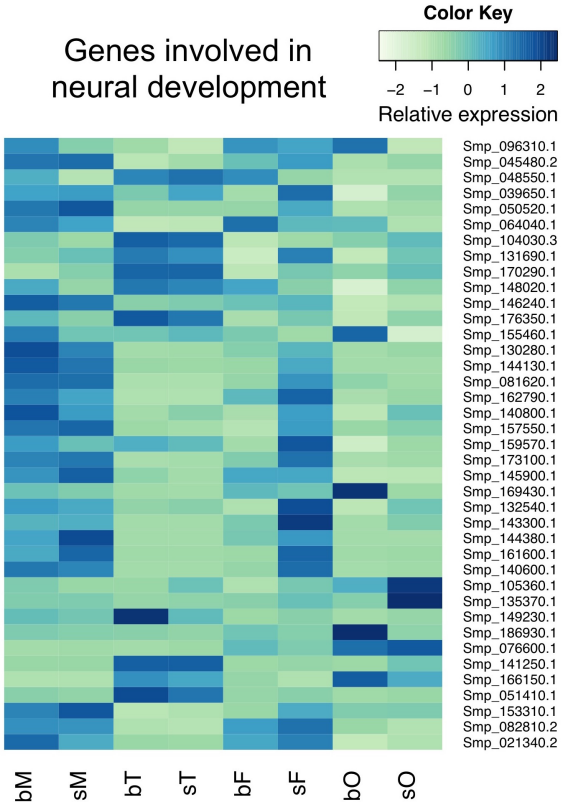

Figure 3.34: Hierarchical clustering of genes related to neural development. Among the 39 analysed genes, several showed dominant expression in testes and/or ovaries.

Neuropeptides

Neuropeptidergic signaling is known to play fundamental roles in flatworm locomotion, reproduction, feeding, host-finding and regeneration (McVeigh et al., 2005). A recent study highlighted the importance of neuropeptides in planarian germline development (Collins et al., 2010). A BLAST approach was performed before to identify potential neuropeptides and precursors in flatworms (McVeigh et al., 2009). Of these some occur in the obtained dataset being highly expressed in gonads: Sm-npp-19 (Smp_044680.1) and Sm-npp-17 (Smp_056360.8) were transcribed in testes and ovaries, Sm-npp-16 (Smp_138560.1) only expressed in testes, Sm-npp-5 (Smp_052880) only in sO, Sm-npp14 (Smp_150650.1) predominantly in sO and a few transcripts in testes (Figure 3.35). A gene predicated to encode a NPF-like peptide (*npy-8*) was demonstrated to be required for maintaining reproductive tissues in

planarian (Collins et al., 2010). *S.mansoni* has two NPY-like prohormone genes: Sm-npp-20a (Smp_088360, 48% similarity with *npy-8*) and Sm-npp-20b (Smp_159950, no significant similarity with *npy-8*), but both genes seem to be low-abundantly transcribed in the gonads (RPKM < 0.4 in all gonads, numbers not shown) (Figure 3.35). Furthermore, a prohormone convertase gene (Smp_077980) showed very low abundance in bT and bO (RPKM < 1.2 in both). The detailed transcription profiles of these genes are included in Supplementary file No. 36.

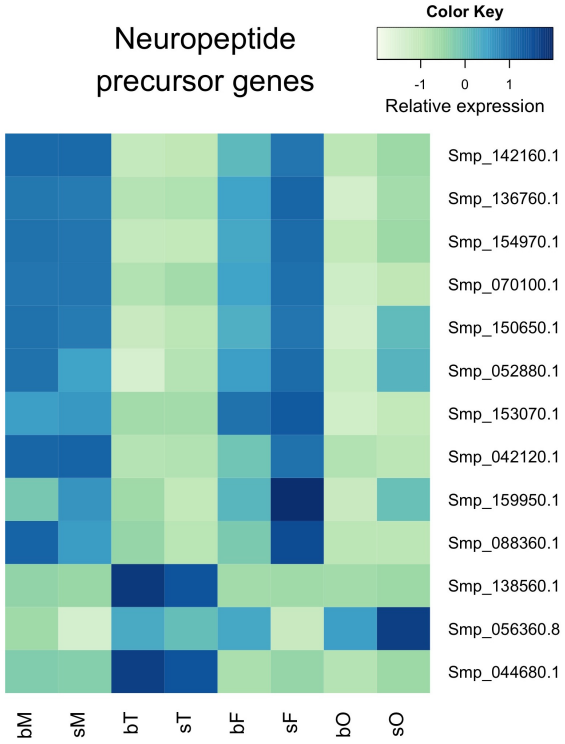

Figure 3.35: Hierarchical clustering of neuropeptide precursor genes. Most of them are enriched in the whole worms.

Protein kinases

Among the 233 protein kinases identified in *S.mansoni* (Andrade et al., 2011), 208 were found to be transcribed in the adult stage (Figure 3.36). Apart from previously well characterized cellular PTKs (SmTK3, SmTK4, SmTK5 and SmTK6), 32 kinases were highly preferentially expressed in the gonads compared to the whole worms, including several CDKs and STKs (Appendix 7.6).

Besides, RPKs preferentially transcribed in specific organs (independent from the above worm-gonad comparison) were also identified. For example, Smp_152680, an epidermal growth factor receptor (EGFR), was found to be dominantly transcribed in

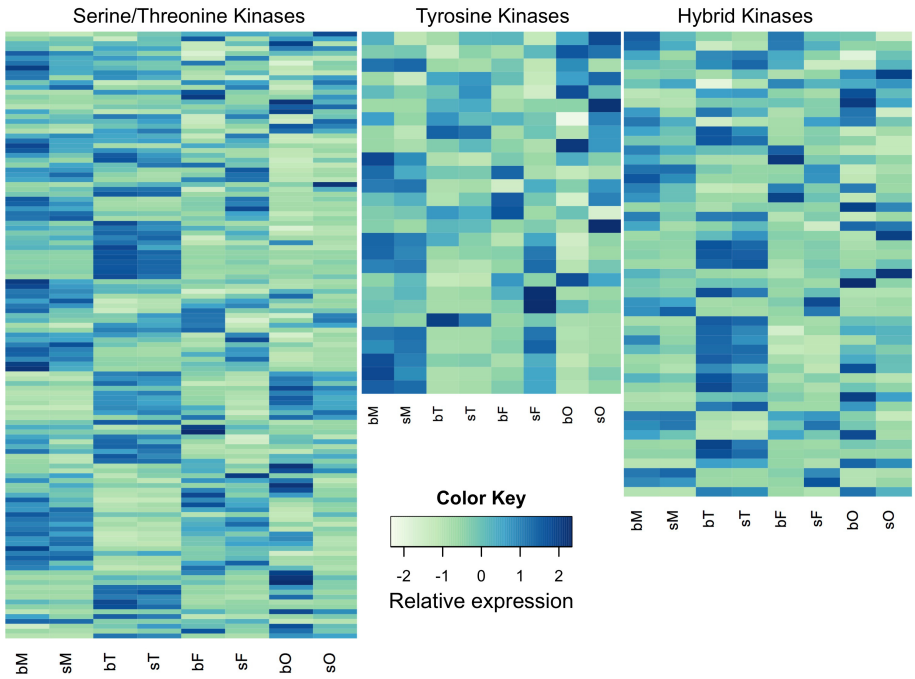

Figure 3.36: Hierarchical clustering of genes encoding protein kinases. These genes are grouped into three categories (serine/threonine kinases, tyrosine kinases and hybrid kinases) and their expression among all samples are shown.

testes with a higher RPKM in bT. Genes with similar expression patterns were also found (Smp_132260, Smp_166540, Smp_009800, Smp_097940 and others). Genes with highest preferential expression in bO included Smp_177120, Smp_125060, Smp_162710 (hybrid protein kinases); Smp_124850 and Smp_172200 (tyrosine kinases); and Smp_136270, Smp_073510, Smp_172240 (serine/threonine kinases). Interesting, several genes that have recently been characterized as important for stem cell in *S. mansoni*, including the FGFR a and b, were found to have highest transcription level in sO.

Transcription factors

Sequence-specific transcription factors were determined based on the conserved domain information (see section 2.7.8). The number for each type in the gonads is shown below (Table 3.27).

By comparing *S. mansoni* genes with the KEGG database, 62 transcription factor orthologs were identified. The complete list and gene expression patterns are available in Supplementary file No. 37. There are several transcription factors that were found to be differentially transcribed in testes and ovaries. For instance,

Smp_062490, a HLH transcription factor, Smp_155250, a hormone receptor, and Smp_175410, which encodes a zinc finger factor protein, were expressed in testes but not in ovaries. Smp_166560, a zinc finger protein gene, was expressed in ovaries but not in testes.

Table 3.27: Numbers of sequence-specific transcription factors

TF classification	bT	sT	bO	sO
POU	2	2	2	2
Homeodomain	22	20	11	14
Forkhead	10	10	5	9
ETS	4	5	2	3
Helix-loop-helix	16	16	15	17
Nuclear hormone receptor	5	5	7	6
Zinc finger, C2H2	25	25	24	23
Transcriptional enhancer factor	3	3	3	2
HMG-box	11	12	13	14
Transcription coactivator	24	24	24	28
Basic-leucine zipper	19	20	20	16

3.3.15 Summary of genes essential for germ-cell development and their orthologs in *S. mansoni*

In *Drosophilla*, genes involved in oogenesis function during different stages of germ-cell development (see http://www.sdbonline.org/sites/fly/aimorph/oocyte.htm for detailed information). Among these (i) some genes are required in the early stage for maintenance and devision of germline stem cells, including armadillo domain-containing genes, *nanos*, *piwi*, *dishevelled*, *bmp*, *vasa* and others; (ii) some genes affect the cytoskeleton, such as *diaphanous*, *frizzled*, *kelch* and PTK-coding genes; and (iii) some genes are involved in cell cycle control including cyclins, CDKs, etc (see Supplementary file No. 38 for relevant expression profiles).

For gene expression in *Drosophilla* testis, the majority of transcription occurs in spermatocytes, which provide products that are required for the elaborate program of spermatid differentiation. For the germinal stem cell (GSC) self-renewal, the JAK-STAT pathway was found to be activated by the cytokine-like ligand *Unpaired* in hub cells (Fuller and Spradling, 2007).

Table 3.28: *S. mansoni* orthologs of genes that are essential for germ-cell development

Gene name	Classification	*Sm* ortholog	Transcript	Function and reference
vasa / *vasa-like*	RNA-binding	Smp_033710, Smp_068440, Smp_154320	Te+Ov	Oocyte differentiation (Styhler et al., 1998); promoting *gurken*, *nanos* and *oskar* mRNA translation (Tomancak et al., 1998; Breitwieser et al., 1996)
nanos	zinc finger	Smp_055740, Smp_051920.2	Te+Ov, sO>bO	translational repression (Forbes and Lehmann, 1998; Deshpande et al., 1999)
tudor (domain)	binding to methylated arginine or lysine residues	Smp_081570	Te+Ov, bO>sO	germ plasm formation (Boswell, 1985), protein-protein interactions (Arkov et al., 2006)
pumilio	RNA-binding	Smp_155000, Smp_180910	Te+Ov	translational repression together with *nanos* (Forbes and Lehmann, 1998), spermatocyte differentiation (Subramaniam and Seydoux, 2003; Chen et al., 2012)
argonaut	binding to small non-coding RNAs	Smp_179320	Te+Ov	maintenance of germline stem cells (Yang et al., 2007)
elav	RNA-binding	Smp_194950	Te only	neuronal differentiation and maintenance (Borgeson and Samson, 2005); spermatid differentiation (Sekii et al., 2009)
armadillo	adherens junction	Smp_105950, Smp_176850, Smp_180680	Te (+ Ov)	cell adhesion and cytoskeleton (Peifer et al., 1993)

dishevelled	cytoplasmic phospho-protein	Smp_020300, Smp_162410	Te+Ov	maintenance and division of germline cells (Wallingford and Habas, 2005)
mago nashi	novel protein	Smp_103470	Te+Ov, bO>sO	germ plasm assembly (Newmark and Boswell, 1994); germline stem cell differentiation (Parma et al., 2007); spermatogenesis (van der Weele et al., 2007)
kinesin	motor protein	multiple	various	germ plasm aggregation (Robb et al., 1996); intracellular polarity (Januschke et al., 2002)
tektin	microtubule stabilizing	multiple	Te preferential	sperm axonemal microtubule–binding (Cao et al., 2006); sperm motility (Roy et al., 2009)
kelch	actin cross-linking	multiple	various	ring canal organization during oogenesis (Robinson and Cooley, 1997)
Arf/Arl	GTP-binding	multiple	various	spermatogenesis (Jacobs et al., 1998)
serpin	serine protease inhibitor	Smp_062080, Smp_062120, Smp_090080, Smp_155530/50/60	Te+Ov	sperm motility and maturation (Zhao et al., 2012; He et al., 2013)

3.3.16 Genes encoding hypothetical proteins

For all the expressed genes, 1,537 were identified to have no obvious conserved domain by NCBI-Batch-CD search, and at the same time they are actually annotated as "hypothetical" on GeneDB. Among them, 238 genes were enriched in gonads indicating potential roles in gonad development, and 343 genes were enriched in whole worms. The rest (956) did not have a significantly different tendency with respect to transcriptional activity (Figure 3.37). The complete transcription profiles for these genes can be found in Supplementary file No. 39.

Figure 3.37: Hierarchical clustering of genes encoding hypothetical proteins. Genes enriched in gonads (238) or whole worms (343), as well as those expressed at similar level between worms and gonads (956), are clustered separately.

3.4 Other tissues obtained by the organ-isolation approach

During the isolation of the gonads, also other tissues were occasionally obtained. This included the vitelloduct and ootype from females, but also gut fragments from both genders. Some males contained pseudo ovaries (Beckmann et al., 2010b), which could also be isolated (Figure 3.38).

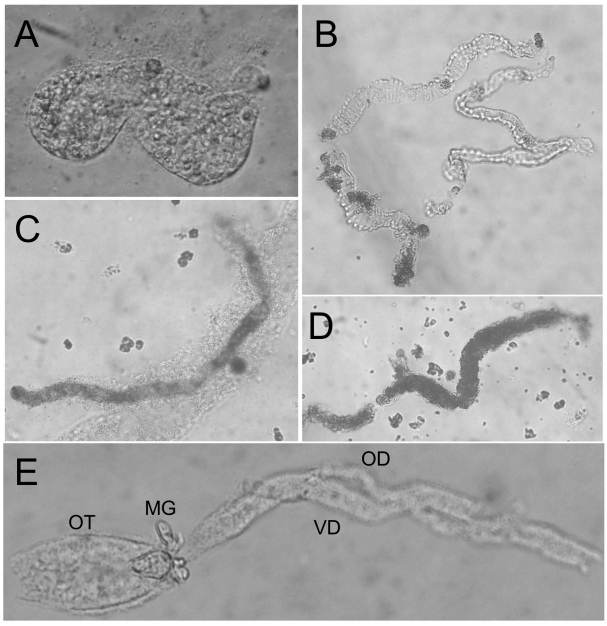

Figure 3.38: Other tissues that were obtained by the organ-isolation approach. A: a pseudo ovary from a male generated by single-sex infection; B: muscle tissue of a female; C: gut fragment of a female; D: a vitelloduct fragment; E: an ootype (OT) with vitelloduct (VD) and oviduct (OD), as well as Mehlis' gland tissue (MG).

3.5 Isolation and primary characterization of vitelline cells

3.5.1 Light microscopy

By a slightly modified protocol based on the organ isolation method, vitellarium tissue and vitelline cells were isolated. Starting with 50 females about 1-5 x 10^5 vitelline cells were obtained.

A previous study showed that vitelline cells undergo four different developmental stages (S1-S4, (Erasmus, 1975)). S1 cells are precursor vitelline cells with a stem cell-like character, having a dominant nucleus and a small amount of cytoplasm. S2- and S3-cells are intermediate stages in which the synthesis of different structures and cell type-specific compounds have been initiated. Besides, the cell volume increases and the proportion nucleus/cytoplasm changes. S4 cells represent the final differentiation stage with the highest amount of cytoplasm and the largest cell size. Besides vitelline droplets accumulating at the periphery of the cell, lipids, and ribosomal complexes appear (Erasmus, 1975).

In my isolates, vitelline cells at various stages of development were obtained. Occasionally vitellarium fragments were also recovered, however, it appeared difficult to harvest them with sufficient purity (Figure 3.39)

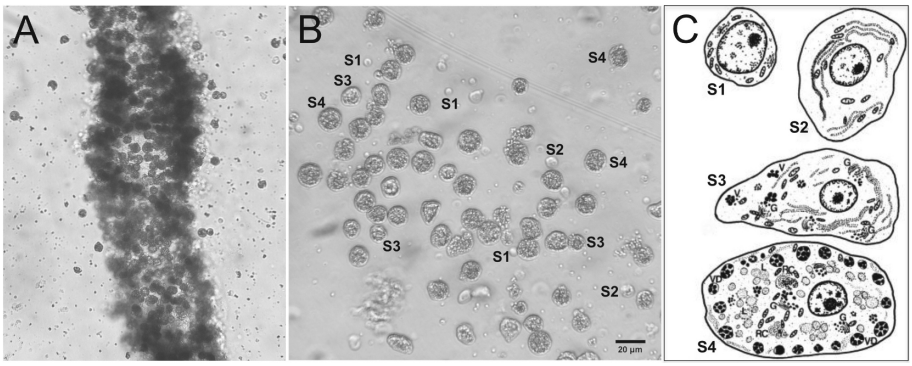

Figure 3.39: Vitellarium tissue and vitelline cells from *S. mansoni* (Lu et al., 2015). A, vitellarium tissue obtained by the organ isolation method. B, vitelline cells collected from fragmented vitellarium tissue. The different sizes and granularities of the cells are representative for the four differentiation stages (S1-S4) occurring inside the vitellarium. C, schematic diagram (modified from (Erasmus, 1975)) showing the four different stages of vitelline-cell differentiation. V, vitelline globules; G, Golgi complexes; VD, vitelline droplets; L, lipids, RC, ribosomal complexes. Scale bar: 20 µm.

Vitelline droplets contain egg-shell precursor proteins, which will be exocytosed to be cross-linked for egg-shell formation (Smyth and Clegg, 1959). During cross-linking, tyrosine-rich precursors are oxidized and this reaction is accompanied by autofluorescence (Cordingley, 1987). The latter covers a wide spectrum, a biological sid effect that is of use for further analyses as reported below. Furthermore, fluorescent dyes such as SYTOX Orange, which was used as a cell vitality indicator, were applied for characterization purposes.

With respect to the known characteristics of mature S4 vitellocytes, staining with Hoechst 33342 was expected to visualize a blue intact nucleus by fluorescence microscopy. In addition green autofluorescing signals were expected in the intracellular periphery of vital S4 cells indicating the presence of vitelline droplets. By a combined staining of Hoechst 33342 and SYTOX Orange, it was expected that dead cells exhibited purple nucleus with red dots in its periphery (Figure 3.40).

The staining of isolated vitellaria (Figure 3.41) and vitelline cells (Figure 3.40) with these dyes indicated that most isolated cells were vital. Cells without autofluorescence represented potential S1 cells because their size is small and because vitelline droplets synthesis has not started at this stage.

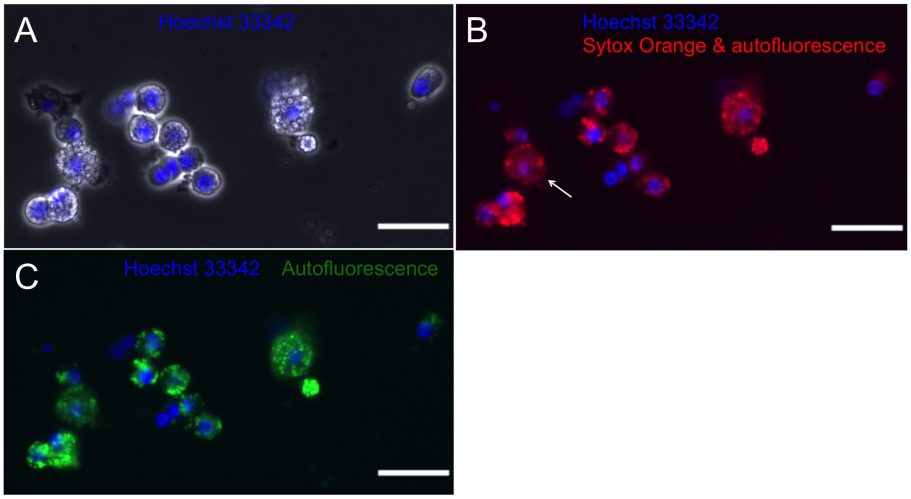

Figure 3.40: Vitelline cells stained with Hoechst 33342 and SYTOX Orange. A: overlay picture of phase-contrast and Hoechst 33342 staining. Nuclei are shown in blue color; B: overlay of Hoechst 33342 (blue) and Syotx Orange (red), which allows to distinguish between vital and dying or dead cells. The arrow shows a dead cell with purple nucleus C: overlay of Hoechst 33342 (blue) and autofluorescence (green) indicating vitelline droplets, whose amount depends on the differentiation status. Scale bars: 25 μm.

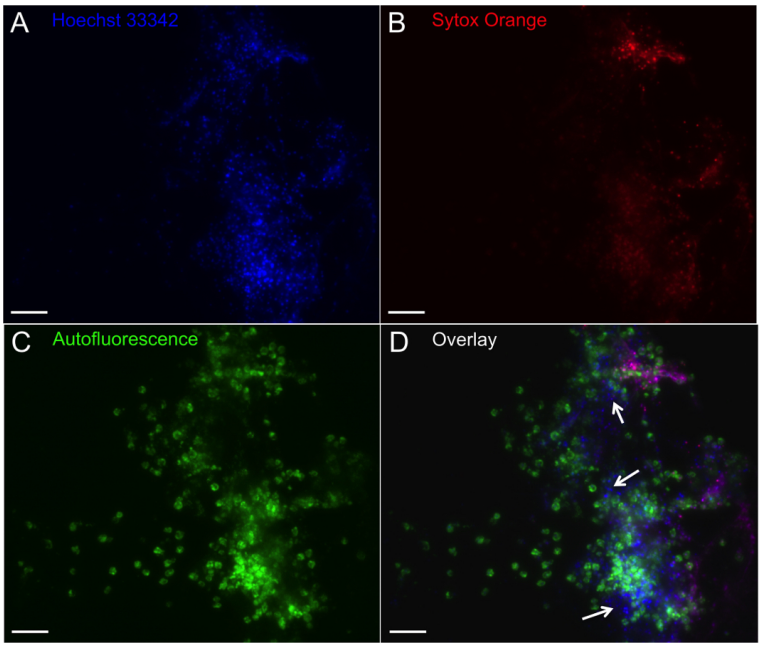

Figure 3.41: Vitellarium tissue stained by Hoechst 33342 (A) and SYTOX Orange (B). Autofluorescence originating from vitelline droplets within vitelline cells appears green (C). Cells without autofluorescence are potential S1 cells (D, see arrows) (Lu et al., 2015). Scale bars: 50 μm.

3.5.2 Identification of S1 to S4 cells

Besides their varying sizes, S1-S4 cells were identified on the basis of vitelline droplets accumulating during the differentiation to mature S4 cells. This coincided with the appearance of green fluorescence. By a combination of phase-contrast and fluorescent microscopy, S1-S4 cells were primarily classified by the intensity of autofluorescence and the nucleus/cytoplasm ratio (Figure 3.42). A S1 cell exhibits a large nucleus and no autofluorescence. S2 cells have very few vitelline globules surrounding the nucleus and the cytoplasm was slightly enlarged. S3 cells show accumulating signals of autofluorescence, and S4 cells besides the largest amount of autofluorescence also the largest size.

Another characteristic of differentiating vitelline cells is the accumulation of lipids (Erasmus, 1975; Furlong, 1991), which parallels the occurrence of vitelline droplets. Staining revealed lipid enrichment during vitelline cell differentiation (Figure 3.43) supporting the previous classification of S cells.

These results demonstrated that S1-S4 vitelline cells can be obtained by the organ-isolation approach (Lu et al., 2015). The identification of different developmental stages were based on cell size, intensity of autofluorescence and lipid content.

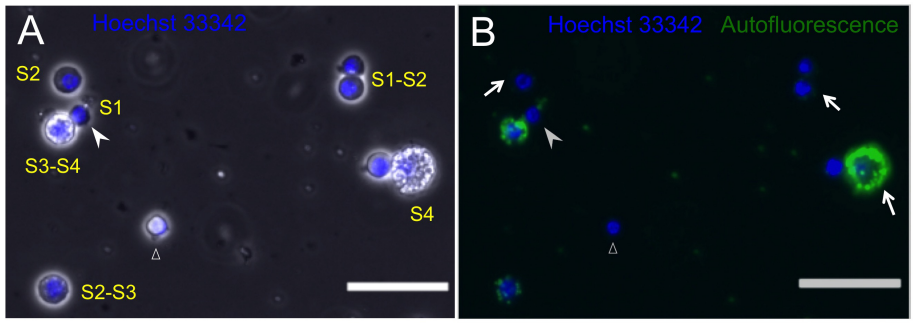

Figure 3.42: Vitelline cells analysed by phase-contrast (A) and fluorescence microscopy (B). A S1 cell (arrow head) contains a large nucleus relative to the cytoplasm, and doesn't show any autofluorescence. The lowest amount of vitelline globules is characteristic for S2-cells that have just started differentiation, whereas S4 cells contain the highest amount of vitelline droplets, which are deposited at the periphery of the cells (see arrows) (Lu et al., 2015). Occasionally, interstitial cells (open triangle; perfectly round nucleus) occur in the preparation. Nuclei were stained by Hoechst 33342 (blue), and fluorescence microscopy was done using an Olympus IX81 microscope. Scale bars: 25 μm.

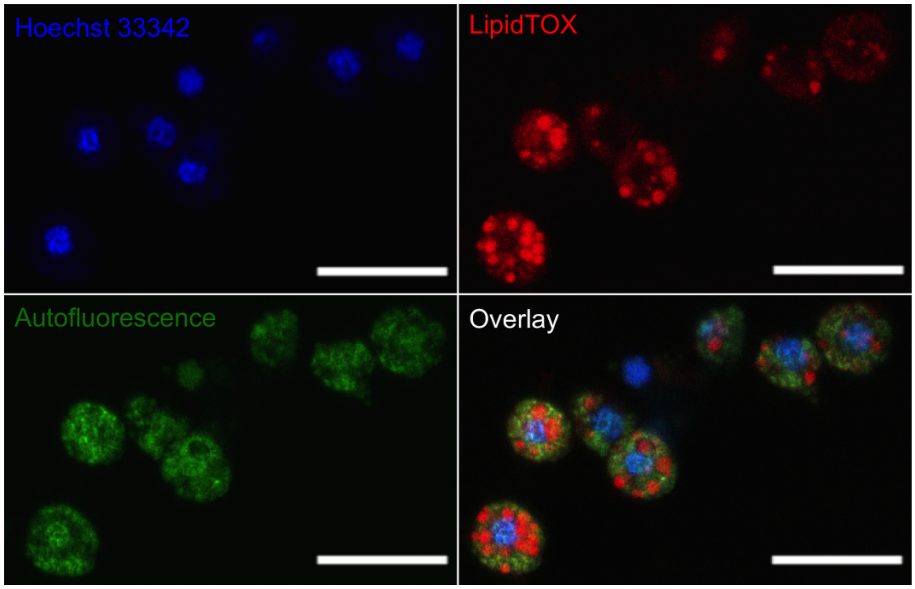

Figure 3.43: Staining of vitelline cells with a neutral lipid stain analysed by CLSM. Analogous to vitelline droplets, lipids accumulate as droplets in vitelline cells during differentiation (Lu et al., 2015). Shown are mainly S3-S4 cells that have accumulated vitelline (green) as well as lipid droplets (red). Nuclei were stained by Hoechst 33342 (blue). Scale bars: 37.5 µm.

3.5.3 Adhesion of vitelline cells

For cell culture as well as a cell characterization purposes it is of importance to find ways for cell adhesion to cell culture dishes and/or glass slides. To adhere vitelline cells to the glass slide for imaging purposes, different substances were tested (see section 2.8). The result showed that laminin alone was not efficient enough to adhere vitelline cells. Testing further substances showed that PLL (poly-L-lysine) + laminin worked best followed by Cell-Tak (hand-spreading), Cell-Tak (absorption, not stable) and serum only. It did not make a difference whether the slide was pre-coated with serum or not. Finally, PLL in combination with laminin was chosen for slide coating. Both coating the whole slide or only in the center worked well, but the center area appeared to be sufficient to adhere cells for imaging purposes.

3.5.4 Electron microscopy

By scanning electron microscopy (SEM), the sizes of differentiating vitelline cells were determined, which varied from about 5 µm for S1, to 6-8 µm for S2, 8-10 µm for S3, and > 10 µm for S4 cells. Vitelline and lipid droplets were detected in damaged S4 cells (Figure 3.44) and revealed sizes of about 0.5-1 µm as determined by SEM.

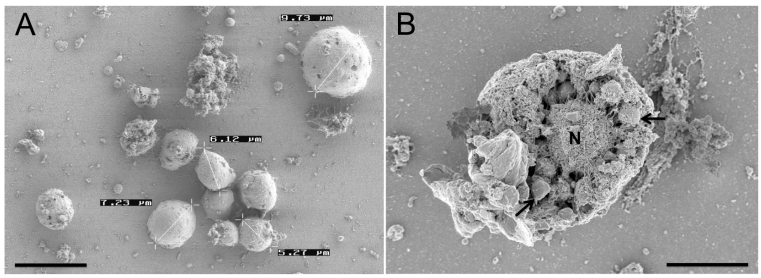

Figure 3.44: Scanning electron microscopy (SEM) analyses of vitelline cells showing the different sizes of S1-S4 vitelline cells (A; as indicated; scale bar: 10 μm), which vary from about 5 μm (S1) to 10 μm (S4). Furthermore, vitelline and/or lipid droplets (see arrows) were detected within an opened vitelline cell (B; scale bare: 5 μm), which according to size (> 10 μm) and content represents a mature S4 cell (Lu et al., 2015). Cell diameters are given as indicated. N = nucleus.

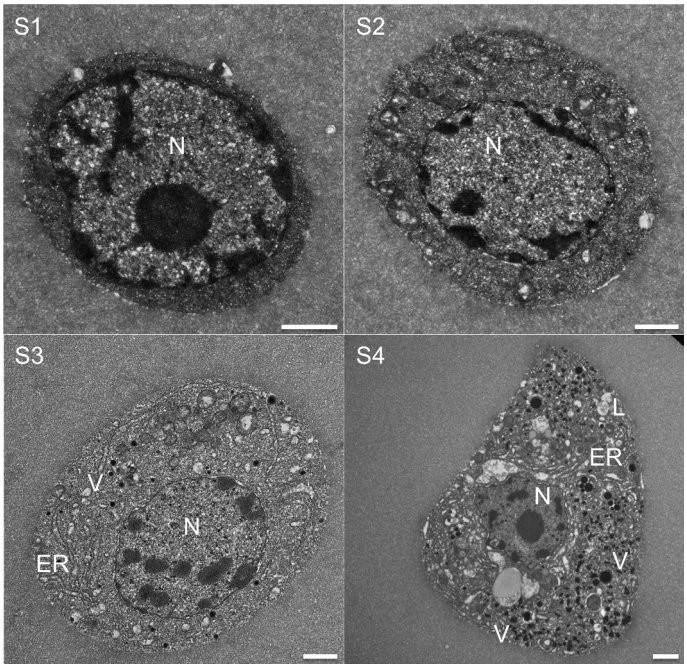

Figure 3.45: Transmission electron microscopy (TEM) analyses of S1-S4 vitelline cells. The following sizes correspond to longitudinal diameters. S1-cells (5 μm) are stem-cell like with a large nucleus relative to the cell volume, and with scattered patches of heterochromatin. Lipid and vitelline globules syntheses start from the S2 stage (7 μm) on and continue through the S3 stage (9 μm), where scattered vitelline globules are clearly visible (V). Finally, vitelline globules form into vitelline droplets and accumulate at the periphery of mature S4 cells (> 10 μm), which show a small nucleus relative to the cell volume (Lu et al., 2015). The cytoplasm is remarkably enlarged at this stage and additionally contains closely packed ribosomes and granular endoplasmic reticulum (ER), which reveals an electron-dense appearance (Erasmus, 1975). N = nucleus. Scale bars: 1 μm.

Transmission electron microscopy (TEM) finally confirmed the size-based classification of S-cells supported by the composition of the cytoplasm of these cells. In contrast to S1-cells, which were characterized by a high nucleus/cytoplasm ratio and nearly no granular content of the cytoplasm, mature S4 cells exhibited the lowest nucleus/cytoplasm ratio but the highest amount of granular content (Figure 3.45). From the EM analyses, cell size and cellular component-based sub-classification of S1-S4 cells were also achieved.

3.5.5 RT-PCR to identify genes transcription in vitelline cells

To characterize vitelline cells at the molecular level, transcriptional analyses were performed by RT-PCR. Following extraction from vitelline cells, the quality of total RNA was tested first by electropherogram analysis indicating a similar quality to RNA obtained from adult females and no significant degradation as proven by the integrity of the 18S rRNA (Figure 3.46. The 28S rRNA was not observed, which is due to a gap region within the 28S RNA molecule of *S. mansoni* leading to its dissociation into two fragments (van Keulen et al., 1991).

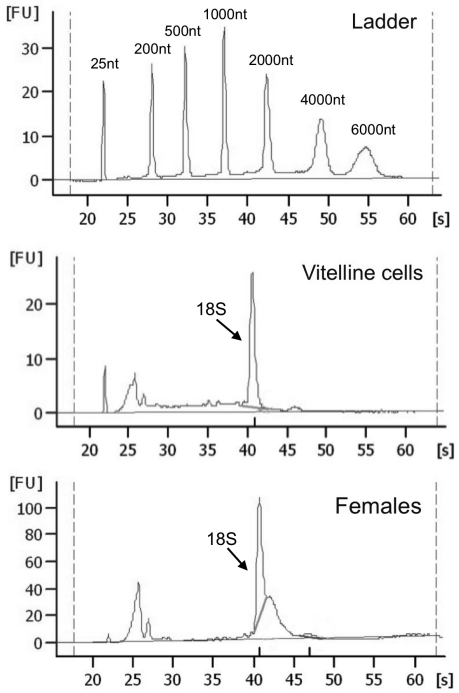

Figure 3.46: Electropherogram (Agilent Bioanalyzer) confirming the high quality of the RNA isolated from vitelline cells and adult females as control. FU: fluorescent units, s: retention time.

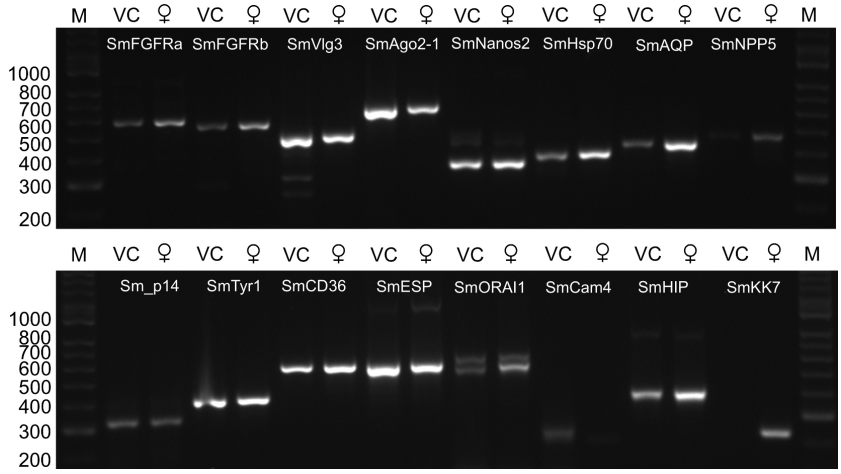

Figure 3.47: Gene transcription in vitelline cells identified by RT-PCR. For the identification of specific transcripts by RT-PCR, primers (Table 2.2) against the following genes were used: SmFGFR a and SmFGFR B (fibroblast growth factor receptors A, B), SmVlg3 (vasa-like 3), SmAgo2-1 (argonaut), SmNanos2 (nanos), SmHsp70 (heat shock protein 70), SmAQP (aquaporin), SmNPP-5 (nucleotide pyrophosphatase/phosphosdiesterase type 5), Sm_p14 (egg shell precursor protein), SmTyr1 (tyrosinase), SmCD36 (HDL cholesteryl ester receptor), SmESP (egg shell precursor protein), SmORAI1 (transmembrane calcium channel protein), SmCam4 (calmodulin 4), SmHIP (hippocalcin), and SmKK7 (potential potassium channel blocker). In each case the occurrence of transcripts in vitelline cells (VC) versus females (♀) was tested (Lu et al., 2015). Marker (M) = Hyperladder I (Bioline).

As targets for RT-PCR analyses the following genes were tested for their transcriptional activities (see also Table 2.2 for primer sequences): (i) genes with already proven localization and/or function in the vitellarium such as the egg-shell precursor protein genes Sm_p14 and SmESP, or the tyrosinase SmTyr1, which is discussed to be important for egg-shell formation processes, the Ca^{2+}-metabolism-associated genes SmORAI1 (transmembrane calcium channel protein), SmCam4 (calmodulin 4), and SmHIP (hippocalcin, a member of the calmodulin superfamily), and the fibroblast growth factor receptor SmFGFR B, (ii) genes with potential roles in gonad and/or reproduction- associated processes such as SmFGFR a, SmVlg3 (vasa-like 3), SmAgo2-1 (argonaut), SmNanos2 (nanos), and SmCD36, a HDL cholesteryl ester receptor discussed to be important for embryogenesis, (iii) genes that seem to be ubiquitously transcribed such as SmHsp70 (heat shock protein 70), and finally (iv) genes with yet unknown and/or unexpected function in the vitellarium such as SmNPP-5 (nucleotide pyrophosphatase / phosphos- diesterase type 5) that was preferentially localized in the tegument of adult worms before, the aquaporin SmAQP that also occurs in the tegument of adult

but was additionally found to be transcribed in testes, and SmKK7, a potential potassium channel blocker detected before to be expressed in peripheral nerve endings of adult *S. mansoni*.

The RT-PCR results showed that all genes except SmKK7 were transcribed in vitelline cells (Figure 3.47). These results confirmed the identity of vitelline cells at the molecular level (Lu et al., 2015).

3.5.6 Vitality testing of vitelline cells by Ca^{2+}-imaging

As a measure for cell vitality, Ca^{2+} signaling was investigated. To this end, freshly isolated vitelline cells were stained with Fura-2 and superfused with a standard Tyrode´s solution containing Ca^{2+} for stabilization. Thereafter, the solution was exchanged with Ca^{2+}-free Tyrode´s solution. Removing extracellular Ca^{2+} induced a decrease in the Fura-2 ratio signal (Figure 3.48) reflecting Ca^{2+} efflux from the cytosol into the extracellular medium.

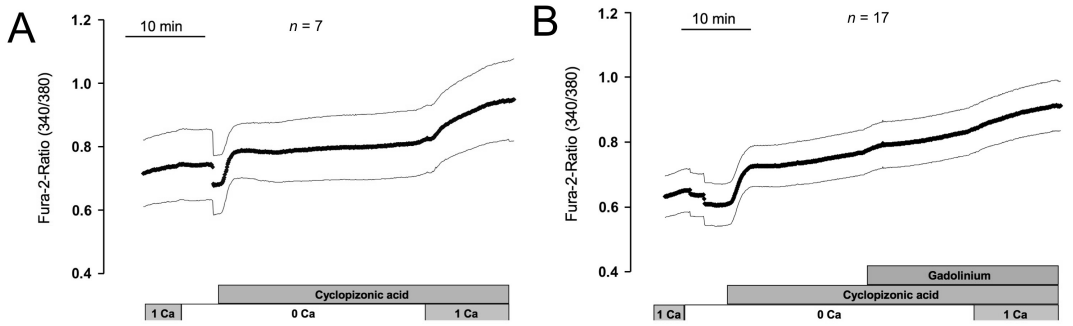

Figure 3.48: Ca^{2+} fluxes in vitelline cells of *S. mansoni* determined by Fura-2 imaging analysis. Cells were superfused with a standard Tyrode´s solution (A and B, 1 Ca) containing 1.25 mM Ca^{2+} for approximately 5 min for stabilization and then incubated in Ca^{2+}-free Tyrode´s solution (A and B, 0 Ca). Intracellular Ca^{2+} stores were depleted using CPA (cyxclopiazonic acid, 10 μm). Afterwards, Ca^{2+} was added by superfusing with standard Tyrode in the absence (A) or presence (B) of the Ca^{2+}-entry blocker gadolinium (5 μm; B) (Lu et al., 2015). X-axis, Fura-2 ratio 340/380 nm; values (thick black line) are means ± SEM (parallel thin lines).

Inhibiting sarcoplasmic-endoplasmic reticulum (SERCA) Ca^{2+}-ATPases with cyclopiazonic acid (CPA) led to a rise of the cytosolic Ca^{2+} concentration reflected by a rise of the Fura-2 ratio signal. Usually, the subsequent depletion of intracellular Ca^{2+} stores leads to the opening of capacitative Ca^{2+} channels in the plasma membrane (Parekh, 2006). This was also the case in vitelline cells, as the readministration of extracellular Ca^{2+} evoked a strong rise in the Fura-2 ratio signal,

which was inhibited, when the cells were pretreated with Gd^{3+}, which is known to inhibit capacitative Ca^{2+} entry (Lu et al., 2015).

3.5.7 FACS analyses of vitelline cells

For future purposes concerning the characterization of vitelline cells, it would be of advantage to enrich subclasses of these cells. To this end first attempts were performed to apply fluorescence-activated cell sorting (FACS). Based on the differences in the intensity of autofluorescence, four clusters of cells (S1-S4) were selected for sorting. Although no clear separation in size was observed (Figure 3.49 A), the cells differed significantly in their degree of granularity (Figure 3.49 B).

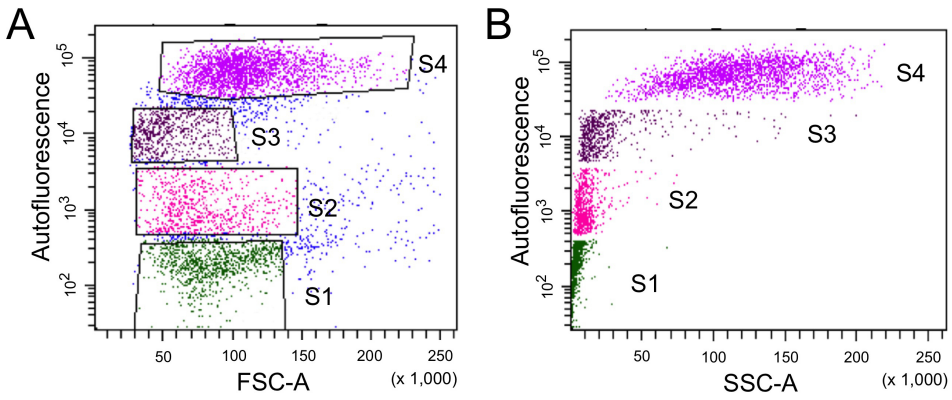

Figure 3.49: Analysis of isolated vitelline cells based on autofluorescence and size or granularity by fluorescence-activated cell sorting (FACS). A: Distribution pattern of isolated cells based on autofluorescence and size (indicated by FSC-A). Cells located in the selected areas were collected after sorting. B: The corresponding distribution pattern of selected cells based on autofluorescence and granularity (indicated by SSC-A).

The obtained cells within each cluster represented the expected sub-populations S1-S4 as determined by morphological criteria (Figure 3.50; Figure 3.39B). Although cells were successfully sorted this way, the total number of cells finally obtained was lower than expected according to the report of the cytometer (around 5% of the total amount). In conclusion, vitelline cells can be sorted and enriched into subclasses at different differentiation stages.

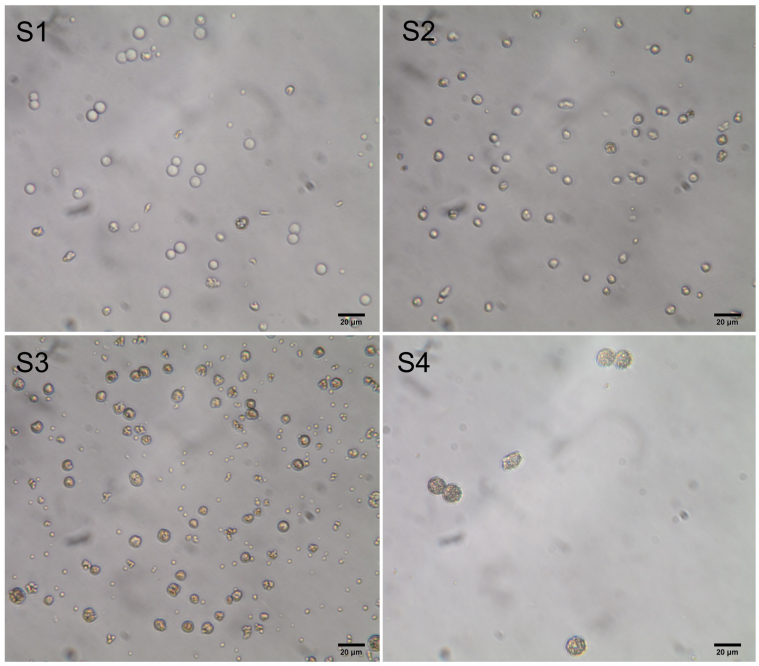

Figure 3.50: Morphology of the obtained cells after FACS. Developmental stages were determined as S1-S4 according to size, shape, and granular content. Scale bars: 20 μm.

3.5.8 Neutral lipids in the vitellaria

As mentioned before, vitelline and lipid droplets are only present in differentiated vitelline cells, and the differentiation process is strictly regulated by pairing. Schistosomes cannot synthesize sterols or free fatty acid *de novo* but they can use complex precursors from the host (Brouwers et al., 1997) to synthesize triacylglycerols (TGs).. As one of the neutral lipids, TG constitutes more than 40% of the lipid content in adult worms, and TG has been shown recently to be essential energy source for egg production (Huang et al., 2012). However, there is no evidence about how male parasites assist females in the synthesis of TGs and how this assistance is associated with the differentiation of viteline cells. To come closer to answers to these two questions, experiments were carried out to stain females from single-sex infection by Oil Red O (ORO).

Oil Red O staining of neutral lipids

By staining whole adult worms from mixed-sex infections, the following tissues were stained by ORO: male tubercles, tegument, vitellaria, and eggs. Ovaries and testes, as well as females from single-sex infection were not stained (Figure 3.51). Similar to the LipidTOX fluorescent dye, ORO can also be used as a dye to indicate the

amount of neural lipids in vitelline cells.

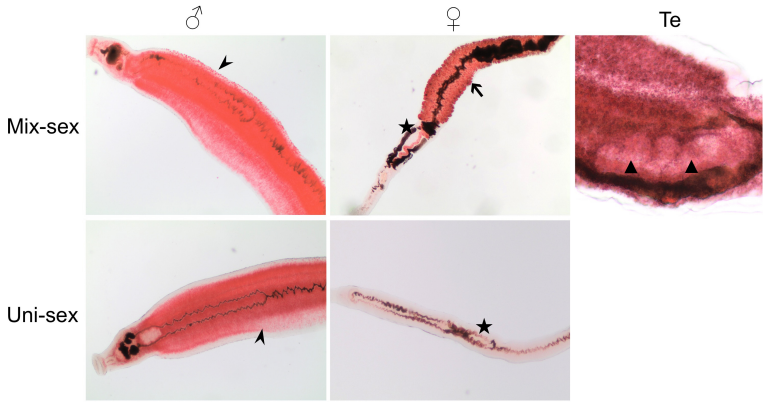

Figure 3.51: Neutral lipids in adult worms stained by Oil Red O. Arrow heads: male tubercles, arrow: vitellarium, stars: ovary, triangles: testis.

Changes in the amount of neutral lipids during *in vitro* culture

Oil Red O staining was also applied to investigate the presence of lipids during culture periods of worms. In contrast to separate males, the amount of neutral lipids dramatically decreased in females after separation of males during 10 days *in vitro*. This effect was also found in paired females and thus appeared to be independent of the pairing status (Figure 3.52).

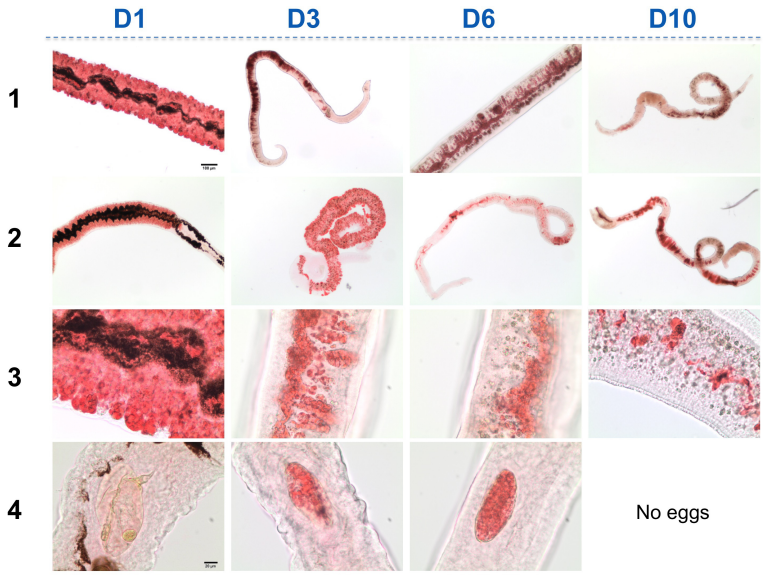

Figure 3.52: Summary of the results of neural lipid staining of *S. mansoni* females in culture. Row 1: separated females in culture (days 1-10 as indicated); row 2: also in paired females the loss of neutral lipids was observed; row 3: close-ups of the vitellarium; row 4: ORO staining in eggs.

In addition, a turnover for neutral lipids was observed in male tubercles and occurred around 3 days in culture (Figure 3.53).

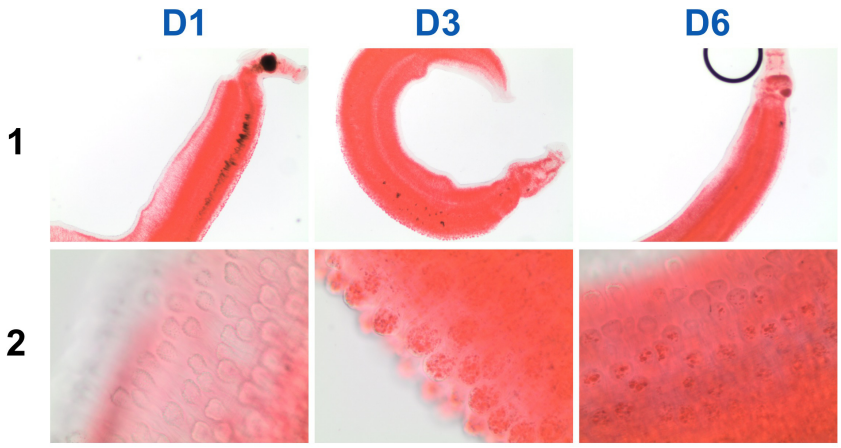

Figure 3.53: Summary of the results of neural lipid staining of *S. mansoni* males in culture (days 1-6 as indicated). Row 1: overview of ORO stain in males; 2: close-ups of tubercles.

Females of single-sex infection in male-conditioned medium

To find out whether male parasites provide or transfer neutral lipids to the females, 5 females obtained by single-sex infection were cultured together with males (bM or sM), or they were cultured in male-conditioned medium (bM or sM in non-supplemented M199 or non-supplemented DMEM or in PBS with 0.1% glucose). The results showed that compared to the control (Figure 3.54 C), pairing dramatically increased the amount of neutral lipids in the posterior area of sF, which was accompanied by the development of vitellaria (cavity formed, and cells appeared) (Figure 3.54 A).

Furthermore, ORO-stained sF cultured in male-conditioned medium showed first signs of vitellaria development (cavity formation), independent of the the pairing status of the males used for collecting the conditioned medium (Figure 3.54 B). However, no further development was observed when sF were cultured for longer time periods up to 6 days.

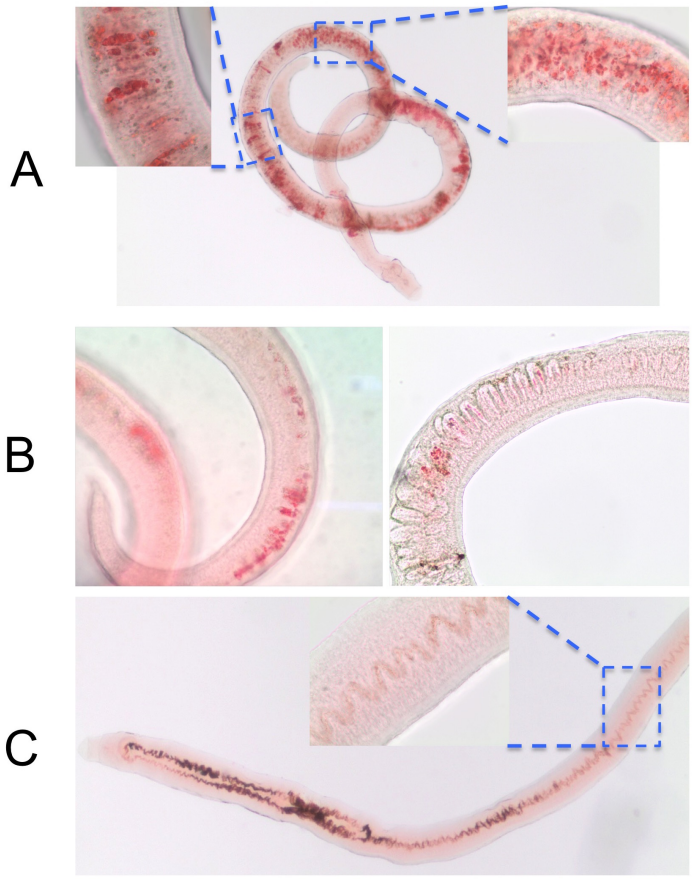

Figure 3.54: Appearance of neutral lipids in sF after pairing with males or in male-conditioned medium. A: sF paired with bM for 1-3 days; B: sF in sM- (left) or bM-conditioned medium (right) for 1-3 days; C: control females.

4 Discussion

Schistosomiasis is still a social-economically important disease for human and animals worldwide. The eggs of schistosomes are not only important for maintaining the completed life-cycle, but also account for pathogenesis. Schistosomes live dioeciously and only paired, fully developed, sexually mature females are capable of producing eggs. Thus it is of great importance to understand the reproductive biology of these parasites. My study focused on the characterization of the gonads from male and female worms, testes, ovaries and vitellaria/vitelline cells at the morphological and molecular levels.

4.1 Characterization of isolated testes and ovaries

4.1.1 Protein expressed in testes and/or ovaries

By Western blotting using antibodies donated by several colleagues the occurrence of proteins was investigated in isolated testes and ovaries, isolated tegument fragments, as well as in whole worms for comparisons. Among these, the schistosome permease SPRM1hc, the heat shock protein HSP70 and the FK506 binding protein FKBP12 were expressed in all samples. Aquaporin protein was not expressed in gonads but in the other samples.

Heat shock proteins (HSPs) such HSP70 are highly conserved, ubiquitous and abundant proteins and have been extensively studied before (Neumann et al., 1993; Levy-Holtzman and Schechter, 1996; Wippersteg et al., 2002; Knudsen et al., 2005; Clerico et al., 2015). SmHSP70 was even found to be part of the egg-shell (DeWalick et al., 2011). In my study, the SmHSP70 protein was found to be abundantly expressed in all worm and tissue samples, which was expected. Hence, it can be used as a house keeper in the analysis.

As a transporter controlling water exchange, aquaporin was detected before to be abundantly expressed in the tegument of adult worms (Faghiri and Skelly, 2009). In

contrast to schistosome adults, aquaporin was not expressed in the gonads but in the tegument. This demonstrates the selectivity of the gonad isolation method and the purity of gonad proteins which seemed to be free of residual tegument proteins.

SPRM1hc was previously characterized as an amino acid transporter and found to be widely distributed throughout adult male and female worms by immunolocalization (Krautz-Peterson et al., 2007). Its high expression in testes and ovaries indicates a further, yet unknown function in gonads.

FKBP12 is a member of the TGFβ-signaling pathway and has been shown before to be transcribed in sub-tegumental cell bodies and in the ovary but not in the testis (Knobloch et al., 2004). In my study SmFKBP12 protein expression was detected in both gonads indicating a role(s) for TGFβ signaling during the reproductive phase of schistosome development, a hypothesis for which independent experimental evidence was obtained before (Freitas et al., 2007; LoVerde et al., 2007; Knobloch et al., 2007; Freitas et al., 2009; Buro et al., 2013; Leutner et al., 2013).

4.1.2 Sub-proteome analyses of ovaries

A first sub-proteome analyses for ovary samples from females obtained from mixed-sex infections resulted in the identification of 814 proteins. This number was lower than expected. This may be due to the technical limitations of the method used to prepared the samples. Although trypsin has been used as a common principle in proteomics, this approach has a limitation: tightly folded proteins might not be digested, resulting in incomplete MS data (Siepen et al., 2007). Therefore, the identified proteins might not represent all proteins present in the ovary. Many proteins that had been supposed to be present were not detected. For instance, *S. mansoni* has three vasa-like genes, SmVlg1, SmVlg2 and SmVlg3, and all have been proven to be transcribed in the ovary (Skinner et al., 2012). However, only SmVlg1 was detected in the ovary sample. Cellular PTKs including, SmTK4, SmTK5 and SmTK6, which were shown before to be transcribed in the ovary (Knobloch et al., 2002b; Beckmann et al., 2010a; Kapp et al., 2001), were also missing. This applied also forthe Src kinase SmTK3, whose presence in the ovary was confirmed before by *in situ* hybridization and immunolocalization (Kapp et al., 2004). By comparing with the ovary transcriptome data, transcripts of genes coding for all identified proteins have been identified.

4.2 RNA-Seq approach

Total RNA was extracted from testes and ovaries as well as from male and female worms to perform RNA-Seq. For the differential gene expression analysis, RPKM < 2 was selected as a cut-off for the background signal. This is arbitrary but a value used in similar studies (Protasio et al., 2012). For choosing the RPKM threshold, there is no predefined value for denoting a gene to be transcribed. A spike-in control approach would be very helpful for this purpose. Besides that, a method for evaluating the cut-off was applied by calculating the false positive and false negative rates from the intronic/intergenic expression (Ramsköld et al., 2009), which is complicated and can be messy. Another study estimated that one transcript copy per cell corresponds to 0.5 to 5 FPKM (fragments per kilobase of transcript per million mapped reads) in polyA$^+$ RNA of whole-cell samples (Kellis et al., 2014).

4.3 Gene transcription in testes and ovaries and the pairing effect

4.3.1 Overview of detected transcripts in the gonads

The RNA-Seq results revealed that > 87% of the transcripts detected in whole worms were also present in the gonads. A recent study conducted to detect tissue-specific transcripts in the carcinogenic liver fluke *Clonorchis sinensis*, Huang et al. (2013) found that 72.4% and 81.2% of all transcribed genes in this parasite were also transcribed in the ovary and testis, respectively. The huge amounts of gonad transcripts might be due to the fact that a number of mRNAs are just stored in either primary spermatocytes until later elongation (Schäfer et al., 1995; Barreau et al., 2008), or in mRNP (message ribonucleoprotein) particles in the oocyte (Varnum and Wormington, 1990; Bettegowda and Smith, 2007; Mtango et al., 2008), which are translated later during embryonic development. Furthermore, the number of transcribed genes in sO of *S. mansoni* was found to be higher than that of bO (7,800 in sO compared to 7,016 in bO), indicating that many mRNAs might be stored in sO for translation during oocyte maturation, a process induced by pairing. At first view, the high number of transcripts present in the gonads appears to be surprisingly high and difficult to explain. However, the storage of RNA in germ cells has been described in other organisms as well, and it has important biological significance. Thus the occurrence of mRNAs, antisense

and microRNAs has been shown in spermatozoa of eukaryotes and that these RNAs are transported via sperm and sperm fluid into the oocyte where they among other functions contribute to epigenetic processes (Spirin, 1994; Boerke et al., 2007; Lalancette et al., 2008). In *Drosophila* diverse maternal mRNAs are deposited in the oocyte, and their post-zygotic translation leads to proteins controlling late stages of oogenesis and early stages of embryogenesis. Subsequently, maternal mRNAs are gradually disintegrated in embryos during the maternal/zygotic transition, while the control of further developmental steps switches from the maternal to the zygotic genome (Dworkin and Dworkin-Rastl, 1990; Seydoux, 1996; Johnstone and Lasko, 2001; Zhou and King, 2004; Barckmann and Simonelig, 2013).

To sort the data into meaningful parts, genes transcribed in testes and ovaries were divided into different categories according to their organ-specificity and pairing-influenced regulation. Here I will discuss the results with respect to the occurrence of transcripts in specific gonads and two exemplary genes of each category will be discussed.

4.3.2 Testis-preferentially or -specifically occurring transcripts

This first category included 42 genes which were found to be transcribed in testes but not in ovaries. Furthermore, their transcription was regulated by pairing. Among other genes, synaptotagmin and CDC25 were identified in this group and showed preferential or specific transcription in testes when compared with all other samples (Figure 3.15).

Synaptotagmins are transmembrane proteins occurring in a variety of species, including human, mouse, *Drosophila* and *C. elegans* (Fukuda, 2003). Usually, they act as Ca^{2+} sensors, and they can regulate multiple cellular processes, including exocytosis, and the acrosome reaction in sperms (Hutt et al., 2002). In this first category, one synaptotagmin-coding gene (Smp_150920) was found to be transcribed in testes but not in ovaries (RPKM < 0.3 in bO and sO) (Figure 3.15). Its low transcription levels in males and females indicate further, gonad-independent functions of this gene. Furthermore, a pairing-influenced difference was observed in females. Since higher transcript amounts were detected in sF, a putative function in the vitellarium appears unlikely.

Smp_152200 encodes a M-phase inducer phosphatase known as Cdc25 (cell division cycle protein). Dual-specificity phosphatases are considered to represent a sub-class of protein tyrosine phosphatases. Cdc25 proteins control entry into and progression

through various phases of the cell cycle including mitosis and S phase by removing inhibitory phosphate residues from target cyclin-dependent kinases (CDKs) (Boutros et al., 2006; Karlsson-Rosenthal and Millar, 2006; Rudolph, 2007). All mammals have three homologues (Cdc25A, Cdc25B and Cdc25C). In *Drosophila* there are two, which are named "String" and "Twine". The *twine* transcripts are present during the stages of meiosis in both male and female germ cells (Courtot et al., 1992). In *C. elegans* four homologues have been found (Cdc25.1 – Cdc25.4). Cdc25.1 was reported before to regulate the rate of germline mitotic cell cycles (Yoon et al., 2012) and Cdc25.2 was demonstrated before to be required for oocyte maturation but not for spermatogenesis (Kim et al., 2010). Cdc25.3 and Cdc25.4 were also shown to be preferentially expressed in germ cells (Yoon et al., 2012). Based on its transcript profile SmCdc25 (Smp_152200) seems to be exclusively transcribed in the testes, which indicates a unique role in regulating spermatogenesis. In *S. mansoni* there is another gene encoding Cdc25, Smp_046810, which is transcribed in both genders and gonad samples, and it is only affected by pairing in testes. This indicates a more general function of this gene.

The category of testes-specific but not pairing-unaffected transcripts included 436 hits. Among other genes, *spatial* and *elav* were identified as interesting candidates for potentially important functions during spermatogenesis.

Smp_194750 contains the SPATIAL (stromal protein associated with thymii and lymph node) domain, which encodes a putative transcription factor and is transcribed in the testis. Studies in mice have shown that *spatial* is involved in spermatid differentiation (Irla et al., 2003). Smp_194750 was found to be preferentially expressed in testes and bs-females but not in the ovaries (Figure 3.16), thus, it might have a role in the vitellarium, too.

ELAV (embryonic lethal, abnormal vision) is a well-studied protein in *Drosophila*. ELAV belongs to a class of proteins that binds to mRNA and presumably has regulatory functions for mRNA stability, pre-mRNA splicing and translational activation. Besides its important role in neuronal stem cells (Yannoni and White, 1996; Ratti et al., 2006; Simionato et al., 2007), ELAV and its homolog HuR have been shown to regulate spermatogenesis in mouse (Chi et al., 2011) and in the flatworm *Macrostomum lignano* (Sekii et al., 2009). The knockdown of *elav1* and *elav2* in planarian resulted in the failure of meiosis, which led to no detectable spermatids in RNAi-treated animals (Wang et al., 2010). The *S.mansoni* ELAV protein shares 63% similarity at amino acid level with Smed_ELAV1 and 62% with Smed_ELAV2 from *Schmidtea mediterranea* (Figure 3.17). Concerning the exclusive expression of SmELAV in the testes in *S. mansoni*, it seems likely that it fullfills similar functions in regulating spermatogenesis.

4.3.3 Ovary-specific transcripts

CPEB (cytoplasmic polyadenylation element binding protein) is a protein containing a cis-acting CPE (cytoplasmic polyadenylation element) sequence, which usually resides about 20 nucleotides 5 of the AAUAAA motif within the untranslated region of mRNAs and dictates which mRNAs will be polyadenylated (Richter, 2007). By promoting polyadenylation-induced translation, CPEB mediates diverse processes including germ-cell development (Hake and Richter, 1994; Luitjens et al., 2000; Tay and Richter, 2001), cell division and cellular senescence. In zebrafish (*Danio rerio*) cytoplasmic polyadenylation initiates translational processes that play important roles during embryogenesis. An oocyte-specific CPEB (zobra) was found that controls the translation of the embryonic transcript ElrA by keeping this transcript in storage until fertilization occurs. When zorba levels decrease, ElrA protein is synthesized to regulate the translation of additional mRNAs during embryogenesis (O'Connell et al., 2014).

Recently, Smp_070360 (CPEB1) transcripts were localized specifically to the posterior part of the ovary in bF, and Smp_137460 (named "CPEB2") transcripts were detected in the posterior area of both bO and sO, as well as in the vitellarium of bF, indicating that this gene may have functions in different reproductive organs (Cogswell et al., 2012). The results obtained in my study are consistent with the localization results of the mentioned study and they show that both CPEB1 and CPEB2 were specifically transcribed in the ovary (Figure 3.18) in a pairing-influenced manner. Thus it is tempting to speculate that in analogy to *zobra* its presumptive orthologs CPEB1/CPEB2 of *S. mansoni* may be involved in controlling pairing-dependent post-zygotic translational events which are associated with early developmental processes.

In contrast to the identified testis-specific synaptotagmin (Smp_150920), another synaptotagmin (Smp_150350) was found to be ovary-specific. This indicates that synaptotagmins may have gonad tissue-specific functions.

For genes whose transcription was not affected by pairing, Smp_076600, the SOX transcription factor gene, and Smp_210800, a potential regulator of G-protein signaling were chosen as exemplary genes. The SOX family of transcription factors plays key roles in development, including the maintenance of embryonic and neural stem cells (Wegner, 2011). When comparing the gene expression profiles of germ balls to cercariae and schistosomula, Parker-Manuel et al. (2011) found a SOX gene ortholog as highly transcribed in the germ balls, indicating its potential role in germinal cell development.

In my data sets this SOX gene was transcribed at the highest level in the ovaries (Figure 3.19), indicating it may have a unique role in oogonia proliferation and/or differentiation.

Smp_210800 contains a RGS (regulator of G-protein signaling) domain and a DEP (found in dishevelled, egl-10, and pleckstrin) domain. The RGS domain is an essential part of the R7 (neuronal RGS) protein subfamily. All of the R7 subfamily members are expressed predominantly in the nervous system and play important roles in the regulation of crucial neuronal processes such as vision, motor control and reward behavior (De Vries et al., 2000; Anderson et al., 2009). Therefore, its highest transcript amount in ovaries suggests a potential role of Smp_210800 in the neuronal process associated with oocyte development and/or differentiation.

4.3.4 Transcripts existing in both testes and ovaries

More than 139 genes were found to be transcribed in both testes and ovaries, and their transcription was regulated by pairing in both gonads. This category includes among other genes a diaphanous-related formin protein-coding gene (Smp_146810) and a TWIK family of potassium channel protein-coding gene (Smp_147550). The former contains a formin homolog 2 (FH2) domain. FH proteins control rearrangements of the actin cytoskeleton during cytokinesis and cell polarisation. The diaphanous protein SmDia (Smp_068720) has been previously characterized in our group. It consists of a Rho-GTPase binding domain, an armadillo repeat /dimerization region, the inter-domain region, the FH1 and FH2 doman and a diaphanous autoregulatory domain, and was shown to interact with the Src kinase SmTK3 and the Rho-GTPase ortholog SmRho of *S. mansoni* (Quack et al., 2009). In my data sets, the diaphanous-related gene (Smp_146810) was predominantly transcribed in bO, and regulated by pairing in both gonads (2.3-fold difference in testes and 20.3-fold difference in ovaries). This implies that the cytoskeleton organization function of this gene may be enhanced after pairing, especially in the ovaries. Since oocyte maturation starting from oogonia to primary oocytes goes along with pairing in schistosomes, it seems plausible that this process is associated with considerable cytoskeleton rearrangements as it was shown for maternal mRNA localization during oogenesis in *Drosophila* (Pokrywka and Stephenson, 1995). Cytoskeleton rearrangement in schistosomes may be governed by SmTK3-SmDia-SmRho signaling processes which have been shown to regulate F-actin assembly (Tominaga et al., 2000; Grosse et al., 2003; Quack et al., 2009).

The transcript amount of the twik-family potassium channel-related gene (Smp_147550) was up-regulated in both testes (1.7-fold) and ovaries (34.7-fold) after pairing (Figure 3.20). In eukaryotic cells, potassium channels are involved in neuronal signaling, and are critical determinants of neuronal excitability and synaptic function (Hobert, 2005). The up-regulation of this gene in both gonads may indicate that pairing affects neuronal processes, which are regarded to be important in gonad development (Leutner et al., 2013). In *C. elegans*, the TWK-1 two-pore potassium channel was found to function cumulatively to enable somatic control of oocyte meiotic maturation (Kim et al., 2012). Therefore, this K^+ channel gene may also have a role in regulating meiosis in *S. mansoni* gonads.

About 50% of gonad genes (4,100 out of 8,411) were found to be pairing-unaffected in both testes and ovaries. This large set includes DNA replication licensing factors MCM2-8, vasa-like genes 1-3, argonaut, origin recognition complex (ORC) subunits, the PTKs SmTK3, SmTK5 and SmVKR2. These genes may function in general, not pairing-influenced processes associated with gonad development and/or differentiation. In this category genes encoding a protein lin-9 (Smp_133660) and a leucine zipper protein (Smp_124570) will be discussed. The line-9 protein of *C. elegans* functions in an Rb-related pathway that acts antagonistically to a RTK/Ras signal transduction pathway controlling vulva induction. Lin-9 has also been shown to be required for the development of male gonad (Beitel et al., 2000). In my data set, lin-9 of *S. mansoni* was transcribed abundantly in all gonad samples (RPKM > 40) at a much higher level than in whole worm samples (18.3-fold difference in average, FDR < 0.0001). This indicates a dominant role of lin-9 for gonad development. The leucine zipper protein gene Smp_124570 contains a trichoplein (mitostatin) domain, which was first detected to be part of a meiosis-specific nuclear structural protein (Vecchione et al., 2009). In *S. mansoni*, Smp_124570 was predominantly transcribed in testes samples. However, its exact function in the gonads remains unclear.

Furthermore, genes were detected whose transcription was differentially regulated by pairing in testes and ovaries. Compared to the number of transcripts that were pairing-affected in testes but not in ovaries, there were more genes (3152 versus 62) that were pairing-affected in ovaries but not in testes. The former situation included a gene encoding a predicted vWA-containing protein (Smp_127480) and another one coding for the rad50 ATPase (Smp_181450). The majority of vWA-containing proteins occurs extracellularly. They participate in cell adhesion, migration, signal transduction and other processes, which involve interaction with a large array of ligands (Colombatti et al., 1993). Because the annotation of this gene

was predicted, it is not clear whether it plays similar roles the gonads. Transcription of Smp_181450 (DNA double-strand break repair rad50 ATPase) was found to be up-regulated in bT but pairing-independently in the ovaries. Although the identity of its sequence is quite low to that in other organism genomes, its high expression in the testes (Figure 3.22) indicates a role in testes development.

The maternal embryonic leucine zipper kinase (MELK) is a cell cycle-dependent protein kinase that belongs to the KIN1/PAR-1/MARK family. It functions by binding to numerous proteins and has been shown to regulate multiple processes, including cell cycle (Cordes et al., 2006), cell proliferation (Nakano et al., 2005), spliceosome assembly (Vulsteke et al., 2004), embryonic development and especially tumorigenesis (Lin et al., 2007; Kuner et al., 2013). Several proteins can interact with MELK, including cdc25b and Smad proteins (Smad2, -3, -4 and -7). In my dataset, the putative *S. mansoni* MEKL ortholog (Smp_166150) shows a high preferential expression in testes and ovaries (Figure 3.23), indicating a role in regulating germinal cell proliferation, and in addition, is is regulated by pairing in ovaries.

Lastly, a gene (Smp_198690) was detected that putatively encodes a HMG-CoA synthase, and which was up-regulated in ovaries but not in testes after pairing (Figure 3.23). HMG-CoA is an intermediate in both cholesterol synthesis and ketogenesis. It catalyses the first step in isoprenoid/mevalonate synthesis and controls the mevalonate pathway flux (Harris et al., 2000). Its expression in testes and ovaries may indicate the role of cholesterol in germinal cell growth and/or differentiation. Moreover, the pairing-influenced transcription in ovaries indicates the possibility of pairing-induced cholesterol metabolism in such organs.

With respect to the expression of SmVKR1 (Smp_019790), a previous study demonstrated that this unusual receptor gene is transcribed at higher levels in primary oocytes than in oogonia, and qPCR results demonstrated that VKR1 transcript amounts are higher in bO than in sO. Knocking-down VKR1 by RNAi led to deformed eggs and a reduction of egg production in paired *S. mansoni* females (Vanderstraete et al., 2014). Furthermore, by *in situ* hybridization the colocalization of SmVKR1 and the PTKs SmTK6, SmTK4 and SmTK3 have been demonstrated as well as their direct interactions by yeast-two-hybrid (Y2H) analyses and co-immunoprecipitation (Beckmann et al., 2011, 2010a). In my data sets, SmVKR1 transcript amounts were detected to be higher in bO than in sO (1.67-fold difference, FDR < 0.0001), which corresponds very well to the results obtained before.

With respect to the gender effect, after comparing the transcription patterns of all genes between each of the gonads to the complete worms, transcript amounts of

1012 genes were higher in all gonads than in complete worms, with at least 1.5-fold difference. The gene ontology enrichment indicated these genes were involved among others in processes such as RNA biosynthesis, cell cycle, and DNA replication. This is similar to the finding of Parker-Manuel et al. (2011), who found that genes up-regulated in germ balls compared to cercariae and schistosomula were mainly involved in DNA replication and cell division.

4.3.5 Role of neuropeptides in *S. mansoni* gonads

In a previous study Collins et al. (2010) demonstrated that a NPF-like peptide (*npy-8*)-coding gene was required for maintaining reproductive tissues in planarian. However, in the present data set, two *S. mansoni* NPF-like prohormone genes were both unlikely to be transcribed in testes and ovaries (RPKM < 0.4). Besides, a prohormone convertase gene (Smp_077980) showed very low abundance in bT and bO (RPKM < 1.2 in both). Thus it is unclear wheather the schistosome npy-genes have similar functions as in planaria, or weather the functions are different. The latter would indicate that planarians and schistosomes may not employ the same set of neuropeptides controlling their reproductive outcomes (Collins et al., 2010).

4.3.6 From hermaphroditism to dioeciousness: RNA-Seq data supports evolutionary hypotheses

In hermaphrodites, protandry as a form of sequential hermaphroditism is common and the development of the male gonad occurs more rapidly than that of the female. In e.g. some nematodes like *C. elegans* sperm is produced during the last larval stage, and afterwards gonad development switches to oocyte production in the adult stage where fertilization takes place (Pires-daSilva, 2007). Within the phylum Platyhelminthes, only schistosomes have developed both genders. It was regarded that this dioecy had been evolved from their hermaphroditic ancestors (Basch, 1990). Adults of most schistosome species live in venous systems of homeotherms as final hosts. Trematodes of the closely related sister group are vascular system generalists of the family Spirorchidae, which occur in poikilotherms like turtles. According to phylogenetic analyses Spirorchidae are basal to the Schistosomatidae (Platt and Brooks, 1997; Snyder, 2004).

During evolution, the successful colonization of homeotherms by vascular trematodes required among others the conquest of a novel host environment, the overcoming of its immunological armament, and the organization and optimizing of assembly-line egg production as well as ensuring easy access for the eggs to the

external environment. At the same time safeguarding hosts´ survival had to be secured by the parasite to increase its chances of evolutionary success (Brant and Loker, 2005). Evolution of dioecy in Schistosomatidae from their hermaphroditic origin may have advanced via androdioecy, hermaphrodites specialized in egg deposition in the vascular system and larger adults developed further to functional males (Platt and Brooks, 1997). To enhance the probability of success, as a next step the "division of labour" between the genders may have been the driving force for the subsequent development of the female gender. Indeed, in schistosomes physiological and metabolic functions are unequally distributed between male and female schistosomes when pairing has occurred (Basch, 1990; Ribeiro-Paes and Rodrigues, 1997; Brant and Loker, 2005). Moreover, the "division of labour" hypothesis was strongly supported by microarray studies performed with the aim to investigate male-female interaction at the molecular level. Among others it was shown that the spectrum of genes transcribed in sF was larger than that of bF. Furthermore, the expression of genes with functions for e.g. egg production was found to be initiated in bF and motor functions were down-regulated in bF at the same time while these functions were up-regulated in bM compared to sM (Fitzpatrick and Hoffmann, 2006). This kind of streamlining of female transcriptional activity had been demonstrated before also in studies with adult *S. mansoni in vitro* demonstrating that the occurrence of transcripts of genes, whose function is associated with egg production, depends on the pairing status. Transcripts of egg-associated genes such as Sm_p14, ferritin-1, and mucin A11 were detected only when females were paired, or when they repaired after a separation period during which the transcription of these genes was stopped (Grevelding et al., 1997). This could mean that the origin of dioecy in schistosomes resulted from the evolution of genes suppressing female function in males and, according to physiological and molecular data also in sF, while male functions are suppressed in bF (Platt and Brooks, 1997).

The situation of schistosomes is similar to protandric hermaphrodites with respect to the direction of gonad development, male gonad first, female gonad second. Indirect support for this view is given by the observation of pseudo-ovaries and vitellaria which have been found in males in addition to testicular lobel although at different positions (Shaw and Erasmus, 1982; Hulstijn et al., 2006; Beckmann et al., 2010b). However, no efferent duct was found in males thus the oocytes may not be able to leave this organ and are biologically probably not functional. Thus they may be represent an an evolutionary set-back (atavism). These observations coincide with former results showing a leaky expression of some female-specific genes associated with egg synthesis

in males (Leutner et al., 2013).

The analysis of the RNAseq data support this evolutionary point of view. A lot of genes were transcribed simultaneously and predominantly in males and in single-sex females. Also the diversity of genes transcribed was higher in sF than in bF. GO analysis of the genes found showed that they were mainly involved in transport processes, cell adhesion, and development. Furthermore, a number of neuronal genes were also found to be transcribed preferentially in bM-sM and sF. Comparing the RNAseq data from adults by hierarchical clustering (Figure 3.9 and 7.2) indicated that the pattern of sF-transcribed genes was more similar to bM and sM than to bF. This tendency was also found by MDS analysis (Figure 3.10) demonstrating that the sF cluster of biological replicates located closer to the sM/bM cluster than to the bF cluster. Remarkably, the same trend was found comparing the gonad samples by these two methods. From these results it can be concluded that before pairing sF are more similar to males than to bF.

Therefore, with respect to the question of hermaphroditism versus dioeciousness, the complete functional separation of the sexes of schistosomes cannot be stated, because female schistosomes still need the constant pairing contact with the male to complete sexual maturation. This, however, represents an obvious reminiscence to schistosomes´ hermaphroditic ancestors.

4.3.7 Comparisons with similar studies

Microarray analyses of gonads obtained by laser microdissection microscopy

Nawaratna et al. (2011) reported a laser microdissection method (LMM) to obtain reproductive tissues. They conducted a microarray approach to analyse the RNA obtained from the extracted tissues and found 4,450 genes in the ovary and 2,171 genes in the testis to be up-regulated with > 2 fold difference compared to whole worm controls. In my dataset, the transcription of 1,309 genes in the ovaries, and 2,008 genes in the testes was up-regulated with > 2 fold difference compared to the whole worm controls (FDR < 0.005 for both). These two datasets had 557 genes in common for the ovary and 677 genes for the testes (Figure 4.1). With respect the fold change values, these two data sets also differed (details for selected genes in (Nawaratna et al., 2011) were attached as Supplementary file No. 40). Among these genes is Smp_145900 (sphingolipid delta(4) desaturase:C4 hydroxylase), which was detected to be up-regulated in bT in the LMM approach but to be up-regulated in bM in my results. The huge difference with respect to ovary data sets might be due to the

fact that Nawaratna et al. only employed one sample whereas three biological replicates were used in my study. In addition, the LMM procedure may be more sensible to transcript contaminations originating from other tissues co-extracted using this method. Furthermore, it seemed that during the microdissection approach only the parts of ovaries containing the primary oocytes were extracted. Lastly, different transcriptome techniques (microarray versus RNA-Seq) and statistics tools (GeneSpring versus edgeR) also resulted in analytical bias.

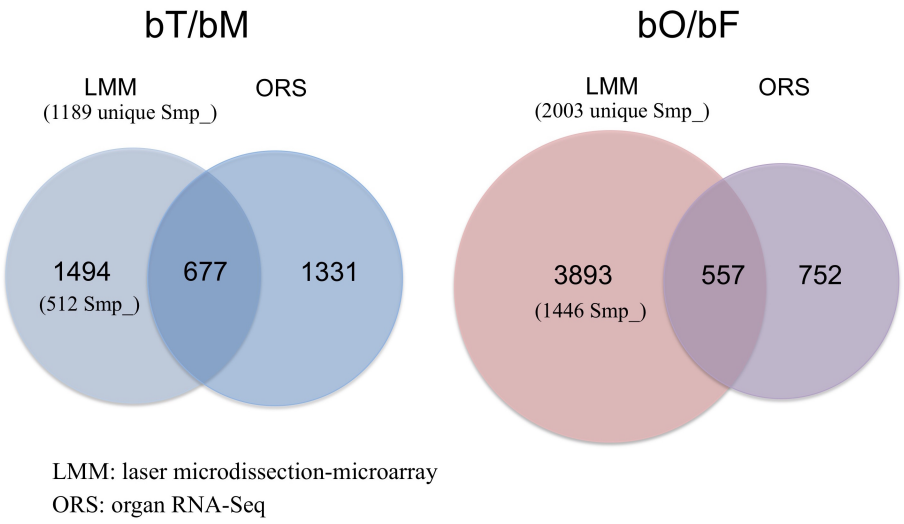

Figure 4.1: Numbers of DEGs compared to the LMM approach by Nawaratna et al. (2011).

Males microarray

By a combination of microarray and Super-SAGE analyses, Leutner et al. (2013) discovered 526 and 253 genes to be differentially transcribed between males from single-sex infections and those from mixed-sex infections. In total 29 DEGs were detected by both approaches. Applying the same parameters (adjusted $p < 0.01$ and fold change cut-off at 1.5), the present RNA-Seq dataset showed 298 genes that were differentially transcribed between single-sex and mixed-sex male worms. Transcription tendency of some genes were consistent in both studies, including Smp_158480 (AMP dependent ligase), Smp_135230 (aromatic-L-amino-acid decarboxylase), and Smp_151490 (nebulin), which showed up-regulation in bM, and Smp_123300 (follistatin), which was detected to be up-regulated in sM in both studies. Detailed comparisons on these 29 genes were shown in Supplementary file No. 41.

4.4 Characterization of vitelline cells

Based on the organ-isolation approach (Hahnel et al., 2013) I made first attempts to isolate vitellaria and vitelline cells, which were characterized. Although interstitial cells were found occasionally, their percentage among vitelline cells was so low that their impact can be ignored. After the isolation of cells, their quality and homogeneity were tested by morphological, molecular, physiological, and physical means. Bright-field microscopy, SEM, and TEM analyses revealed stage-depending characteristics of vitelline cells including their varying sizes and cytoplasmic compositions, in particular the vitelline and lipid droplets, which are both needed for egg production and embryogenesis (Erasmus, 1975; Erasmus et al., 1982).

In addition, the isolation of high quality RNA allowed the characterisation of isolated vitelline cell populations at the molecular level. Supporting data of previous studies, transcripts were detected for genes encoding Sm_p14, SmESP, SmTyr1, SmORAI1, SmCam4, SmHIP and SmFGFR B. Genes with hypothesised roles in reproduction- associated processes were also transcribed and included those encoding SmFGFR a, the stem cell function-associated SmVlg3, SmAgo2-1, SmNanos2 (nanos) and SmCD36, supporting the hypothesis that this protein is important for embryogenesis (Okumura-Noji et al., 2013). HSP70 is known to be a ubiquitously expressed protein thus it is no surprise to find it expressed in the vitellarium. Unexpectedly, SmNPP-5 transcripts were detected in vitelline cells. SmNPP-5 may a function within the tegument of adult schistosomes (Rofatto et al., 2009), but its transcripts were also detected in testes or ovaries in a previous study (Hahnel et al., 2013). Thus SmNPP-5 may have a yet unknown function for reproduction. This may also be true for SmAQP which was previously hypothesised to play also a role within the tegument of adults (Faghiri et al., 2010). SmAQP was found to be transcribed in testes but not in ovaries, however its translation in testes was not confirmed (Hahnel et al., 2013). Thus, although transcripts of this gene were found in vitelline cells its expression as well as its role in schistosome gonads remains elusive. Finally, no SmKK7 transcripts were found in the vitelline cells, which indicated that this potential potassium channel blocker has no function in vitelline cells. SmKK7 was first detected in cercarial secretions by proteomics (Curwen et al., 2006) and subsequently in peripheral nerve endings of adult *S. mansoni* (Reimers et al., 2015).

In a previous microarray study using RNA isolated from inhibitor-treated *S. mansoni* females, evidence was obtained that Ca^{2+} contributes to physiological

processes during egg production. *In situ*-hybridisation confirmed the expression of the Ca^{2+} transporter ORAI-1 in ovary and vitellarium, the Ca^{2+} sensor SmHIP in ovary, vitellarium and Mehlis' gland, and the Ca^{2+}-binding protein calmodulin-4 within the vitelloduct and around the ootype (Buro et al., 2013). Organ-specific RT-PCRs confirmed and complemented the *in situ* findings, providing additional evidence for the presence of ORAI-1 transcripts in testes and ovaries, and calmodulin-4 transcripts in testes (Buro et al., 2013). With respect to my results, RNA transcripts were detected for ORAI-1, SmHIP and calmodulin-4 in the vitellarium, supporting the role(s) of Ca^{2+}-dependent processes in this organ, and consequently for egg production. Independent support for this hypothesis was gained by physiological studies using Ca^{2+}-imaging which revealed Ca^{2+} fluxes in freshly isolated vitelline cells. In addition, this result showed that the isolated cells were viable and physiologically active. Previous studies that measured either Ca^{2+} levels of schistosome females (Shaw and Erasmus, 1983) or used Ca^{2+}-ionophore to treat schistosome females *in vitro* followed by electron microscopic analysis (Wells and Cordingley, 1991) had already hypothesised a role of Ca^{2+} during egg formation processes.

FACS analysis indicated that sorting of vitelline cells based on autofluorescence and size or granularity is possible. However, the total number of cells obtained was lower than expected. This could be due to unique physical characteristics of vitelline cells, which may be different from cells used to optimise the FACS system e.g. human cells. Future studies will include efforts to improve the FACS sorting efficiency. Nonetheless, the ability to sort vitelline cells will allow further studies that elucidate vitelline-cell development and that aim for cell-culture establishment. FACS sorting will also enable the enrichment of vitelline cell sub-populations for more detailed molecular analyses of processes during S1–S4 cell differentiation. In addition, the feasibility of S1-cell enrichment is of great interest with respect to its proliferative potential as stem cell-like precursor cells. This biological capacity together with the organ isolation-based enrichment of this cell type will open novel research perspectives towards cell-line establishment that have not previously been available.

Neutral lipid staining of adult worms showed that the lipid content, especially within the vitellarium, decreased dramatically *in vitro*, independent of the pairing-status of the females. This implied that the available lipid source was missing in the used culture system, or the uptake of neutral lipids was inhibited. Further experiments culturing sF in male-conditioned medium indicated that lipids either released by males may have been taken up by females. Thus direct feeding may be possible, a hypothesis

being discussed over decades in the schistosome literature (Popiel, 1986; Gupta and Basch, 1987a,b; Skelly et al., 2014). Although initial development of the vitellarium was observed in "feeded females", no continuation of development was observed after prolonged incubation periods in male-conditioned medium. This indicates that besides the neutral lipids there are probably other stimuli that induce and maintain vitelline cell differentiation. This interesting topic should be subject of further studies.

5 Summary / Zusammenfassung

5.1 Summary

Schistosomiasis remains a devastating disease in many tropical and subtropical countries worldwide. Its pathology is caused by the eggs laid by constantly paired adult schistosome females. Without pairing, female worms remain virgin-like, or they will lose their fecundity, which includes the de-differentiation of their gonads if they have been paired but get separated from their male partners.

To come closer to answers to the unsolved questions about the molecular basis of male-female interaction of schistosomes, my study aimed at the application of RNA-Seq to elucidate the transcriptomes of male and female worms of *S. mansoni* and, in addition, of testes and ovaries that were obtained by an organ-isolation method established in our laboratory. In this context, the effects of gender, pairing-status, and tissue-origin on gene transcription were analysed. Furthermore, based on the organ-isolation approach I isolated and characterised vitellarium tissue and vitelline cells of different differentiation stages.

RNA-Seq analyses were performed on testes (T) isolated from paired (b) and unpaired (s) males (= bT, sT) and ovaries (O) from paired and unpaired females (= bO, sO), as well as their whole worm counterparts (bM, sM and bF, sF). The effects of gender, pairing-status, and tissue origin on gene expression among these samples were compared. The data sets revealed that tissue origin (organ versus worm) has a large effect on gene expression in general, which resulted in 4,534-5,478 (35% - 51%) differentially expressed genes (DEGs; 1.5-fold difference). In addition, 1,012 genes were shown to be up-regulated in all gonads compared to whole worms (> 1.5-fold change). Gene ontology analyses showed that these genes were mainly involved in processes like RNA biosynthesis, cell cycle and ribosome biogenesis, which are essential for gonad development.

The number of DEGs induced by gender varied, with the lowest number of 1,445 (out of 8,590; 7.8%) for sM/sF comparison to 4,629 (out of 7,970; 41.3%) for the bT/bO

comparison (1.5-fold difference). Furthermore, detailed bioinformatics analyses revealed that sF, which had never been paired before, were much closer related to males (bM or sM) than to paired females at the transcriptome level, based on the fact that 841 genes were transcribed preferentially in bM/sM/sF. This important finding sheds also new light on the question of hermaphroditism versus dioeciousness and provides a molecular fundament for the actual hypothesis of schistosome evolution and its roots originating from the Spirorchidae. In these hermaphroditic worms the male gonad develops ahead of the female gonad (protandry). This principle appears to be conserved in schistosomes as well, although apportioned to two genders.

When comparing the male and female gonads, 182 and 33 genes were identified as testis- and ovary-specifically transcribed markers, respectively, which can be used in future studies as reference genes for different kinds of molecular analyses such as comparative qPCRs.

Furthermore, investigating the pairing effect in detail demonstrated its fundamental impact on molecular processes in males and females, and more importantly, in their gonads. Of note, transcription of only 243 (1.4%) and 426 (1.7%) genes was influenced by pairing in testes and males, respectively. However, for ovaries and females the numbers of DEGs were 3,748 for females and 3,600 for ovaries (about 30% each). Consistent with former studies, a number of egg biosynthesis-related genes were found to be up-regulated in paired females, including egg-shell protein genes (e.g. *p14* and *p48*) and genes encoding tyrosinases that are involved in egg-shell formation. Pairing-affected transcripts in the gonads might have functions in spermatogenesis (e.g. *synaptotagmin 1* and *cdc25*), oogenesis (e.g. *synaptotagmin 2* and *cpeb*), or both processes (e.g. *melk*).

Moreover, a number of 15 genes were found to be equally transcribed among all samples, and, therefore, represented potential house-keeping genes useful in future studies.

Furthermore, the RNA-Seq data also aided in the prediction in the biological context of the activities of hypothetical genes. Thus the occurrence of 238 gonad-preferentially transcribed genes indicated their hypothetical roles in testis- and/or ovary-associated functions.

Finally, with the help of a modified version of the organ-isolation protocol established in our group, I succeeded in the isolation and purification of S1-S4 vitelline cells. These cells were characterized at the molecular level by RT-PCR experiments and morphologically analysed by various microscopic techniques including bright field, fluorescent, and electron microscopy. Their vitality and

physiological activity was confirmed by cytological staining procedures and Ca^{2+}-imaging analyses. It was even possible to enrich subpopulations of S1 to S4 vitelline cells by FACS analysis, which is a prerequisite for further studies. Thus S1-cell enrichment provides a basis for novel approaches towards cell-culture establishment.

In summary the results obtained in my study provide novel and diverse insights into the developmental processes of the gonads as well as a broad basis for future studies aiming to unravel the role of specific factors controlling the unusual reproductive biology of schistosomes.

5.2 Zusammenfassung

Die Schistosomiasis ist nach wie vor eine der bedeutendsten Infektionskrankheiten in den Tropen und Subtropen weltweit. Die Pathologie der Schistosomiasis wird durch Eier verursacht, die nur von dauerhaft gepaarten Schistosomen-Weibchen gelegt werden. Weibchen haben einen jungfräulichen Status, solange sie ungepaart sind, oder sie verlieren ihre Fertilität, wenn sie von ihrem Paarungspartner getrennt werden. Letzteres geht mit der Dedifferenzierung der Gonaden einher.

Um der Frage nach der molekularen Basis der Männchen-Weibchen-Interaktion bei *S. mansoni* nachzugehen, zielte meine Studie auf die Durchführung von RNA-Seq-Experimenten ab, um die Transkriptome von Männchen und Weibchen sowie von Testis und Ovar zu analysieren. Diese Gonaden wurden die über eine in unserem Labor etablierte Organ-Isolationsmethode gewonnen. In diesem Zusammenhang wurden auch gewebespezifische Effekte sowie der Einfluss der Paarung auf die Gentranskription in den Gonaden analysiert. Weiterhin wurde auf Basis der Organ-Isolationsmethode Vitellarium-Gewebe gewonnen sowie Vitellinzellen charakterisiert.

RNA-Seq-Experimente wurden mit Gonaden verschiedenen Ursprungs durchgeführt wie Testis (T) aus gepaarten (b) und ungepaarten (s) Männchen (= bT, sT) bzw. Ovar (O) aus gepaarten und ungepaarten Weibchen (= bO, sO) sowie zum Vergleich mit ganzen Würmern (bM, sM, bF, sF). Die Effekte des Geschlechts, des Paarungszustands und des Gewebeursprungs wurden bei der Datenauswertung verglichen. Die Ergebnisse zeigten, dass im Vergleich zum ganzen Wurm der Gewebeursprung einen beträchtlichen Effekt auf die Genexpression hat. So wurden 4,534-5,478 (35% - 51%) der insgesamt in Schistosomen vorkommenden Gene als differentiell exprimierte Gene (DEGs; > 1.5-facher Unterschied) ausgemacht. Zudem waren im Vergleich zum ganzen Wurm 1,012 Gene in den Gonaden transkriptionell hochreguliert (> 1.5-fach). „Gene ontology"- Analysen offenbarten, dass diese Gene hauptsächlich für Prozessen wie RNA-Synthese, Zellzyklus und Ribosomen-Biogenese von Bedeutung sind, die alle bei der Gonaden- Entwicklung eine Rolle spielen.

Die Anzahl an DEGs, die durch Paarung beeinflusst wurden, variierte stark. Der niedrigste Wert von 1,445 (aus 8,590; 7.8%) wurde beim Vergleich sM/sF gefunden, der höchste Wert war 4,629 (aus 7,970; 41.3%) für bT/bO (> 1.5-fach). Weitergehende bioinformatische Untersuchungen deckten auf der Basis von 841 in bM/sM/sF gleicher- maßen transkribierten Genen auf, dass Weibchen, die niemals mit einem

Männchen gepaart gewesen sind, vom Transkriptomprofil dieser 841 Gene her den Männchen (bM oder sM) ähnlicher waren als paarungserfahrenen Weibchen. Dieser Befund bringt einen neuen Aspekt in Debatte um Zwittrigkeit versus Getrenntgeschlechtlichkeit und liefert ein molekulares Fundament für die favorisierte Hypothese, dass die evolutionären Wurzeln der Schistosomen bei den Spirorchidae liegen. In diesen hermaphroditischen Würmern entwickelt sich die männliche Gonade vor der weiblichen (Protandrie). Dieses Prinzip scheint in den Schistosomen weiterhin zu bestehen, auch wenn sie zwei Geschlechter entwickelt haben.

In den Gonaden selber wurden 182 bzw. 33 Gene als Testis- bzw. Ovar-spezifisch transkribiert identifiziert. Diese können in zukünftigen Studien als Referenzgene für verschiedene molekulare Analysen wie z.B. vergleichende qPCRs genutzt werden.

Ferner deckte die Detailanalyse der erhaltenen Daten einen fundamentalen Einfluss der Paarung auf molekulare Prozesse in Männchen und Weibchen auf und besonders in ihren Gonaden. Bemerkenswert war hierbei, dass durch die Paarung nur 426 (1.7%) Transkripte in Männchen beeinflusst wurden sowie 243 (1.4%) der in Testis gewebe-spezifisch auftretenden Transkripte. Demgegenüber lagen die Transkript-Zahlen für Weibchen und die gewebespezifisch im Ovar auftretenden DEGs bei 3,748 in Weibchen und 3,600 im Ovar (je über 30%). In Übereinstimmung mit vorherigen Studien zeigte sich hierbei u.a., dass Eiproduktions-assoziierte Gene im Ovar gepaarter Weibchen hochreguliert waren, was Gene für Eischal-Proteine (z.B. *p14* and *p48*) und Tyrosinasen umfasste, die an der Eischalbildung beteiligt sind. Paarungs-beeinflusste Gene wurden aber auch übereinstimmend in beiden Gonadentypen gefunden, wo sie Funktion für die Spermatogenese (z.B. *synaptogagmin 1* und *cdc25*) wie für die Oogenese (*synaptotagmin 2* und *cpeb*) oder für beide Prozesse (z.B. *melk*) ausüben könnten. Darüber hinaus wurden 15 Gene entdeckt, die in allen Proben auf gleichem Niveau transkribiert wurden und somit potentielle „house-keeping"-Funktionen erfüllen, was ebenfalls für zukünftige Experimente von Wert sein kann.

Ferner gaben die RNA-Seq-Daten auch erste Hinweise auf den biologischen Kontext, in dem die Aktivitäten vorhergesagter Gene (hypothetical proteins) zu sehen sind. So deutete das Auftreten von 238 Gonaden-präferentiell transkribierter Gene auf ihre möglichen Funktionen in Testis und/oder Ovar hin.

Mit Hilfe einer modifizierten Version des Organ-Isolationsprotokolls ist es mir schließlich auch gelungen, S1-S4 Vitellinzellen zu isolieren und aufzureinigen. Diese Zellen wurden mit RT-PCRs molekular charakterisiert und über verschiedene mikroskopische Techniken, die Lichtmikroskopie, Fluoreszenz- und Elektronen-

mikroskopie umfassten, analysiert. Ihre Vitalität und physiologische Aktivität wurden über cytologische Färbungen and „Ca2+-imaging“ bestätigt. Es war sogar möglich, Subpopulationen von S1- bis S4-Zellen über FACS anzureichern, eine Voraussetzung für Folgestudien. So stellt z.B. die Anreicherung der Mitose-kompetenten S1-Zellen eine Basis für neue Ansätze zur Etablierung einer Zellkultur dar.

Zusammengefasst liefern die Resultate meiner Untersuchungen neuartige und vielfältige Erkenntnisse zu Entwicklungsprozessen in den Gonaden sowie eine breite Grundlage für zukünftige Studien mit dem Ziel, die Rolle spezifischer Faktoren zu untersuchen, die die ungewöhnliche Reproduktionsbiologie der Schistosomen steuern.

6 References

Alexa, A. and Rahnenfuhrer, J. (2010). topGO: topGO: Enrichment analysis for Gene Ontology. R package version 2.16.0.

Almeida, G. T., Amaral, M. S., Beckedorff, F. C. F., Kitajima, J. a. P., DeMarco, R., and Verjovski-Almeida, S. (2012). Exploring the *Schistosoma mansoni* adult male transcriptome using RNA-seq. *Exp. Parasitol.*, 132(1):22–31.

Anderson, G. R., Posokhova, E., and Martemyanov, K. A. (2009). The R7 RGS protein family: Multi-subunit regulators of neuronal G protein signaling. *Cell Biochem. Biophys.*, 54(1-3):33–46.

Andrade, L. F., Nahum, L. A., Avelar, L. G. a., Silva, L. L., Zerlotini, A., Ruiz, J. C., and Oliveira, G. (2011). Eukaryotic protein kinases (ePKs) of the helminth parasite *Schistosoma mansoni*. *BMC Genomics*, 12(1):215.

Arkov, A. L., Wang, J.-Y. S., Ramos, A., and Lehmann, R. (2006). The role of Tudor domains in germline development and polar granule architecture. *Development*, 133(20):4053–4062.

Armstrong, J. C. (1965). Mating behavior and development of schistosomes in the mouse. *J. Parasitol.*, 51:605–16.

Ashburner, M., Ball, C. A., Blake, J. A., Botstein, D., Butler, H., Cherry, J. M., Davis, A. P., Dolinski, K., Dwight, S. S., Eppig, J. T., Harris, M. A., Hill, D. P., Issel-Tarver, L., Kasarskis, A., Lewis, S., Matese, J. C., Richardson, J. E., Ringwald, M., Rubin, G. M., and Sherlock, G. (2000). Gene ontology: tool for the unification of biology. *Nat. Genet.*, 25(1):25–29.

Ashcroft, N. R., Kosinski, M. E., Wickramasinghe, D., Donovan, P. J., and Golden, A. (1998). The four cdc25 genes from the nematode *Caenorhabditis elegans*. *Gene*, 214(1-2):59–66.

Barakat, R. and El Morshedy, H. (2011). Efficacy of two praziquantel treatments among primary school children in an area of high *Schistosoma mansoni* endemicity, Nile Delta, Egypt. *Parasitology*, 138(4):440–446.

Barckmann, B. and Simonelig, M. (2013). Control of maternal mRNA stability in germ cells and early embryos. *Biochim. Biophys. Acta*, 1829(6-7):714–24.

Barreau, C., Benson, E., Gudmannsdottir, E., Newton, F., and White-Cooper, H. (2008). Post-meiotic transcription in *Drosophila* testes. *Development*, 135(11):1897–1902.

Basch, P. F. (1981). Cultivation of *Schistosoma mansoni in vitro*. I. Establishment of cultures from cercariae and development until pairing. *J. Parasitol.*, 67(2):179–185.

Basch, P. F. (1990). Why do schistosomes have separate sexes? *Parasitol. Today*, 6(5):160–163.

Basch, P. F. and Basch, N. (1984). Intergeneric reproductive stimulation and parthenogenesis in *Schistosoma mansoni*. *Parasitology*, 89 (Pt 2):369–76.

Basch, P. F. and Nicolas, C. (1989). *Schistosoma mansoni*: pairing of male worms with artificial surrogate females. *Exp. Parasitol.*, 68(2):202–207.

Beckmann, S., Buro, C., Dissous, C., Hirzmann, J., and Grevelding, C. G. (2010a). The Syk kinase SmTK4 of *Schistosoma mansoni* is involved in the regulation of spermatogenesis and oogenesis. *PLoS Pathog.*, 6(2):e1000769.

Beckmann, S., Hahnel, S., Cailliau, K., Vanderstraete, M., Browaeys, E., Dissous, C., and Grevelding, C. G. (2011). Characterization of the Src/Abl hybrid kinase SmTK6 of *Schistosoma mansoni*. *J. Biol. Chem.*, 286(49):42325–42336.

Beckmann, S., Quack, T., Burmeister, C., Buro, C., Long, T., Dissous, C., and Grevelding, C. G. (2010b). *Schistosoma mansoni*: signal transduction processes during the development of the reproductive organs. *Parasitology*, 137(3):497–520.

Beckmann, S., Quack, T., Dissous, C., Cailliau, K., Lang, G., and Grevelding, C. G. (2012). Discovery of platyhelminth-specific α/β-integrin families and evidence for their role in reproduction in *Schistosoma mansoni*. *PLoS One*, 7(12):e52519.

Beitel, G. J., Lambie, E. J., and Horvitz, H. R. (2000). The *C. elegans* gene *lin-9*, which acts in an Rb-related pathway, is required for gonadal sheath cell development and encodes a novel protein. *Gene*, 254(1-2):253–263.

Benamrouz, S., Conseil, V., Creusy, C., Calderon, E., Dei-Cas, E., and Certad, G. (2012). Parasites and malignancies, a review, with emphasis on digestive cancer induced by *Cryptosporidium parvum* (Alveolata: Apicomplexa). *Parasite*, 19(2):101–15.

Benjamini, Y. and Hochberg, Y. (1995). Controlling the False Discovery Rate: A practical and powerful approach to multiple testing. *J. R. Stat. Soc. Ser. B*, 57(1):289 – 300.

Berriman, M., Haas, B. J., LoVerde, P. T., Wilson, R. A., Dillon, G. P., Cerqueira, G. C., Mashiyama, S. T., Al-Lazikani, B., Andrade, L. F., Ashton, P. D., Aslett, M. A., Bartholomeu, D. C., Blandin, G., Caffrey, C. R., Coghlan, A., Coulson, R., Day, T. a., Delcher, A., DeMarco, R., Djikeng, A., Eyre, T., Gamble, J. A., Ghedin, E., Gu, Y., Hertz-Fowler, C., Hirai, H., Hirai, Y., Houston, R., Ivens, A., Johnston, D. A., Lacerda, D., Macedo, C. D., McVeigh, P., Ning, Z., Oliveira, G., Overington, J. P., Parkhill, J., Pertea, M., Pierce, R. J., Protasio, A. V., Quail, M. a., Rajandream, M.-A., Rogers, J., Sajid, M., Salzberg, S. L., Stanke, M., Tivey, A. R., White, O., Williams, D. L., Wortman, J., Wu, W., Zamanian, M., Zerlotini, A., Fraser-Liggett, C. M., Barrell, B. G., and El-Sayed, N. M. (2009). The genome of the blood fluke *Schistosoma mansoni*. *Nature*, 460(7253):352–8.

Bettegowda, A. and Smith, G. W. (2007). Mechanisms of maternal mRNA regulation: implications for mammalian early embryonic development. *Front. Biosci.*, 12:3713–26.

Boerke, A., Dieleman, S. J., and Gadella, B. M. (2007). A possible role for sperm RNA in early embryo development. *Theriogenology*, 68 Suppl 1:S147–55.

Bogitsh, B. J., Carter, C. E., and Oeltmann, T. N. (2013). *Human Parasitology*. Academic Press.

Borgeson, C. D. and Samson, M. L. (2005). Shared RNA-binding sites for interacting members of the *Drosophila* ELAV family of neuronal proteins. *Nucleic Acids Res.*, 33(19):6372–6383.

Boswell, R. (1985). *tudor*, a gene required for assembly of the germ plasm in Drosophila melanogaster. *Cell*, 43(1):97–104.

Boutros, R., Dozier, C., and Ducommun, B. (2006). The when and wheres of CDC25 phosphatases. *Curr. Opin. Cell Biol.*, 18(2):185–191.

Brant, S. V. and Loker, E. S. (2005). Can specialized pathogens colonize distantly related hosts? Schistosome evolution as a case study. *PLoS Pathog.*, 1(3):167–9.

Breitwieser, W., Markussen, F. H., Horstmann, H., and Ephrussi, A. (1996). Oskar protein interaction with vasa represents an essential step in polar granule assembly. *Genes Dev.*, 10(17):2179–2188.

Brouwers, J. F. H. M., Smeenk, I. M. B., van Golde, L. M. G., and Tielens, A. G. M. (1997). The incorporation, modification and turnover of fatty acids in adult *Schistosoma mansoni*. *Mol. Biochem. Parasitol.*, 88(1–2):175–185.

Buro, C., Oliveira, K. C., Lu, Z., Leutner, S., Beckmann, S., Dissous, C., Cailliau, K., Verjovski-Almeida, S., and Grevelding, C. G. (2013). Transcriptome analyses of inhibitor-treated schistosome females provide evidence for cooperating Src-kinase and TGFβ receptor pathways controlling mitosis and eggshell formation. *PLoS Pathog.*, 9(6):e1003448.

Camacho, C., Coulouris, G., Avagyan, V., Ma, N., Papadopoulos, J., Bealer, K., and Madden, T. L. (2009). BLAST+: architecture and applications. *BMC Bioinformatics*, 10(1):421.

Cao, W., Gerton, G. L., and Moss, S. B. (2006). Proteomic profiling of accessory structures from the mouse sperm flagellum. *Mol. Cell. Proteomics*, 5(5):801–810.

Capron, A. and Dupas, H. (1972). Attempts at obtaining cell cultures from explants of *Schistosoma mansoni* (Sambon, 1907). *C. R. Acad. Sci. Hebd. Seances Acad. Sci. D.*, 275(12):1243–6.

Cheever, A. W., Macedonia, J. G., Mosimann, J. E., and Cheever, E. A. (1994). Kinetics of egg production and egg excretion by *Schistosoma mansoni* and *S. japonicum* in mice infected with a single pair of worms. *Am. J. Trop. Med. Hyg.*, 50(3):281–95.

Chen, D., Zheng, W., Lin, A., Uyhazi, K., Zhao, H., and Lin, H. (2012). Pumilio 1 suppresses multiple activators of p53 to safeguard spermatogenesis. *Curr. Biol.*, 22(5):420–425.

Chen, L. L., Rekosh, D. M., and LoVerde, P. T. (1992). *Schistosoma mansoni* p48 eggshell protein gene: characterization, developmentally regulated expression and comparison to the p14 eggshell protein gene. *Mol. Biochem. Parasitol.*, 52:39–52.

Cheng, G.-F., Lin, J.-J., Feng, X.-G., Fu, Z.-Q., Jin, Y.-M., Yuan, C.-X., Zhou, Y.-C., and Cai, Y.-M. (2005). Proteomic analysis of differentially expressed proteins between the male and female worm of *Schistosoma japonicum* after pairing. *Proteomics*, 5(2):511–21.

Chi, M. N., Auriol, J., Jegou, B., Kontoyiannis, D. L., Turner, J. M. A., de Rooij, D. G., and Morello, D. (2011). The RNA-binding protein ELAVL1/HuR is essential for mouse spermatogenesis, acting both at meiotic and postmeiotic stages. *Mol. Biol. Cell*, 22(16):2875–2885.

Chuan, J., Feng, Z., Brindley, P. J., McManus, D. P., Han, Z., Jianxin, P., and Hu, W. (2010). Our wormy world. Genomics, proteomics and transcriptomics in east and southeast Asia. *Adv. Parasitol.*, 73:327–371.

Clerico, E. M., Tilitsky, J. M., Meng, W., and Gierasch, L. M. (2015). How hsp70 molecular machines interact with their substrates to mediate diverse physiological functions. *J. Mol. Biol.*, 427(7):1575–88.

Clough, E. R. (1981). Morphology and reproductive organs and oogenesis in bisexual and unisexual transplants of mature *Schistosoma mansoni* females. *J. Parasitol.*, 67(4):535–9.

Cogswell, A. a., Kommer, V. P., and Williams, D. L. (2012). Transcriptional analysis of a unique set of genes involved in *Schistosoma mansoni* female reproductive biology. *PLoS Negl. Trop. Dis.*, 6(11):e1907.

Collins, J. J., Hou, X., Romanova, E. V., Lambrus, B. G., Miller, C. M., Saberi, A., Sweedler, J. V., and Newmark, P. A. (2010). Genome-wide analyses reveal a role for peptide hormones in planarian germline development. *PLoS Biol.*, 8(10):e1000509.

Collins, J. J. and Newmark, P. A. (2013). It's no fluke: the planarian as a model for understanding schistosomes. *PLoS Pathog.*, 9(7):e1003396.

Collins, J. J., Wang, B., Lambrus, B. G., Tharp, M. E., Iyer, H., and Newmark, P. a. (2013). Adult somatic stem cells in the human parasite *Schistosoma mansoni*. *Nature*, 494(7438):476–9.

Colombatti, A., Bonaldo, P., and Doliana, R. (1993). Type A modules: interacting domains found in several non-fibrillar collagens and in other extracellular matrix proteins. *Matrix*, 13(4):297–306.

Conlon, C. P. (2005). Schistosomiasis. *Medicine (Baltimore).*, 33(8):64–67.

Cordes, S., Frank, C. A., and Garriga, G. (2006). The *C. elegans* MELK ortholog PIG-1 regulates cell size asymmetry and daughter cell fate in asymmetric neuroblast divisions. *Development*, 133(14):2747–2756.

Cordingley, J. (1987). Trematode eggshells: Novel protein biopolymers. *Parasitol. Today*, 3(11):341–344.

Correia da Costa, J. M., Vale, N., Gouveia, M. J., Botelho, M. C., Sripa, B., Santos, L. L., Santos, J. H., Rinaldi, G., and Brindley, P. J. (2014). Schistosome and liver fluke derived catechol-estrogens and helminth associated cancers. *Front. Genet.*, 5:444.

Courtot, C., Fankhauser, C., Simanis, V., and Lehner, C. F. (1992). The *Drosophila* cdc25 homolog twine is required for meiosis. *Development*, 116(2):405–416.

Curwen, R. S., Ashton, P. D., Johnston, D. A., and Wilson, R. A. (2004). The *Schistosoma mansoni* soluble proteome: a comparison across four life-cycle stages. *Mol. Biochem. Parasitol.*, 138(1):57–66.

Curwen, R. S., Ashton, P. D., Sundaralingam, S., and Wilson, R. A. (2006). Identification of novel proteases and immunomodulators in the secretions of schistosome cercariae that facilitate host entry. *Mol. Cell. Proteomics*, 5(5):835–44.

De Bont, J. and Vercruysse, J. (1998). Schistosomiasis in cattle. *Adv. Parasitol.*, 41:285–364.

de Laval, F., Savini, H., Biance-Valero, E., and Simon, F. (2014). Human schistosomiasis: an emerging threat for Europe. *Lancet*, 384(9948):1094–5.

De Vries, L., Zheng, B., Fischer, T., Elenko, E., and Farquhar, M. G. (2000). The regulator of G protein signaling family. *Annu. Rev. Pharmacol. Toxicol.*, 40:235–271.

Deshpande, G., Calhoun, G., Yanowitz, J. L., and Schedl, P. D. (1999). Novel functions of nanos in downregulating mitosis and transcription during the development of the *Drosophila* germline. *Cell*, 99(3):271–81.

Dettman, C. D., Higgins-Opitz, S., and Saikoolal, A. (1989). Enhanced efficacy of the paddling method for schistosome infection of rodents by a four-step pre-soaking procedure. *Parasitol. Res.*, 76(2):183–184.

DeWalick, S., Bexkens, M. L., van Balkom, B. W. M., Wu, Y.-P., Smit, C. H., Hokke, C. H., de Groot, P. G., Heck, A. J. R., Tielens, A. G. M., and van Hellemond, J. J. (2011). The proteome of the insoluble *Schistosoma mansoni* eggshell skeleton. *Int. J. Parasitol.*, 41(5):523–32.

DeWalick, S., Tielens, A. G. M., and van Hellemond, J. J. (2012). *Schistosoma mansoni*: The egg, biosynthesis of the shell and interaction with the host. *Exp. Parasitol.*, 132(1):7–13.

Dissous, C., Morel, M., and Vanderstraete, M. (2014). Venus kinase receptors: prospects in signaling and biological functions of these invertebrate kinases. *Front. Endocrinol. (Lausanne).*, 5:72.

Doenhoff, M. J., Cioli, D., and Utzinger, J. (2008). Praziquantel: mechanisms of action, resistance and new derivatives for schistosomiasis. *Curr. Opin. Infect. Dis.*, 21(6):659–667.

Doenhoff, M. J., Hagan, P., Cioli, D., Southgate, V., Pica-Mattoccia, L., Botros, S., Coles, G., Tchuem Tchuenté, L. A., Mbaye, A., and Engels, D. (2009). Praziquantel: its use in control of schistosomiasis in sub-Saharan Africa and current research needs. *Parasitology*, 136(13):1825–35.

Duvall, R. H. and DeWitt, W. B. (1967). An improved perfusion technique for recovering adult schistosomes from laboratory animals. *Am. J. Trop. Med. Hyg.*, 16(4):483–6.

Dworkin, M. B. and Dworkin-Rastl, E. (1990). Functions of maternal mRNA in early development. *Mol. Reprod. Dev.*, 26(3):261–97.

El Ridi, R. A. F. and Tallima, H. A.-M. (2013). Novel therapeutic and prevention approaches for schistosomiasis: review. *J. Adv. Res.*, 4(5):467–78.

Erasmus, D. A. (1975). *Schistosoma mansoni*: Development of the vitelline cell, its role in drug sequestration, and changes induced by Astiban. *Exp. Parasitol.*, 38(2):240–256.

Erasmus, D. A., Popiel, I., and Shaw, J. R. (1982). A comparative study of the vitelline cell in *Schistosoma mansoni*, *S. haematobium*, *S. japonicum* and *S. mattheei*. *Parasitology*, 84:283–287.

Faghiri, Z., Camargo, S. M. R., Huggel, K., Forster, I. C., Ndegwa, D., Verrey, F., and Skelly, P. J. (2010). The tegument of the human parasitic worm *Schistosoma mansoni* as an excretory organ: The surface aquaporin SmAQP is a lactate transporter. *PLoS One*, 5.

Faghiri, Z. and Skelly, P. J. (2009). The role of tegumental aquaporin from the human parasitic worm, *Schistosoma mansoni*, in osmoregulation and drug uptake. *FASEB J.*, 23(8):2780–9.

Fenwick, A., Savioli, L., Engels, D., Robert Bergquist, N., and Todd, M. H. (2003). Drugs for the control of parasitic diseases: current status and development in schistosomiasis. *Trends Parasitol.*, 19(11):509–515.

Fitzpatrick, J. M. and Hoffmann, K. F. (2006). Dioecious *Schistosoma mansoni* express divergent gene repertoires regulated by pairing. *Int. J. Parasitol.*, 36(10-11):1081–9.

Forbes, A. and Lehmann, R. (1998). Nanos and Pumilio have critical roles in the development and function of *Drosophila* germline stem cells. *Development*, 125:679–690.

Franco, G. R., Rabelo, E. M., Azevedo, V., Pena, H. B., Ortega, J. M., Santos, T. M., Meira, W. S., Rodrigues, N. A., Dias, C. M., Harrop, R., Wilson, A., Saber, M., Abdel-Hamid, H., Faria, M. S., Margutti, M. E., Parra, J. C., and Pena, S. D. (1997). Evaluation of cDNA libraries from different developmental stages of *Schistosoma mansoni* for production of expressed sequence tags (ESTs). *DNA Res.*, 4(3):231–40.

Freitas, T. C., Jung, E., and Pearce, E. J. (2007). TGF-beta signaling controls embryo development in the parasitic flatworm *Schistosoma mansoni*. *PLoS Pathog.*, 3(4):489–497.

Freitas, T. C., Jung, E., and Pearce, E. J. (2009). A bone morphogenetic protein homologue in the parasitic flatworm, *Schistosoma mansoni*. *Int. J. Parasitol.*, 39(3):281–287.

Fried, B. and Graczyk, T. K. (1997). Reproductive Physiology and Behavior of Digenetic Trematodes. In *Adv. Parasitol.*, chapter 5, pages 117–148. CRC Press.

Fukuda, M. (2003). Molecular cloning, expression, and characterization of a novel class of synaptotagmin (Syt XIV) conserved from *Drosophila* to humans. *J. Biochem.*, 133(5):641–649.

Fuller, M. T. and Spradling, A. C. (2007). Male and female *Drosophila* germline stem cells: two versions of immortality. *Science*, 316(5823):402–4.

Furlong, S. T. (1991). Unique roles for lipids in *Schistosoma mansoni*. *Parasitol. Today*, 7(2):59–62.

Gobert, G. N. (2010). Applications for profiling the schistosome transcriptome. *Trends Parasitol.*, 26(9):434–439.

Gobert, G. N., McManus, D. P., Nawaratna, S., Moertel, L., Mulvenna, J., and Jones, M. K. (2009). Tissue specific profiling of females of *Schistosoma japonicum* by integrated laser microdissection microscopy and microarray analysis. *PLoS Negl. Trop. Dis.*, 3(6):e469.

Gonnert, R. (1955a). Schistosomiasis studies. II. Oogenesis of *Schistosoma mansoni* and the development of the eggs in the host organism. *Z. Tropenmed. Parasitol.*, 6(1):33–52.

Gonnert, R. (1955b). Schiztosomiasis studies. I. Contributions to the anatomy and histology of *Schistosoma mansoni. Z. Tropenmed. Parasitol.*, 6(1):18–33.

Gray, D. J., Williams, G. M., Li, Y., Chen, H., Forsyth, S. J., Li, R. S., Barnett, A. G., Guo, J., Ross, A. G., Feng, Z., and McManus, D. P. (2009). A cluster-randomised intervention trial against *Schistosoma japonicum* in the Peoples' Republic of China: Bovine and human transmission. *PLoS One*, 4(6).

Grevelding, C. G. (1995). The female-specific W1 sequence of the Puerto Rican strain of *Schistosoma mansoni* occurs in both genders of a Liberian strain. *Mol. Biochem. Parasitol.*, 71(2):269–72.

Grevelding, C. G. (1999). Genomic instability in *Schistosoma mansoni*. *Mol. Biochem. Parasitol.*, 101(1-2):207–16.

Grevelding, C. G. (2004). Schistosoma. *Curr. Biol.*, 14(14):R545.

Grevelding, C. G., Sommer, G., and Kunz, W. (1997). Female-specific gene expression in *Schistosoma mansoni* is regulated by pairing. *Parasitology*, 115 (Pt 6:635–640.

Grigoryan, G. and Keating, A. E. (2008). Structural specificity in coiled-coil interactions. *Curr. Opin. Struct. Biol.*, 18(4):477–483.

Grimes, J. E. T., Croll, D., Harrison, W. E., Utzinger, J., Freeman, M. C., and Templeton, M. R. (2014). The relationship between water, sanitation and schistosomiasis: a systematic review and meta-analysis. *PLoS Negl. Trop. Dis.*, 8(12):e3296.

Grobusch, M. P., Mühlberger, N., Jelinek, T., Bisoffi, Z., Corachán, M., Harms, G., Matteelli, A., Fry, G., Hatz, C., Gjø rup, I., Schmid, M. L., Knobloch, J., Puente, S., Bronner, U., Kapaun, A., Clerinx, J., Nielsen, L. N., Fleischer, K., Beran, J., da Cunha, S., Schulze, M., Myrvang, B., and Hellgren, U. (2003). Imported schistosomiasis in Europe: sentinel surveillance data from TropNetEurop. *J. Travel Med.*, 10(3):164–9.

Grosse, R., Copeland, J. W., Newsome, T. P., Way, M., and Treisman, R. (2003). A role for VASP in RhoA-Diaphanous signalling to actin dynamics and SRF activity. *EMBO J.*, 22(12):3050–61.

Grossman, A. I., Short, R. B., and Cain, G. D. (1981). Karyotype evolution and sex chromosome differentiation in Schistosomes (Trematoda, Schistosomatidae). *Chromosoma*, 84(3):413–430.

Gryseels, B., Mbaye, A., De Vlas, S. J., Stelma, F. F., Guissé, F., Van Lieshout, L., Faye, D., Diop, M., Ly, A., Tchuem-Tchuenté, L. A., Engels, D., and Polman, K. (2001). Are poor responses to praziquantel for the treatment of *Schistosoma mansoni* infections in Senegal due to resistance? An overview of the evidence. *Trop. Med. Int. Heal.*, 6(11):864–873.

Gryseels, B., Polman, K., Clerinx, J., and Kestens, L. (2006). Human schistosomiasis. *Lancet*, 368(9541):1106–18.

Gupta, B. C. and Basch, P. F. (1987a). Evidence for transfer of a glycoprotein from male to female *Schistosoma mansoni* during pairing. *J. Parasitol.*, 73(3):674–5.

Gupta, B. C. and Basch, P. F. (1987b). The role of *Schistosoma mansoni* males in feeding and development of female worms. *J. Parasitol.*, 73(3):481–6.

Hahnel, S., Lu, Z., Wilson, R. A., Grevelding, C. G., and Quack, T. (2013). Whole-organ isolation approach as a basis for tissue-specific analyses in *Schistosoma mansoni*. *PLoS Negl. Trop. Dis.*, 7(7):e2336.

Hahnel, S., Quack, T., Parker-Manuel, S. J., Lu, Z., Vanderstraete, M., Morel, M., Dissous, C., Cailliau, K., and Grevelding, C. G. (2014). Gonad RNA-specific qRT-PCR analyses identify genes with potential functions in schistosome reproduction such as SmFz1 and SmFGFRs. *Front. Genet.*, 5:1–15.

Hake, L. E. and Richter, J. D. (1994). CPEB is a specificity factor that mediates cytoplasmic polyadenylation during *Xenopus* oocyte maturation. *Cell*, 79:617–627.

Harris, I. R., Höppner, H., Siefken, W., Farrell, A. M., and Wittern, K. P. (2000). Regulation of HMG-CoA synthase and HMG-CoA reductase by insulin and epidermal growth factor in HaCaT keratinocytes. *J. Invest. Dermatol.*, 114(1):83–87.

Hatz, C. F. R. (2005). Schistosomiasis: an underestimated problem in industrialized countries? *J. Travel Med.*, 12(1):1–2.

He, L., Jiang, H., Cao, D., Liu, L., Hu, S., and Wang, Q. (2013). Comparative transcriptome analysis of the accessory sex gland and testis from the Chinese mitten crab (*Eriocheir sinensis*). *PLoS One*, 8(1):e53915.

Hobert, O. (2005). *The neuronal genome of* Caenorhabditis elegans. Pasadena (CA): WormBook.

Hoffmann, K. F., Brindley, P. J., and Berriman, M. (2014). Medicine. Halting harmful helminths. *Science*, 346(6206):168–9.

Hokke, C. H., Fitzpatrick, J. M., and Hoffmann, K. F. (2007). Integrating transcriptome, proteome and glycome analyses of *Schistosoma* biology. *Trends Parasitol.*, 23(4):165–74.

Honeycutt, J., Hammam, O., Fu, C.-L., and Hsieh, M. H. (2014). Controversies and challenges in research on urogenital schistosomiasis-associated bladder cancer. *Trends Parasitol.*, 30(7):324–32.

Huang, H.-H., Rigouin, C., and Williams, D. L. (2012). The redox biology of schistosome parasites and applications for drug development. *Curr. Pharm. Des.*, 18(24):3595–611.

Huang, Y., Chen, W., Wang, X., Liu, H., Chen, Y., Guo, L., Luo, F., Sun, J., Mao, Q., Liang, P., Xie, Z., Zhou, C., Tian, Y., Lv, X., Huang, L., Zhou, J., Hu, Y., Li, R., Zhang, F., Lei, H., Li, W., Hu, X., Liang, C., Xu, J., Li, X., and Yu, X. (2013). The carcinogenic liver fluke, *Clonorchis sinensis*: new assembly, reannotation and analysis of the genome and characterization of tissue transcriptomes. *PLoS One*, 8.

Huang, Y.-X. X. and Manderson, L. (2005). The social and economic context and determinants of schistosomiasis japonica. *Acta Trop.*, 96(2-3):223–31.

Hulstijn, M., Barros, L. A., Neves, R. H., Moura, E. G., Gomes, D. C., and Machado-Silva, J. R. (2006). Hermaphrodites and supernumerary testicular lobes in *Schistosoma mansoni* (Trematoda: Schistosomatidae) analyzed by brightfield and confocal microscopy. *J. Parasitol.*, 92(3):496–500.

Hutt, D. M., Cardullo, R. A., Baltz, J. M., and Ngsee, J. K. (2002). Synaptotagmin VIII is localized to the mouse sperm head and may function in acrosomal exocytosis. *Biol. Reprod.*, 66(1):50–6.

Inaba, K. (2003). Molecular architecture of the sperm flagella: molecules for motility and signaling. *Zoolog. Sci.*, 20(9):1043–1056.

Irla, M., Puthier, D., Le Goffic, R., Victorero, G., Freeman, T., Naquet, P., Samson, M., and Nguyen, C. (2003). Spatial, a new nuclear factor tightly regulated during mouse spermatogenesis. *Gene Expr. Patterns*, 3(2):135–138.

Ivanchenko, M. G., Lerner, J. P., McCormick, R. S., Toumadje, A., Allen, B., Fischer, K., Hedstrom, O., Helmrich, A., Barnes, D. W., and Bayne, C. J. (1999). Continuous *in vitro* propagation and differentiation of cultures of the intramolluscan stages of the human parasite *Schistosoma mansoni*. *Proc. Natl. Acad. Sci.*, 96(9):4965–4970.

Jacobs, S., Schürmann, A., Becker, W., Böckers, T. M., Copeland, N. G., Jenkins, N. A., and Joost, H. G. (1998). The mouse ADP-ribosylation factor-like 4 gene: two separate promoters direct specific transcription in tissues and testicular germ cell. *Biochem. J.*, 335 (Pt 2:259–265.

Januschke, J., Gervais, L., Dass, S., Kaltschmidt, J. A., Lopez-Schier, H., St. Johnston, D., Brand, A. H., Roth, S., and Guichet, A. (2002). Polar transport in the *Drosophila* oocyte requires Dynein and Kinesin I cooperation. *Curr. Biol.*, 12(23):1971–1981.

Johnstone, O. and Lasko, P. (2001). Translational regulation and RNA localization in *Drosophila* oocytes and embryos. *Annu. Rev. Genet.*, 35:365–406.

Kapp, K., Knobloch, J., Schüssler, P., Sroka, S., Lammers, R., Kunz, W., and Grevelding, C. G. (2004). The *Schistosoma mansoni* Src kinase TK3 is expressed in the gonads and likely involved in cytoskeletal organization. *Mol. Biochem. Parasitol.*, 138(2):171–82.

Kapp, K., Schüssler, P., Kunz, W., and Grevelding, C. G. (2001). Identification, isolation and characterization of a Fyn-like tyrosine kinase from *Schistosoma mansoni*. *Parasitology*, 122(Pt 3):317–327.

Karlsson-Rosenthal, C. and Millar, J. B. A. (2006). Cdc25: mechanisms of checkpoint inhibition and recovery. *Trends Cell Biol.*, 16(6):285–292.

Kellis, M., Wold, B., Snyder, M. P., Bernstein, B. E., Kundaje, A., Marinov, G. K., Ward, L. D., Birney, E., Crawford, G. E., Dekker, J., Dunham, I., Elnitski, L. L., Farnham, P. J., Feingold, E. a., Gerstein, M., Giddings, M. C., Gilbert, D. M., Gingeras, T. R., Green, E. D., Guigo, R., Hubbard, T., Kent, J., Lieb, J. D., Myers, R. M., Pazin, M. J., Ren, B., Stamatoyannopoulos, J. a., Weng, Z., White, K. P., and Hardison, R. C. (2014). Defining functional DNA elements in the human genome. *Proc. Natl. Acad. Sci. U. S. A.*, 111(17):6131–8.

Kim, J., Kawasaki, I., and Shim, Y.-H. (2010). cdc-25.2, a *C. elegans* ortholog of cdc25, is required to promote oocyte maturation. *J. Cell Sci.*, 123(Pt 6):993–1000.

Kim, S., Govindan, J. A., Tu, Z. J., and Greenstein, D. (2012). SACY-1 DEAD-Box helicase links the somatic control of oocyte meiotic maturation to the sperm-to-oocyte switch and gamete maintenance in *Caenorhabditis elegans*. *Genetics*, 192(3):905–28.

Knobloch, J., Beckmann, S., Burmeister, C., Quack, T., and Grevelding, C. G. (2007). Tyrosine kinase and cooperative TGFbeta signaling in the reproductive organs of *Schistosoma mansoni*. *Exp. Parasitol.*, 117(3):318–36.

Knobloch, J., Kunz, W., and Grevelding, C. G. (2002a). Quantification of DNA synthesis in multicellular organisms by a combined DAPI and BrdU technique. *Dev. Growth Differ.*, 44(6):559–63.

Knobloch, J., Rossi, A., Osman, A., Loverde, P. T., Klinkert, M. Q., and Grevelding, C. G. (2004). Cytological and biochemical evidence for a gonad-preferential interplay of SmFKBP12 and SmTβR-I in *Schistosoma mansoni*. *Mol. Biochem. Parasitol.*, 138(2):227–236.

Knobloch, J., Winnen, R., Quack, M., Kunz, W., and Grevelding, C. G. (2002b). A novel Syk-family tyrosine kinase from *Schistosoma mansoni* which is preferentially transcribed in reproductive organs. *Gene*, 294(1-2):87–97.

Knudsen, G. M., Medzihradszky, K. F., Lim, K.-C., Hansell, E., and McKerrow, J. H. (2005). Proteomic analysis of *Schistosoma mansoni* cercarial secretions. *Mol. Cell. Proteomics*, 4(12):1862–75.

Krautz-Peterson, G., Camargo, S., Huggel, K., Verrey, F., Shoemaker, C. B., and Skelly, P. J. (2007). Amino acid transport in schistosomes: Characterization of the permeaseheavy chain SPRM1hc. *J. Biol. Chem.*, 282(30):21767–75.

Kuner, R., Fälth, M., Pressinotti, N. C., Brase, J. C., Puig, S. B., Metzger, J., Gade, S., Schäfer, G., Bartsch, G., Steiner, E., Klocker, H., and Sültmann, H. (2013). The maternal embryonic leucine zipper kinase (MELK) is upregulated in high-grade prostate cancer. *J. Mol. Med.*, 91(2):237–248.

Kunz, W. (2001). Schistosome male-female interaction: induction of germ-cell differentiation. *Trends Parasitol.*, 17(5):227–231.

Kunz, W., Gohr, L., Grevelding, C., Schüssler, P., Sommer, G., Menrath, M., and Michel, A. (1995). *Schistosoma mansoni*: control of female fertility by the male. *Mem. Inst. Oswaldo Cruz*, 90(2):185–189.

Kusel, J. and Hagan, P. (1999). Praziquantel – its use, cost and possible development of resistance. *Parasitol. Today*, 15(9):352–354.

Lalancette, C., Miller, D., Li, Y., and Krawetz, S. A. (2008). Paternal contributions: new functional insights for spermatozoal RNA. *J. Cell. Biochem.*, 104(5):1570–9.

Leutner, S., Oliveira, K. C., Rotter, B. B., Beckmann, S., Buro, C., Hahnel, S., Kitajima, J. P., Verjovski-Almeida, S., Winter, P., and Grevelding, C. G. (2013). Combinatory microarray and SuperSAGE analyses identify pairing-dependently transcribed genes in *Schistosoma mansoni* males, including follistatin. *PLoS Negl. Trop. Dis.*, 7(11):e2532.

Levy-Holtzman, R. and Schechter, I. (1996). Expression of different forms of the heat-shock factor during the life cycle of the parasitic helminth *Schistosoma mansoni*. *Biochim. Biophys. Acta*, 1317(1):1–4.

Li, H., Handsaker, B., Wysoker, A., Fennell, T., Ruan, J., Homer, N., Marth, G., Abecasis, G., and Durbin, R. (2009). The Sequence Alignment/Map format and SAMtools. *Bioinformatics*, 25(16):2078–9.

Lin, M.-L., Park, J.-H., Nishidate, T., Nakamura, Y., and Katagiri, T. (2007). Involvement of maternal embryonic leucine zipper kinase (MELK) in mammary carcinogenesis through interaction with Bcl-G, a pro-apoptotic member of the Bcl-2 family. *Breast Cancer Res.*, 9(1):R17.

Liu, F., Lu, J., Hu, W., Wang, S.-Y., Cui, S.-J., Chi, M., Yan, Q., Wang, X.-R., Song, H.-D., Xu, X.-N., Wang, J.-J., Zhang, X.-L., Zhang, X., Wang, Z.-Q., Xue, C.-L., Brindley, P. J., McManus, D. P., Yang, P.-Y., Feng, Z., Chen, Z., and Han, Z.-G. (2006). New perspectives on host-parasite interplay by comparative transcriptomic and proteomic analyses of *Schistosoma japonicum*. *PLoS Pathog.*, 2(4):e29.

Long, T., Cailliau, K., Beckmann, S., Browaeys, E., Trolet, J., Grevelding, C. G., and Dissous, C. (2010). *Schistosoma mansoni* Polo-like kinase 1: A mitotic kinase with key functions in parasite reproduction. *Int. J. Parasitol.*, 40(9):1075–86.

Long, T., Vanderstraete, M., Cailliau, K., Morel, M., Lescuyer, A., Gouignard, N., Grevelding, C. G., Browaeys, E., and Dissous, C. (2012). SmSak, the second Polo-like

kinase of the helminth parasite *Schistosoma mansoni*: conserved and unexpected roles in meiosis. *PLoS One*, 7(6):e40045.

LoVerde, P. T., Andrade, L. F., and Oliveira, G. (2009). Signal transduction regulates schistosome reproductive biology. *Curr. Opin. Microbiol.*, 12(4):422–8.

LoVerde, P. T. and Chen, L. (1991). Schistosome female reproductive development. *Parasitol. Today*, 7(11):303–8.

LoVerde, P. T., Hirai, H., Merrick, J. M., Lee, N. H., and El-Sayed, N. (2004a). *Schistosoma mansoni* genome project: An update. *Parasitol. Int.*, 53(2):183–192.

LoVerde, P. T., Niles, E. G., Osman, A., and Wu, W. (2004b). *Schistosoma mansoni* male–female interactions. *Can. J. Zool.*, 82(2):357–374.

LoVerde, P. T., Osman, A., and Hinck, A. (2007). *Schistosoma mansoni*: TGF-beta signaling pathways. *Exp. Parasitol.*, 117(3):304–317.

Lu, Z., Quack, T., Hahnel, S., Gelmedin, V., Pouokam, E., Diener, M., Hardt, M., Michel, G., Baal, N., Hackstein, H., and Grevelding, C. G. (2015). Isolation, enrichment and primary characterisation of vitelline cells from *Schistosoma mansoni* obtained by the organ isolation method. *Int. J. Parasitol.*, 45(9-10):663–672.

Luitjens, C., Gallegos, M., Kraemer, B., Kimble, J., and Wickens, M. (2000). CPEB proteins control two key steps in spermatogenesis in *C. elegans*. *Genes Dev.*, 14:2596–2609.

McCarthy, D. J., Chen, Y., and Smyth, G. K. (2012). Differential expression analysis of multifactor RNA-Seq experiments with respect to biological variation. *Nucleic Acids Res.*, 40(10):4288–4297.

McVeigh, P., Kimber, M. J., Novozhilova, E., and Day, T. A. (2005). Neuropeptide signalling systems in flatworms. *Parasitology*, 131 Suppl:S41–55.

McVeigh, P., Mair, G. R., Atkinson, L., Ladurner, P., Zamanian, M., Novozhilova, E., Marks, N. J., Day, T. A., and Maule, A. G. (2009). Discovery of multiple neuropeptide families in the phylum Platyhelminthes. *Int. J. Parasitol.*, 39(11):1243–52.

Mehlhorn, H. (2008). *Encyclopedia of Parasitology*. Springer.

Michaels, R. M. (1969). Mating of *Schistosoma mansoni in Vitro*. *Exp. Parasitol.*, 25:58–71.

Ming, Z., Dong, H., Zhong, Q., Grevelding, C. G., and Jiang, M. (2006). The effect of a mutagen (N-methyl-N-nitro-N-nitrosoguanidine) on cultured cells from adult *Schistosoma japonicum*. *Parasitol. Res.*, 98(5):430–7.

Moore, D. V. and Sandground, J. H. (1956). The relative egg producing capacity of *Schistosoma mansoni* and *Schistosoma japonicum*. *Am. J. Trop. Med. Hyg.*, 5(5):831–40.

Moser, D., Doumbo, O., and Klinkert, M. Q. (1990). The humoral response to heat shock protein 70 in human and murine Schistosomiasis mansoni. *Parasite Immunol.*, 12(4):341–52.

Mtango, N. R., Potireddy, S., and Latham, K. E. (2008). Oocyte quality and maternal control of development. *Int. Rev. Cell Mol. Biol.*, 268:223–90.

Nagy, S., Ricca, B. L., Norstrom, M. F., Courson, D. S., Brawley, C. M., Smithback, P. A., and Rock, R. S. (2008). A myosin motor that selects bundled actin for motility. *Proc. Natl. Acad. Sci. U. S. A.*, 105(28):9616–9620.

Nahum, L. A., Mourão, M. M., and Oliveira, G. (2012). New frontiers in schistosoma genomics and transcriptomics. *J. Parasitol. Res.*, 2012.

Nakano, I., Paucar, A. A., Bajpai, R., Dougherty, J. D., Zewail, A., Kelly, T. K., Kim, K. J., Ou, J., Groszer, M., Imura, T., Freije, W. A., Nelson, S. F., Sofroniew, M. V., Wu, H., Liu, X., Terskikh, A. V., Geschwind, D. H., and Kornblum, H. I. (2005). Maternal embryonic leucine zipper kinase (MELK) regulates multipotent neural progenitor proliferation. *J. Cell Biol.*, 170(3):413–427.

Nawaratna, S. S. K., Gobert, G. N., Willis, C., Chuah, C., McManus, D. P., and Jones, M. K. (2014). Transcriptional profiling of the oesophageal gland region of male worms of *Schistosoma mansoni*. *Mol. Biochem. Parasitol.*, 196(2):82–89.

Nawaratna, S. S. K., McManus, D. P., Moertel, L., Gobert, G. N., and Jones, M. K. (2011). Gene atlasing of digestive and reproductive tissues in *Schistosoma mansoni*. *PLoS Negl. Trop. Dis.*, 5(4):e1043.

Neumann, S., Ziv, E., Lantner, F., and Schechter, I. (1993). Regulation of HSP70 gene expression during the life cycle of the parasitic helminth *Schistosoma mansoni*. *Eur. J. Biochem.*, 212(2):589–96.

Neves, R. H., de Lamare Biolchini, C., Machado-Silva, J. R., Carvalho, J. J., Branquinho, T. B., Lenzi, H. L., Hulstijn, M., and Gomes, D. C. (2005). A new description of the

reproductive system of *Schistosoma mansoni* (Trematoda: Schistosomatidae) analyzed by confocal laser scanning microscopy. *Parasitol. Res.*, 95(1):43–9.

Newmark, P. A. and Boswell, R. E. (1994). The mago nashi locus encodes an essential product required for germ plasm assembly in *Drosophila*. *Development*, 120(5):1303–1313.

O'Connell, M. L., Cavallo, W. C., and Firnberg, M. (2014). The expression of CPEB proteins is sequentially regulated during zebrafish oogenesis and embryogenesis. *Mol. Reprod. Dev.*, 81(4):376–87.

Okumura-Noji, K., Miura, Y., Lu, R., Asai, K., Ohta, N., Brindley, P. J., and Yokoyama, S. (2013). CD36-related protein in *Schistosoma japonicum*: candidate mediator of selective cholesteryl ester uptake from high-density lipoprotein for egg maturation. *FASEB J.*, 27(3):1236–44.

Olveda, D. U., Li, Y., Olveda, R. M., Lam, A. K., McManus, D. P., Chau, T. N. P., Harn, D. A., Williams, G. M., Gray, D. J., and Ross, A. G. P. (2014). Bilharzia in the Philippines: Past, present, and future. *Int. J. Infect. Dis.*, 18(1):52–56.

Osman, A., Niles, E. G., Verjovski-Almeida, S., and LoVerde, P. T. (2006). *Schistosoma mansoni* TGF-beta receptor II: role in host ligand-induced regulation of a schistosome target gene. *PLoS Pathog.*, 2(6):e54.

Pan, S. C. (1980). The fine structure of the miracidium of *Schistosoma mansoni*. *J. Invertebr. Pathol.*, 36(3):307–72.

Parekh, A. B. (2006). On the activation mechanism of store-operated calcium channels. *Pflügers Arch. - Eur. J. Physiol.*, 453(3):303–311.

Parker-Manuel, S. J., Ivens, A. C., Dillon, G. P., and Wilson, R. A. (2011). Gene expression patterns in larval *Schistosoma mansoni* associated with infection of the mammalian host. *PLoS Negl. Trop. Dis.*, 5(8):e1274.

Parma, D. H., Bennett, P. E., and Boswell, R. E. (2007). Mago Nashi and Tsunagi/Y14, respectively, regulate *Drosophila* germline stem cell differentiation and oocyte specification. *Dev. Biol.*, 308(2):507–519.

Peifer, M., Orsulic, S., Sweeton, D., and Wieschaus, E. (1993). A role for the *Drosophila* segment polarity gene armadillo in cell adhesion and cytoskeletal integrity during oogenesis. *Development*, 118(4):1191–1207.

Pires-daSilva, A. (2007). Evolution of the control of sexual identity in nematodes. *Semin. Cell Dev. Biol.*, 18(3):362–370.

Platt, T. R. and Brooks, D. R. (1997). Evolution of the schistosomes (Digenea: Schistosomatoidea): the origin of dioecy and colonization of the venous system. *J. Parasitol.*, 83(6):1035–44.

Pokrywka, N. J. and Stephenson, E. C. (1995). Microtubules are a general component of mRNA localization systems in *Drosophila* oocytes. *Dev. Biol.*, 167(1):363–70.

Popiel, I. (1986). Male-stimulated female maturation in *Schistosoma*: A review. *J. Chem. Ecol.*, 12(8):1745–54.

Popiel, I. and Basch, P. F. (1984). Reproductive development of female *Schistosoma mansoni* (Digenea: Schistosomatidae) following bisexual pairing of worms and worm segments. *J. Exp. Zool.*, 232(1):141–50.

Protasio, A. V., Tsai, I. J., Babbage, A., Nichol, S., Hunt, M., Aslett, M. A., de Silva, N., Velarde, G. S., Anderson, T. J. C., Clark, R. C., Davidson, C., Dillon, G. P., Holroyd, N. E., LoVerde, P. T., Lloyd, C., McQuillan, J., Oliveira, G., Otto, T. D., Parker-Manuel, S. J., Quail, M. A., Wilson, R. A., Zerlotini, A., Dunne, D. W., and Berriman, M. (2012). A systematically improved high quality genome and transcriptome of the human blood fluke *Schistosoma mansoni*. *PLoS Negl. Trop. Dis.*, 6(1):e1455.

Quack, T., Knobloch, J., Beckmann, S., Vicogne, J., Dissous, C., and Grevelding, C. G. (2009). The formin-homology protein SmDia interacts with the Src kinase SmTK and the GTPase SmRho1 in the gonads of *Schistosoma mansoni*. *PLoS One*, 4(9):e6998.

Quack, T., Wippersteg, V., and Grevelding, C. G. (2010). Cell cultures for schistosomes - Chances of success or wishful thinking? *Int. J. Parasitol.*, 40(9):991–1002.

Ramsköld, D., Wang, E. T., Burge, C. B., and Sandberg, R. (2009). An abundance of ubiquitously expressed genes revealed by tissue transcriptome sequence data. *PLoS Comput. Biol.*, 5(12):e1000598.

Raso, G., N'Goran, E. K., Toty, A., Luginbühl, A., Adjoua, C. A., Tian-Bi, N. T., Bogoch, I. I., Vounatsou, P., Tanner, M., and Utzinger, J. (2004). Efficacy and side effects of praziquantel against *Schistosoma mansoni* in a community of western Côte d'Ivoire. *Trans. R. Soc. Trop. Med. Hyg.*, 98(1):18–27.

Ratti, A., Fallini, C., Cova, L., Fantozzi, R., Calzarossa, C., Zennaro, E., Pascale, A., Quattrone, A., and Silani, V. (2006). A role for the ELAV RNA-binding proteins in neural stem cells: stabilization of Msi1 mRNA. *J. Cell Sci.*, 119(Pt 7):1442–1452.

Reimers, N., Homann, A., Höschler, B., Langhans, K., Wilson, R. A., Pierrot, C., Khalife, J., Grevelding, C. G., Chalmers, I. W., Yazdanbakhsh, M., Hoffmann, K. F., Hokke, C. H., Haas, H., and Schramm, G. (2015). Drug-induced exposure of *Schistosoma mansoni* antigens SmCD59a and SmKK7. *PLoS Negl. Trop. Dis.*, 9(3):e0003593.

Ribeiro-Paes, J. T. and Rodrigues, V. (1997). Sex determination and female reproductive development in the genus *Schistosoma*: a review. *Rev. do Inst. Med. Trop. SÃ\poundso Paulo*, 39:337–344.

Richter, J. D. (2007). CPEB: a life in translation. *Trends Biochem. Sci.*, 32(6):279–85.

Robb, D. L., Heasman, J., Raats, J., and Wylie, C. (1996). A kinesin-like protein is required for germ plasm aggregation in *Xenopus*. *Cell*, 87(5):823–831.

Robinson, D. N. and Cooley, L. (1997). *Drosophila* kelch is an oligomeric ring canal actin organizer. *J. Cell Biol.*, 138(4):799–810.

Robinson, M. D., McCarthy, D. J., and Smyth, G. K. (2010). edgeR: a Bioconductor package for differential expression analysis of digital gene expression data. *Bioinformatics*, 26(1):139–140.

Rofatto, H. K., Tararam, C. A., Borges, W. C., Wilson, R. A., Leite, L. C. C., and Farias, L. P. (2009). Characterization of phosphodiesterase-5 as a surface protein in the tegument of *Schistosoma mansoni*. *Mol. Biochem. Parasitol.*, 166(1):32–41.

Ross, A. G. P., Bartley, P. B., Sleigh, A. C., Olds, G. R., Li, Y., Williams, G. M., and McManus, D. P. (2002). Schistosomiasis. *N. Engl. J. Med.*, 346(16):1212–20.

Rossi, A., Pica-Mattoccia, L., Cioli, D., and Klinkert, M.-Q. (2002). Rapamycin insensitivity in *Schistosoma mansoni* is not due to FKBP12 functionality. *Mol. Biochem. Parasitol.*, 125(1-2):1–9.

Roy, A., Lin, Y. N., Agno, J. E., Demayo, F. J., and Matzuk, M. M. (2009). Tektin 3 is required for progressive sperm motility in mice. *Mol. Reprod. Dev.*, 76(5):453–459.

Rudolph, J. (2007). Cdc25 phosphatases: Structure, specificity, and mechanism. *Biochemistry*, 46(12):3595–3604.

Schäfer, M., Nayernia, K., Engel, W., and Schäfer, U. (1995). Translational control in spermatogenesis. *Dev. Biol.*, 172(2):344–352.

Schneider, C. A., Rasband, W. S., and Eliceiri, K. W. (2012). NIH Image to ImageJ: 25 years of image analysis. *Nat. Methods*, 9(7):671–675.

Sekii, K., Salvenmoser, W., De Mulder, K., Scharer, L., and Ladurner, P. (2009). Melav2, an elav-like gene, is essential for spermatid differentiation in the flatworm *Macrostomum lignano*. *BMC Dev. Biol.*, 9:62.

Seydoux, G. (1996). Mechanisms of translational control in early development. *Curr. Opin. Genet. Dev.*, 6(5):555–61.

Shaw, J. R., Marshall, I., and Erasmus, D. A. (1977). *Schistosoma mansoni*: *In vitro* stimulation of vitelline cell development by extracts of male worms. *Exp. Parasitol.*, 42(1):14–20.

Shaw, M. K. (1987). *Schistosoma mansoni*: vitelline gland development in females from single sex infections. *J. Helminthol.*, 61:253–259.

Shaw, M. K. and Erasmus, D. A. (1982). *Schistosoma mansoni*: the presence and ultrastructure of vitelline cells in adult males. *J. Helminthol.*, 56(1):51–3.

Shaw, M. K. and Erasmus, D. A. (1983). *Schistosoma mansoni*: changes in elemental composition in relation to the age and sexual status of the worms. *Parasitology*, 86 (Pt 3):439–53.

Siepen, J. A., Keevil, E.-J., Knight, D., and Hubbard, S. J. (2007). Prediction of missed cleavage sites in tryptic peptides aids protein identification in proteomics. *J. Proteome Res.*, 6(1):399–408.

Simionato, E., Barrios, N., Duloquin, L., Boissonneau, E., Lecorre, P., and Agnès, F. (2007). The *Drosophila* RNA-binding protein ELAV is required for commissural axon midline crossing via control of commissureless mRNA expression in neurons. *Dev. Biol.*, 301(1):166–177.

Skelly, P. J., Da'dara, A. A., Li, X.-H., Castro-Borges, W., and Wilson, R. A. (2014). Schistosome feeding and regurgitation. *PLoS Pathog.*, 10(8):e1004246.

Skinner, D. E., Rinaldi, G., Suttiprapa, S., Mann, V. H., Smircich, P., Cogswell, A. a., Williams, D. L., and Brindley, P. J. (2012). Vasa-like DEAD-box RNA helicases of *Schistosoma mansoni*. *PLoS Negl. Trop. Dis.*, 6(6):e1686.

Smithers, S. R. and Terry, R. J. (1965). The infection of laboratory hosts with cercariae of *Schistosoma mansoni* and the recovery of the adult worms. *Parasitology*, 55(4):695–700.

Smyth, J. D. and Clegg, J. A. (1959). Egg-shell formation in trematodes and cestodes. *Exp. Parasitol.*, 8(3):286–323.

Snyder, S. D. (2004). Phylogeny and paraphyly among tetrapod blood flukes (Digenea: Schistosomatidae and Spirorchiidae). *Int. J. Parasitol.*, 34(12):1385–92.

Spirin, A. S. (1994). Storage of messenger RNA in eukaryotes: envelopment with protein, translational barrier at 5′ side, or conformational masking by 3′ side? *Mol. Reprod. Dev.*, 38(1):107–17.

Styhler, S., Nakamura, A., Swan, A., Suter, B., and Lasko, P. (1998). vasa is required for GURKEN accumulation in the oocyte, and is involved in oocyte differentiation and germline cyst development. *Development*, 125(9):1569–1578.

Subramaniam, K. and Seydoux, G. (2003). Dedifferentiation of primary spermatocytes into germ cell tumors in *C. elegans* lacking the pumilio-like protein PUF-8. *Curr. Biol.*, 13(2):134–139.

Taft, A. S., Vermeire, J. J., Bernier, J., Birkeland, S. R., Cipriano, M. J., Papa, A. R., McArthur, A. G., and Yoshino, T. P. (2009). Transcriptome analysis of *Schistosoma mansoni* larval development using serial analysis of gene expression (SAGE). *Parasitology*, 136(5):469–485.

Tay, J. and Richter, J. D. (2001). Germ cell differentiation and synaptonemal complex formation are disrupted in CPEB knockout mice. *Dev. Cell*, 1(2):201–213.

The *Schistosoma japonicum* Genome Sequencing and Functional Analysis Consortium (2009). The *Schistosoma japonicum* genome reveals features of host-parasite interplay. *Nature*, 460(7253):345–51.

Tomancak, P., Guichet, A., Zavorszky, P., and Ephrussi, A. (1998). Oocyte polarity depends on regulation of gurken by Vasa. *Development*, 125(9):1723–1732.

Tominaga, T., Sahai, E., Chardin, P., McCormick, F., Courtneidge, S. A., and Alberts, A. S. (2000). Diaphanous-related formins bridge Rho GTPase and Src tyrosine kinase signaling. *Mol. Cell*, 5(1):13–25.

van der Weele, C. M., Tsai, C.-W., and Wolniak, S. M. (2007). Mago nashi is essential for spermatogenesis in *Marsilea*. *Mol. Biol. Cell*, 18(10):3711–3722.

van Keulen, H., Mertz, P. M., LoVerde, P. T., Shi, H., and Rekosh, D. M. (1991). Characterization of a 54-nucleotide gap region in the 28S rRNA gene of *Schistosoma mansoni*. *Mol. Biochem. Parasitol.*, 45(2):205–214.

Vanderstraete, M., Gouignard, N., Cailliau, K., Morel, M., Hahnel, S., Leutner, S., Beckmann, S., Grevelding, C. G., and Dissous, C. (2014). Venus kinase receptors control reproduction in the platyhelminth parasite *Schistosoma mansoni*. *PLoS Pathog.*, 10(5):e1004138.

Varnum, S. M. and Wormington, W. M. (1990). Deadenylation of maternal mRNAs during *Xenopus* oocyte maturation does not require specific cis-sequences: a default mechanism for translational control. *Genes Dev.*, 4(12B):2278–86.

Vecchione, A., Fassan, M., Anesti, V., Morrione, A., Goldoni, S., Baldassarre, G., Byrne, D., D'Arca, D., Palazzo, J. P., Lloyd, J., Scorrano, L., Gomella, L. G., Iozzo, R. V., and Baffa, R. (2009). MITOSTATIN, a putative tumor suppressor on chromosome 12q24.1, is downregulated in human bladder and breast cancer. *Oncogene*, 28(2):257–69.

Verjovski-Almeida, S., DeMarco, R., Martins, E. a. L., Guimarães, P. E. M., Ojopi, E. P. B., Paquola, A. a. C. M., Piazza, J. a. P., Nishiyama, M. Y., Kitajima, J. a. P., Adamson, R. E., Ashton, P. D., Bonaldo, M. F., Coulson, P. S., Dillon, G. P., Farias, L. P., Gregorio, S. P., Ho, P. L., Leite, R. a., Malaquias, L. C. C., Marques, R. C. P., Miyasato, P. A., Nascimento, A. L. T. O., Ohlweiler, F. P., Reis, E. M., Ribeiro, M. a., Sá, R. G., Stukart, G. C., Soares, M. B., Gargioni, C., Kawano, T., Rodrigues, V., Madeira, A. M. B. N., Wilson, R. A., Menck, C. F. M., Setubal, J. a. C., Leite, L. C. C., and Dias-Neto, E. (2003). Transcriptome analysis of the acoelomate human parasite *Schistosoma mansoni*. *Nat. Genet.*, 35(2):148–57.

Vulsteke, V., Beullens, M., Boudrez, A., Keppens, S., Van Eynde, A., Rider, M. H., Stalmans, W., and Bollen, M. (2004). Inhibition of spliceosome assembly by the cell cycle-regulated protein kinase MELK and involvement of splicing factor NIPP1. *J. Biol. Chem.*, 279(10):8642–8647.

Wallingford, J. B. and Habas, R. (2005). The developmental biology of Dishevelled: an enigmatic protein governing cell fate and cell polarity. *Development*, 132:4421–4436.

Wang, B., Collins, J. J., and Newmark, P. A. (2013). Functional genomic characterization of neoblast-like stem cells in larval *Schistosoma mansoni*. *Elife*, 2:e00768.

Wang, L.-D., Chen, H.-G., Guo, J.-G., Zeng, X.-J., Hong, X.-L., Xiong, J.-J., Wu, X.-H., Wang, X.-H., Wang, L.-Y., Xia, G., Hao, Y., Chin, D. P., and Zhou, X.-N. (2009). A strategy to control transmission of *Schistosoma japonicum* in China. *N. Engl. J. Med.*, 360(2):121–128.

Wang, S. and Hu, W. (2014). Development of "-omics" research in *Schistosoma* spp. and -omics-based new diagnostic tools for schistosomiasis. *Front. Microbiol.*, 5:313.

Wang, S.-F., Oh, S., Si, Y.-X., Wang, Z.-J., Han, H.-Y., Lee, J., and Qian, G.-Y. (2012). Computational prediction of protein-protein interactions of human tyrosinase. *Enzyme Res.*, 2012(Oca 1):192867.

Wang, Y., Stary, J. M., Wilhelm, J. E., and Newmark, P. A. (2010). A functional genomic screen in planarians identifies novel regulators of germ cell development. *Genes Dev.*, 24(18):2081–92.

Wegner, M. (2011). SOX after SOX: SOXession regulates neurogenesis. *Genes Dev.*, 25(23):2423–2428.

Wells, K. E. and Cordingley, J. S. (1991). *Schistosoma mansoni*: Eggshell formation is regulated by pH and calcium. *Exp. Parasitol.*, 73(3):295–310.

Werner, M. and Simmons, L. W. (2008). Insect sperm motility. *Biol. Rev.*, 83(2):191–208.

Williams, D. L., Sayed, A. A., Bernier, J., Birkeland, S. R., Cipriano, M. J., Papa, A. R., McArthur, A. G., Taft, A., Vermeire, J. J., and Yoshino, T. P. (2007). Profiling *Schistosoma mansoni* development using serial analysis of gene expression (SAGE). *Exp. Parasitol.*, 117(3):246–258.

Wilson, R. A. (2012). Proteomics at the schistosome-mammalian host interface: any prospects for diagnostics or vaccines? *Parasitology*, 139(09):1178–1194.

Wippersteg, V., Kapp, K., Kunz, W., Jackstadt, W. P., Zahner, H., and Grevelding, C. G. (2002). HSP70-controlled GFP expression in transiently transformed schistosomes. *Mol. Biochem. Parasitol.*, 120(1):141–50.

Yang, L., Chen, D., Duan, R., Xia, L., Wang, J., Qurashi, A., Jin, P., and Chen, D. (2007). Argonaute 1 regulates the fate of germline stem cells in *Drosophila*. *Development*, 134(23):4265–4272.

Yannoni, Y. M. and White, K. (1996). Association of the neuron-specific RNA binding domain-containing protein ELAV with the coiled body in *Drosophila* neurons. *Chromosoma*, 105(6):332–341.

Ye, Q., Dong, H.-F., Grevelding, C. G., and Hu, M. (2013). *In vitro* cultivation of *Schistosoma japonicum*-parasites and cells. *Biotechnol. Adv.*, 31(8):1722–37.

Yoon, S., Kawasaki, I., and Shim, Y. H. (2012). CDC-25.1 controls the rate of germline mitotic cell cycle by counteracting WEE-1.3 and by positively regulating CDK-1 in *Caenorhabditis elegans*. *Cell Cycle*, 11(7):1354–1363.

Young, N. D., Jex, A. R., Li, B., Liu, S., Yang, L., Xiong, Z., Li, Y., Cantacessi, C., Hall, R. S., Xu, X., Chen, F., Wu, X., Zerlotini, A., Oliveira, G., Hofmann, A., Zhang, G., Fang, X., Kang, Y., Campbell, B. E., Loukas, A., Ranganathan, S., Rollinson, D., Rinaldi, G., Brindley, P. J., Yang, H., Wang, J. J., and Gasser, R. B. (2012). Whole-genome sequence of *Schistosoma haematobium*. *Nat. Genet.*, 44(2):221–5.

Zhao, Y., Sun, W., Zhang, P., Chi, H., Zhang, M.-J., Song, C.-Q., Ma, X., Shang, Y., Wang, B., Hu, Y., Hao, Z., Huhmer, A. F., Meng, F., L'Hernault, S. W., He, S.-M., Dong, M.-Q., and Miao, L. (2012). Nematode sperm maturation triggered by protease involves sperm-secreted serine protease inhibitor (Serpin). *Proc. Natl. Acad. Sci.*, 109(5):1542–1547.

Zhou, Y. and King, M. L. (2004). Sending RNAs into the future: RNA localization and germ cell fate. *IUBMB Life*, 56(1):19–27.

7 Appendix

7.1 RNA-Seq reads statistics

Sample	Total	Mapped	Prop. paired	Singletons	Unmapped	%unmapped
bM1	82157621	71801485	57615006	5011317	10356136	12.61
bM2	61413861	51649806	42911100	2509444	9764055	15.90
bM3	58786566	51179327	42452604	2580515	7607239	12.94
sM1	63319818	53852252	45111588	2701856	9467566	14.95
sM2	63888404	53738964	44763160	2691940	10149440	15.89
sM3	54258554	47564797	38200040	2435665	6693757	12.34
bT1	43373743	38119993	30926682	2511925	5253750	12.11
bT2	43840647	32048217	26063698	2199055	11792430	26.90
bT3	65099133	48212772	24158538	2332190	16886361	25.94
sT1	44595566	38876508	29982900	2376020	5719058	12.82
sT2	56767832	49722004	40360354	3168100	7045828	12.41
sT3	68875916	56457897	46779174	2740915	12418019	18.03
bF1	42049886	36204716	19131978	2683370	5845170	13.90
bF2	56720483	45482737	33138056	4739835	11237746	19.81
bF3	48461371	39592784	28397394	4281282	8868587	18.30
sF1	62724794	54360068	45920862	2718634	8364726	13.34
sF2	111348638	94437658	78762590	4987700	16910980	15.19
sF3	80824593	61321111	52127848	2868193	19503482	24.13
bO1	60987961	54988691	29669282	2960611	5999270	9.84
bO2	83483600	74676180	63194578	4419900	8807420	10.55
bO3	73599576	66211423	55763652	3971051	7388153	10.04
sO1	62449538	53494629	43577282	3214019	8954909	14.34
sO2	68107686	58533720	47044524	3714416	9573966	14.06

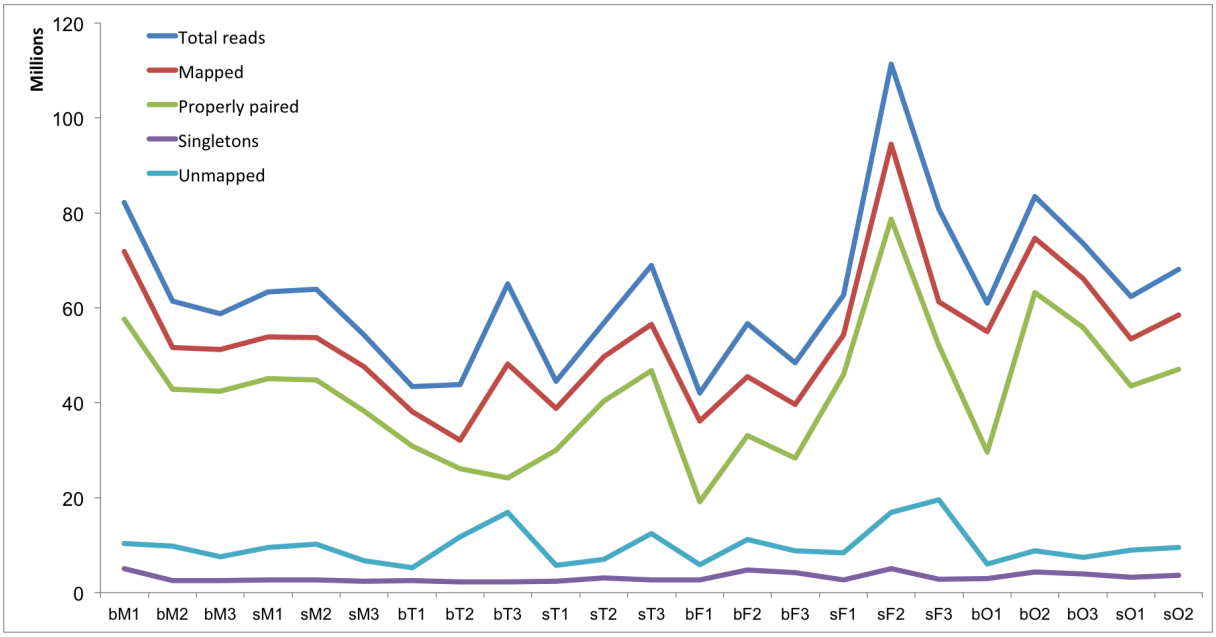

Figure 7.1: Overview of RNA-Seq reads in all samples. Properly paired: the read and its mate are both mapped within a reasonable distance and are correctly oriented with respect to one another; singletons: the read itself is unmapped the mate is mapped.

7.2 Hierarchical clustering of all expressed genes

Hierarchical clustering of all genes with RPKM > 2 was shown below.

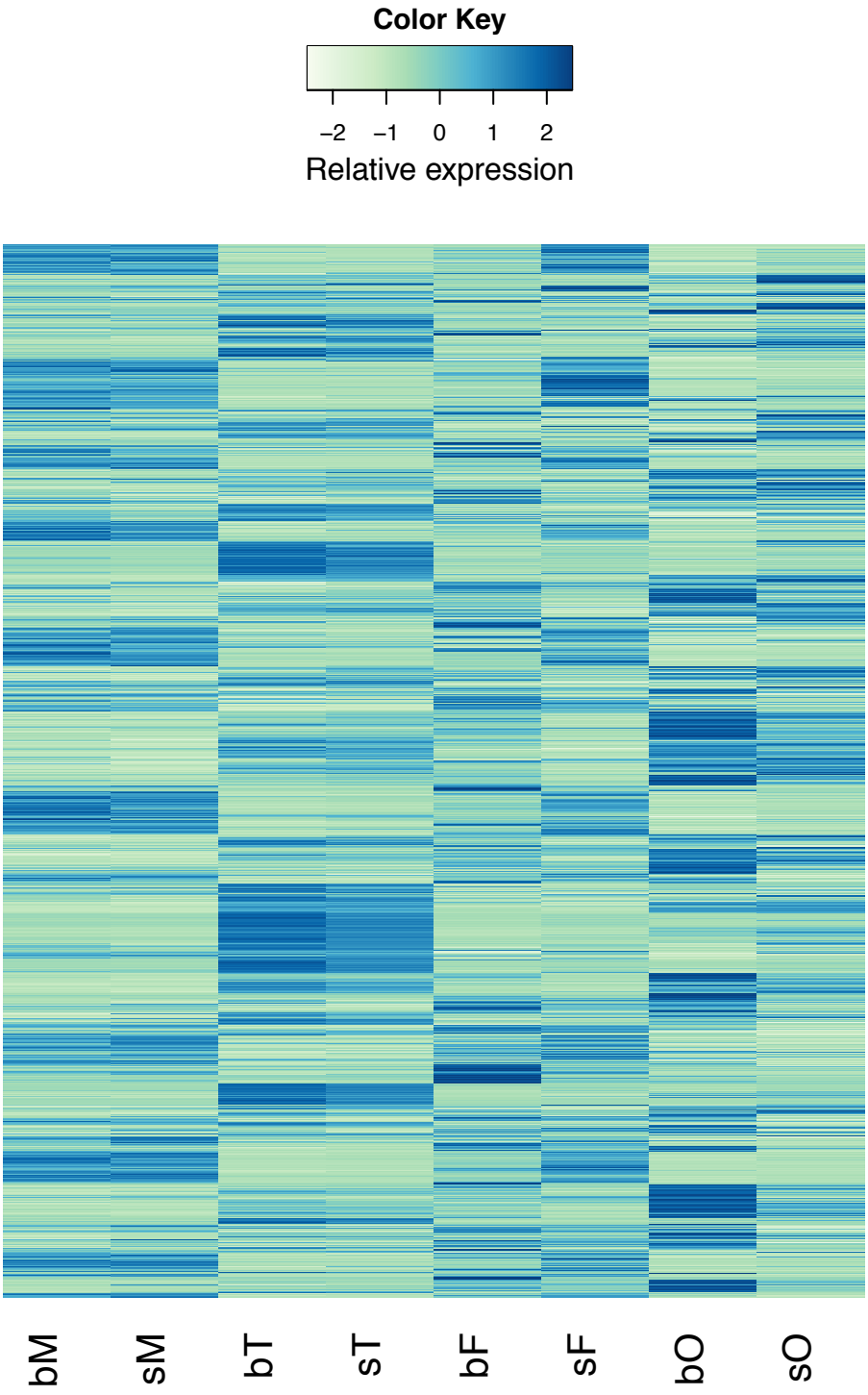

7.3 List of bT markers

Gene_ID	RPKM_bT	Product
Smp_001160.1	20.33	sperm-associated antigen 16 protein
Smp_004690.1	16.20	hypothetical protein
Smp_007670.1	45.42	hypothetical protein
Smp_008190.1	15.58	rho guanine nucleotide exchange factor 11
Smp_008920.1	2.12	voltage-gated hydrogen channel 1
Smp_009630.1	20.67	homeobox protein SIX6
Smp_010450.1	297.61	hypothetical protein
Smp_015820.1	12.81	protein notum
Smp_018120.1	14.23	[K] kinesin protein KIF9
Smp_019200.1	423.83	hypothetical protein
Smp_020540.2	7.63	LIM and senescent cell antigen-containing
Smp_024810.1	2.87	protein FAM82B
Smp_026670.1	5.09	transmembrane protein 26
Smp_028130.1	67.38	protein FAM78B
Smp_046120.1	4.72	[K] vesicular acetylcholine transporter
Smp_047020.1	8.24	hypothetical protein
Smp_052290.1	2.82	fibroblast growth factor receptor 1 like
Smp_053520.1	5.92	homeobox protein aristaless 3-like
Smp_056770.1	3.81	hypothetical protein
Smp_059600.1	9.89	[K] tektin 3
Smp_062490.1	56.55	[K] heart and neural crest derivatives expressed
Smp_062760.1	4.56	[K] regulator of G-protein signaling 3
Smp_075330.1	2.30	hypothetical protein
Smp_075350.1	2.74	hypothetical protein
Smp_079260.1	5.54	LIM:homeobox protein Lhx2
Smp_079600.1	67.04	two pore calcium channel protein 1
Smp_080650.1	224.50	cAMP-dependent protein kinase regulatory chain CAP-ED
Smp_080820.1	69.08	G-protein coupled receptor fragment
Smp_085180.1	2.10	cathepsin B (C01 family)

Gene_ID	RPKM_bT	Product
Smp_085690.1	33.66	cAMP-dependent protein kinase catalytic subunit PKA/STK
Smp_085700.1	3.61	cAMP-dependent protein kinase catalytic subunit
Smp_087820.1	67.09	hypothetical protein
Smp_088090.1	2.08	hypothetical protein
Smp_090160.1	3.02	zinc-finger homeobox protein 3
Smp_094930.1	41.50	early growth response protein 1 (egr)
Smp_099670.1	6.03	lipoprotein receptor
Smp_099680.1	8.25	hypothetical protein
Smp_104210.1	51.41	[K] opsin receptor
Smp_112450.1	2.54	trematode egg-shell synthesis domain-containing protein
Smp_114970.1	51.58	WD repeat-containing protein 52
Smp_118710.1	20.32	hypothetical protein
Smp_121230.1	22.34	hypothetical protein
Smp_122170.1	155.27	phd finger protein 10
Smp_123430.1	30.22	coiled coil domain-containing protein
Smp_123810.1	21.23	interferon regulatory factor 2-binding protein
Smp_124380.1	16.10	leucine rich
Smp_124510.1	37.40	hypothetical protein
Smp_124750.1	4.90	hypothetical protein
Smp_125620.1	48.14	hypothetical protein
Smp_126250.1	48.08	tetratricopeptide repeat protein 21b
Smp_126530.1	3.02	v ets erythroblastosis virus E26 oncogene
Smp_126820.1	27.05	hypothetical protein
Smp_126870.1	7.24	homeobox protein Nkx 6
Smp_127720.1	12.74	biogenic amine (dopamine) receptor
Smp_127850.1	8.88	hypothetical protein
Smp_128340.1	12.18	NAD-dependent epimerase:dehydratase
Smp_128510.1	283.87	hypothetical protein
Smp_130710.1	10.91	wd repeat containing
Smp_130810.1	22.94	[K] dynein heavy chain
Smp_131240.1	61.75	transcription factor

Gene_ID	RPKM_bT	Product
Smp_132220.1	22.62	G-protein coupled receptor fragment
Smp_132490.1	3.47	hypothetical protein
Smp_134380.1	11.79	hypothetical protein
Smp_134960.1	2.04	peptide (allatostatin:somatostatin)
Smp_135550.1	45.52	hypothetical protein
Smp_136100.1	163.87	kelch protein 10
Smp_137140.1	6.01	[K] nk homeobox protein
Smp_137280.1	36.35	coiled coil domain-containing protein 87
Smp_137690.1	27.83	hypothetical protein
Smp_137880.1	2.33	hypothetical protein
Smp_137890.1	3.61	[K] ATP-binding cassette sub family G
Smp_138340.1	2.84	hypothetical protein
Smp_138350.1	3.43	zinc-finger protein basonuclin 2
Smp_138560.1	28.25	hypothetical protein (Sm-npp-16
Smp_140150.1	36.83	katanin p60 ATPase containing subunit A
Smp_140190.1	5.53	G-protein coupled receptor fragment
Smp_140350.1	19.22	homeobox protein ARX
Smp_140540.1	16.53	hypothetical protein
Smp_141170.1	2.54	hypothetical protein
Smp_141230.1	183.38	[K] dual specificity tyrosine (Y) phosphorylation DYRK
Smp_141340.1	11.39	hypothetical protein
Smp_141460.1	54.64	protein FAM92A1 uncharacterized
Smp_141490.1	13.22	hypothetical protein
Smp_141670.1	6.04	hypothetical protein
Smp_142220.1	123.22	apobec1 complementation factor
Smp_142420.1	20.19	hypothetical protein
Smp_142730.1	2.10	rho GTPase activating protein 100F
Smp_143190.1	25.46	hypothetical protein
Smp_143950.1	14.50	hypothetical protein
Smp_143970.1	110.32	kelch protein 10
Smp_144120.1	8.18	arrowhead
Smp_144540.1	109.22	zinc-finger and putative transcriptional repressor
Smp_145140.1	3.85	[K] wnt5

Gene_ID	RPKM_bT	Product
Smp_145380.1	2.08	Beta ketoacyl synthase,domain-containing protein
Smp_146420.1	20.24	spindle assembly checkpoint component MAD1
Smp_147390.1	3.06	glutamate (NMDA) receptor subunit epsilon 2
Smp_148030.1	127.51	DC STAMP domain-containing protein 1
Smp_148040.1	53.14	DC STAMP domain-containing protein 1
Smp_148160.1	62.55	spermatogenesis-associated protein 6
Smp_149310.1	4.83	lipoxygenase y domain-containing protein
Smp_149710.1	17.56	hypothetical protein
Smp_149860.1	11.07	cat eye syndrome critical region protein 5
Smp_149870.1	5.81	cat eye syndrome critical region protein
Smp_150180.1	2.17	octopamine receptor oamb
Smp_150920.1	28.20	[K] synaptotagmin
Smp_151660.1	40.03	hypothetical protein
Smp_151740.1	21.15	run and tbc1 domain-containing protein
Smp_151920.1	8.31	paladin
Smp_152170.1	3.75	forkhead box protein A2 hepatocyte nuclear
Smp_152200.1	129.97	M-phase inducer phosphatase 3 cdc25
Smp_152390.1	26.88	hypothetical protein
Smp_152680.1	7.49	epidermal growth factor receptor EGFR
Smp_152970.1	53.69	hypothetical protein
Smp_153070.1	2.63	hypothetical protein (Sm-npp-13)
Smp_153080.1	47.87	hypothetical protein
Smp_153260.1	177.87	hypothetical protein
Smp_154260.1	4.51	venom allergen (val) protein
Smp_154410.1	2.05	[K] core alpha 1,3 fucosyltransferase
Smp_154790.1	34.78	DC STAMP domain-containing protein 2
Smp_154800.1	85.10	DC STAMP domain-containing protein 2
Smp_155250.1	5.46	[K] nuclear receptor subfamily 2 group E member
Smp_155730.1	9.33	acidic fibroblast growth factor intracellular
Smp_156030.1	11.96	hypothetical protein

Gene_ID	RPKM_bT	Product
Smp_156080.1	14.90	[K] dynein heavy chain
Smp_156600.1	4.55	hypothetical protein
Smp_156800.1	23.20	hypothetical protein
Smp_156810.1	7.04	hypothetical protein
Smp_156820.1	5.39	normocyte-binding protein 2a
Smp_157010.1	4.89	titin
Smp_157860.1	16.01	hypothetical protein
Smp_158370.1	22.73	[K] tubulin monoglycylase TTLL3
Smp_159320.1	3.77	hypothetical protein
Smp_159430.1	4.15	[K] Bardet Biedl syndrome 1 protein
Smp_159510.1	4.87	hypothetical protein
Smp_159520.1	26.19	acidic fibroblast growth factor intracellular
Smp_160310.1	41.31	lysosomal alpha mannosidase
Smp_160320.1	25.22	DNA double strand break repair rad50 ATPase
Smp_160960.1	14.40	asparagine rich protein
Smp_162480.1	2.50	asparagine rich protein
Smp_162690.1	8.88	hypothetical protein
Smp_162760.1	3.00	homeobox protein prospero:prox 1:ceh 26
Smp_164150.1	46.85	tau tubulin kinase 1 STK-CK1
Smp_164460.1	3.45	hypothetical protein
Smp_165040.1	15.18	tbc1 domain family member
Smp_165090.1	5.13	serine:threonine protein phosphatase 2A 56 kDa
Smp_167370.1	14.97	copine 8
Smp_167960.1	66.56	hypothetical protein
Smp_168360.1	29.00	hypothetical protein
Smp_168440.1	3.35	hypothetical protein
Smp_168670.1	2.92	[K] cGMP-dependent protein kinase 1
Smp_169100.1	6.29	monocarboxylate transporter
Smp_171010.1	147.42	EF hand domain (C terminal) containing 2
Smp_171690.1	74.26	hypothetical protein
Smp_173870.1	2.93	anosmin 1
Smp_174150.1	6.70	myeloid ecotropic viral integration site 1
Smp_175410.1	11.55	[K] zinc-finger protein 398

Gene_ID	RPKM_bT	Product
Smp_175730.1	15.03	hypothetical protein
Smp_176170.1	14.78	venom allergen (val) protein
Smp_176250.1	2.18	hypothetical protein
Smp_176300.1	34.35	[K] dynein heavy chain
Smp_176820.1	9.01	hypothetical protein
Smp_179050.1	41.02	[K] homomeric kinesin Kif17
Smp_179920.1	22.83	tetratricopeptide repeat protein 21b
Smp_179970.1	7.77	egg protein CP391S
Smp_182470.1	24.71	hypothetical protein
Smp_186630.1	12.89	hypothetical protein
Smp_192200.1	9.41	hypothetical protein
Smp_196950.1	105.55	one cut domain family member
Smp_196990.1	2.02	protocadherin 11
Smp_197400.1	17.13	hypothetical protein
Smp_197580.1	31.11	tetratricopeptide repeat protein 21b
Smp_198810.1	19.37	mitogen activated protein kinase 15
Smp_200940.1	5.66	hypothetical protein
Smp_201090.1	74.93	hypothetical protein
Smp_202930.1	5.01	hypothetical protein
Smp_203200.1	2.11	hypothetical protein
Smp_203470.1	3.80	hypothetical protein
Smp_203550.1	2.50	hypothetical protein
Smp_204250.1	7.62	hypothetical protein
Smp_205580.1	2.10	hypothetical protein
Smp_212280.1	99.07	dynein heavy chain
Smp_212290.1	11.50	[K] dynein heavy chain

7.4 List of bO markers

Gene_ID	RPKM_bO	Product
Smp_032970.1	6.78	calmodulin protein
Smp_037430.1	4.44	hypothetical protein
Smp_054430.1	4.01	[K] hypothetical protein
Smp_070360.1	223.60	[K] cytoplasmic polyadenylation element binding
Smp_077850.1	2.02	actin
Smp_081620.1	4.73	[K] SmHox4
Smp_082410.1	10.20	hypothetical protein
Smp_087320.1	227.30	TPA-induced protein 11B mouse
Smp_093790.1	2.50	prokaryotic membrane lipoprotein lipid
Smp_098340.1	8.27	[K] gamma glutamylcyclotransferase
Smp_106010.1	4.56	hypothetical protein
Smp_118960.1	17.42	jun protein
Smp_126070.1	6.76	hypothetical protein
Smp_134490.1	8.27	thyroid hormone receptor alpha
Smp_137460.1	119.35	cytoplasmic polyadenylation element binding
Smp_139480.1	2.21	[K] ephrin receptor
Smp_142700.1	8.43	neuronal acetylcholine receptor subunit alpha 4
Smp_143900.1	6.58	hypothetical protein
Smp_145020.1	4.92	[K] glutamate semialdehyde dehydrogenase
Smp_146940.1	3.10	innexin
Smp_156140.1	6.63	tripartite motif protein trim9
Smp_160930.1	9.54	hypothetical protein
Smp_163750.1	4.07	otoferlin
Smp_164140.1	131.53	opsin receptor
Smp_168410.1	4.52	tripartite motif protein trim9
Smp_169160.1	3.19	ATP-dependent DNA ligase, IPR000859
Smp_174260.1	26.24	[U]thyroid hormone receptor alpha
Smp_176510.1	5.33	RIMS-binding protein 2

Gene_ID	RPKM_bO	Product
Smp_179600.1	112.93	hypothetical protein
Smp_191690.1	14.32	tumor susceptibility gene 101 protein
Smp_201900.1	12.16	hypothetical protein
Smp_206150.1	5.83	hypothetical protein
Smp_206240.1	2.22	hypothetical protein

7.5 Additional 42 house-keeping candidates for worm samples

Gene_ID	Product
Smp_005780.1	hypothetical protein
Smp_006320.1	[K] KH domain-containing, RNA binding, signal
Smp_007260.2	sarco:endoplasmic reticulum calcium ATPase
Smp_012560.1	o-methyltransferase
Smp_012970.1	myotubularin
Smp_016340.1	[K] mediator of RNA polymerase II transcription
Smp_020400.1	zinc metalloproteinase YIL108W
Smp_025510.1	[K] vacuolar protein sorting associated protein 4A
Smp_032240.1	hypothetical protein
Smp_046780.1	plasminogen activator inhibitor 1 RNA-binding
Smp_054750.1	brain tumor protein
Smp_074650.1	*Schistosoma* protein, unknown function
Smp_091800.1	guanine nucleotide exchange factor mss4
Smp_096320.1	[K] kelch protein 20 like
Smp_102920.1	[K] tRNA dimethylallyltransferase
Smp_102930.1	hypothetical protein
Smp_120440.1	nucleic acid binding
Smp_127700.1	hypothetical protein
Smp_130750.1	enhancer of mRNA decapping protein 4
Smp_132530.1	hypothetical protein
Smp_136990.1	[K] dynactin subunit 3 (dynactin light chain p24)
Smp_137030.1	SET domain protein
Smp_143040.1	cullin 5
Smp_145440.1	zinc-finger protein; homeobox protein meis
Smp_149830.1	hypothetical protein
Smp_150050.1	TBC1-domain family
Smp_154420.1	[K] clathrin heavy chain
Smp_155210.1	tetratricopeptide repeat protein 5
Smp_160740.1	[K] choline transporter protein 2
Smp_162270.1	[K] ATP-synthase mitochondrial F1 complex assembly
Smp_163640.1	[K] phosphatidylinositol

Gene_ID	Product
Smp_165920.1	guanine nucleotide exchange factor dbs
Smp_167070.1	peptidase M8, leishmanolysin,domain-containing protein
Smp_168780.1	hypothetical protein
Smp_186260.1	hypothetical protein
Smp_186830.1	oligomeric Golgi complex component
Smp_188270.1	metastasis-associated protein MTA1
Smp_191380.1	DNA-binding SAP,domain-containing protein
Smp_193410.1	mitochondrial uncoupling protein
Smp_194450.1	hypothetical protein
Smp_198650.1	ankyrin :unc
Smp_210000.1	sterol response element-binding protein

7.6 Gonad-preferentially transcribed ePKs

Gene_ID	Product
Smp_009600.1	[K] STK PlK1
Smp_018290.1	serine:threonine protein kinase 17A
Smp_050380.1	[K] mitogen activated protein kinase kinase kinase
Smp_057360.1	serine:threonine protein kinase SIK3
Smp_058790.1	mitogen-activated protein kinase kinase kinase
Smp_077180.1	[K] serine:threonine protein kinase Chk1 CAMK
Smp_080730.1	cyclin-dependent kinase 1 (CDC2
Smp_090980.1	[K] cyclin-dependent kinase 20
Smp_094250.1	[K] 3-phosphoinositide-dependent protein kinase 1
Smp_124770.1	hypothetical protein
Smp_125060.1	kinase suppressor of Ras (KSR)
Smp_128670.1	dual specificity testis specific protein kinase
Smp_131630.1	testis expressed protein 14 / STK
Smp_133420.1	[K] serine:threonine protein kinase
Smp_134260.1	[K] mitogen-activated protein kinase 15
Smp_135360.1	serine:threonine protein kinase 12 B
Smp_141380.1	serine:threonine protein kinase VRK1
Smp_141580.1	[K] serine:threonine protein kinase tousled
Smp_150040.2	[K] cyclin-dependent kinase 7
Smp_157300.1	fgfrB
Smp_158950.1	[K] serine:threonine protein kinase haspin
Smp_162710.1	serine:threonine protein kinase 6
Smp_166150.1	maternal embryonic leucine zipper kinase MELK
Smp_167940.1	wee1 protein kinase 2
Smp_169950.1	casein kinase I delta
Smp_171370.1	[K] serine:threonine protein kinase Chk2
Smp_171610.1	[K] dual specificity serine:threonine tyrosine
Smp_171920.1	[K] serine:threonine protein kinase LATS1
Smp_172700.1	cyclin-dependent kinase 6
Smp_174820.1	hypothetical protein
Smp_176620.1	[K] cyclin-dependent kinase 11
Smp_176970.1	[K] serine:threonine protein kinase Nek4

7.7 GO enrichment of sT genes by Biological Process

Significantly enriched biological process categories ($p < 0.01$) are shown in the figure below.

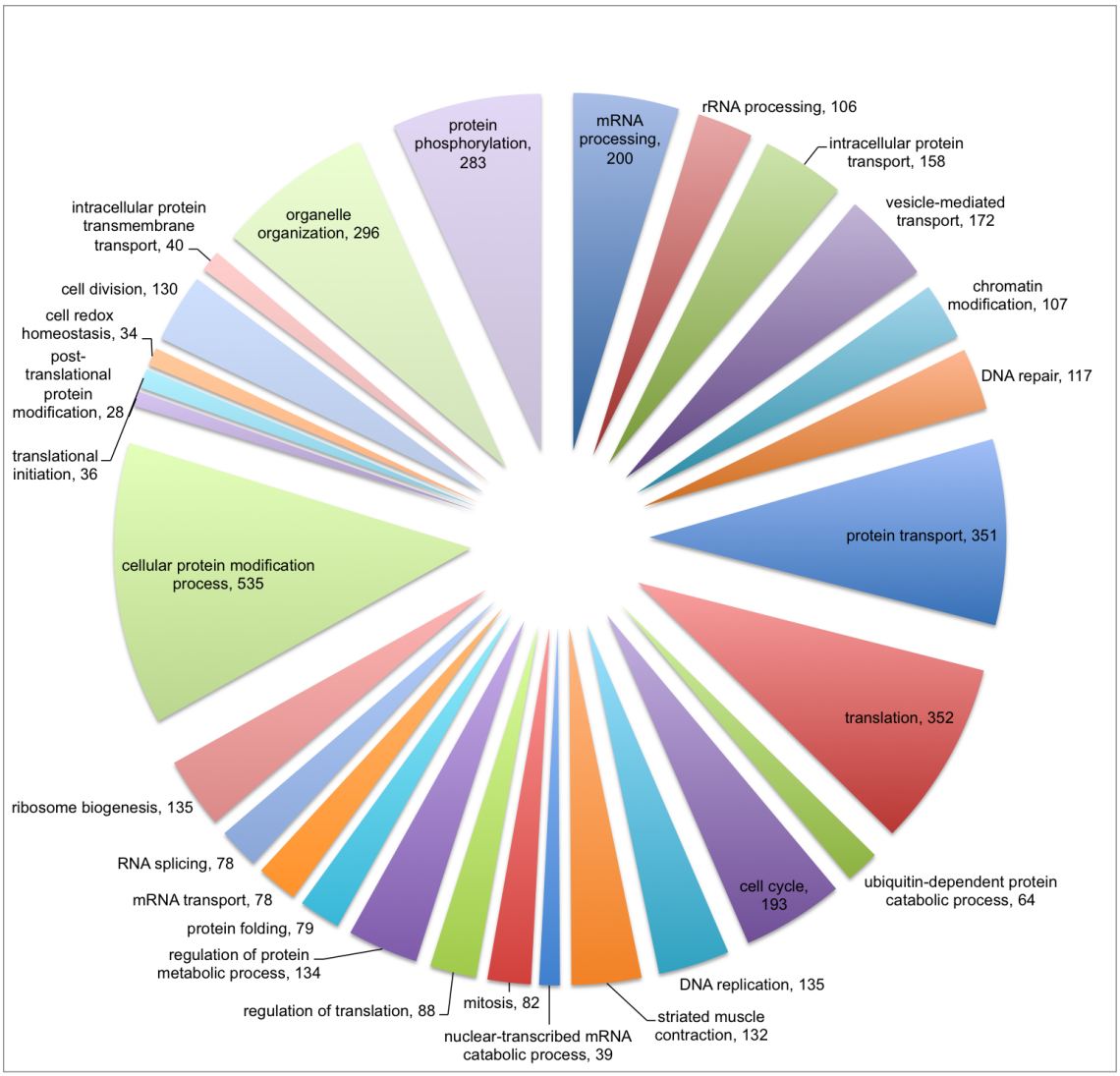

7.8 GO enrichment of sO genes by Biological Process

Significantly enriched biological process categories ($p < 0.01$) are shown in the figure below.

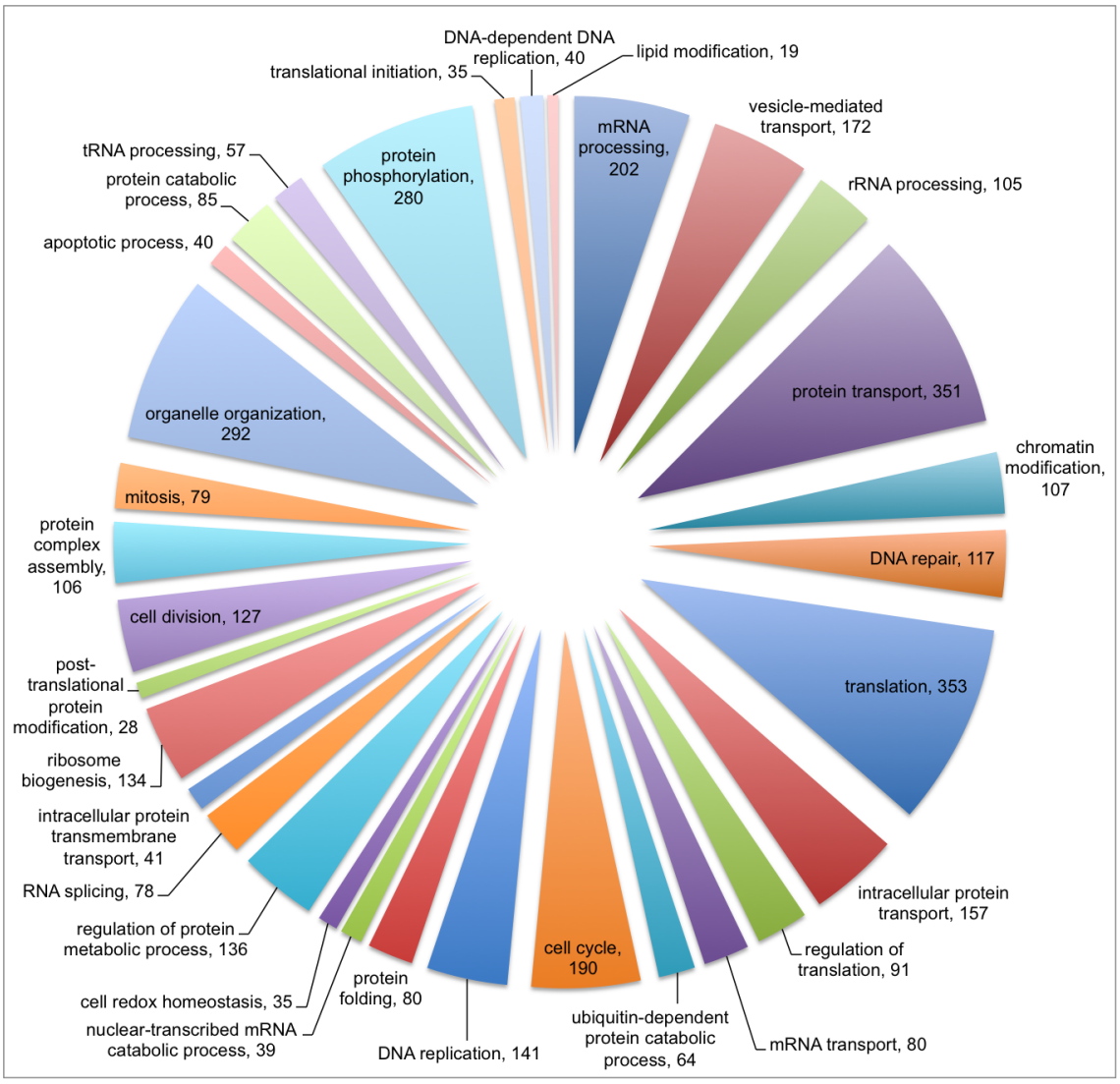

7.9 RNA-Seq data confirmed previous RT-PCR results

RPKM values of genes that had been determined in bT or bO samples by RT-PCR (Hahnel et al., 2013) were shown below. In nearly all cases my RNA-Seq data was consistent with the RT-PCR results.

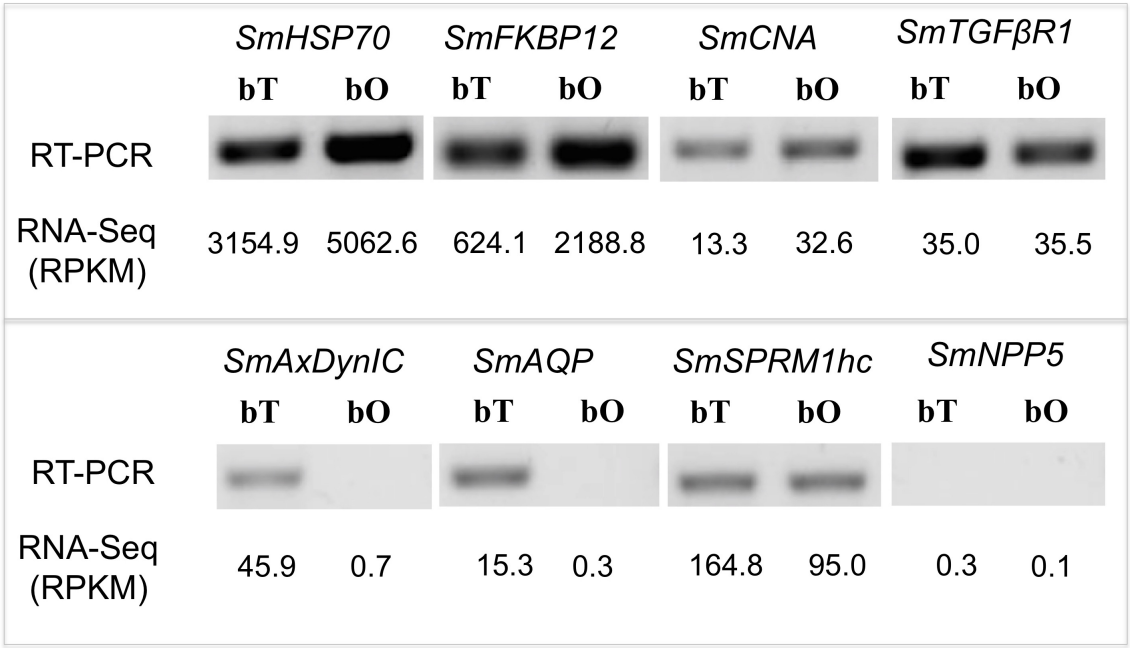

7.10 An example of the final plots with expression profile data

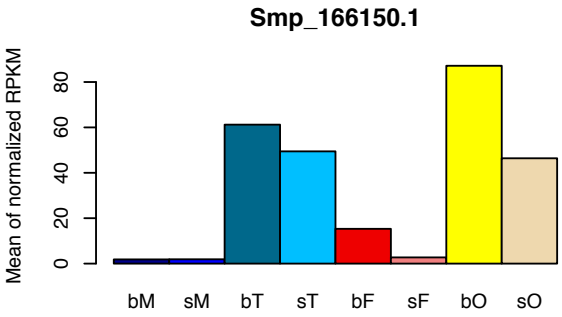

maternal embryonic leucine zipper kinase MELK

Pairing

comp	log2FC	PAdjust
bM/sM	NA	NA
bT/sT	0.3078	1.716e–01
bF/sF	2.4807	2.553e–60
bO/sO	0.9091	1.926e–08

Gender

comp	log2FC	PAdjust
bM/bF	–3.0570	8.421e–85
sM/sF	–0.5319	2.581e–03
bT/bO	–0.5097	2.981e–04
sT/sO	0.0916	6.365e–01

Tissue

comp	log2FC	PAdjust
bT/bM	5.0561	7.746e–206
sT/sM	4.7039	1.525e–181
bO/bF	2.5088	1.179e–66
sO/sF	4.0804	9.398e–139

```
NA (if indicated): original RPKM < 2 in both samples
```

(see Supplementary file No. 42 for plots of all genes.)

List of Figures

List of Tables

Supplementary files

Suppl_01-1_raw-counts-length.dat
This files contains all the raw read counts for each gene in the RNA-Seq analysis. Column names are indicated. The last column is the information of gene length.

Suppl_01-2_RPKM-raw.dat
This contains the raw RPKM values for each gene. It was generated by the 'rpkm()' function of the edgeR package. This file was used to calculated the top 100 highly expressed genes and to generate the heat map for those.

Suppl_02_rpkmMean_norm_prod
This file contains the means of RPKM values that were calculated based on normalized reads. Gene annotations are also shown in the last column. Genes whose RPKM was < 2 in any replicate, were discarded.

Suppl_03-1_R-shell-scripts-DGE.pdf
This file includes the used shell commands for editing files and the R script for the differential gene expression analysis.

Suppl_03-2_R-topGO.R
This file contains the R script for Gene Ontology enrichment analysis.

Suppl_04_ID.Product2
This file contains the annotation for each gene. Additional information on the existence of KEGG orthologs was indicated by '[K]'.

Suppl_05_SmK_150216_ed.txt
This file contains all genes with KEGG orthologs. The first column indicates the Smp number, and the second column is the K identifier in the KEGG database. Blast was

done on 16.02.2015.

Suppl_06_SmCD_150220_std.xlsx
This file contains information on conserved domains of all *S. mansoni* proteins. This file was generated by the NCBI Batch-CD search tool on 20.02.2015. Default database (CDD) was used, *p*-value cut-off was set at < 0.01 and maximum number of hits was set to 500.

Suppl_07-1_Prot-Ov_score100_395-splice.prod.txt
This file contains the list of proteins identified in bO by the nano-LC-ESI-MS/MS approach, with a score > 100. The first column indicates the Smp number and the second column contains the product annotations.

Suppl_07-2_Prot-Ov_all_814.txt
This file contains all the proteins identified in bO by nano-LC-ESI-MS/MS approach.The first column indicates the Smp number and the second column contains the product annotations.

Suppl_08_top100_expressed_all.txt
This file contains the top 100 highly expressed genes. These were selected by comparing the mean RPKM values across all samples. Genes were organised in a descending manner according to their mean RPKM values. Product information is supplied in the 3rd column.

Suppl_09_teDEG_005-0585-prod_243.txt
This file contains all the differentially expressed genes, their $\log_2$ (fold change) values and product information from bT/sT comparison. Cut-off: FDR < 0.05 and $|\log_2$ (Fold Change)| > 0.585.

Suppl_10_ovDEG_0005-0585-prod_3600.txt
This file contains all the differentially expressed genes, their $\log_2$ (fold change) values and product information from bO/sO comparison. Cut-off: FDR < 0.005 and $|\log_2$ (Fold Change)| > 0.585.

Suppl_11_maDEG_005-0585_prod426.txt
This file contains all the differentially expressed genes, their $\log_2$ (fold change) values

and product information from bM/sM comparison. Cut-off: FDR < 0.05 and $|\log_2$ (Fold Change)| > 0.585.

Suppl_12_feDEG_0005-0585_prod3748.txt
This file contains all the differentially expressed genes, their $\log_2$ (fold change) values and product information from bF/sF comparison. Cut-off: FDR < 0.005 and $|\log_2$ (Fold Change)| > 0.585.

Suppl_13_bM-bF_0005-0585_prod-4383.txt
This file contains all the differentially expressed genes, their $\log_2$ (fold change) values and product information from bM/bF comparison. Cut-off: FDR < 0.005 and $|\log_2$ (Fold Change)| > 0.585.

Suppl_14_bT-bO_0005-0585_prod-4629.txt
This file contains all the differentially expressed genes, their $\log_2$ (fold change) values and product information from bT/bO comparison. Cut-off: FDR < 0.005 and $|\log_2$ (Fold Change)| > 0.585.

Suppl_15_sM-sF_0005-0585_prod-1445.txt
This file contains all the differentially expressed genes, their $\log_2$ (fold change) values and product information from sM/sF comparison. Cut-off: FDR < 0.005 and $|\log_2$ (Fold Change)| > 0.585.

Suppl_16_sT-sO_0005-0585_prod-2837.txt
This file contains all the differentially expressed genes, their $\log_2$ (fold change) values and product information from sT/sO comparison. Cut-off: FDR < 0.005 and $|\log_2$ (Fold Change)| > 0.585.

Suppl_17_bT-bM_0005-0585-prod5478.txt
This file contains all the differentially expressed genes, their $\log_2$ (fold change) values and product information from bT/bM comparison. Cut-off: FDR < 0.005 and $|\log_2$ (Fold Change)| > 0.585.

Suppl_18_sT-sM_0005-0585-prod_5409.txt
This file contains all the differentially expressed genes, their $\log_2$ (fold change) values and product information from sT/sM comparison. Cut-off: FDR < 0.005 and $|\log_2$

(Fold Change)| > 0.585.

Suppl_19_bO-bF_0005-0585-prod_4534.txt
This file contains all the differentially expressed genes, their $\log_2$ (fold change) values and product information from bO/bF comparison. Cut-off: FDR < 0.005 and |$\log_2$ (Fold Change)| > 0.585.

Suppl_20_sO-sF_0005-0585-prod_5080.txt
This file contains all the differentially expressed genes, their $\log_2$ (fold change) values and product information from sO/sF comparison. Cut-off: FDR < 0.005 and |$\log_2$ (Fold Change)| > 0.585.

Suppl_21_1-1.pdf
This file contains all genes from category 1.1 (see section 3.3.6), the $\log_2$(Fold Change) and FDR values, gene products and their expression profiles. Genes were organised in a ascending manner according to the Smp numbers.

Suppl_22_1-2.pdf
This file contains all genes from category 1.2 (see section 3.3.6), the $\log_2$(Fold Change) and FDR values, gene products and their expression profiles. Genes were organised in a ascending manner according to the Smp numbers.

Suppl_23_2-1.pdf
This file contains all genes from category 2.1 (see section 3.3.6), the $\log_2$(Fold Change) and FDR values, gene products and their expression profiles. Genes were organised in a ascending manner according to the Smp numbers.

Suppl_24_2-2.pdf
This file contains all genes from category 2.2 (see section 3.3.6), the $\log_2$(Fold Change) and FDR values, gene products and their expression profiles. Genes were organised in a ascending manner according to the Smp numbers.

Suppl_25_3-1.pdf
This file contains all genes from category 3.1 (see section 3.3.6), the $\log_2$(Fold Change) and FDR values, gene products and their expression profiles. Genes were organised in a ascending manner according to the Smp numbers.

Suppl_26_3-2.pdf
This file contains all genes from category 3.2 (see section 3.3.6), the $\log_2$(Fold Change) and FDR values, gene products and their expression profiles. Genes were organised in a ascending manner according to the Smp numbers.

Suppl_27_3-3.pdf
This file contains all genes from category 3.3 (see section 3.3.6), the $\log_2$(Fold Change) and FDR values, gene products and their expression profiles. Genes were organised in a ascending manner according to the Smp numbers.

Suppl_28_3-4.pdf
This file contains all genes from category 3.4 (see section 3.3.6), the $\log_2$(Fold Change) and FDR values, gene products and their expression profiles. Genes were organised in a ascending manner according to the Smp numbers.

Suppl_29_MaTe-specific168.pdf
This file contains identified male samples-specific transcripts from section 3.3.8. RPKM values in all female samples (bF, sF, bO and sO) are < 2. Their transcription patterns are attached.

Suppl_30_FeOv-specific73.pdf
This file contains identified female samples-specific transcripts from section 3.3.8. RPKM values in all female samples (bM, sM, bT and sT) are less than 2. Their transcription patterns are attached after.

Suppl_31_Gonads-Worms-all-up-1.5fold-join1012.txt
This list contains genes whose transcriptions are higher in all gonads than in whole worms, with > 1.5-fold difference. Their protein products are shown in the 2nd column.

Suppl_32_gonad_enriched_905.pdf
This file contains all gonad-enriched transcripts from section 3.3.11 and their protein product. Their expression profiles are also attached.

Suppl_33_worm_enriched_1326.pdf

This file contains all worm-enriched transcripts from section 3.3.11 and their protein product. Their expression profiles are also attached.

Suppl_34_Ma+sF841-sort-prod.pdf
This file contains the list of males-sF enriched transcripts from section 3.3.12. Their transcription pattern plots were sorted by the annotations.

Suppl_ 35-1_Actin-tubulin-GAPDH.pdf
This file shows the expression profiles of *S. mansoni* actins, tubulins and GAPDH.

Suppl_35-2_Housekeeper15.pdf
This file contains the expression profiles of all identified 15 potential housekeeping genes (section 3.3.13).

Suppl_36_neuropeptide14-13.pdf
This file contains expression profiles of *S. mansoni* neuropeptide precursor genes.

Suppl_37_Sm_transcription_factors_KEGG.pdf
This file shows the expression profiles of all identified transcription factors by blasting against the KEGG database.

Suppl_38_Appendix-genes.pdf
This file contains expression profiles of the following genes: *cyclin*, *CDK*, *MCM*, *ORC*, *vlg*, *kinesin*, *tektin*, *kelch*, *dynein*, *myosin*, *arf*, *serpin*, *diaphanous* and *frizzled*.

Suppl_39_hypothetical-noCD1537.pdf
This file contains transcription profiles of all 1537 genes whose products were annotated as "hypothetical protein" and contain none conserved domains.

Suppl_40_LMM-ORS.xlsx
This file contains results of comparisons to the laser microdissection microarray analysis by (Nawaratna et al., 2011). Sheet "bO-bF": comparison on up-regulated genes in bO that were listed in the LMM study; sheet "bT-bM": comparison on up-regulated genes in bT that were listed in the LMM study; sheet "shared-ov557": fold-changes of up-regulated genes in bO identified by both approaches; sheet "shared-te677": fold-changes of up-regulated genes in bT identified by both

approaches.

Suppl_41_MICROARRAY-SAGE-SEQ.xlsx
This file contains the result of comparisons to the microarray-SuperSAGE analysis by (Leutner et al., 2013). Listed genes were the 29 DEGs identified by both microarray and SuperSAGE.

Suppl_42_GW_RNA-Seq_plot.zip
This is a compressed file containing 9,224 plots. Each plot represents the expression profile of one of the 9,224 genes analysed in this study. In addition, $\log_2$FC and corresponding FDR (shown as PAdjust) values from all comparisons (based on pairing, gender and tissue) are indicated below each plot. An example is given in Appendix 7.10.

Note: all supplementary files can be found in the attached CD.

Acknowledgements

First I would like to thank Prof. Dr. Albrecht Bindereif for his willingness to be my first supervisor and to review my thesis.

To my supervisor Prof. Christoph Grevelding I express my deepest gratitude for his generous support, extreme patience, continuous encouragement and valuable suggestions to me, to my life and to this project. I thank him for giving me the opportunity to work in a different field, for providing me direct help and information on our living in Germany, for guiding me into the amazing world of parasites, and most importantly, for directing me on the way to be a good researcher. His broad knowledge in various aspects of parasitology benefits me at both experimental and theoretical levels. He is very conductive and also patient in improving my skills in English speaking and writing. I am also grateful for his efforts in finding collaboration partners and supporting organisations.

Thanks also go to all past and present members of Grevelding's lab, for their encouragement, information, fun and help with this work: Alex, Ariane, Bianca, Christin, Christina, David, Gabriela, Helena, Katja, Matze, Richard, Silke, Sophie, Steffen, Svenja, Thomas, and Verena. In particular, I would like to thank Dr. Thomas Quack for assisting me to be adapted in the first two years, including lab equipment, materials and protocols, regulations, and writing revisions. Thanks to Steffen, Sophie and Verena for valuable discussions and suggestions, as well as partial experimental work. Tina, Bianca, Katja, David and Matze had done excellent work in maintaining schistosome life-cycle, which resulted in available worm material every week.

This work had been made possible with the help and contributions from different collaboration partners. Firstly, I was really glad to work together with people from the Wellcome Trust Sanger Institute, especially those from the Parasite Genomics Group. I appreciate a lot the willingness of Dr. Matt Berriman to establish such a corporation and to host me in his group. Dr. Nancy Holroyd did excellent work in organisation of the RNA-Seq project. Florian Sessler had done a lot in lab work, sequence mapping and counting, as well as valuable introduction to data analysis and result discussions. Dr. James Cotton introduced me the concept of factors. Dr. Magdalena Zarowiecki generously shared her shell and perl scripts for data analysis.

I also appreciate and enjoy the corporation with Dr. Ervice Pouokam from Prof. Martin Diener's group in Ca^{2+}-imaging, with Dr. Martin Hardt in EM analyses, and with Ms. Gabriele Michel and Dr. Nelli Baal from Prof. Holger Hackstein's lab in FACS analysis. They have contributed a lot in solving problems during the establishment of

analyses with schistosome cells.

Thanks to the Giessen Graduate Centre for the Life Sciences (GGL), who had organized diverse courses including statistics, grant writing, German language and bioinformatics. The annual conferences also broadened my view in other fields. The Career Day events provided useful insights into the bio- and chem-industry. Apart form that, I appreciate the assistance from Prof. Eveline Baumgart-Vogt in finding potential supervisors before my PhD work.

Thanks to all the friends in Giessen for sharing their time and making fun: Adrian, Ame, Changwu, Christian, Hong, Huijuan, Ilya, Jiangping, Junpei, Kai, Qin, Rong, Tian, and Xiaodan.

Thanks are due to the China Scholarship Council (CSC), who provided me financial support for pursuing the doctorate degree for three years.

Last but not least I wish to thank my family and my wife's family for their continuous understanding and support during our studies. I would like to express my deepest appreciation to my wife Yanyan, who encourages, supports and cheers on me all the time. I feel so lucky to meet her ten years ago and to share my time with her in the past eight years. My great gratitude is also delivered to our little daughter Sunnie, who brought new air and a lot of fun to our life.

To my father and grandmother: I will always be with you.

Contributions

Publications

Lu, Z., Sessler, F., Holroyd, N.E., Hahnel, S., Quack, T., Berriman, M., Grevelding, C.G., 2015. Comparative sub-transcriptomics reveal gonad-specific and paring-dependent gene expression patterns in *Schistosoma mansoni*. (In preparation)

Lu, Z., Quack, T., Hahnel, S., Gelmedin, V., Pouokam, E., Diener, M., Hardt, M., Michel, G., Baal, N., Hackstein, H., Grevelding, C.G., 2015. Isolation, enrichment and primary characterisation of vitelline cells from *Schistosoma mansoni* obtained by the organ isolation method. Int. J. Parasitol. 45, 663–672. doi:10.1016/j.ijpara.2015.04.002

Hahnel, S., Quack, T., Parker-Manuel, S.J., **Lu, Z.**, Vanderstraete, M., Morel, M., Dissous, C., Cailliau, K., Grevelding, C.G., 2014. Gonad RNA-specific qRT-PCR analyses identify genes with potential functions in schistosome reproduction such as SmFz1 and SmFGFRs. Front. Genet. 5. doi:10.3389/fgene.2014.00170

Buro, C., Oliveira, K.C., **Lu, Z.**, Leutner, S., Beckmann, S., Dissous, C., Cailliau, K., Verjovski-Almeida, S., Grevelding, C.G., 2013. Transcriptome analyses of inhibitor-treated schistosome females provide evidence for cooperating Src-kinase and TGF receptor pathways controlling mitosis and eggshell formation. PLoS Pathog. 9, e1003448. doi:10.1371/journal.ppat.1003448

Hahnel, S., **Lu, Z.**, Wilson, R.A., Grevelding, C.G., Quack, T., 2013. Whole-organ isolation approach as a basis for tissue-specific analyses in *Schistosoma mansoni*. PLoS Negl. Trop. Dis. 7, e2336. doi:10.1371/journal.pntd.0002336

Conferences

International Symposium on Waterborne Diseases and Emerging Parasitic Diseases, 25-27 November 2014, Guangzhou, China. (Talk: "Towards an in-depth view of the reproductive biology of *Schistosoma mansoni*: from gonad isolation to subtranscriptomics and cell culture")

7th Annual GGL Conference 2014, 17-18 September 2014, Giessen, Germany. (Talk:

"Organ-specific sub-transcriptome analyses reveal pairing-dependent processed in the gonads of *Schistosoma mansoni*"

Molecular and Cellular Biology of Helminths VIII, 1-6 September 2014, Hydra, Greece. (Poster: "Isolation and characterization of vitelline cells from *Schistosoma mansoni*")

6th Annual GGL Conference 2013, 11-12 September 2013, Giessen, Germany. (Poster: "Understanding female development in *Schistosoma mansoni*: ovaries and vitellaria as a basis"

5th Annual GGL Conference 2012, 18-19 September 2012, Giessen, Germany. (Poster: "Improved method for the isolation of reproductive organs from *Schistosoma mansoni*")

Open Talks

"Current Topics in Infection Biology" Seminar, 15 July 2014, Biomedical Research Centre Seltersberg (BFS), Giessen, Germany. Talk title "Understanding the sexual maturation of schistosome females: lessons from isolated organs and cells"

Declaration

I declare that this thesis is my original work and other sources of information have been properly quoted. This work has not been previously presented to obtain any other degree from any other university.

Ich erkläre: Ich habe die vorgelegte Dissertation selbständig und ohne unerlaubte fremde Hilfe und nur mit den Hilfen angefertigt, die ich in der Dissertation angegeben habe. Alle Textstellen, die wörtlich oder sinngemäß aus veröffentlichten Schriften entnommen sind, und alle Angaben, die auf mündlichen Auskünften beruhen, sind als solche kenntlich gemacht. Bei den von mir durchgeführten und in der Dissertation erwähnten Untersuchungen habe ich die Grundsätze guter wissenschaftlicher Praxis, wie sie in der "Satzung der Justus-Liebig-Universität Gießen zur Sicherung guter wissenschaftlicher Praxis" niedergelegt sind, eingehalten.

Gießen, November 6, 2015

_____

Zhigang Lu